

2013

Oligomers of beta-L-arabinosides of hydroxyproline : synthesis of the carbohydrate epitope of the Art v 1 allergen

Ning Xie

Louisiana State University and Agricultural and Mechanical College, nxie2@tigers.lsu.edu

Follow this and additional works at: https://digitalcommons.lsu.edu/gradschool_dissertations



Part of the [Chemistry Commons](#)

Recommended Citation

Xie, Ning, "Oligomers of beta-L-arabinosides of hydroxyproline : synthesis of the carbohydrate epitope of the Art v 1 allergen" (2013). *LSU Doctoral Dissertations*. 249.
https://digitalcommons.lsu.edu/gradschool_dissertations/249

This Dissertation is brought to you for free and open access by the Graduate School at LSU Digital Commons. It has been accepted for inclusion in LSU Doctoral Dissertations by an authorized graduate school editor of LSU Digital Commons. For more information, please contact gradetd@lsu.edu.

**OLIGOMERS OF BETA-L-ARABINOSIDES OF HYDROXYPROLINE:
SYNTHESIS OF THE CARBOHYDRATE EPI TOPE OF THE ART V 1 ALLERGEN**

A Dissertation

Submitted to the Graduate Faculty of the
Louisiana State University and
Agricultural and Mechanical College
in Partial Fulfillment of the
Requirements for the Degree of
Doctor of Philosophy

In

The Department of Chemistry

by

Ning Xie

B.S., Louisiana State University, 2007
December 2013

To My Family...

To my wife Thao, without whom I would not be the man I am today.

To my son Andrew, whose mere existence inspires me to become an even better man.

To my mom and dad, I love you more than you'll ever know, more than I'll ever say...

...This Dissertation Is For You

ACKNOWLEDGMENTS

First and foremost, I would like to give many, many thanks to my adviser, Dr. Carol M. Taylor, for her guidance and support during my tenure as a graduate student at LSU. I have learned many things from Dr. Taylor in the past 5 years, most important of which is her relentless work ethic. I can truly say that Dr. Taylor is the hardest working woman that I've ever had the pleasure of knowing. She tries her best to instill the same diligence in me, as she does all her students, and for that I am forever grateful.

I would like to thank my committee members from the Chemistry department: Dr. William Crowe, Dr. Megan Macnaughtan, and Dr. Graca Vicente, for all their help over the years and providing me aid whenever I needed it. I would also like to thank my Dean's Representative, Dr. Jack Losso, for taking this commitment upon very short notice.

I wish to thank my fellow labmates Benson, Doug, Saroj, Chamini, Chyree, and Molly. Whether it's helping me fill a balloon of hydrogen (I hate balloons), coming along to grab a quick bite at the union, or offering helpful opinions on my research, there is always someone there willing to share their time. It has been a pleasure to work alongside you for the past five years and I am truly fortunate to have experienced graduate school with you all.

Special thanks to Dr. Thomas Weldeghiorghis and the late Dr. Dale Treleven, I truly appreciate everything you have done to help me acquire the best NMR spectra possible. I wish to thank Dr. Fritz Altmann for their work on the biological studies of our synthetic glycopeptides. And finally, I would like to thank the Department of Chemistry at LSU for all their support.

TABLE OF CONTENTS

ACKNOWLEDGMENTS.....	iii
LIST OF TABLES.....	vi
LIST OF FIGURES	vii
LIST OF SCHEMES.....	ix
LIST OF ABBREVIATIONS AND SYMBOLS	xii
ABSTRACT.....	xvi
CHAPTER 1:	
INTRODUCTION	1
1.1 Carbohydrates in Biology.....	1
1.2 Hydroxyproline-Rich Glycoproteins.....	3
1.3 Art v 1: the Major Allergen of Mugwort.....	4
1.4 Natural Versus Recombinant Art v 1	6
1.5 Two Novel O-Glycans in the Polyproline Domain.....	6
1.6 Immunological Studies.....	10
1.6.1 <i>In vitro</i> and <i>In vivo</i> testing of Art v 1	10
1.6.2 IgE recognition of Art v 1.....	12
1.7 A Related Allergen from <i>Ambrosia</i>	13
1.8 <i>Arabidopsis</i> CLV3 Glycopeptide: Another β -L-Arabinoside of Hyp.....	14
1.9 Closing Comments	15
CHAPTER 2:	
SYNTHESIS OF A MONOMER OF 4-O-[β -L-ARABINOFURANOSYL]-(2S,4R)-4-HYDROXYPROLINE.....	16
2.1 Importance of Arabinosides	16
2.2 Challenge of β -Arabinoside Synthesis	16
2.2.1 The anomeric effect	17
2.2.2 Neighboring group participation	18
2.3 Previous Efforts to Produce β -Arabinosides.....	19
2.4 Current Investigation.....	28
2.4.1 Glycosylation with the conformationally-restricted glycosyl donor	32
2.4.2 Conformationally unrestrained donor	38
2.5 Experimental Section.....	41
2.5.1 Experimental procedures	41
2.5.2 Spectra	51
CHAPTER 3:	
SYNTHESIS OF OLIGOMERS OF 4-O-[β -L-ARABINOFURANOSYL]-(2S,4R)-4-HYDROXYPROLINE.....	71
3.1 Previous Syntheses of Glycoclusters	71
3.2 Dimer Synthesis	75
3.3 Oligomer Synthesis.....	82
3.4 Oligomer End-Capping	84

3.5	Pre-End-Capped Glycosides	86
3.6	Global Deprotection	89
3.7	Experimental Section	90
3.7.1	Experimental procedures	90
3.7.2	Spectra	103
CHAPTER 4:		
	STRUCTURAL STUDIES OF POLYPROLINE GLYCOSIDES	128
4.1	Circular Dichroism	128
4.1.1	Polyproline helices	128
4.1.2	Effect of pH on peptide conformation	132
4.1.3	Glycosylated oligomers of proline	134
4.1.4	CD spectra of Ara-Hyp glycopeptides	136
4.2	Nuclear Magnetic Resonance Spectroscopy	140
4.2.1	Characterization of Ara-Hyp glycopeptides of nArt v 1 by Leonard <i>et al.</i>	140
4.2.2	Characterization of synthetic Ara-Hyp glycopeptides	141
4.3	Enzyme Linked Immunosorbent Assays	147
4.4	Summary	149
4.5	Future Work	152
4.5.1	Incorporation of the β -Ara-Hyp motif into longer peptides	152
4.5.2	Antibody generation	153
4.5.3	Effect of glycosylation on oligoproline conformation	154
4.5.4	Synthetic glycopeptides as diagnostic tools	154
4.6	Experimental Section	155
4.6.1	Circular dichroism spectroscopy	155
4.6.2	NMR spectroscopy	155
	REFERENCES	156
	APPENDIX: LETTERS OF PERMISSION	166
	VITA	173

LIST OF TABLES

Table 1.1	Amino acid residues in the “Head” domain	5
Table 1.2	Amino acid residues in the “Tail” domain	5
Table 1.3	Proline-rich domains of Art v 1 and Amb a 4.....	14
Table 2.1	Selected examples of glycosylation with <i>L</i> -arabinosyl donors. Reagents and conditions: NIS/AgOTf, DCM, -30 °C	24
Table 2.2	Selected comparisons of <i>L</i> - vs <i>D</i> -arabinofuranosyl donors	27
Table 2.3	Chemical Shifts for β -Glycoside 55β	35
Table 4.1	NMR resonances of Hyp in Art v 1.....	140
Table 4.2	NMR resonances of β -Ara in Art v 1	141
Table 4.3	Amino acid sequence in the polyproline domain	152
Table 4.4	Target oligoproline compounds	154

LIST OF FIGURES

Figure 1.1	Structure of heparan sulfate subunit.....	1
Figure 1.2	<i>N</i> -acetyl glucosamine (GlcNAc).....	2
Figure 1.3	G _{D3} -Protein conjugate vaccine for melanoma.....	2
Figure 1.4	Synthetic hexasaccharide GPI	3
Figure 1.5	<i>Artemisia vulgaris</i> plant	5
Figure 1.6	Gel filtration chromatogram of alkali-degraded nArt v 1. Reprint with permission from Journal of Biological Chemistry	7
Figure 1.7	The unusual arabinogalactan (Hyp PS); arrows indicate potential sites for further arabinosylation	8
Figure 1.8	β -Glucosyl Yariv reagent.....	8
Figure 1.9	Enzymatic degradation of Art v 1	9
Figure 1.10	a) The single β -L-Ara-Hyp motif, b) Tetramer of Hyp- β -arabinofuranoside	10
Figure 1.11	NMR solution structure of Art v 1. a) Defensin domain in dark blue, intermediate region in blue, and polyproline domain in light blue. b) Ribbon illustration of Art v 1. Reprinted with permission from Elsevier	13
Figure 1.12	Cartoon representations of Art v 1 and Amb a 4.....	13
Figure 1.13	CLV3.....	14
Figure 2.1	Arabinofuranosyl residue found in the cell wall of mycobacterium	16
Figure 2.2	Factors that influence stereochemistry in glycosylation. a) The anomeric effect, although strong for pyranoses, offers little selectivity for its furanose counterpart. b) Neighboring group participation favors the 1,2- <i>trans</i> -glycoside	17
Figure 2.3	a) In the ³ E conformation, the C-2 substituent is axial, resulting in steric interactions that favor axial attack. The E ₃ conformation allows the C-2 substituent to be in a pseudo-equatorial orientation, favoring a beta attack at the anomeric carbon. b) C-3 and C-5 alcohols protected as a silyl acetal.....	23
Figure 2.4	Benzylidene method adapted for β -D-arabinofuranoside formation	25
Figure 2.5	Crystal structure of 3,5-O-(di- <i>tert</i> -butyl-silane) arabinofuranoside derivative. Reprint with permission from iUCR.....	26
Figure 2.6	Hyperconjugation via $\sigma \rightarrow \sigma^*$ interaction	32
Figure 3.1	MUC1 core related diglycohexapeptide and diglycodecapeptide	72

Figure 3.2	T _N and TF antigen	73
Figure 3.3	a) Guanidinium and uronium salts of HATU and HBTU, b) Neighboring group effect	80
Figure 4.1	Polyproline type I and II helices	128
Figure 4.2	Phi (Φ), psi (Ψ), and omega (ω) backbone dihedral angles of peptides.....	129
Figure 4.3	n→π* Interaction in a proline tetramer.....	129
Figure 4.4	CD Spectrum of Ac-(Pro) ₇ -Gly-Tyr-NH ₂ taken at 5 °C. Reprint with permission from American Chemical Society.....	130
Figure 4.5	Host PPII helix sequence with insertion of guest amino acids. Reprint with permission from American Chemical Society.....	131
Figure 4.6	CD spectra of synthetic polyproline peptides H-(Pro) _n -OH	132
Figure 4.7	<i>Cis/Trans</i> isomerization of Alanylproline.....	133
Figure 4.8	CD Spectra of H-Gly-(Pro) ₂ -OH. Reprint with permission from John Wiley and Sons	133
Figure 4.9	CD Spectra of model peptides. Reprint with permission from American Chemical Society.....	134
Figure 4.10	CD spectrum of Ac-([β-L-Araf]Hyp)-NHMe	136
Figure 4.11	CD spectrum of Ac-([β-L-Araf]Hyp) ₂ -NHMe.....	137
Figure 4.12	CD spectrum of Ac-([β-L-Araf]Hyp) ₃ -NHMe and Ac-([β-L-Araf]Hyp) ₄ -NHMe	138
Figure 4.13	CD Spectra of all four synthetic glycopeptides.....	139
Figure 4.14	NOESY spectrum of Ac-([β-L-Araf]Hyp)-NHMe	142
Figure 4.15	HSQC spectrum of Ac-([β-L-Araf]Hyp)-NHMe	143
Figure 4.16	COSY spectrum of Ac-([β-L-Araf]Hyp)-NHMe	144
Figure 4.17	¹ H NMR of all four synthetic glycopeptides	146
Figure 4.18	ELISA inhibition experiments of synthetic glycopeptides	148
Figure 4.19	Varied concentrations of synthetic glycopeptides inhibition experiments	149
Figure 4.20	Protected oligomers	150
Figure 4.21	Proposed conjugation of synthetic glycopeptides to carrier proteins.....	153

LIST OF SCHEMES

Scheme 1.1	Two sequential post translational modifications.....	6
Scheme 2.1	Stereoselectivity utilizing the anomeric effect	17
Scheme 2.2	Conformational restriction leading to increased anomeric effect in furanoside.....	18
Scheme 2.3	Neighboring group participation.....	19
Scheme 2.4	Stereocontrol via neighboring group participation	19
Scheme 2.5	Early efforts to obtain 1,2- <i>cis</i> -arabinosides.....	19
Scheme 2.6	Use of 1,2,5-orthoester as donor and acceptor.....	20
Scheme 2.7	Intramolecular aglycon delivery	21
Scheme 2.8	Synthesis of CLV3 glycopeptide utilizing IAD	21
Scheme 2.9	Stereoselective β -arabinosylation through a 2,3-anhydro sugar intermediate.....	22
Scheme 2.10	Sulfide and sulfoxide donors. a) Cyclohexanol, NIS/AgOTf, CH ₂ Cl ₂ -30 °C \rightarrow RT, b) Tf ₂ O -78 °C, 30 min, then cyclohexanol	26
Scheme 2.11	Retrosynthetic analysis of tetramer	28
Scheme 2.12	Peracylated arabinofuranoside synthesis	29
Scheme 2.13	Preparation of bicyclic silyl acetal donor.....	30
Scheme 2.14	Benzylation of C-2 alcohol.....	31
Scheme 2.15	Preparation of hydroxyproline acceptor	31
Scheme 2.16	Glycosylation of hydroxyproline with silyl acetal donor	33
Scheme 2.17	Glycosylation of hydroxyproline with sulfoxide donor.....	36
Scheme 2.18	Intramolecular aglycon delivery strategies.....	37
Scheme 2.19	Preparation of disiloxane donor	38
Scheme 2.20	Preparation of two conformationally unrestrained donors	38
Scheme 2.21	Low temperature glycosylation method	39
Scheme 2.22	Glycosylation of hydroxyproline with benzylated sulfide donor	40
Scheme 2.23	Glycosylation of hydroxyproline with benzylated sulfoxide donor.....	40

Scheme 3.1	Fragment condensation using HOBt and EDC	72
Scheme 3.2	Synthesis of a triglycopeptide cluster (T _N only).....	73
Scheme 3.3	Solid phase peptide synthesis of a nonaglycopeptide.....	74
Scheme 3.4	Retrosynthetic analysis of dimer.....	75
Scheme 3.5	Boc deprotection of monomer	76
Scheme 3.6	Known methods of allyl ester deprotection	76
Scheme 3.7	Deallylation of monomer.....	77
Scheme 3.8	Difficult coupling of a dipeptide of aminoisobutyric acid	77
Scheme 3.9	Fragment condensation to produce dimer with PyBrOP	78
Scheme 3.10	Mechanism of PyBrOP/DMAP mediated coupling	78
Scheme 3.11	Classical preparation of acid fluorides; acid chloride side reactions.....	79
Scheme 3.12	Preparation of TFFH.....	79
Scheme 3.13	Fragment condensation to produce dimer with TFFH.....	80
Scheme 3.14	Pathways of amide formation using HATU	81
Scheme 3.15	Fragment condensation to produce dimer using HATU	82
Scheme 3.16	[2+1] and [1+2] Trimer coupling strategy	82
Scheme 3.17	Preparation of dimer building blocks.....	83
Scheme 3.18	Fragment condensation to produce trimer	83
Scheme 3.19	Fragment condensation to produce tetramer	84
Scheme 3.20	End-capping of glycopeptides	84
Scheme 3.21	Monomer end-capping	85
Scheme 3.22	Dimer end-capping	85
Scheme 3.23	Oligomer-specific glycosidic building blocks	86
Scheme 3.24	Pre-end-capped glycosyl acceptors.....	86
Scheme 3.25	Preparation of pre-end-capped monomers	87

Scheme 3.26 Alternate strategy for preparation of C-terminal amide glycoside.....	87
Scheme 3.27 Pre-end-capped trimer synthesis.....	88
Scheme 3.28 Pre-end-capped tetramer synthesis.....	89
Scheme 3.29 Global debenzylation.....	90
Scheme 4.1 Activation of ALP with <i>p</i> -nitrophenyl phosphate.....	148
Scheme 4.2 Glycosylation of Boc-Hyp-OAll by sulfide donor.....	150
Scheme 4.3 Global debenzylation.....	151

LIST OF ABBREVIATIONS AND SYMBOLS

Å	Angstrom
Ac	Acetyl
AgOTf	silver triflate
AGP	arabinogalactan proteins or arabinogalactan polysaccharides
Amb	<i>Ambrosia artemisiifolia</i>
Ara(f)	arabinose(furanose)
Art v 1	<i>Artemisia vulgaris</i>
Bn	benzyl
Boc	<i>tert</i> -butyloxycarbonyl
BOP	benzotriazol-1-yloxytris(dimethylamino)-phosphonium
^t Bu	<i>tert</i> -butyl
° C	degrees Celsius
CD	circular dichroism
CLV3	CLAVATA3
COSY	correlation spectroscopy
<i>m</i> CPBA	<i>meta</i> -chloroperoxybenzoic acid
DCC	dicyclohexylcarbodiimide
DCM	dichloromethane
DIEA	<i>N,N</i> -diisopropylethylamine
DFT	density functional theory
DMAP	4-dimethylaminopyridine
DMF	dimethylformamide
DTBMP	di- <i>tert</i> -butyl methyl pyridine
<i>E. Coli</i>	<i>Escherichia coli</i>

EDC	1-(3-dimethylaminopropyl)-3-ethylcarbodiimide hydrochloride
ELISA	Enzyme-linked immunosorbent assay
ESI	electrospray ionization
Fmoc	9-fluorenylmethoxycarbonyl
Gal	galactose
GlcNAc	<i>N</i> -acetyl glucosamine
GPI	glycosylphosphatidylinositol
HATU	<i>O</i> -(7-azabenzotriazol-1-yl)-1,1,3,3-tetramethyluronium
HBTU	<i>O</i> -(benzotriazol-1-yl)-1,1,3,3-tetramethyluronium hexafluorophosphate
HIV	human immunodeficiency virus
HMBC	heteronuclear multiple bond coherence
HOAt	1-hydroxy-7-azabenzotriazole
HOBt	1-hydroxybenzotriazole
HPLC	high performance liquid chromatography
HRGP	hydroxyproline-rich glycoproteins
HRMS	high resolution mass spectrometry
HSQC	heteronuclear single quantum correlation
Hyp	<i>trans</i> -4-L-hydroxyproline
Hyp-PS	hydroxyproline polysaccharide
IAD	intramolecular aglycon delivery
IgE	Immunoglobulin E
IIDQ	<i>N</i> -isobutyloxy-carbonyl-2-isobutyloxy-1,3-dihydroquinone
KLH	keyhole limpet hemocyanin
MA	mixed anhydride
Me	methyl

MS	mass spectrometry
NaH	sodium hydride
nArt v 1	natural Art v 1
NIS	<i>N</i> -iodosuccinimide
NMM	<i>N</i> -methylmorpholine
NMR	nuclear magnetic resonance
nOe	nuclear Overhauser effect
NPT	nasal provocation test
PMA	phosphomolybdic acid
PMB	<i>para</i> -methoxybenzyl
PMBC	peripheral blood mononuclear cells
ppm	parts per million
PPI	polyproline 1
PPII	polyproline 2
PRP	proline-rich proteins
PTM	post translational modification
PyBOP	benzotriazol-1-yloxytri(pyrrolidino)phosphonium hexafluorophosphate
PyBroP	bromotris(pyrrolidino)phosphonium hexafluorophosphate
R_f	retention factor
rArt v 1	recombinant Art v 1
RAST	radioallergosorbent test
rt	room temperature
s	singlet
SPT	skin prick test
q	quartet

Ser	serine
SPPS	solid phase peptide synthesis
TBAF	tetra- <i>n</i> -butylammonium fluoride
TBAH	tetra- <i>n</i> -butylammonium hydroxide
TBTU	O-benzotriazol-1-yl-1,1,3,3-tetramethyluronium tetrafluoroborate
TCL	T-cell lines
TF	Thomsen-Friedenreich
Tf ₂ O	triflic anhydride
TFA	trifluoroacetic acid
TFFH	tetramethylfluoroformamidinium hexafluorophosphate
THF	tetrahydrofuran
TLC	thin layer chromatography
TOF	time of flight
UV	ultraviolet

ABSTRACT

The major allergen of mugwort pollen, Art v 1, is a significant contributor to hay fever in Europe and North America. A notable motif in Art v 1 – characterized by clusters of contiguous β -arabinosides of hydroxyproline – was found to be a key recognition element for antibodies generated in response to the natural protein. This dissertation details the synthesis of oligomers of β -arabinosides of hydroxyproline and the search to establish the minimal carbohydrate epitope of Art v 1.

The key issue pertaining to the formation of glycosidic bonds is the α/β selectivity at the anomeric carbon. To this end, using a 2,3,5-*O*-benzyl-1-thio- α -L-arabinofuranoside donor, we were able to obtain the Ara-Hyp monomer in 60% yield with 4:1 β : α selectivity using silver triflate and *N*-iodosuccinamide as activators.

A dimer of β -Ara-Hyp was prepared by deprotection of the *N*- and *C*- termini of the β -Ara-Hyp monomer respectively, after which peptide coupling of the two compounds was performed using HATU as coupling reagent to give the product, Boc-([β -L-Araf]Hyp)₂-OAll, in 60% yield. Similar approaches were employed using a [2+1] or [1+2] fragment condensation strategy to produce the trimer, Boc-([β -L-Araf]Hyp)₃-OAll, in 35% yield. The tetramer, Boc-([β -L-Araf]Hyp)₄-OAll was produced using a [2+2] strategy in 49% yield.

We've installed terminal amides on the oligomers to best mimic the extended peptide found in the natural allergen. Production of oligomer-specific building blocks (Ac-([β -L-Araf]Hyp)-OMe, Boc-([β -L-Araf]Hyp)-NHMe) allowed a more convergent synthesis towards the end-capped oligomers. With this strategy, end-capped dimer, trimer, and tetramer were synthesized by fragment condensation in 48%, 35%, and 15% respectively. The end-capped glycopeptides could then be fully deprotected by global debenzylation to give the final products in quantitative yield.

Nuclear magnetic resonance and circular dichroism spectra were obtained for all synthetic glycopeptides. Analysis of the CD spectra showed that the glycosylated proline oligomers exhibit a polyproline type II helical conformation. While CD spectrum of the monomer showed that it was unordered, the elliptical curve of dimer, trimer, and tetramer all exhibited significant PPII characteristics. Spectra obtained from ^1H , ^{13}C , and various 2D NMR was used for comparison with NMR data taken from the natural allergen.

CHAPTER 1: INTRODUCTION

1.1 Carbohydrates in Biology

It has been shown over the past couple of decades that carbohydrates play a more important role in biology¹ than previously appreciated. Sugars are found in abundance in nature as biopolymers. Sugars can exist as oligosaccharides, polysaccharides, and/or glycosides in natural products, many of which display important biological activity. Many carbohydrates have specific roles in biological processes ranging from signal transduction² to immune response³.

The functions of carbohydrates in living organisms are diverse. For example, heparan sulphate (Figure 1.1), a linear polysaccharide in proteoglycans, is found on the plasma membrane of all animal cells and regulates a wide variety of biological activities.⁴ Gene mutation leading to the expression of modified proteoglycans has been implicated in conditions including rib malformations, craniofacial defects, and eye and lens defects.

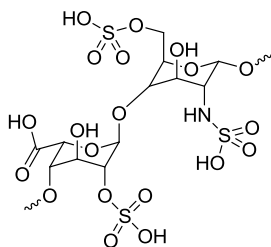


Figure 1.1 Structure of heparan sulfate subunit

Over 500 *N*-acetylglucosamine (Figure 1.2) protein conjugates are involved in almost all aspects of cellular function.⁵ Both hypo- and hyper-glycosylation of these proteins have been associated with disease. For example, altered glycosylation of proteins due to nutrient excess and/or stress has been associated with glucose toxicity,⁶ a.k.a. type-2 diabetes. Reduced glycosylation leading to the hyperphosphorylation of tau proteins may also affect neuronal

function. The hyperphosphorylated tau proteins aggregate into neurofibrillary tangles, one of the proposed mechanisms in the onset of Alzheimer's disease.⁷

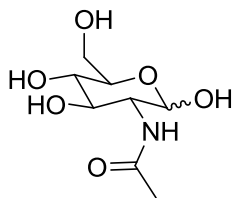


Figure 1.2 *N*-acetyl glucosamine (GlcNAc)

Advances in glycobiology and glycochemistry have enabled the development of carbohydrate-based experimental therapeutics for a variety of diseases, including HIV and cancer.⁸ Carbohydrate-based tumor antigens that induce only weak immunological responses have been successfully conjugated to carrier proteins to illicit a more powerful immune response.⁹ Advances in glycopeptide assembly have led to synthetic antitumor vaccines such as G_{D3} (Figure 1.3) that are conjugated to keyhole limpet hemocyanin (KLH), a well-known carrier protein.

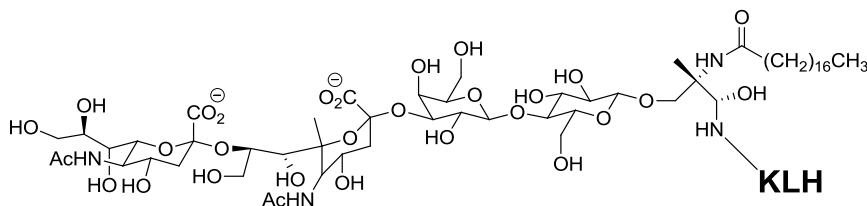


Figure 1.3 G_{D3}-Protein conjugate vaccine for melanoma

Various pathogenic bacteria are coated with polysaccharides, glycoproteins, and/or glycolipids which can be targeted by carbohydrate-rich protein-conjugated antibacterial vaccines.¹⁰ Vaccines against *Streptococcus pneumonia*, *Neisseria meningitidis*, and *Salmonella typhi* are now commercially available.

ten percent.¹³

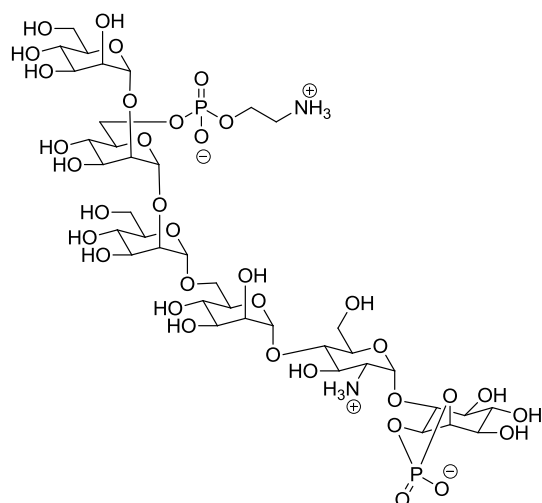


Figure 1.4 Synthetic hexasaccharide GPI

1.2. Hydroxyproline-Rich Glycoproteins

plant defense.¹⁶ The HRGPs can be divided into four groups:

- 1) Extensins - Hyp-rich glycoproteins with repeating sequences such as Ser(Hyp)₄ and are highly glycosylated with oligosaccharides of arabinose.
- 2) Arabinogalactan proteins (AGPs) - typically contain arabinogalactan (Ara-Gal) chains that are attached to the protein via a Gal-Hyp linkage.
- 3) Solanaceous lectins - Hyp-rich lectins that consist of a carbohydrate-binding domain and an extensin-like domain.
- 4) proline-rich proteins (PRPs) - a broad classification of molecules that are rich in Pro/Hyp, but which cannot be classified as any of the previous three groups.

While the HRGP can be divided into groups, there are no distinct boundaries between them. In fact, Art v 1 draws characteristics of all four HRGP groups.

1.3 Art v 1: the Major Allergen of Mugwort

Artemisia vulgaris (Figure 1.5) is a widespread weed that belongs to the *Asteraceae* family. The plant is native to temperate Europe, Asia, parts of North Africa, and has been naturalized in North America. This species is known by several common names, amongst them are chrysanthemum weed, wild woodworm, felon herb, and mugwort, and typically blooms from July to September. The pollen of this plant is a major contributor to hay fever (*allergic rhinitis*) in late summer to early fall. Art v 1, the major allergen of mugwort, is recognized by up to 95% of mugwort pollen-sensitized patients.¹⁷ In Europe, mugwort pollen affects up to 14% of all patients with pollinosis.¹⁸ In industrialized countries of the world, Immunoglobulin E (IgE) mediated allergy affects more than 40% of the population.¹⁹



Figure 1.5 *Artemisia vulgaris* plant

A modular glycoprotein, Art v 1 has a tadpole-like structure that is comprised of two major domains known as the “head” and “tail” domains. The head domain is similar to protein sequences found in plant defensins. This globular domain, comprised of amino acids residues 1-55 (Table 1.1), is cysteine-rich and stabilized by disulfide bonds. The tail domain, comprised of amino acid residues 56-108 (Table 1.2), is the proline-rich domain. This section contains about 20 proline residues and is heavily hydroxylated and glycosylated. The prolyl domain facilitates protein folding²⁰ and influences the conformation of the globular domain.²¹

Table 1.1 Amino acid residues in the “Head” domain

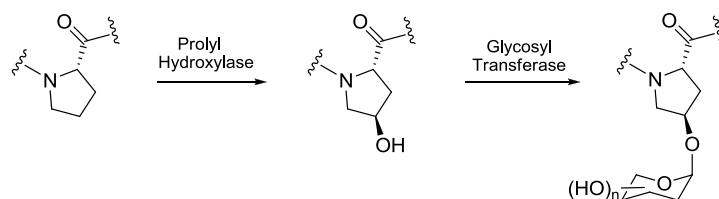
1-10	11-20	21-30	31-40	41-50	51-55
AGSKLCEKTS	KTYSGKCDNK	KCDKKCIEWE	KAQHGACHKR	EAGKESCFCY	FDCSK

Table 1.2 Amino acid residues in the “Tail” domain

56-60	61-70	71-80	81-90	91-100	100-108
SPPGA	TPAPPGAAPP	PAAGGSPSPP	ADGGSPPPA	DGGSPPVDGG	SPPPPSTH

1.4 Natural Versus Recombinant Art v 1

During the primary post-translational modification (PTM) of the polyproline domain of HRGPs, most of the proline residues are hydroxylated by a prolyl-4 hydroxylase (Scheme 1.1). The hydroxyprolines are further modified by subsequent O-glycosylation with some type of carbohydrate molecule(s) during the secondary PTM. The carbohydrates in natural Art v 1 constitute about 30-40% of the mass of the molecule.



Scheme 1.1 Two sequential post translational modifications

The cDNA sequence of the Art v 1 glycoprotein was determined.¹⁷ Natural Art v 1 (nArt v 1) was characterized and expressed in *Escherichia coli* and produced as the recombinant allergen (rArt v 1). The major difference between the natural and recombinant allergen is that rArt v 1 lacks the post translational modifications of the proline rich domain. Any differences found in biological reactivity of the two allergens could be attributed to the carbohydrate moiety of the natural versus recombinant allergen.

1.5 Two Novel O-Glycans in the Polyproline Domain

The hydroxyproline-rich domain of Art v 1, also known as the tail section, contains amino acid residues 56-108. Post translational modification of the tail section gives rise to two novel O-glycans that have been described by Leonard *et al.*²² Through the use of high field NMR, in conjunction with chemical and enzymatic degradation and mass spectrometry, Leonard reported the existence of a new carbohydrate determinant in Art v 1. The three major peaks of the gel filtration chromatogram of alkali-degraded nArt v 1 are shown in Figure 1.6.

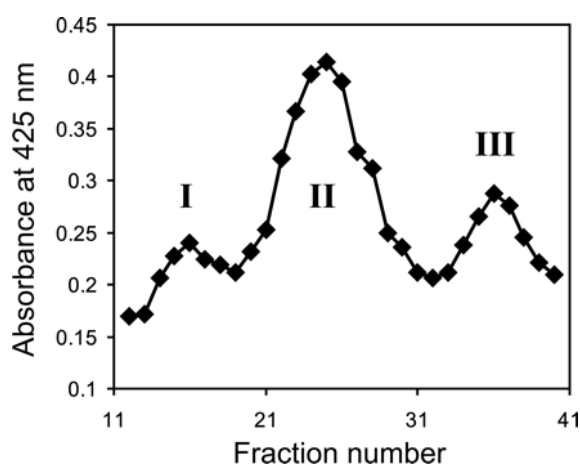


Figure 1.6 Gel filtration chromatogram of alkali-degraded nArt v 1. Reprint with permission from Journal of Biological Chemistry

The first and smallest peak (I) of the gel filtration chromatogram was attributed to incompletely digested material (Figure 1.6). The second peak (II) was most intense and attributed to hydroxyproline-linked arabinogalactan, which the authors termed Hyp-polysaccharide (Hyp-PS). Natural Art v 1 was found to contain an 11.4:1 ratio of arabinose and galactose residues. Analysis of Hyp-PS showed that it contained arabinose and galactose residues in a 5.5:1 ratio, about half of all arabinose residues in the glycoprotein. Limited acid hydrolysis of Hyp-PS saw cleavage of the arabinose units while leaving the trigalactosyl-Hyp intact with a calculated $[M+Na]^+$ ion mass of 640 Da. When Hyp-PS was treated with α -L-arabinosidase, similar results were found indicating that Hyp-PS composed of a galactosyl-core with α -L-arabinose residues attached. Hyp PS has a β -1,3-linked galactan backbone with side chains of β -1,6-linked units similar to type II arabinogalactans (arabino-3,6-galactan),²³ but with differing patterns of substituted arabinose residues. Leonard *et al.* proposed that this be termed a type III arabinogalactan polysaccharide (AGP). Mass spectrometry indicated that Hyp-PS has isoforms that contain 5-28 α -linked arabinofuranose residues in the positions indicated in Figure 1.7. β -Glucosyl Yariv reagent (Figure 1.8), a synthetic phenyl glycoside that specifically binds to arabinogalactan polysaccharides (AGP),²⁴ was used to precipitate natural Art v 1. This positive test confirms that Hyp-PS is an AGP.

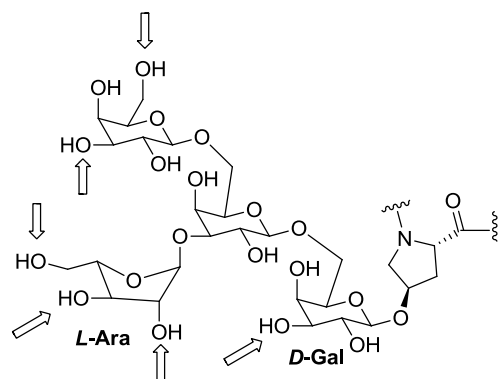


Figure 1.7 The unusual arabinogalactan (Hyp PS); arrows indicate potential sites for further arabinosylation

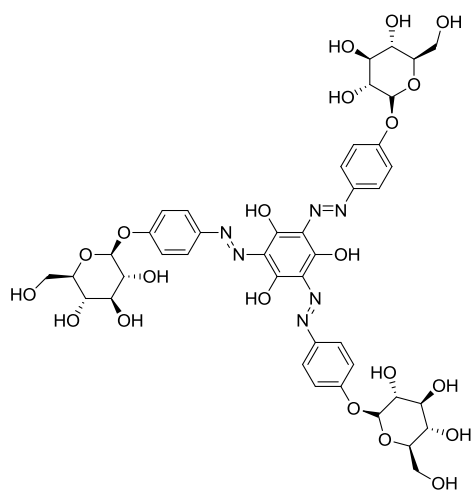


Figure 1.8 β -glucosyl Yariv reagent

Type II arabinogalactans have known to be immunogenic with monoclonal antibodies binding to arabinose-containing epitopes.²⁵ Surprisingly, Hyp-PS bound very weakly to antibodies from the sera of mugwort-allergic patients.²² A similar glycoprotein from *Phleum pratense* also disappointed investigators by its insignificant binding to IgE of patients.²⁶

The final peak (III) in the gel filtration chromatogram of alkali degraded nArt v 1 represents β -L-arabinoside of hydroxyproline (β -L-Araf-Hyp) (Figure 1.6). Initially, it was thought that the carbohydrate domain of Art v 1 comprised only of α -arabinose and β -galactose residues. However, upon treatment of nArt v 1 with α -arabinofuranosidase and β -galactosidase,

the product had a calculated mass much larger than the total peptide mass of the carbohydrate region of nArt v 1 (Figure 1.9). The authors calculated that about 2.5 kDa of unaccounted mass still remained in the enzymatically treated glycoprotein. This mass was eventually attributed to 16-17 arabinose residues that were resistant to the α -arabinosidase.

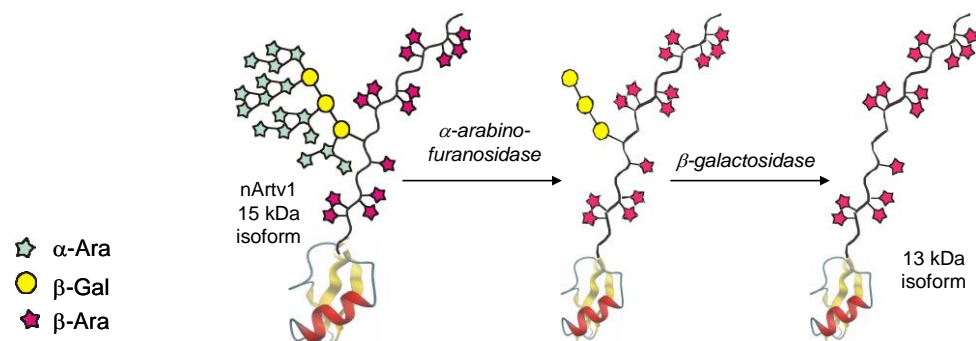


Figure 1.9 Enzymatic degradation of Art v 1.

Proton and two dimensional NMR data suggested that the 16-17 residues of “dark matter” were single β -arabinofuranosides linked to hydroxyproline (Figure 1.10a). This novel O-glycan does occur as a monomer, but anywhere from two to four adjacent β -arabinosylated prolines may be present (Figure 1.10b, 1). Unlike other well-known HRGPs having the Ser-Hyp₄ motif, no oligo-arabinosides were found in Art v 1. This second new type of O-glycan *did* react with antibodies from the sera of mugwort-allergic patients. As reported earlier, comparison of the recombinant and natural allergen showed that a number of patients responded only to the natural Art v 1.²⁷ This means that the post translational modifications, namely proline hydroxylation and subsequent β -arabinosylation, are influencing the conformation of the epitopes of the mugwort allergen. While the exact mechanism of the stabilizing effects of arabinoglycosylated prolines are yet unclear, it has been implicated that β -arabinosides in the polyproline-domain does influence the allergenicity of Art v 1.²¹

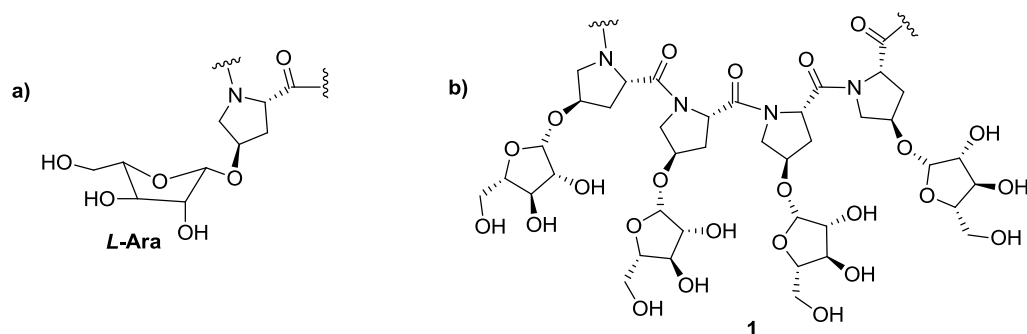


Figure 1.10 a) The single β -L-Ara-Hyp motif, b) Tetramer of Hyp- β -arabinofuranoside

1.6 Immunological Studies

1.6.1 *In vitro* and *in vivo* testing of Art v 1

T-cells, or T-lymphocytes, are a specialized type of white blood cell that play a central role in cell-mediated immunity. Initial testing showed that the post-translational modifications did not influence T-cell recognition of Art v 1.¹⁷ In a related study by Jahn-Schmid *et al.*, peripheral blood from eighteen mugwort pollen-sensitized patients was collected based on case history and positive *in vitro* and *in vivo* tests. These patients were found to have IgE that recognized both nArt v 1 and rArt v 1. For this patient group, the nArt v 1 and its recombinant form elicited similar T-cell responses in peripheral blood mononuclear cells (PBMC) and in allergen-specific T-cell lines (TCL).²⁸

T-cell epitopes were determined by TCL against both the natural and recombinant allergen. The T cell proliferation assays utilized thirty-three overlapping 12-mer peptides that spanned the entire amino acid sequence of rArt v 1. Out of seventeen patients, fourteen recognized an Art v 1 epitope at amino acids 22-36 in the cysteine rich region of Art v 1. Five patients recognized an epitope at amino acids 43-54, also in the cysteine domain. Only two of seventeen patients exhibited multiple dispersed epitopes, a rather low number in comparison to

known epitopes of other pollen allergens. A follow up study by this group reported that the single T cell epitope Art v 1₂₂₋₃₆ is associated with the expression of HLA-DRB1*01.^{1*},²⁹

In the first clinical study of mugwort allergens, Schmid-Grendelmeier and co-workers investigated the allergenicity of nArt v 1 and rArt v 1 by both *in vitro* and *in vivo* experiments.³⁰ Thirty-two patients with mugwort pollen allergy (17 female, 15 male; 16-43 years old) and 10 control subjects (7 female, 3 male; 21-41 years old) were included in this study. The thirty-two mugwort allergic patients were selected based on having a clinical history of recurrent rhinitis, a positive skin prick test (SPT) response to mugwort extracts, and increased IgE levels to mugwort pollen.

The *in vitro* results agreed with the findings of Jahn-Schmid and co-workers. It was reported that both nArt v 1 and rArt v 1 alone were able to induce T-cell proliferation in mugwort-sensitized patients. The proliferative responses of PBMCs to rArt v 1 and nArt v 1 were comparable, the only difference being that the recombinant form required longer incubation periods to induce lymphocyte proliferation.

The *in vivo* tests, however, showed that the recombinant allergen elicits a lower SPT and nasal provocation test (NPT) reactivity than the natural allergen. While rArt v 1 was still able to elicit positive SPT and NPT, the amount of rArt v 1 required was significantly higher than that for nArt v 1. The recombinant allergen showed a decrease in the size of the wheals induced in the SPT, while having a reduced response compared to that of its natural counterpart in the NPT.

^{1*}Human Leukocyte Antigen (HLA) is the name of the major histocompatibility complex (MHC) in humans. MHC mediates the interaction of leukocyte (white blood cells) with other leukocytes or body cells.

1.6.2 IgE recognition of Art v 1

Immunoblots, radioallergosorbent tests (RAST), and enzyme-linked immunosorbent assays (ELISA) were used to evaluate the IgE binding properties of natural and recombinant Art v 1.¹⁷ Immunoblots and RAST showed that two groups of patients exist: one group that exhibits similar IgE recognition of nArt v 1 and rArt v 1, and a second group that showed significantly lower or no reactivity to the recombinant allergen. ELISA experiments showed that rArt v 1 only caused a partial (30%) inhibition of IgE binding to nArt v 1.

Oberhuber and co-workers published a paper in 2008 detailing the analysis of IgE binding profiles in a group of mugwort-allergic patients.²⁷ Sera from 100 pediatric mugwort allergic patients (62 males, 38 females; 1-19 years old) were tested. Patients all showed hypersensitivity to mugwort based on a SPT from mugwort pollen extract and a positive RAST.

In order to evaluate IgE binding activity, ELISA experiments were performed with purified nArt v 1 and rArt v 1. The natural allergen was recognized by the serum of 79 of the 100 patients. As for the recombinant allergen, only 39 patients' sera recognized the protein, a 50% drop in allergen recognition as compared to nArt v 1.

More recent work has shown that glycosylation of the natural Art v 1 protein contributes to the thermal stability of the allergen in that it aids in the complete refolding of the glycoprotein after heat denaturation, something that the recombinant allergen could not replicate.²⁰ Razzera and co-workers reported, after comparing NMR chemical shifts of the recombinant and naturally glycosylated Art v 1, that the carbohydrates in the polyproline domain affect the defensin domain in the natural molecule (Figure 1.11).²¹ These results, in combination with the findings of Himly and Oberhuber *et al.*,^{17, 27} strongly suggest that, for a significant group of patients, the involvement of post-translational modification and the resulting carbohydrates are crucial in the formation of IgE binding epitopes of Art v 1.

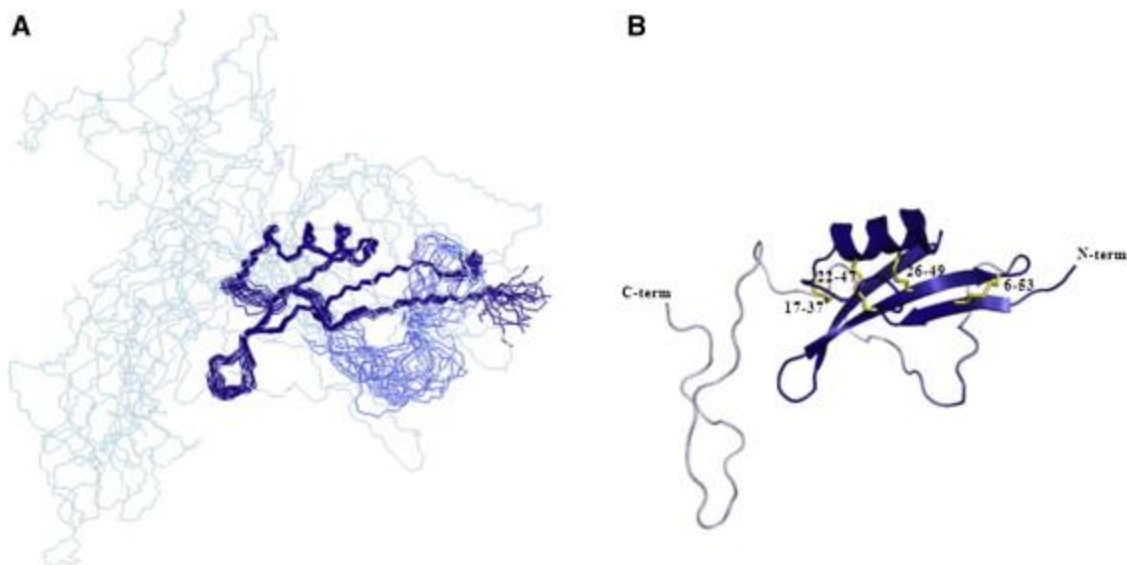


Figure 1.11 NMR solution structure of Art v 1. a) Defensin domain in dark blue, intermediate region in blue, and polyproline domain in light blue. b) Ribbon illustration of Art v 1. Reprinted with permission from Elsevier.

1.7 A Related Allergen from *Ambrosia*

Altmann and coworkers recently characterized a new allergen, Amb a 4 (Figure 1.12), from ragweed (*Ambrosia artemisiifolia*).³¹ The isolated ragweed pollen protein consisted of a defensin-like domain with a 50% homology to Art v 1 (Table 1.3). The C-terminal hydroxyproline-rich domain contained small amounts of the single hydroxyproline-linked β -arabinoside residues also found in Art v 1. The recombinant ragweed protein reacted with the sera of more than 30% of weed pollen allergic patients.

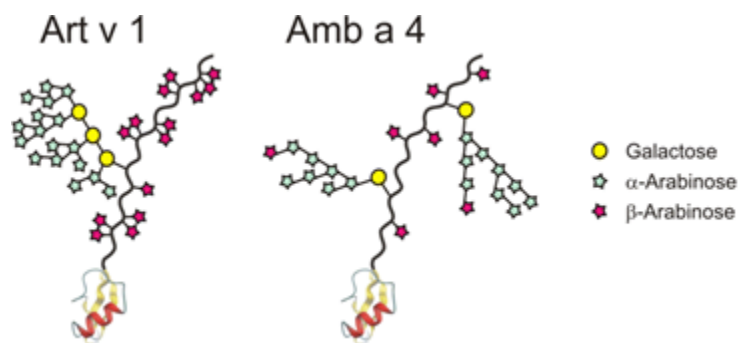


Figure 1.12 Cartoon representations of Art v 1 and Amb a 4

Table 1.3 Proline-rich domains of Art v 1 and Amb a 4.

	56	61	71	81	91	101
Art v 1	SPPGA	TPAPPGAAPP	PAAGGSPSP	ADGGSPPPPA	DGGSPPV DGG	SPPPPSTH
Amb a 4	-NPGP	PPGAPK GKAP	APSPPSGGGA	PPPSGGEGGD	GPPPEGGEGG	GGDGGGE

1.8 *Arabidopsis* CLV3 Glycopeptide: Another β -L-Arabinoside of Hyp

CLAVATA3 (CLV3) is a glycopeptide gene secreted from *Arabidopsis thaliana* plants.³² The CLV3 gene is expressed in the shoot apical meristem (SAM), which continuously produces organs for the plants, and is a key component in the regulation of stem cell renewal and differentiation.³³ Overexpression in the CLV3 gene can lead to developmental retardation.³² It has been reported that the mature CLV3 peptide found in CLV3-overexpressing *Arabidopsis* plants feature a 13 amino acid peptide.³⁴ This peptide features a *trans*-4-hydroxyproline at the seventh residue (Hyp7) that is attached to three L-arabinose residues via β -1,2-linkages (Figure 1.13). In testing the restrictions of stem cell activity by synthetic peptides varying in the number of carbohydrates attached to Hyp7, it was found that the biological activity increased with the length of the arabinose chain.

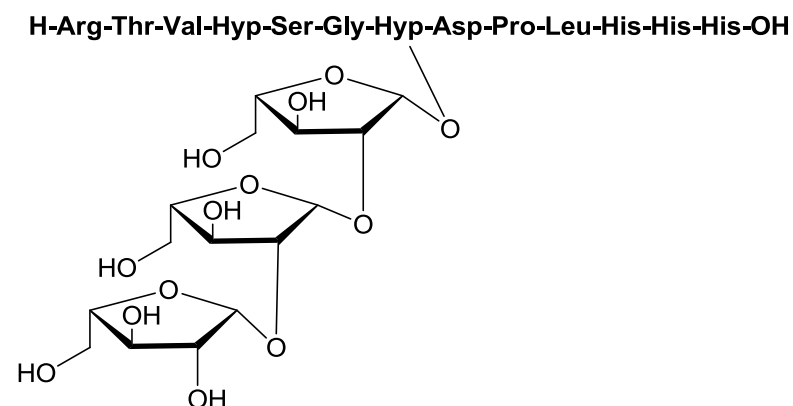


Figure 1.13 CLV3

1.9 Closing Comments

Small amounts of Art v 1 have been isolated from the pollen of *Artemisia vulgaris*. The isolation and chemical characterization of the allergenic epitope of Art v 1, however, is not practical through extraction and partial degradation of the natural protein. There is much difficulty in obtaining pure compounds due to the heterogeneous nature of the glycoprotein. Chemical degradation techniques typically lead to a complex mixture of amino acids. In order to clearly identify the carbohydrate motif that contributes to the epitopes of Art v 1, homogenous compounds of monomer, dimer, trimer, and tetramer must be obtained by way of chemical synthesis. This dissertation describes our efforts to synthesize homogenous oligomers of hydroxyproline β -arabinosides. The following chapters will present the synthetic methods, challenges, and triumphs we've endured upon our path to this goal.

CHAPTER 2: SYNTHESIS OF A MONOMER OF 4-O-[β -L-ARABINOFURANOSYL]-(2S,4R)-4-HYDROXYPROLINE

2.1 Importance of Arabinosides

Both enantiomers of arabinose exist in nature. β -Linked homopolymers of *D*-arabinose can be found in the cell wall of *Mycobacterium tuberculosis* and *Mycobacterium leprae* (Figure 2.1),³⁵ while the *L*-form is an important component of plant cell walls.³⁶ As described in Chapter 1, we are specifically interested in contiguous β -L-arabinofuranosides of hydroxyproline, a motif that is found in mugwort pollen. We believe this constitutes a significant allergenic epitope of the Art v 1 glycoprotein. The chemical synthesis of arabinosides, to further investigate their biological significance, has therefore become an important endeavor.

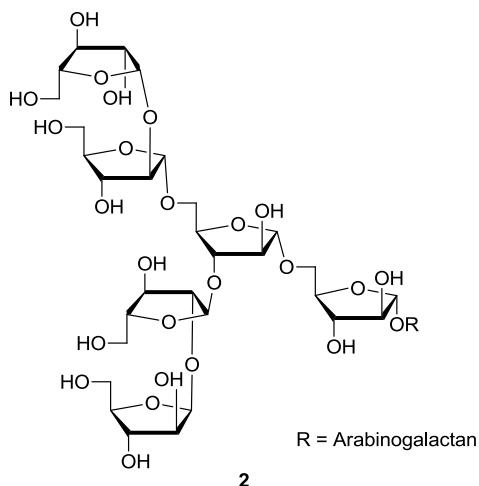


Figure 2.1 Arabinofuranosyl residues found in the cell wall of mycobacterium

2.2 Challenge of β -Arabinoside Synthesis

Methods for the stereoselective introduction of furanosides are not as well developed as for their pyranoside counterparts.³⁷ The key issue pertaining to the formation of glycosidic bonds is the α/β selectivity at the anomeric carbon. Two major factors that influence this

stereochemistry are highlighted in Figure 2.2 and will be discussed in more detail in the following sections.

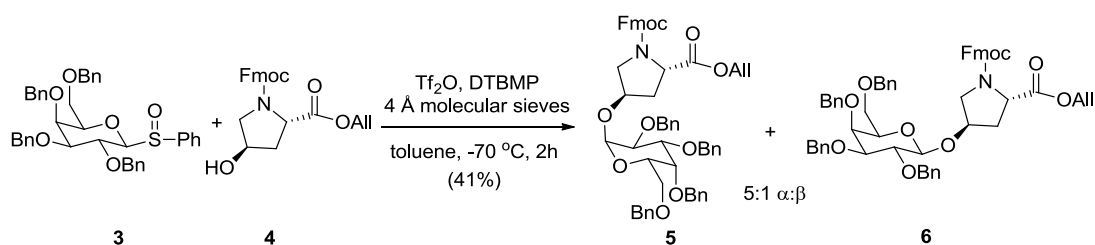


Figure 2.2 Factors that influence stereochemistry in glycosylation. a) The anomeric effect, although strong for pyranoses, offers little selectivity for its furanose counterpart. b) Neighboring group participation favors the 1,2-*trans*-glycoside.

2.2.1 The anomeric effect

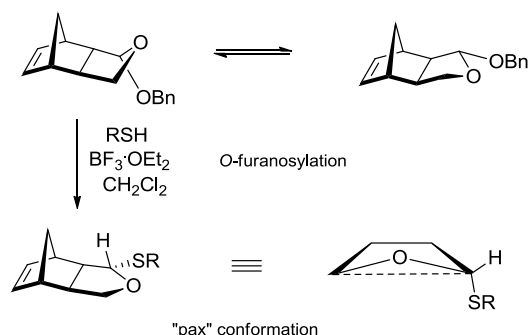
The anomeric effect is a stereoelectronic effect that describes the tendency of incoming substituents on the anomeric carbon of a pyranose ring to prefer the axial orientation. This effect is typically used by carbohydrate chemists to control the stereoselectivity of a glycosylation reaction.

The anomeric effect is well understood and controlled for pyranoses that have a strong conformational preference for a chair (Scheme 2.1),³⁸ but the effect is weak for furanoses and by itself is not sufficient to influence α/β selectivity.³⁹ Furanoses may have up to 20 low energy twist and envelope conformations, while able to adopt an infinite number of conformations differing slightly from those ideal conformations.⁴⁰ These numerous low energy conformations can lead to many different transition states during glycosylation that does not bias the anomeric selectivity. If the conformations were more rigid, it might be possible to have more stereocontrol.



Scheme 2.1 Stereoselectivity utilizing the anomeric effect

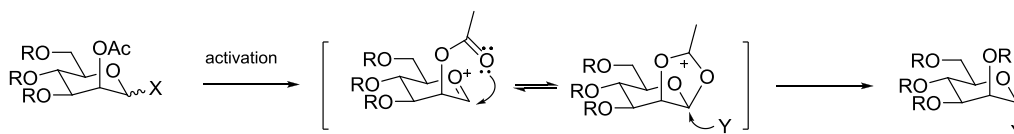
The Magnusson group published a paper in 1994 detailing the anomeric effect in conformationally restricted furanosides.³⁹ They chose a furanose that was fused, at C-3 and C-4, with a norbornane ring system (Scheme 2.2). The rigidity of the norbornane ring restricts the conformational flexibility of the furanose ring. With all the carbons in one plane, the only two conformations allowed would be those with the oxygen either above ($^{\circ}\text{E}$) or below (E_o) the plane of the ring. Upon O- and S-furanosylation of this fused ring system, they found that the anomeric substituent did indeed favor what they called the “pax” conformation, which is the pseudo-axial conformation. This work showed that with strict conformational control of the furanose ring, one can control the stereoselectivity of the furanosylation by invoking the anomeric effect.



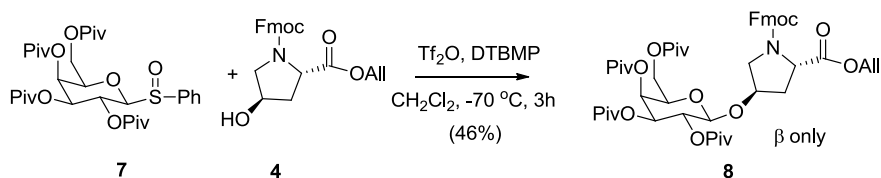
Scheme 2.2 Conformational restriction leading to increased anomeric effect in furanoside

2.2.2 Neighboring group participation

Neighboring group participation (Scheme 2.3), a phenomenon widely used to good advantage by carbohydrate chemists to control stereoselectivity at the anomeric carbon, heavily favors the formation of the 1,2-*trans* product. Scheme 2.4 shows the glycosylation of Fmoc-protected hydroxyproline allyl ester (**4**) with a sulfoxide donor **7** having a participating pivaloyl group at C-2 giving the only the *trans* product **8**.³⁸ Unfortunately for us, this would lead to the formation of the α -arabinoside.



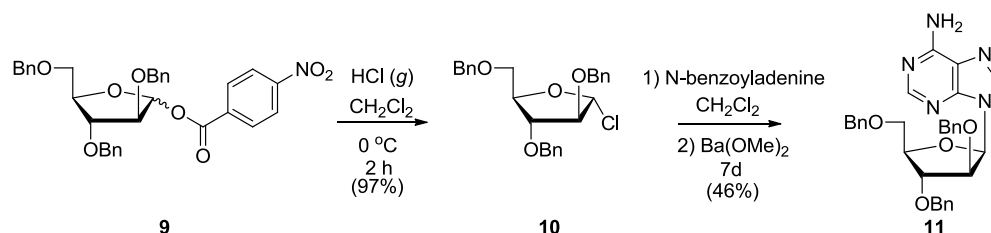
Scheme 2.3 Neighboring group participation



Scheme 2.4 Stereocontrol via neighboring group participation

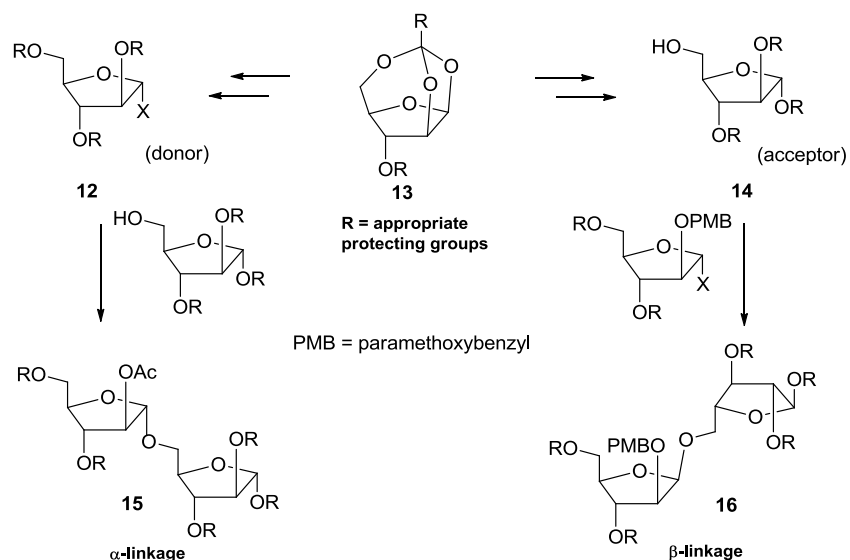
2.3 Previous Efforts to Produce β-Arabinosides

Amongst some of the earliest work in the effort to obtain 1,2-*cis*-arabinosides, Claudemans and coworkers employed glycosyl halides (e.g., **10**) which were masked at C-2 by a nonparticipating group, viz a benzyl ether, for the synthesis of 9-β-D-arabinofuranosyladenine (**11**) (Scheme 2.5).⁴¹ They later reported that, mechanistically, the glycosylation exhibited both S_N1- and S_N2-type properties and, regardless of the configuration of the C-1 halide, having a nonparticipating group at C-2 gave the more stable *trans* ion pair which would yield the *cis*-product.⁴² Furthermore, the rate of glycosylation was increased with each hydroxyl group having been protected as an “armed”⁴³ benzyl ether as opposed to a more electron withdrawing species.⁴⁴



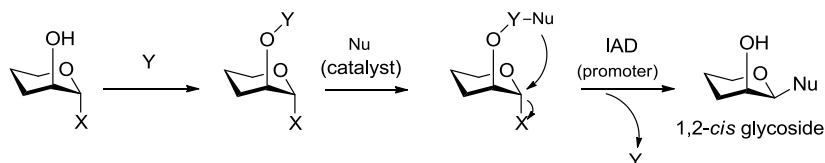
Scheme 2.5 Early efforts to obtain 1,2-*cis*-arabinosides

Prandi and coworkers published papers in 2000 showcasing 1,2,5-orthoester **13** in the synthesis of a penta-arabinofuranoside of the mycobacterial cell wall (Scheme 2.6).⁴⁵ The orthoester intermediate **13** can be converted to either a glycosidic donor **12** or acceptor **14**. The stereoselectivity of the subsequent glycosylation reaction is controlled by the protecting group at C-2. α -Arabinosidic linkages (*viz*, **15**) could be made with a participating C-2 acetate, while β -linkages (*viz*, **16**) are accessed through a *para*-methoxybenzyl (PMB) ether at C-2.



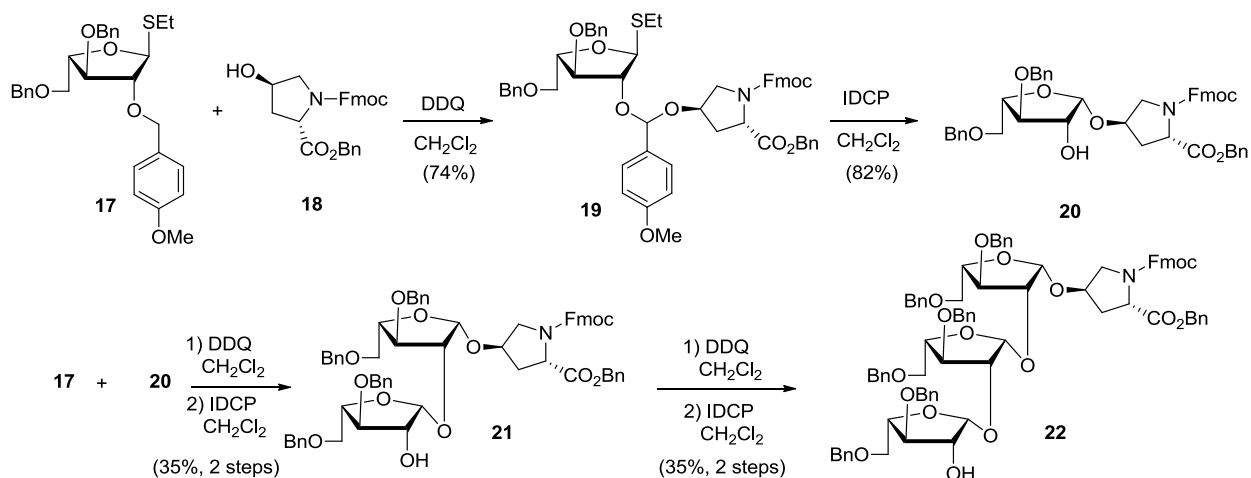
Scheme 2.6 Use of 1,2,5-orthoester as donor and acceptor

Intramolecular aglycon delivery (IAD) is a more recent approach to synthesize 1,2-*cis*-glycosides (Scheme 2.7). In this method, the glycosyl acceptor is first tethered to the protecting group at C-2. Activation of the anomeric leaving group, along with subsequent formation of the oxacarbenium ion, allows for the delivery of the tethered nucleophile from the same face to form the new glycosidic bond. Prandi's use of a PMB ether (Scheme 2.6) at C-2 to facilitate an intramolecular aglycon delivery to give only the β -linked polysaccharides is an example of this strategy.



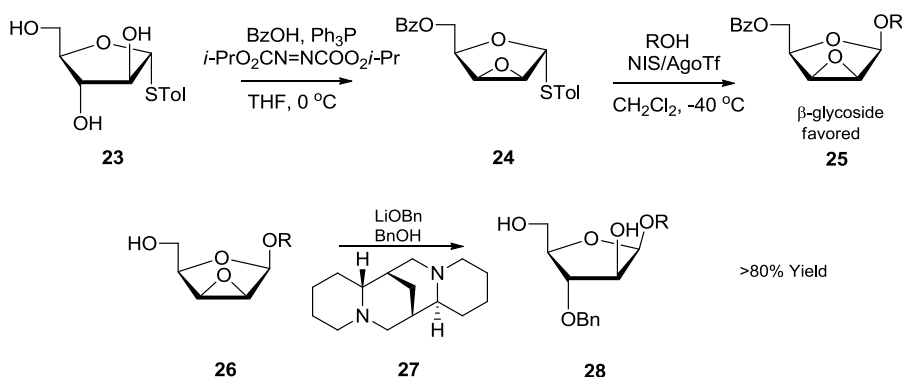
Scheme 2.7 Intramolecular aglycon delivery

More recently, Shinohara *et al.* reported on the synthesis of *Arabidopsis* CLV3 glycopeptide utilizing IAD for the installation of its β -arabinofuranosidic linkages.³⁴ The CLV3 peptide is a 13 amino acid glycopeptide containing a β -*L*-triarabinosylated hydroxyproline (Scheme 2.8, **22**). The three arabinose residues are linked to one another via β -1,2-linkages. *N* α -Fmoc hydroxyproline benzyl ester (**18**) and thioglycoside donor **17** were treated with DDQ to give the mixed acetal **19** in 74% yield. Activation of the anomeric thio leaving group gave the β -glycoside **20** in 82% yield. This process is repeated twice more to give the protected Hyp triarabinofuranoside **22**. Incorporation of the synthetic glycopeptide into the 13 amino acid chain was done by solid phase peptide synthesis. Comparison of the mono-, di-, and triarabinosylated CLV3 peptides showed that increased arabinosylation corresponded to increased biological activity.



Scheme 2.8 Synthesis of CLV3 glycopeptide utilizing IAD

Lowary's group showed that β -arabinofuranosides could be made with high stereoselectivity through a 2,3-anhydro sugar intermediate **24** (Scheme 2.9).⁴⁶ Transformation of a thioglycoside triol **23** into a 5-benzoyl-2,3-epoxide donor **24** was achieved in one step. Subsequent activation of the leaving group and addition of an alcohol nucleophile gave glycosides **25** with good β -selectivity. However, increasing the steric bulk of the alcohol nucleophile led to lower β -selectivity. Acceptors bearing electron withdrawing protecting groups also suffered a slight loss in selectivity. Nonetheless, upon treatment of the epoxide **26** with LiOBn in benzyl alcohol and sparteine (**27**), the β -arabinoside **28** could be obtained in desired regioselectivity and great yield.



Scheme 2.9 stereoselective β -arabinylation through a 2,3-anhydro sugar intermediate

Boons and co-workers devised a practical approach to the stereoselective synthesis of β -*L*-arabinofuranosides.⁴⁷ Bearing in mind that furanosides have many low energy conformations, the Boons group sought to lock the thioglycoside donor into a conformation that would favor nucleophilic attack from the β -face. Using density functional theory (DFT) quantum mechanical calculations, the optimized geometries of the arabinofuranosyl oxacarbenium ion were found to be the ^3E and E_3 conformations (Figure 2.3a). The E_3 conformation permits a staggered relative orientation of the substituents for the 1,2-*cis* attack and thus would favor the formation of a β -glycoside. In order to apply the principle of conformational restraint, they employed a 3,5-*O*-di-*tert*-butylsilane protecting group that gave a [6,5] bicyclic molecule (Figure

2.3b), in which the 6-membered ring would be a chair, locking the furanose ring in the desired E_3 conformation.

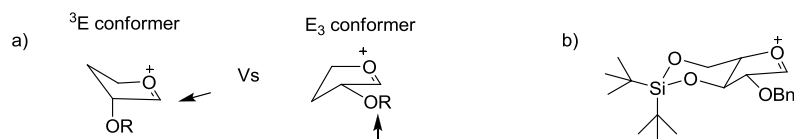
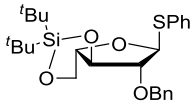
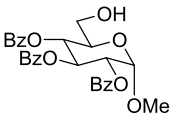
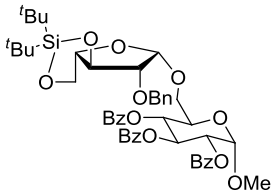
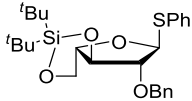
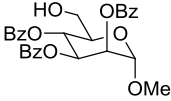
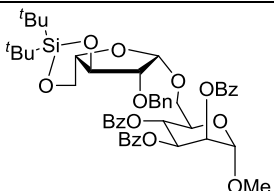
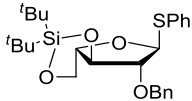
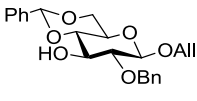
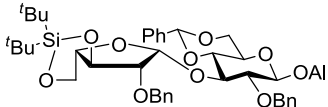
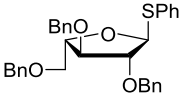
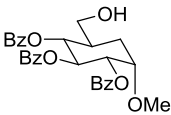
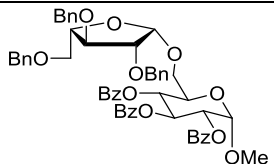
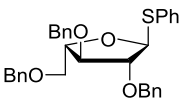
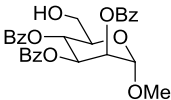
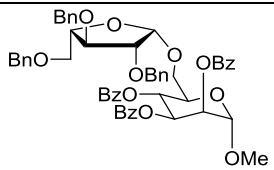


Figure 2.3 a) In the 3E conformation, the C-2 substituent is axial, resulting in steric interactions that favor alpha attack. The E_3 conformation allows the C-2 substituent to be in a pseudo-equatorial orientation, favoring a beta attack at the anomeric carbon. b) C-3 and C-5 alcohols protected as a silyl acetal.

With the thioglycoside donor **29** in-hand, Boons' group investigated several different glycosyl acceptors (Table 2.1, Entries 1-3). For most pyranose derivatives with a free primary alcohol at C-6 (Entries 1 and 2), activation of the donor with NIS/AgOTf provided excellent selectivity ranging from 15:1 β/α to 100% β , along with good chemical yields, ranging from 82% to 95%. In the one case where the overall yield was only 69%, β -selectivity was 100% (not shown). Pyranoses with a secondary C-3-OH acceptor (e.g., Entry 3) were also studied under the same activation conditions. Stereoselectivity in these reactions slipped to 8:1 β/α , while the yields were in the mid-80's.

Table 2.1 Selected examples of glycosylation with *L*-arabinosyl donors. Reagents and conditions: NIS/AgOTf, DCM, -30 °C

	DONOR	ACCEPTOR	β/α ratio / YIELD	GLYCOSIDE
1	 29	 30	$\beta/\alpha = 15/1$ 91%	 31
2	 29	 32	β only 94%	 33
3	 29	 34	$\beta/\alpha = 8/1$ 82%	 35
4	 36	 30	$\beta/\alpha = 3/1$ 88%	 37
5	 36	 32	$\beta/\alpha = 2/1$ 85%	 38

In order to prove that the conformationally restricted donor **29** was responsible for the excellent β -selectivity, the same primary alcohols mentioned above were reacted with a 2,3,5-tri-*O*-benzylated thioglycoside donor **36** (Entries 4 & 5). Although the chemical yield remained good, as expected, the β/α ratio dropped significantly (Entries 1 vs 4, 2 vs 5). This provides empirical proof of the effectiveness of conformational control in the synthesis of β -arabinofuranosides.

Crich and co-workers simultaneously developed a similar approach to assemble the β -D-arabinofuranothioglycosyl donor, but first investigated a 3,5-*O*-benzylidene protected donor (**39**, Figure 2.4) since the six membered ring had provided good conformational control in the case of pyranoses (e.g., glycosylations with **40**).⁴⁸ Unfortunately, in the case of furanosides, donor **39** was difficult to synthesize and found to not be as stable as the silylene protected donor. In addition to being less stable, the benzylidene-protected thioglycoside **39** gave rise to lower $\beta:\alpha$ selectivity and typically poor yields.⁴⁹

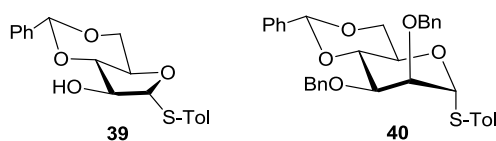
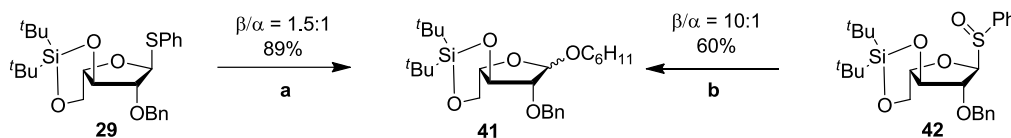


Figure 2.4 Benzylidene method adapted for β -D-arabinofuranoside formation

Since a more robust protecting group was needed, Crich and coworkers chose to move ahead with the 3,5-*O*-(di-*tert*-butyl-silane) arabinofuranoside donor **29** (Scheme 2.10). The list of acceptors they employed included methanol, cyclohexanol, and pyranoses with free primary or secondary alcohols. Based on their success with the synthesis of β -thiomannopyranosides,⁵⁰ they also decided to investigate the sulfoxide method⁵¹ for the formation of β -arabinofuranosides. It was interesting that activation of the thioglycoside donor **29** (Scheme 2.10) with NIS/AgOTf and reaction with cyclohexanol provided a β/α ratio of only 1.5:1 (**41**),

while activation of the corresponding sulfoxide donor **42** with Tf_2O and reaction with cyclohexanol provided a β/α ratio of 10:1.



Scheme 2.10 Sulfide and sulfoxide donors. a) cyclohexanol, NIS/AgOTf, CH_2Cl_2 $-30^\circ\text{C} \rightarrow \text{RT}$, b) Tf_2O -78°C , 30 min, then cyclohexanol

Other activators were also employed, but in the end the NIS/AgOTf combination employed by Boons and co-workers still gave the best β/α ratio when it came to using the *L*-arabinofuranosylthioglycoside as donor. Other methods of activation that did not prove useful were believed to be less successful because the activators did not completely convert the donors into glycosyl triflates, a hypothesis that was supported by low-temperature NMR experiments.⁴⁹ A point to bear in mind is that only *L*-arabinosides were activated with NIS/AgOTf. The *D*-thioarabinosides in this study were activated in other ways.

Crich concurred with Boons' hypothesis that the intermediate in the glycosylation is most likely the oxacarbenium ion in the E_3 conformation. Since the publication of these two key papers, Lowary and co-workers have reported a crystal structure of a 3,5-*O*-(di-*tert*-butyl-silane) arabinofuranoside derivative in which the furanose ring is in an E_4 conformation (Figure 2.5).⁵²

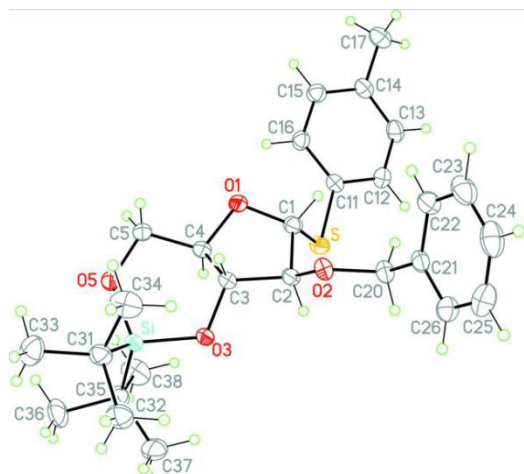
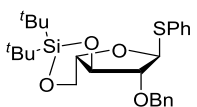
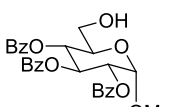
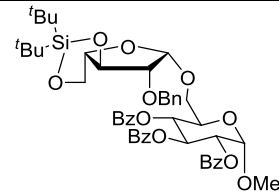
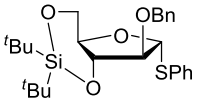
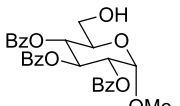
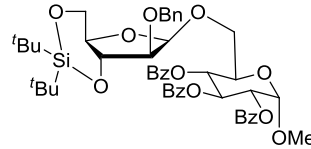


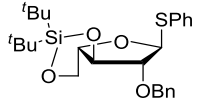
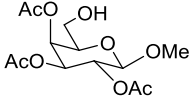
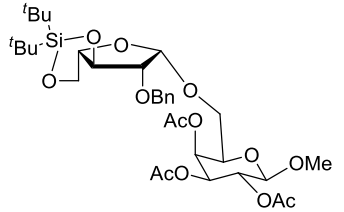
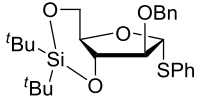
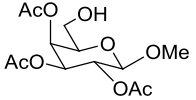
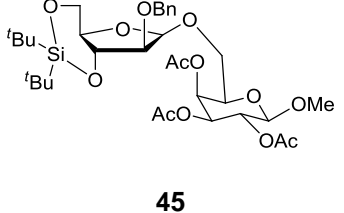
Figure 2.5 Crystal structure of 3,5-*O*-(di-*tert*-butyl-silane) arabinofuranoside derivative. Reprint with permission from IUCr.

Zhu, the first author on the 2007 paper from the Boons group, is now at University College, Dublin. The Zhu Group's goal, in a more recent paper, was to directly compare the NIS/AgOTf activation for glycosylation with *L*- and *D*-arabinofuranosyl donors (Table 2.2), something that neither the Boons nor Crich groups had done.⁵³ 3,5-*O*-(Di-*tert*-butyl-silane)-*D*-arabinothiofuranoside (**ent-29**) was used as the donor while several sugars with free primary and secondary alcohols were used as acceptors. Some of these acceptors were a lot like the ones that were used by Crich. Glycosylation of the primary alcohols proceeded in good yields (78% to 90%), with β/α ratios in the range of 2:1 to as high as 6:1. Glycosylation of secondary alcohols gave comparable β/α ratios, but the yield dropped slightly (not shown). Zhu concluded that, given the state-of-the-art for the synthesis of β -D-arabinosides, this can still be regarded as an efficient glycosylating agent.

Table 2.2 Selected comparisons of *L*- vs *D*-arabinofuranosyl donors.¹⁷

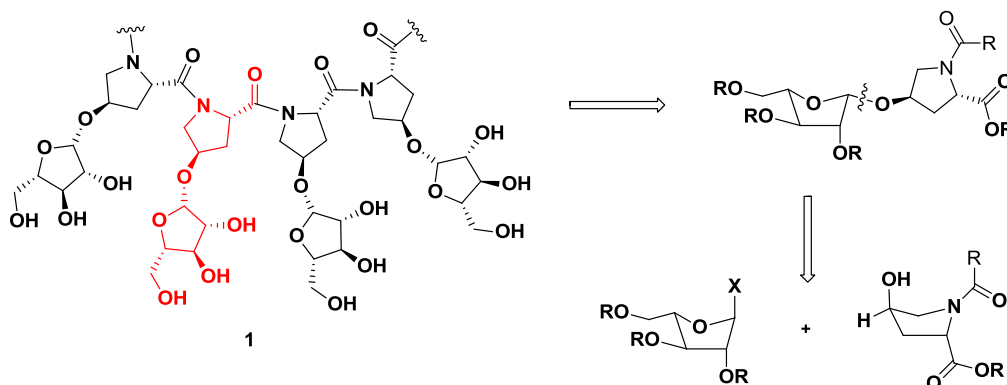
DONOR	ACCEPTOR	$\beta:\alpha$ ratio / YIELD	GLYCOSIDE
 29	 30	$\beta:\alpha = 15:1$ 91%	 31
 ent-29	 30	$\beta:\alpha = 8:1$ 83%	 43

(Table 2.2 continued)

DONOR	ACCEPTOR	$\beta:\alpha$ ratio / YIELD	GLYCOSIDE
 <p>29</p>	 <p>44</p>	<p>β only</p> <p>95%</p>	 <p>45</p>
 <p>ent-29</p>	 <p>44</p>	<p>$\beta:\alpha = 5:1$</p> <p>90%</p>	 <p>45</p>

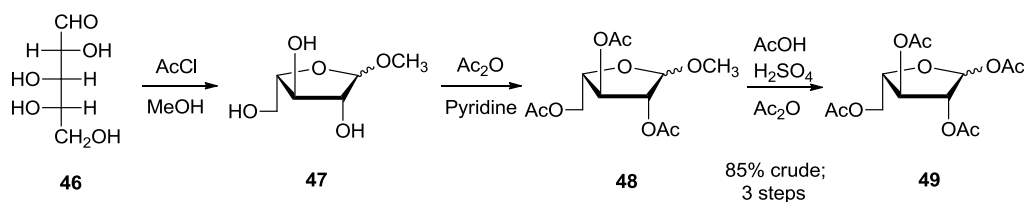
2.4 Current Investigation

Scheme 2.11 shows a tetramer of hydroxyproline- β -arabinoside (**1**). Retrosynthetic analysis shows that we must first prepare the monomer, which in turn requires us to prepare a donor and acceptor for glycosylation. In light of published results described above, we chose to adopt the Crich/Boons approach of using a conformationally restricted donor for the synthesis of our β -glycosides.



Scheme 2.11 Retrosynthetic analysis of tetramer

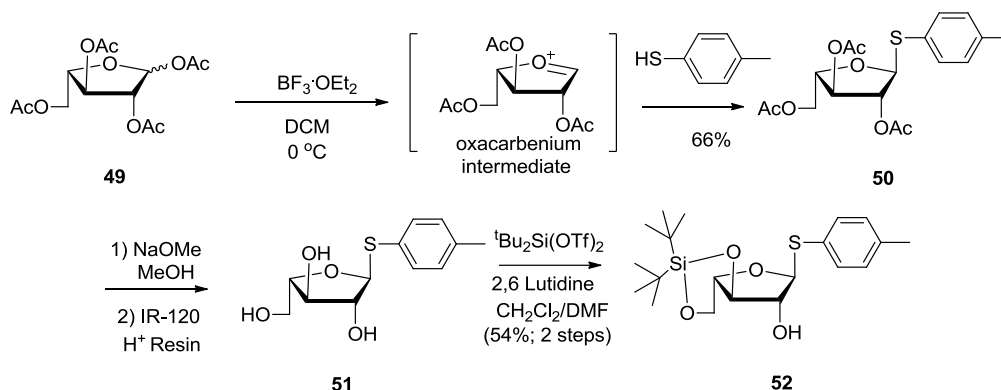
The synthesis of the donor begins with a variation on the Guthrie-Smith method⁵⁴ for the synthesis of peracylated arabinofuranose (Scheme 2.12).⁵⁵ This “general” method was also adopted by Crich. Commercially available *L*-arabinose (**46**) is present in solution as an equilibrium mixture of the linear and cyclic (both furanose and pyranose) forms. Low concentrations of HCl are generated *in situ* with acetyl chloride and methanol; these reaction conditions lock the arabinose into the methyl furanoside form. In order to obtain this kinetic product, the reaction must be stopped at three hours to prevent equilibration to the unwanted methyl pyranosides. The triol **47** was esterified with acetic anhydride in pyridine to give the 2,3,5-O-acylated methyl furanoside **48**. Treatment of the methyl glycoside in acetic acid, followed by sulfuric acid, gave the anomeric acetate **49**. Work up with several washes of NaHCO₃ is crucial as the excess acetic acid side product is extremely hard to remove. We believe compound **49** to be mostly α -furanoside due to neighboring group participation of the C-2 acetate. Unfortunately, due to the many low energy conformations of this compound,³⁷ the NMR spectra were complex and thus an α : β ratio was not determined.



Scheme 2.12 Peracylated arabinofuranoside synthesis

With compound **49** in hand, the next step was to form the thioglycoside donor (Scheme 2.13). Upon coordination of boron trifluoride to the oxygen of the anomeric acetate, an oxacarbenium ion is formed that undergoes nucleophilic attack by thiocresol to give thioglycoside **50**. The apparent singlet assigned to the anomeric proton confirms the formation of the α -anomer, the major product. The β -anomer (not shown in scheme) is hardly visible in NMR spectra, suggesting <10%. Temperature control during this glycosylation is crucial to limit the formation of unwanted side products. It is also important that BF₃·OEt₂ is added slowly to

the reaction mixture over a span of 10 to 15 minutes. The median yield for this reaction, under these optimal conditions, is 66% and reproducible on multigram scale.

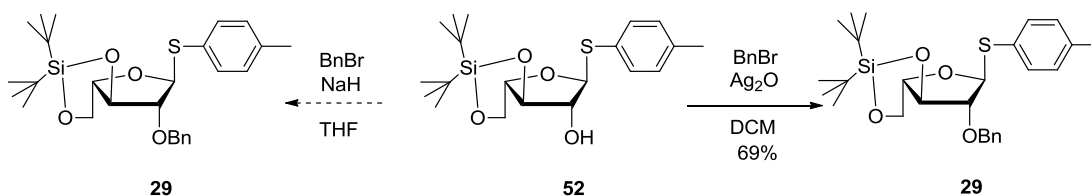


Scheme 2.13 Preparation of bicyclic silyl acetal donor

Methanolysis of the acetate esters, followed by work-up with an acidic resin, afforded compound **51**. The triol was dissolved in a 5:1 ratio of $\text{CH}_2\text{Cl}_2/\text{DMF}$ with 2,6-lutidine as base/buffer. The dimethylformamide is essential to fully dissolve the very polar triol. After cooling to 0°C , di-*tert*-butylsilyl-*bis*-triflate was added slowly and the reaction was allowed to warm up to room temperature overnight. While the 54% yield of silyl acetal **52** is modest, the purity of the compound obtained is evidenced by the NMR spectra.

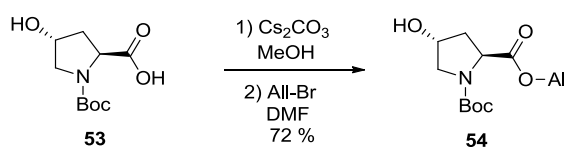
We originally attempted benzylation of the C-2 alcohol in compound **52** with sodium hydride and benzyl bromide according to Crich/Boons (Scheme 2.14),^{47, 49} but this combination of reagents gave us product mixtures in which most components were more polar than the starting material. Upon isolation of these side products, it was apparent that the *tert*-butyl silyl group was being cleaved from one of the oxygens, presumably due to adventitious sodium hydroxide. Around this time, a new paper was published by the Zhu group.⁵³ Interestingly, a change was noted in the procedure for the benzylation reaction. Silver(I) oxide in dichloromethane is now used as the reagent/solvent in place of NaH in THF. When we contacted Zhu about the new procedure, he also cited problems with the cleavage of the silyl

acetal as the reason for the change. In this improved strategy, the silver polarizes the C-Br bond of the benzyl bromide, facilitating nucleophilic attack by the secondary alcohol of the arabinoside without subjecting the silyl protecting group to harsh, basic conditions. Compound **29** was the first glycosyl donor prepared in our lab for hydroxyproline arabinosylation.



Scheme 2.14 Benzylation of C-2 alcohol

Synthesis of the glycosyl acceptor was accomplished in one step from commercially available Boc-*L-trans*-4-hydroxyproline (**53**). The carboxylic acid functionality was converted to the corresponding cesium salt, which reacts with allyl bromide to give the allyl ester **54** (Scheme 2.15). We chose these protecting groups based on how we would like to deprotect them downstream. The Boc carbamate would be easily removed by trifluoroacetic acid and is orthogonal to the allyl ester, which could be removed in a mild manner by palladium (0).⁵⁶



Scheme 2.15 Preparation of hydroxyproline acceptor

While synthesis of the hydroxyproline acceptor is straightforward, we anticipated that it would likely give us problems in glycosylation due to its poor nucleophilicity. Aside from the secondary alcohol being hindered, the pyrrolidine ring is in a C γ -exo conformation due to gauche interactions between the substituents (Figure 2.6).⁵⁷ This places the hydroxyl functionality in a pseudo-axial orientation, favored by a hyperconjugative interaction between the axial hydrogens at C β and C δ and the alcohol at C γ .⁵⁸ These effects contribute to the overall poor nucleophilicity of the alcohol.

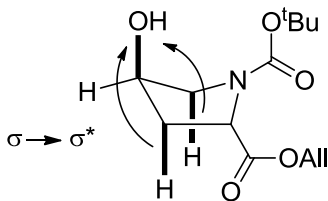
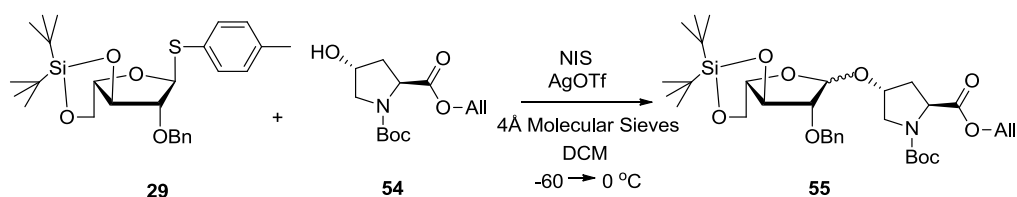


Figure 2.6 Hyperconjugation via $\sigma \rightarrow \sigma^*$ interaction

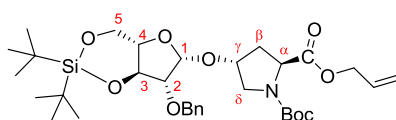
2.4.1 Glycosylation with the conformationally-restricted glycosyl donor

In our first attempt at the glycosylation of hydroxyproline we followed the procedure published by Crich, wherein the glycosyl donor was *ent*-**29** (derived from *D*-Ara) and the glycosyl acceptor was cyclohexanol (Scheme 2.16). *N*-Iodosuccinimide was used as the activator to form the oxacarbenium ion, followed by the addition of silver triflate to form the anomeric triflate. The six-membered silyl acetal ring should serve to lock the furanose into the conformation that favors β -attack. The reaction is messy, however, with a plethora of side products. Monitoring of the reaction and separation of compounds is also hampered by the fact that product **55** is not very UV active. Due to low concentrations of analyte in the test tubes after flash chromatography, anisaldehyde staining, which is generally used to detect sugar molecules, is not sufficiently sensitive. Portions of α - and β -anomers collected, even after flash chromatography, are still rather crude. We have isolated pure β -glycoside in milligram quantities by normal phase HPLC that has enabled ^1H , ^{13}C , COSY, HSQC, and HMBC NMR spectra to be acquired. While we do believe that there is a slight preference for the formation of the β -glycoside, the poor overall yield (~12% after HPLC) and stereoselectivity ultimately led us to investigate other glycosidic donors. We were, however, able to fully assign all protons and carbons in the NMR spectra (Table 2.3).



Scheme 2.16 Glycosylation of hydroxyproline with silyl acetal donor

NMR resonance assignments are based on the information obtained from one-pulse ^{13}C and ^1H experiments as well as COSY, double-quantum filtered COSY, 135° DEPT, TOCSY, and HSQC. These assignments are summarized in Table 2.3.



(a) The Proline Domain

Due to the rotational isomerization of the molecule, a 2:1 ratio of rotamers can be seen in the ^{13}C and ^1H NMR spectra. The ^{13}C resonances at 118.7 (118.3) ppm correlate to a single carbon, which is secondary according to the 135° DEPT spectrum. Correlation between this carbon and resonance 5.21-5.35 ppm leads to assignment of these signals to the terminal $=\text{CH}_2$ of the allyl ester. The COSY spectrum shows correlation of the signals arising from these olefinic CH_2 to a multiplet at 5.85-5.96 ppm, which was therefore assigned as the C-H of the monosubstituted alkene. This proton is further coupled to two protons of signals 4.55-4.69 ppm in the COSY ^1H spectrum, which is the allylic CH_2 , as supported also by the ^{13}C 135° DEPT spectrum. The TOCSY spectrum shows correlation between all five protons.

Multiplets at 2.08-2.15 ppm and 2.35-2.49 ppm can be attributed to a pair of diastereotopic protons with rotational isomerization peaks identifiable by the HSQC spectrum. The chemical shifts would suggest that they are the beta protons of the proline. As expected,

the beta proton signals showed correlation with two other proton signals at 4.40 ppm and 4.29 ppm in the ^1H - ^1H COSY spectrum, that were assigned to $\text{H}\alpha$ (showed no other cross peak) and $\text{H}\gamma$ respectively. The $\text{H}\gamma$ showed further correlation with a pair of diastereotopic protons (3.58-3.69 ppm) (who are also correlated with each other) assigned to $\text{H}\delta$. The HSQC spectrum confirms that they are connected to a single carbon. TOCSY spectrum shows correlation between all six protons of the pyrrolidine ring spin system.

The ^{13}C resonances at 172.7 (172.4) ppm can be assigned to the ester carbonyl functionality of the Boc group. The quaternary carbon of the *tert*-butyl group can be assigned to the ^{13}C resonances at 80.2 (80.1) ppm, and 135° DEPT spectra shows those resonances to be missing. The primary carbons of the *tert*-butyl group can be assigned to the ^{13}C resonances at 28.2 (28.4) ppm, and the HSQC spectra confirms that there are 3 protons connected to each at 1.38 (1.45) ppm on the ^1H spectrum.

(b) The Arabinose Domain

The anomeric proton signal can be confidently assigned to the resonance at 4.97 (4.93) ppm. The coupling constant here is 5.3 Hz, and is in the expected range for β -anomers of arabinosides (c.f., $^3J_{12} = 1\text{-}3$ Hz for α -arabinosides).¹⁰ There are two doublets for H1, as a consequence of the rotational isomerization of the molecule. The anomeric signal is in correlation with one other proton at 3.90 ppm (COSY), which we assign as H2. The TOCSY spectrum shows correlation between the anomeric proton, H2, and four other signals. Two of these signals, 4.30 ppm and 3.88 ppm, show correlations to the same carbon in the ^{13}C - ^1H HSQC spectrum; they are diastereotopic H5 protons of the arabinose ring. The remaining two signals, 3.59 ppm and 4.28 ppm, are assigned to H4 and H3 respectively.

The aromatic protons can easily be assigned to the multiplet at 7.29-7.40 ppm. HSQC data shows five distinct carbon peaks ranging from 127.7-128.3 ppm, along with a quaternary

carbon at 137.7 ppm, that directly correlate to the aromatic carbons of the benzyl group. One of the two benzyl CH₂ signals can be seen clearly in the ¹H NMR spectra with a coupling constant of 12.2 Hz. TOCSY shows correlation between all aromatic protons and even long range cross peaks with the benzyl CH₂.

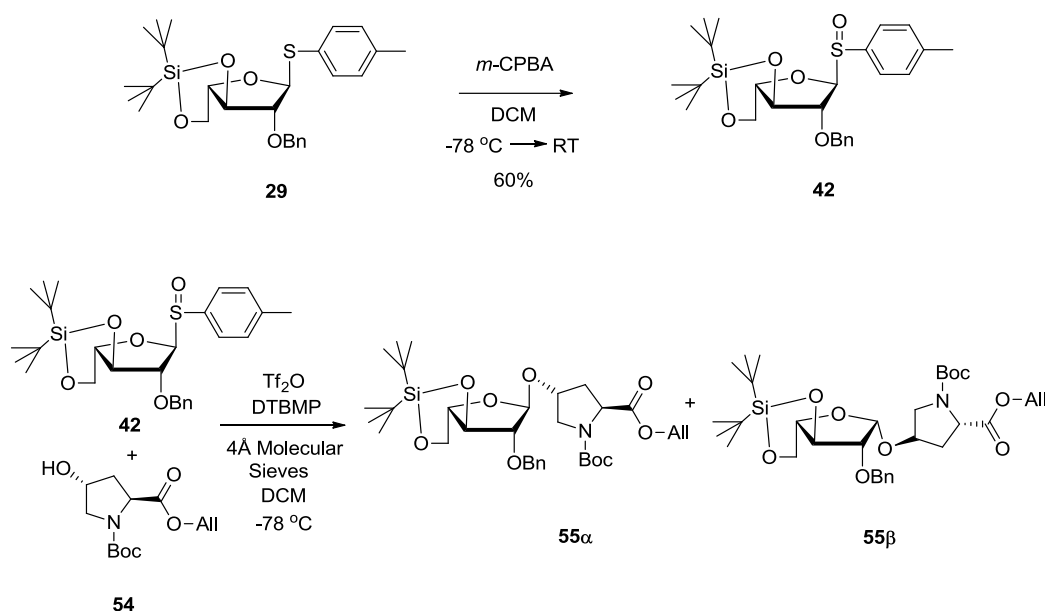
The two singlets at 0.99 ppm and 1.07 ppm, with a total of 18 Hs, can be assigned to the protons of the two *tert*-butyl groups of the silyl acetal. The resonances 27.1 ppm and 27.5 ppm in the ¹³C spectra can be assigned to the primary carbons of the *tert*-butyl group, while the quaternary carbons are at 20.1 ppm and 22.6 ppm.

Table 2.3 Chemical Shifts for β-Glycoside **55β**.

<u>L -Ara</u>	¹ H ppm	¹³ C ppm
H1	4.97 (4.93)	99.2 (100.0)
H2	3.90	80.7
H3	4.31	78.4
H4	3.59	73.6 (73.4)
H5	3.88, 4.31	68.4
CH ₂ Ph	4.69-4.80	71.8 (71.9)
Si ^t Bu ₂	0.99, 1.07	20.1 (4°), 22.6 (4°), 27.1 (1°), 27.5 (1°)
CH ₂ Ph	7.29-7.40	127.7, 127.8, 127.9, 128.0, 128.4, 137.7 (4°)
<u>Hyp</u>		
Hα	4.36-4.44	58.1 (57.7)
Hβ	2.08-2.15, 2.35-2.42 (2.43-2.49)	37.6 (36.8)
Hγ	4.30	75.2
Hδ	3.64	51.1 (51.6)
Boc (<i>tert</i> -butyl)	1.38 (1.45)	80.2 (80.1) (4°) 28.2 (28.4) (1°)
COOR	-	153.7 (154.2), 172.7 (172.4)
CH ₂ CH=CH ₂	4.55-4.69	65.5 (65.6)
CH ₂ CH=CH ₂	5.85-5.96	131.7 (131.9)
CH ₂ CH=CH ₂	5.21-5.35	118.7 (118.3)

*Values in parentheses relate to the minor rotamer about C(=O)N bond of the carbamate.

Crich's glycosylation of cyclohexanol with a sulfoxide donor (Scheme 2.10, **42**) gave an average yield but great diastereoselectivity. With the Taylor Group's past experience with sulfoxide donors,³⁸ this was the next logical approach. Developed by Kahne and coworkers in 1989,⁵⁹ the sulfoxide method has proven useful in the glycosylation of sterically hindered nucleophiles. The sulfoxide donor **42** was made by oxidation of the sulfide donor **29** with *m*-CPBA, after which we were able to separate the pair of diastereomers (Scheme 2.17). Unfortunately, the same problems that plagued the sulfide glycosylation still existed, and we were not able to acquire better yields or selectivity under these conditions.



Scheme 2.17 Glycosylation of hydroxyproline with sulfoxide donor

We also briefly investigated a method that would give absolute β -selectivity in glycosylation. Intramolecular aglycon delivery (IAD) allows for the tethering of the nucleophile to the O-2 substituent in a process that would only allow for the formation of a 1,2-*cis*-glycoside. As described in Section 2.3, Prandi published a paper in 2000 that utilizes this method for the construction of β -arabinofuranosides that used a *para*-methoxybenzyl ether as the tethering agent (Scheme 2.18, *vide supra*).^{45a} Efforts to synthesize **56** with *para*-methoxybenzyl bromide

The reaction scheme illustrates the synthesis of 1,2:5,6-di-O-isopropylidene-3-O-(4-methoxyphenyl)-D-glucopyranan (56) and its conversion to 1,2:5,6-di-O-isopropylidene-3-O-(4-methoxyphenyl)-D-glucopyranan (57).

Synthesis of 56: 1,2:5,6-di-O-isopropylidene-3-O-(4-methoxyphenyl)-D-glucopyranan (56) is synthesized from 1,2:5,6-di-O-isopropylidene-3-O-(4-methoxyphenyl)-D-glucopyranan (52) using PMBBBr, NaH, and THF. The reaction is indicated by a crossed-out arrow, suggesting it is not the preferred method.

Conversion of 56 to 57: 56 is converted to 57 using DDQ.

Synthesis of 57: 1,2:5,6-di-O-isopropylidene-3-O-(4-methoxyphenyl)-D-glucopyranan (57) is synthesized from 1,2:5,6-di-O-isopropylidene-3-O-(4-methoxyphenyl)-D-glucopyranan (52) using NAPBr, Ag₂O, and DCM, yielding 40%.

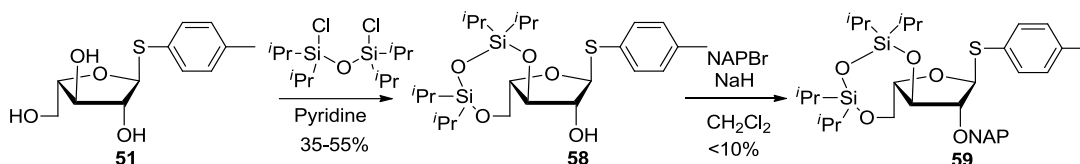
Conversion of 57 to 56: 57 is converted to 56 using ROH/DDQ.

Definitions:

- PMB = 4-methoxybenzyl group (4-MeO-C₆H₄-CH₂-)
- MP = 4-methoxyphenyl group (4-MeO-C₆H₄-)
- NAP = 1-naphthyl group (1-Naph-)
- Naph = 2-naphthyl group (2-Naph-)
- R = 1-(4-methoxyphenyl)-2-(4-methoxyphenyl)-2-methyl-1,3-dioxane-5-carboxylate group (4-MeO-C₆H₄-CH₂-C(CH₃)₂-CH₂-C(=O)-O-4-MeO-C₆H₄-)

Ito and coworkers have shown that a 3,5-O-tetra-*i*-propyldisiloxanylidene protection was optimal in giving β -selectivity when applied to arabinofuranosides.⁶¹ This method, much like the silyl acetal employed by Boons and Crich, used the conformational restriction of the eight membered disiloxane ring to promote the synthesis of the β -anomer. We decided to try this method in the hope that the eight membered disiloxane ring would be more robust under both basic and glycosylating conditions. Treatment of thioglycoside triol **51** in amine base and 1,3-dichloro-1,1,3,3-tetraisopropyldisiloxane gave the bicyclic donor **58** in modest yield (Scheme 2.19). Much to our dismay, the eight membered disiloxane ring was no more stable than the

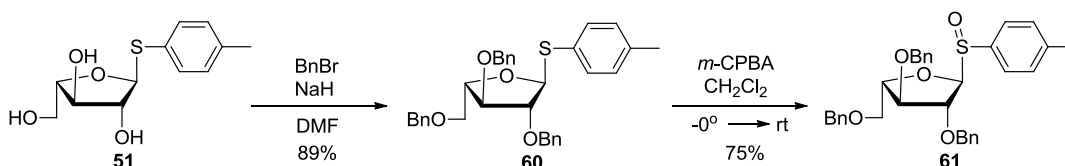
six-membered silyl acetal ring. Subsequent exposure to sodium hydride again showed the cleavage of the 3,5-*O*-protecting group and compound **59** was obtained in unsatisfactory yield.



Scheme 2.19 Preparation of disiloxane donor

2.4.2 Conformationally unrestrained donor

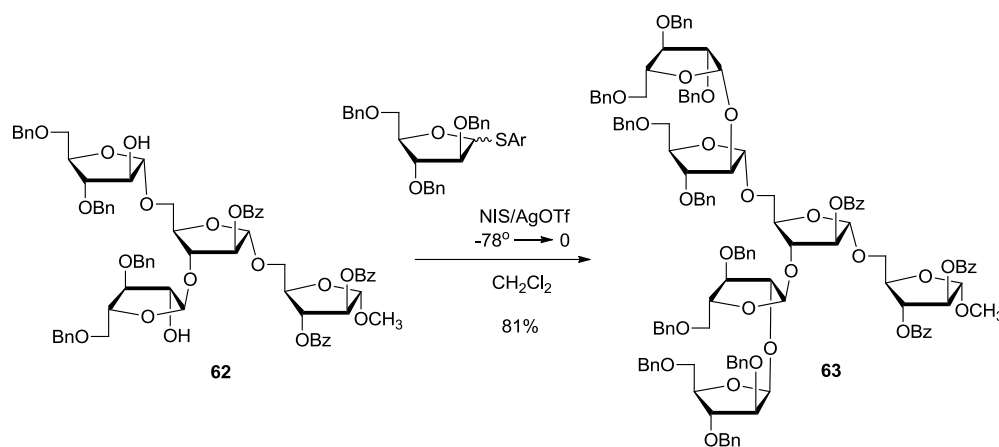
We decided to test a fully benzylated thioglycoside donor (compound **60**, Scheme 2.20) to confirm our suspicion that the labile silyl protecting groups were the cause of our low yields. Compound **51** was transformed into the tri-*O*-benzyl arabinofuranothioglycoside **60** using standard methods (benzyl bromide, NaH, DMF) in great yield. The success of this benzylation reaction reinforced our hypothesis about the shortcomings of the 3,5-*O*-silyl protecting groups. Just to be thorough, we also made the corresponding sulfoxide **61** in good yield.



Scheme 2.20 Preparation of two conformationally unrestrained donors

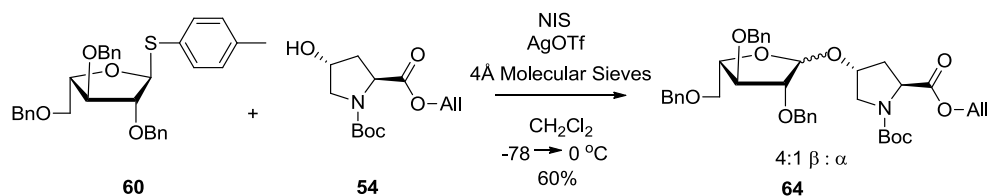
Lowary and coworkers, in their synthesis of a naturally-occurring, highly branched arabinofuranosyl hexasaccharide, had reported a surprising highly stereoselective synthesis of β -arabinofuranosides.⁶² Using *N*-iodosuccinimide and silver triflate as activator, the hexasaccharide **63** was obtained in high yield and with 100% β -selectivity (Scheme 2.21). The authors reported that careful control of temperature is critical as an increase in side products

was observed when the reaction was run at -40 or 0 °C. We employed this procedure in the hope of finding similar success for our purpose.



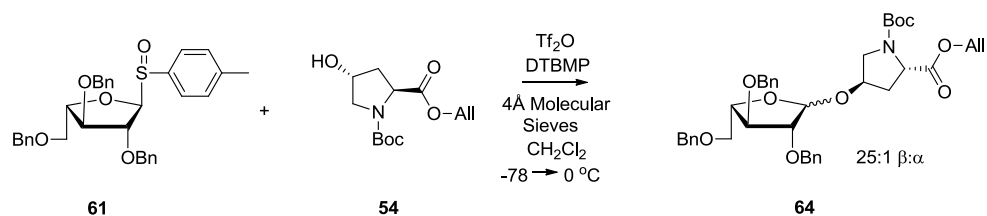
Scheme 2.21 Low temperature glycosylation method

To our delight, reaction of thioglycoside **60** with our hydroxyproline acceptor gave a reasonable yield (60%) with an average β : α ratio of 4:1 (Scheme 2.22), a significant improvement relative to Scheme 2.16 in both aspects. Also important is the fact that we are able to separate the α - and β -anomers by means of flash chromatography, an added bonus that would save us much time and grief as compared to HPLC. Careful upscaling of this reaction has allowed us to do the glycosylation on a multigram level, and we are able to obtain spectroscopically pure β -glycoside up to a gram at a time. Further advantages of this route include saving one linear step in the overall synthesis while also substituting for two reactions that gave typical yields of ~35% (silyl acetal protection, benzyl ether protection) with a single protection step that yields up to 90% (benzylation). The tri-O-benzylated arabinofuranosides are robust and can withstand a variety of acidic and basic conditions. Down the line, the perbenzylated arabinosides can be deprotected by a single hydrogenolytic step to remove all benzyl ethers.



Scheme 2.22 Glycosylation of hydroxyproline with benzylated sulfide donor

We also applied the sulfoxide method to making our β -arabinosides of hydroxyproline (Scheme 2.23). The sulfoxide donor **61** is activated by triflic anhydride and a sterically hindered amine base acts as a buffer for the reaction. The sulfoxide glycosylation gave similar yields but offered far superior selectivity (25:1 β : α by integration of anomeric proton) than its sulfide counterpart. However, the reaction was plagued by side products that are indistinguishable chromatographically from our wanted compounds. Moreover, the stability of the triflic anhydride, even when left unopened, is a deterrent for this reaction compared to the relatively stable NIS/AgOTf. This practical application, in combination with the extra step required to form the sulfoxide, led us to favor the sulfide donor **60** for the large scale preparation of the β -monomer. β -Glycoside **64 β** has been fully characterized by mass spectrometry, ^1H , ^{13}C , and 2-D NMR spectra.

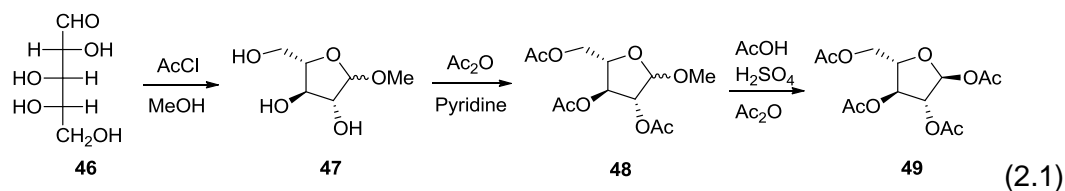


Scheme 2.23 Glycosylation of hydroxyproline with benzylated sulfoxide donor

2.5 Experimental Section

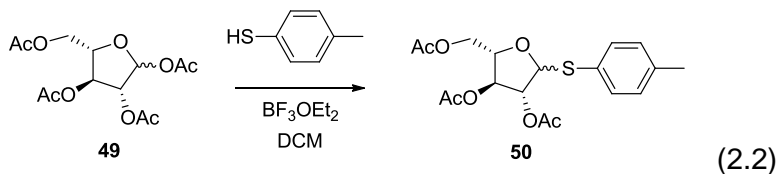
General methods: All reactions were performed under a dry nitrogen atmosphere unless otherwise noted. Reagents were obtained from commercial sources and used directly; exceptions are noted. Diisopropylethylamine, triethylamine, and pyridine were dried and distilled from CaH_2 and stored over KOH pellets. Ethanol and methanol were distilled from Mg turnings and stored over 3 Å molecular sieves. Flash chromatography was performed using flash silica gel (32-63 μ) from Dynamic Adsorbents Inc. Reactions were followed by TLC on precoated silica plates (200 μm , F-254 from Dynamic Adsorbents Inc.). The compounds were visualized by UV fluorescence or by staining with ninhydrin, KMnO_4 , or 10% sulfuric acid in ethanol stains. NMR spectra were recorded on Bruker DPX-250, AV-400-liquid, or Varian 700 MHz spectrometers. Proton NMR data is reported in ppm downfield from TMS as an internal standard. Disodium 3-trimethylsilyl-1-propane-sulfonate (DSS) was used to reference ^1H NMR spectra run in D_2O . High resolution mass spectra were recorded using either time-of-flight or electrospray ionization.

2.5.1 Experimental procedures



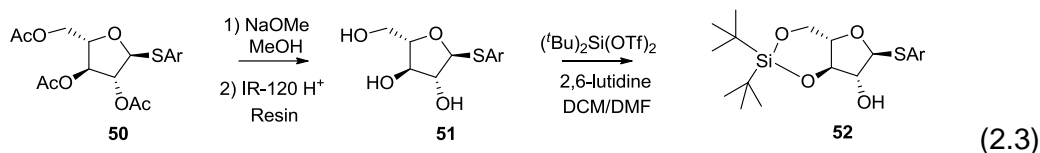
Peracetylated- α -L-Arabinoside (49). L-Arabinose (5.0 g, 33.3 mmol, 1 equiv.) was dissolved in methanol (100 mL) and treated with a solution of acetyl chloride (2.5 mL) in methanol (30 mL) at rt under N_2 . The mixture was stirred for 3 h, during which time the solid completely dissolved. The reaction was quenched dropwise with pyridine. The solvent was evaporated, followed by azeotropeing with DCM to give the methyl arabinoside as a mixture of anomers. The crude product was dissolved in pyridine (40 mL) and cooled to 0 °C, after which acetic anhydride (20

mL) was added and the reaction was stirred overnight at rt. The solvent was evaporated and the mixture was diluted with CH₂Cl₂ (250 mL), washed with water (250 mL), 1 M HCl (250 mL), sat. NaHCO₃ (250 mL), and brine (250 mL). The organic phase was filtered through MgSO₄ and concentrated to give the triacetate. The crude product was dissolved in acetic anhydride (80 mL) and cooled to 0 °C. Acetic acid (20 mL) was added dropwise. After 15 min, sulfuric acid (5 mL) was added dropwise. The mixture was warmed to rt while stirring for approximately 2 h. The solution was poured over a mixture of ice (50 g), CH₂Cl₂ (250 mL) and sat'd aq. NaHCO₃ (200 mL). The organic layer was separated and washed again with several volumes of sat'd aq. NaHCO₃, filtered through MgSO₄, and concentrated to give the crude peracylated furanoside as a light oil (9.071 g, 85%; 3 steps).

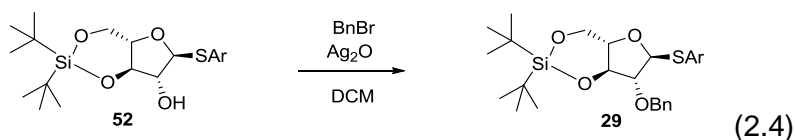


p-Cresyl 2,3,5-O-acetyl-1-thio- α -L-arabinofuranoside (**50**). A solution of **49** (4.47 g, 14 mmol, 1.0 equiv.) and *p*-thiocresol (2.64 g, 21 mmol, 1.5 equiv.) in dry CH₂Cl₂ (60 mL) was cooled to 0 °C under N₂. Boron trifluoride diethyl etherate (1.0 mL, 1.17 g, 8.1 mmol, 0.5 equiv.) was added dropwise and the mixture stirred for 5 h under N₂ at 0 °C. The reaction was quenched with Et₃N (4 mL) and concentrated. The mixture was diluted with EtOAc (150 mL) and washed with H₂O (150 mL) and brine (150 mL). The organic layer was filtered through MgSO₄ and concentrated. The residue was purified by flash chromatography eluting with 3:1 Hex/EtOAc to give **50** as a light colored oil (3.54 g, 66 %). *R*_f 0.25 (3:1 Hexanes/EtOAc). [α]_D²⁵ -170.2 (*c* = 1, CH₂Cl₂). ¹H NMR (400 MHz, CDCl₃) δ 2.10 (s, 3H), 2.11 (s 3H), 2.13 (s, 3H), 2.34 (s, 3H), 4.28 (dd, *J* = 12.1, 5.5 Hz, 1H), 4.39 (dd, *J* = 12.1, 3.6 Hz, 1H), 4.48 (app. q, *J* = 4.7 Hz, 1H), 5.07 (d, *J* = 5.5 Hz, 1H), 5.27 (s, 1H), 5.47 (s, 1H), 7.13 (d, *J* = 7.8 Hz, 2H), 7.40 (d, *J* = 7.8 Hz, 2H); ¹³C NMR (100

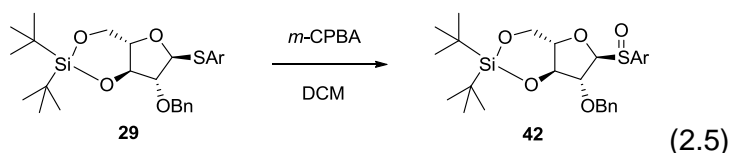
MHz, CDCl₃) δ 20.7 (3C), 21.1, 62.8, 77.2, 79.9, 81.4, 91.2, 129.6, 129.8, 132.7, 138.1, 169.6, 170, 170.5; HRMS (ESI) calcd for C₁₈H₂₁O₇SNa (M+Na)⁺: 405.0978; obsd: 405.0985.



p-Cresyl 3,5-*O*-(*Di*-*tert*-butylsilylene)-1-thio- α -L-arabinofuranoside (**52**). Thioglycoside triacetate **50** (694 mg, 1.8 mmol) was dissolved in MeOH (15 mL). Sodium methoxide (200 μ L, 25% in MeOH) was added and stirred under N₂ overnight. Amberlite® IR-120 acid resin was added portionwise while stirring until solution was neutralized, after which it was filtered and rinsed with MeOH, and concentrated. The crude triol **51** (363 mg, 1.4 mmol, 1.0 equiv.) was suspended in a mixture of dry CH₂Cl₂ (13 mL) and DMF (2.5 mL) and cooled to 0 °C under N₂. 2,6-Lutidine (762 μ L, 705 mg, 6.6 mmol, 4.7 equiv.) and di-*tert*-butylsilyl bis-(trifluoromethanesulfonate) (545 μ L, 741 mg, 1.7 mmol, 1.2 equiv.) were then added sequentially. The mixture was stirred overnight under N₂ at room temperature. The mixture was concentrated and the residue diluted with EtOAc (30 mL) and washed with H₂O (30 mL) and brine (30 mL). The organic layer was filtered through MgSO₄ and concentrated. The residue was purified by flash chromatography eluting with 15:1 Hex/EtOAc to give **52** as an amorphous colorless solid (297 mg, 53%). *R*_f 0.49 (3:1 Hexanes/EtOAc). [α]_D²⁵ -181.0 (*c* = 1.0, CH₂Cl₂). ¹H NMR (400 MHz, CDCl₃) δ 1.00 (s, 9H), 1.08 (s, 9H), 2.33 (s, 3H), 3.58 (d, *J* = 4.2 Hz, 1H), 3.87-3.98 (m, 2H), 4.02 (app. t, *J* = 8.3 Hz, 1H), 4.14 (app. q, *J* ~ 5 Hz, 1H), 4.35 (dd, *J* = 8.3, 4.2 Hz, 1H), 5.27 (d, *J* = 5.9 Hz, 1H), 7.12 (d, *J* = 7.8 Hz, 2H), 7.42 (d, *J* = 7.9 Hz, 2H); ¹³C NMR (100 MHz, CDCl₃) δ 20.1, 21.1, 22.7, 27.1, 27.5, 67.4, 73.7, 80.6, 77.4, 91.5, 129.8, 130.3, 132.3, 137.9; HRMS (ESI) calcd for C₂₀H₃₃O₄SSi (M+H)⁺: 397.1863; obsd: 397.1856.

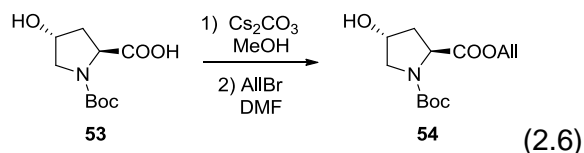


p-Cresyl 2-*O*-Benzyl-3,5-*O*-(di-*tert*-butylsilylene)-1-thio- α -L-arabinofuranoside (**29**). Compound **52** (400 mg, 1.1 mmol, 1 equiv.) was dissolved in dry CHCl₂ (11 mL) and stirred under N₂. Benzyl bromide (240 μ L, 345 mg, 2.0 mmol, 2 equiv.) was added, followed by Ag₂O (714 mg, 3.1 mmol, 3 equiv.). The mixture was stirred for 3 d, filtered through an inch of silica and washed with CHCl₂, and concentrated. The residue was purified by flash chromatography eluting with 120:1 Hex/Ether \rightarrow 60:1 Hex/EtOAc to give **29** as a colorless solid (336 mg, 64%). *R*_f 0.62 (3:1 Hexanes/EtOAc). [α]_D²⁵ -129.93 (*c* = 1, CH₂Cl₂). ¹H NMR (400 MHz, CDCl₃) δ 0.97 (s, 9H), 1.06 (s, 9H), 2.28 (s, 3H), 3.84-3.98 (m, 3H), 4.12 (app. t, *J* = 8.4 Hz, 1H), 4.31 (dd, *J* = 8.2, 4.1 Hz, 1H), 4.72 (d, *J* = 12.0 Hz, 1H), 4.81 (d, *J* = 12.0 Hz, 1H), 5.34 (d, *J* = 5.2 Hz, 1H), 7.05 (d, *J* = 7.9 Hz, 2H), 7.26-7.40 (m, 7H); ¹³C NMR (100 MHz, CDCl₃) δ 20.2, 21.2, 22.7, 27.2, 27.6, 67.4, 72.2, 73.8, 81.4, 86.8, 90.3, 127.9, 128.1, 128.5, 129.8, 130.6, 132.3, 137.71, 137.74; HRMS (ESI) calcd for C₂₇H₃₉O₄SSi (M+H)⁺: 487.2333; obsd: 487.2324.



p-Cresyl 2-*O*-Benzyl-3,5-*O*-(di-*tert*-butylsilylene)-1-thio- α -L-arabinofuranoside *S*-Oxide (**42**). A solution of 3-chloroperoxybenzoic acid (63.5 mg, 77 wt %, 2.8 mmol, ~1.2 equiv.) in dry CH₂Cl₂ (1 mL) was added dropwise to a solution of compound **29** (116 mg, 0.24 mmol, 1 equiv.) in dry CH₂Cl₂ (4 mL) at -80 °C under Argon and stirred. The reaction mixture was gradually warmed to room temperature over 2 h. The solution was diluted with CH₂Cl₂ (30 mL), washed with sat'd aq NaHCO₃ (30 mL), filtered through MgSO₄, and concentrated. The residue was purified by column chromatography, eluting with 10:1 Hex/EtOAc to afford **42** as a colorless gel (68 mg,

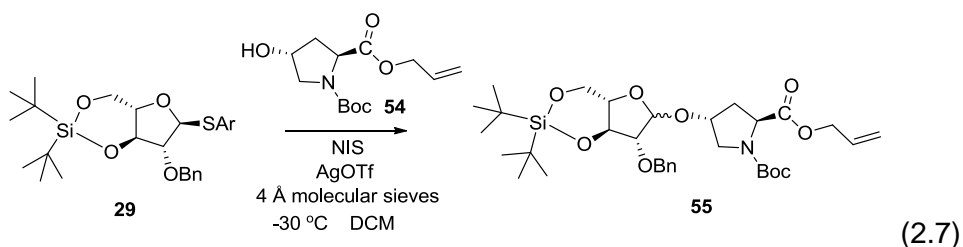
57%) and a mixture of diastereomers varying in their configuration at sulfur. Diastereomer A: R_f 0.42 (3:1 Hexanes/EtOAc). $[\alpha]_D^{25}$ 101.4 ($c = 1$, CHCl_3). ^1H NMR (400 MHz, CDCl_3) δ 1.00 (s, 9H), 1.05 (s, 9H), 2.40 (s, 3H), 3.89 (app. t, $J = \sim 10$ Hz, 1H), 3.99-4.05 (td, $J = 10$, 5.0 Hz, 1H), 4.22 (dd, $J = \sim 10$, 7.2 Hz, 1H), 4.30 (d, $J = 11.4$ Hz, 1H), 4.35 (dd, $J = 9.0$, 5.0 Hz, 1H), 4.57-4.59 (m, 1H), 4.58 (d, $J = 11.4$ Hz, 1H), 4.65 (d, $J = 5.1$ Hz, 1H), 6.98 (app. t, $J = 3.6$ Hz, 2H), 7.25-7.27 (m, 3H), 7.30 (d, $J = 8.0$ Hz, 2H), 7.47 (d, $J = 8.0$ Hz, 2H); ^{13}C NMR (100 MHz, CDCl_3) δ 20.2, 21.4, 22.6, 27.1, 27.4, 67.4, 72.0, 77.0, 78.5, 82.0, 99.3, 124.4, 127.7, 127.9, 128.2, 129.9, 136.2, 137.3, 141.7; HRMS (ESI) calcd for $\text{C}_{27}\text{H}_{39}\text{O}_5\text{SSi}$ ($\text{M}+\text{H}$) $^+$: 503.2282; obsd: 503.2298; Diastereomer B: R_f 0.33 (3:1 Hexanes/EtOAc). $[\alpha]_D^{25}$ -178.6 ($c = 1.35$, CHCl_3). ^1H NMR (400 MHz, CDCl_3) δ 0.95 (s, 9H), 1.05 (s, 9H), 2.40 (s, 3H), 3.78-3.84 (m, 1H), 3.86 (app. t, $J = \sim 9.4$ Hz, 1H), 4.20 (app. t, $J = 8.2$ Hz, 1H), 4.30 (dd, $J = 8.6$, 4.5 Hz, 1H), 4.35 (app. t, $J = 6.4$ Hz, 1H), 4.58 (d, $J = 11.7$ Hz, 1H), 4.63 (d, $J = 5.6$ Hz, 1H), 4.76 (d, $J = 11.7$ Hz, 1H), 7.23-7.36 (app. m, 7H), 7.52 (d, $J = 8.1$ Hz, 2H); ^{13}C NMR (100 MHz, CDCl_3) δ 20.0, 21.5, 22.6, 27.0, 27.4, 67.3, 72.3, 76.9, 81.1, 81.5, 98.2, 125.6, 128.0, 128.1, 128.4, 129.9, 136.4, 137.3, 142.3; HRMS (ESI) calcd for $\text{C}_{27}\text{H}_{39}\text{O}_5\text{SSi}$ ($\text{M}+\text{H}$) $^+$: 503.2282; obsd: 503.2294.



N-tert-Butoxycarbonyl-*trans*-4-hydroxy-L-proline allyl ester (**54**). To a suspension of Boc-Hyp-OH (**53**) (1.77 g, 7.7 mmol, 1.0 equiv.) in dry MeOH (16 mL) was added cesium carbonate (1.37 g, 4.2 mmol, 0.55 equiv.). The mixture was stirred under N_2 for 1.5 h during which time the reaction mixture became a homogeneous solution. The solvent was evaporated, and the residue dissolved in dry DMF (10 mL) and treated immediately with allyl bromide (1.2 g, 0.86 mL, 9.9 mmol, 1.3 equiv.). The mixture was stirred overnight at RT under N_2 . The mixture was diluted with EtOAc (150 mL) and washed with H_2O (150 mL) and brine (150 mL). The organic

layer was filtered through MgSO_4 and concentrated. The residue was purified by flash column chromatography, eluting with 2:1 EtOAc/Hex to give the ester **54** as a light oil (1.86 g, 89%). R_f 0.34 (2:1 EtOAc/Hex). $[\alpha]_D^{25}$ -65.0 (c 1.0, CH_2Cl_2). ^1H NMR (400 MHz, CDCl_3) δ 1.40 (1.46)* (s, 9H), 2.03-2.10 (m, 1H), 2.25-2.35 (m, 1H), 2.96 (s, 1H), 3.44-3.65 (m, 2H), 4.40-4.48 (m, 2H), 4.56-4.71 (m, 2H), 5.25 (app. t, $J = \sim 11.3$ Hz, 1H), 5.35 (dt, $J = 17.1, 3.8, 1.2$ Hz, 1H), 5.87-5.95 (m, 1H); ^{13}C NMR (100 MHz, CDCl_3) δ 28.2 (28.3), 39.1 (38.3), 54.6, 58.0 (57.7), 65.6, 69.1 (69.8), 80.5 (80.2), 118.8 (118.3), 131.6 (131.8), 154.1 (154.6), 172.9 (172.6); HRMS (ESI) calcd for $\text{C}_{13}\text{H}_{21}\text{NO}_5\text{Na}$ ($\text{M}+\text{Na}$) $^+$: 294.1312, obsd: 294.1320.

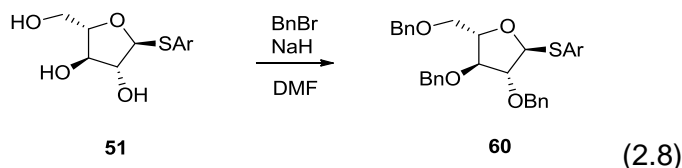
* values in parentheses signify a second signal due to a minor rotamer



N α -tert-Butyloxycarbonyl-trans-4-hydroxy-4-O-[2-O-Benzyl-3,5-O-(di-tert-butylsilylene)-L-arabinofuranosyl]-L-proline Allyl Ester **55**. A solution of compounds **29** (219 mg, 0.45 mmol, 1.0 equiv.) and **54** (250 mg, 0.92 mmol, 2.0 equiv.) in dry CH_2Cl_2 (30 mL) were added to a flask containing activated 4 Å crushed molecular sieves under N_2 . The suspension was stirred for ~20 min at RT then cooled to -65 °C (ethylene glycol and dry ice). The temperature dropped to -30 °C and NIS (173 mg, 0.68 mmol, 1.5 equiv.) was added, followed by a solution of AgOTf (57 mg, 0.22 mmol, 0.5 equiv) in toluene (0.6 mL) as the temperature continued to drop to -65 °C. The suspension was stirred for 1 hr during which it was allowed to gradually warm to RT. Solution continued to stir until room temperature was reached. After ~20 mins at room temperature, the reaction was quenched with Et_3N , filtered, and concentrated. The residue was diluted with EtOAc (50 mL) and washed with sat'd aq. $\text{Na}_2\text{S}_2\text{O}_3$ (50 mL) and brine (50 mL),

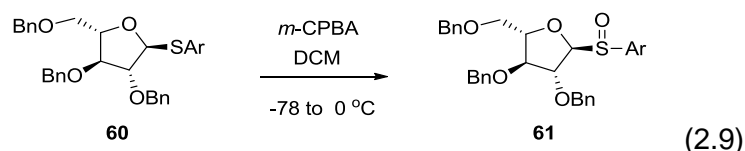
filtered through MgSO_4 , and concentrated. The residue was purified by column chromatography, eluting with 10:1 Hex/EtOAc to afford crude **55** as a colorless oil (147 mg, 51%) as a mixture of anomers and rotamers. Crude compound **55** was subjected to HPLC, eluting with 20% EtOAc in Hexanes at 13.0 mL min^{-1} on a 21 mm silica column detecting with UV at 254 nm. $R_T(\alpha) = 13 \text{ min}$, $R_T(\beta) = 23 \text{ min}$; β -anomer: R_f 0.30 (3:1 Hexanes/EtOAc). ^1H NMR (400 MHz, CDCl_3) δ 0.99 (s, 9H), 1.07 (s, 9H), 1.38 (1.45)* (1 s, 9H), 2.08-2.15 (m, 1H), 2.35-2.42 (2.43-2.49) (m, 1H), 3.58-3.69 (m, 3H), 3.86-3.91 (m, 2H), 4.26-4.32 (m, 3H), 4.36-4.44 (m, 1H), 4.56-4.73 (m, 3H), 4.79 (d, $J = 12.2 \text{ Hz}$, 1H), 4.97 (4.93) (d, $J = \sim 5.3 \text{ Hz}$, 1H), 5.24 (app. t, $J = 11.6 \text{ Hz}$, 1H), 5.32 (ddd, $J = 17.2, 5.9, 1.3 \text{ Hz}$, 1H), 5.85-5.96 (m, 1H), 7.29-7.40 (m, 5H); ^{13}C NMR (100 MHz, CDCl_3) δ 20.1, 22.6, 27.1, 27.5, 28.2 (28.4), 37.6 (36.8), 51.1 (51.6), 58.1 (57.7), 65.5 (65.6), 68.4, 71.8 (71.9), 73.6 (73.4), 75.2, 78.4, 80.2 (80.1), 80.7, 99.2 (100.0), 118.7 (118.3), 127.7, 127.8, 127.9, 128.0, 128.4, 131.7 (131.9), 137.7, 153.7 (154.2), 172.7 (172.4); HRMS (ESI) calcd for $\text{C}_{33}\text{H}_{52}\text{NO}_9\text{Si}$ ($\text{M}+\text{H}$) $^+$: 634.3406; obsd: 634.3408.

* values in parentheses signify a second signal due to a minor rotamer

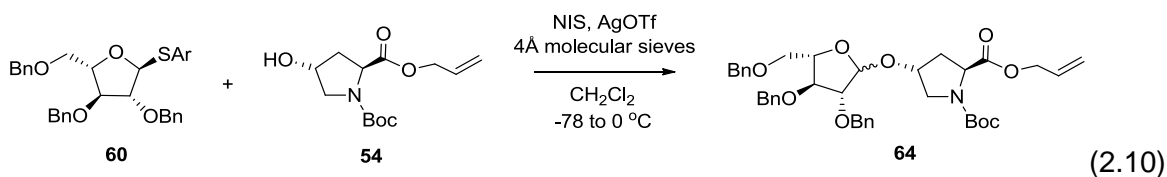


p-Cresyl 2,3,5-*O*-Benzyl-1-thio- α -*L*-arabinofuranoside (**60**). Triol **51** (1.91 g, 7.5 mmol, 1.0 equiv.) was dissolved in dry DMF (15 mL) and cooled to 0 °C under N_2 . Benzyl bromide (5.3 mL, 7.61 g, 44.5 mmol, 6.0 equiv.) and NaH (1.78 g, 60% dispersion, 44.5 mmol, 6.0 equiv.) were added sequentially. The reaction mixture was allowed to warm to RT while it stirred under N_2 for 3 h. The reaction was quenched with sat'd NaHCO_3 (150 mL) and extracted with CH_2Cl_2 (150 mL). The organic layer was washed with H_2O (150 mL) and brine (150 mL), filtered through MgSO_4 , and concentrated. The residue was purified by flash chromatography eluting with 20:1 \rightarrow 10:1 \rightarrow 1:2 Hex/EtOAc to give **60** as a clear gel (3.26 g, 84%; 2 steps). R_f 0.46 (3:1

Hexanes/EtOAc). $[\alpha]_D^{25}$ -107.9 ($c = 1.0$, CH_2Cl_2). ^1H NMR (400 MHz, CDCl_3) δ 2.32 (s, 3H), 3.63 (dd, $J = 10.8, 4.7$ Hz, 1H), 3.68 (dd, $J = 10.8, 3.9$ Hz, 1H), 4.03 (app. q, $J = 3.3$ Hz, 1H), 4.11 (t, $J = 2.9$ Hz, 1H), 4.36-4.38 (m, 1H), 4.48-4.65 (m, 6H), 5.53 (d, $J = 2.0$ Hz, 1H), 7.10 (d, $J = 7.8$ Hz, 2H), 7.26-7.35 (m, 15H), 7.41 (d, $J = 7.8$ Hz, 2H); ^{13}C NMR (100 MHz, CDCl_3) δ 21.2, 69.1, 72.7, 72.3, 73.4, 80.5, 83.5, 88.4, 90.6, 127.6, 127.7, 127.8, 127.9, 127.9, 128.0, 128.3, 128.4, 128.5, 129.7, 131.0, 132.0, 137.4, 137.8, 138.2; HRMS (ESI) calcd for $\text{C}_{33}\text{H}_{34}\text{NaO}_4\text{S}$ ($\text{M}+\text{Na}$) $^+$: 549.2070; obsd: 549.2067.



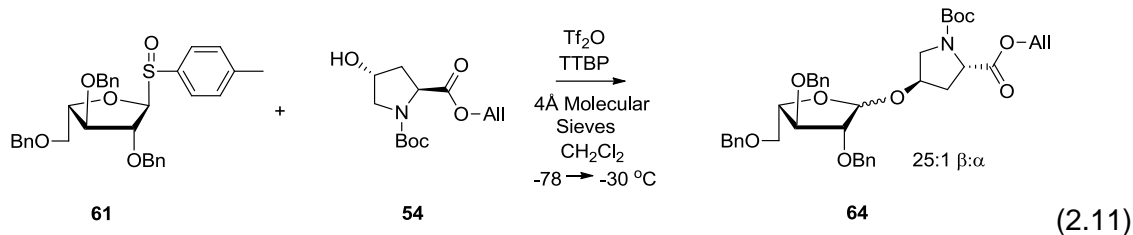
p-Cresyl 2,3,5-*O*-Benzyl-1-thio- α -L-arabinofuranoside S-Oxide **61**. A solution of 3-chloroperoxybenzoic acid (283 mg, 77 wt %, 1.3 mmol, 1.2 equiv.) in dry CH_2Cl_2 (4 mL) was added dropwise to a solution of compound **60** (555 mg, 1.1 mmol, 1.0 equiv.) in dry CH_2Cl_2 (16 mL) at -78 $^\circ\text{C}$ under N_2 and stirred. The reaction mixture was gradually warmed to RT over 1.5 h. The solution was diluted with CH_2Cl_2 (70 mL), washed with sat'd NaHCO_3 (70 mL), filtered through MgSO_4 , and concentrated. The residue was purified by column chromatography, eluting with 3:1 Hex/EtOAc to afford **61** as a colorless gel (429mg, 75%) and essentially a single diastereomer (uneven mixture in which the amount of minor isomer is negligible). Major diastereomer: R_f 0.19 (3:1 Hexanes/EtOAc). $[\alpha]_D^{25}$ +30.1 (c 1.0, CH_2Cl_2). ^1H NMR (400 MHz, CDCl_3) δ 2.39 (s, 3H), 3.53 (dd, $J = 10.6, 5.5$ Hz, 1H), 3.60 (dd, $J = 10.6, 4.8$ Hz, 1H), 4.15 (dd, $J = 5.5, 2.8$ Hz, 1H), 4.37-4.51 (m, 6H), 4.59 (d, $J = 11.8$ Hz, 1H), 4.63 (d, $J = 1.8$ Hz, 1H), 4.74 (app. t, $J = \sim 2.4$ Hz, 1H), 7.20-7.32 (m, 17H), 7.57 (d, $J = 8.1$ Hz, 2H); ^{13}C NMR (100 MHz, CDCl_3) δ 21.5, 69.1, 71.9, 72.2, 73.3, 83.3, 83.9, 84.4, 102.0, 124.8, 127.7, 127.9, 128.0 (2 signals), 128.4 (2 signals), 128.5, 129.9, 137.3, 137.4, 137.9, 138.7, 141.8; HRMS (ESI) calcd for $\text{C}_{33}\text{H}_{35}\text{O}_5\text{S}$ ($\text{M}+\text{H}$) $^+$: 543.2160; obsd: 543.2206.



Na-tert-Butyloxycarbonyl-trans-4-hydroxy-4-O-[2,3,5-O-Benzyl-L-arabinofuranosyl]-L-proline

Allyl Ester (64). A solution of compounds **60** (1.17 g, 2.2 mmol, 1.0 equiv.) and **54** (0.688 g, 2.5 mmol, 1.1 equiv.) in dry CH₂Cl₂ (40 mL) was stirred with activated 4 Å molecular sieves (3.5 g) under N₂ for ~30 min at RT. The suspension was cooled to -78 °C (acetone/dry ice) and then NIS (0.747 g, 3.2 mmol, 1.5 equiv.) and AgOTf (0.285 g, 0.55 mmol, 0.5 equiv.) were added. The reaction was allowed to gradually reach 0 °C over 1.5 h, at which time it was quenched with Et₃N (3 mL) and filtered. The filtrate was diluted with EtOAc (150 mL) and washed with 10% aqueous Na₂S₂O₃ (2 x 200 mL) and brine (200 mL). The organic layer was filtered through MgSO₄ and concentrated. The residue, determined to be a 4:1 β:α ratio by NMR, was purified by column chromatography, eluting with 3:1 Hex/EtOAc to afford **64β** (the β-anomer) (0.732 g, 50%, 2:1 ratio of rotamers) as an orange oil. *R*_f 0.56 (1:1 Hexanes/EtOAc). [α]_D²⁵ +17.9 (c 1.0, CH₂Cl₂). ¹H NMR (400 MHz, CDCl₃) δ 1.37 (1.44)* (s, 9H), 1.96-2.07 (m, 1H), 2.27-2.37 (m, 1H), 3.44-3.67 (m, 4H), 4.03-4.12 (m, 3H), 4.25-4.71 (m, 10H), 4.96 (4.92) (d, *J* = 3.2 Hz, 1H), 5.20-5.34 (m, 2H), 5.86-5.91 (m, 1H), 7.28-7.33 (m, 15H); ¹³C NMR (100 MHz, CDCl₃) δ 28.3 (28.4), 37.4 (36.5), 50.7 (51.4), 58.1 (57.8), 65.6 (65.7), 72.0, 72.4, 73.3, 75.5, 80.1, 80.3, 82.7, 83.8, 83.9, 99.0 (99.9), 118.8 (118.4), 127.6, 127.8, 127.9, 128.0, 128.1, 128.2, 128.3, 128.4, 128.5; 131.7 (131.9), 137.4, 137.9, 138.1, 153.7 (155.4), 172.7 (172.4). HRMS (ESI) calcd for C₃₉H₄₈NO₉ (M+H)⁺: 674.3324, obsd: 674.3343.

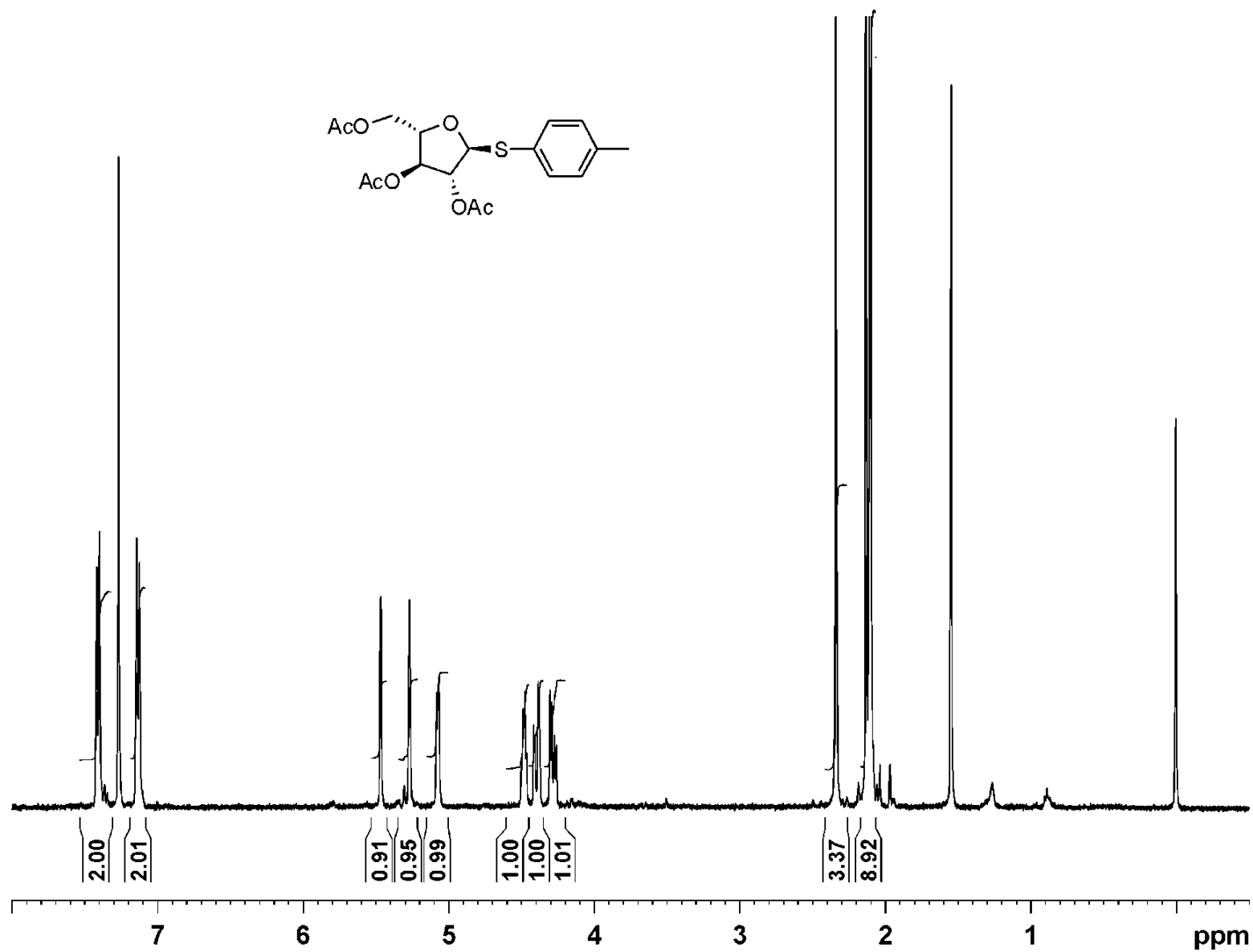
* values in parentheses signify a second signal due to a minor rotamer



N-*tert*-Butyloxycarbonyl-*trans*-4-hydroxy-4-*O*-[2,3,5-*O*-Benzyl-*L*-arabinofuranosyl]-*L*-proline Allyl Ester (**64**) – Sulfoxide method. A solution of compound **61** (133 mg, 0.25 mmol, 1.0 equiv.) and 2,4,6-tri-*tert*-butyl pyridine (121 mg, 0.49 mmol, 2 equiv.) (TTBP) in dry CH₂Cl₂ (5 mL) was stirred with activated 4Å molecular sieves (500 mg) under N₂ for ~30 min at RT. The suspension was cooled to -78 °C (acetone/dry ice) and then triflic anhydride (49 µL, 82 mg, 0.29 mmol, 1.2 equiv.) was added, followed by compound **54** (66 mg, 0.24 mmol, 1.0 equiv.). The reaction was allowed to gradually reach -30 °C over 2 h, at which time it was quenched with Et₃N (3 mL), filtered, and concentrated. The residue, determined to contain a 25:1 β:α ratio of **64** by NMR, was purified by column chromatography, eluting with 3:1 Hex/EtOAc to afford the β-anomer **64β** (84 mg, 51%) as an orange oil.

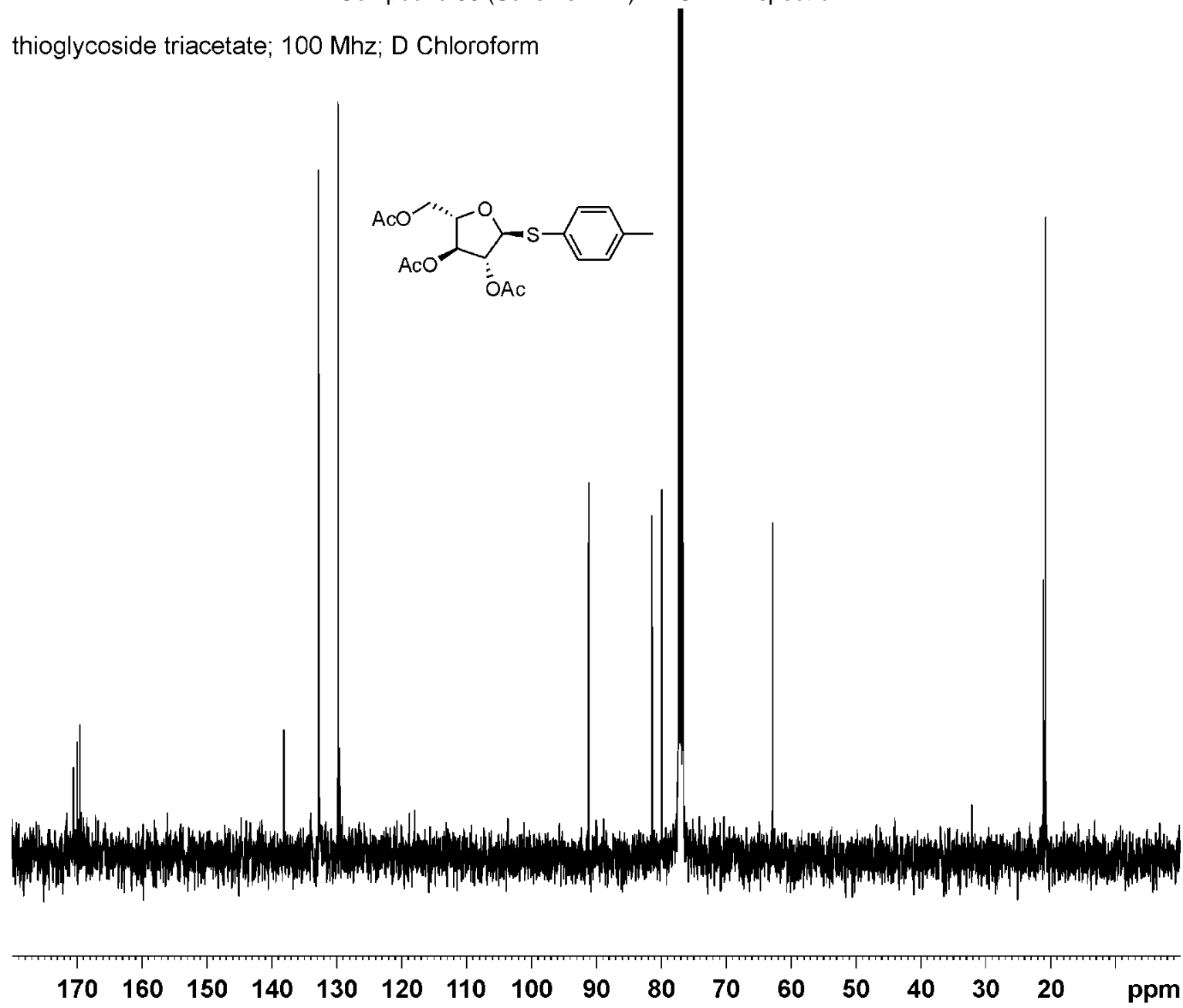
2.5.2 Spectra

Compound **50** (Scheme 2.11) - ^1H NMR spectrum
thioglycoside triacetate; 400 Mhz; D Chloroform



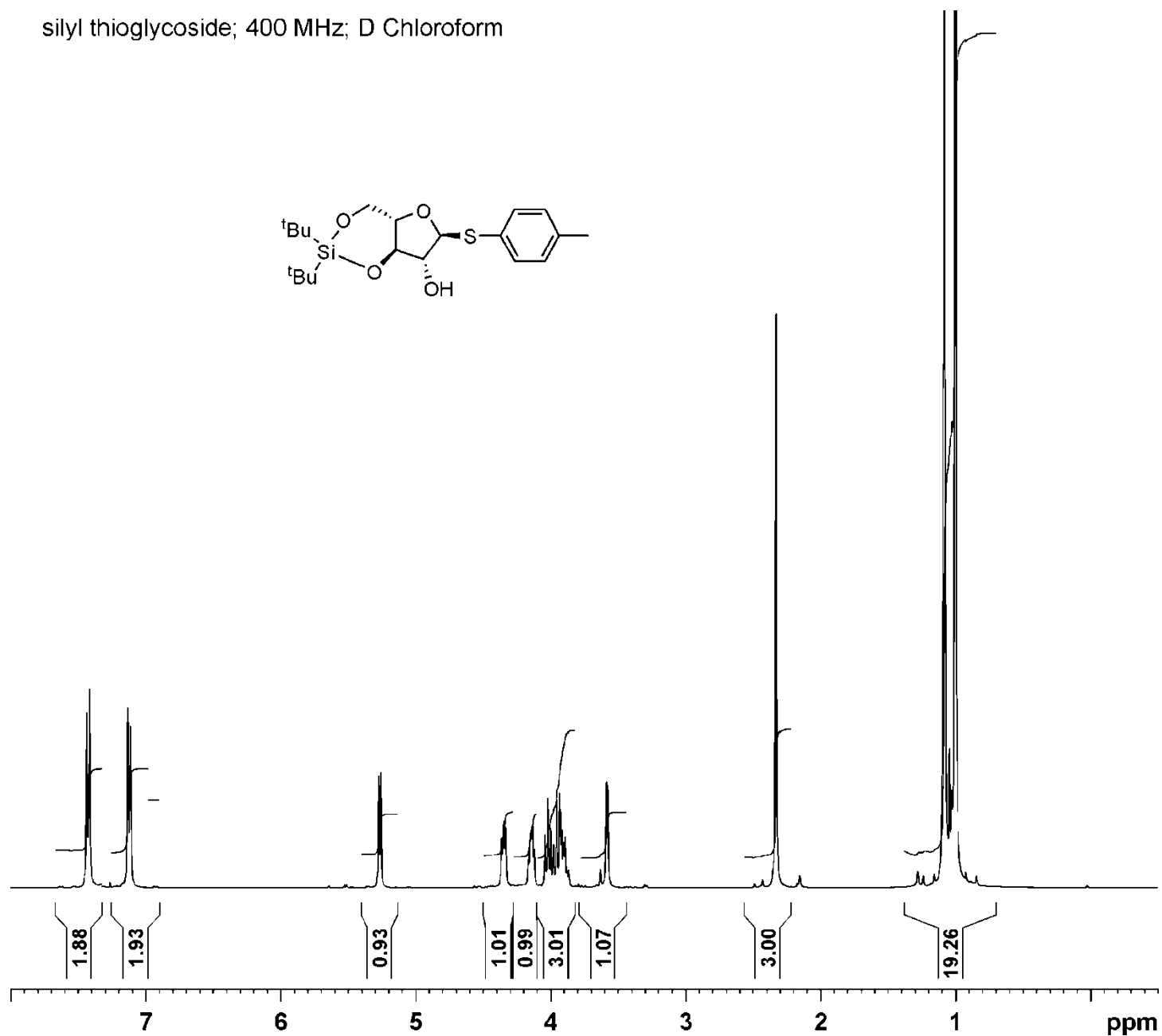
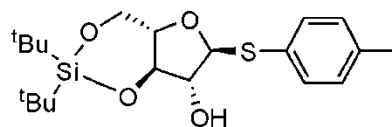
Compound **50** (Scheme 2.11) – ^{13}C NMR spectrum

thioglycoside triacetate; 100 Mhz; D Chloroform

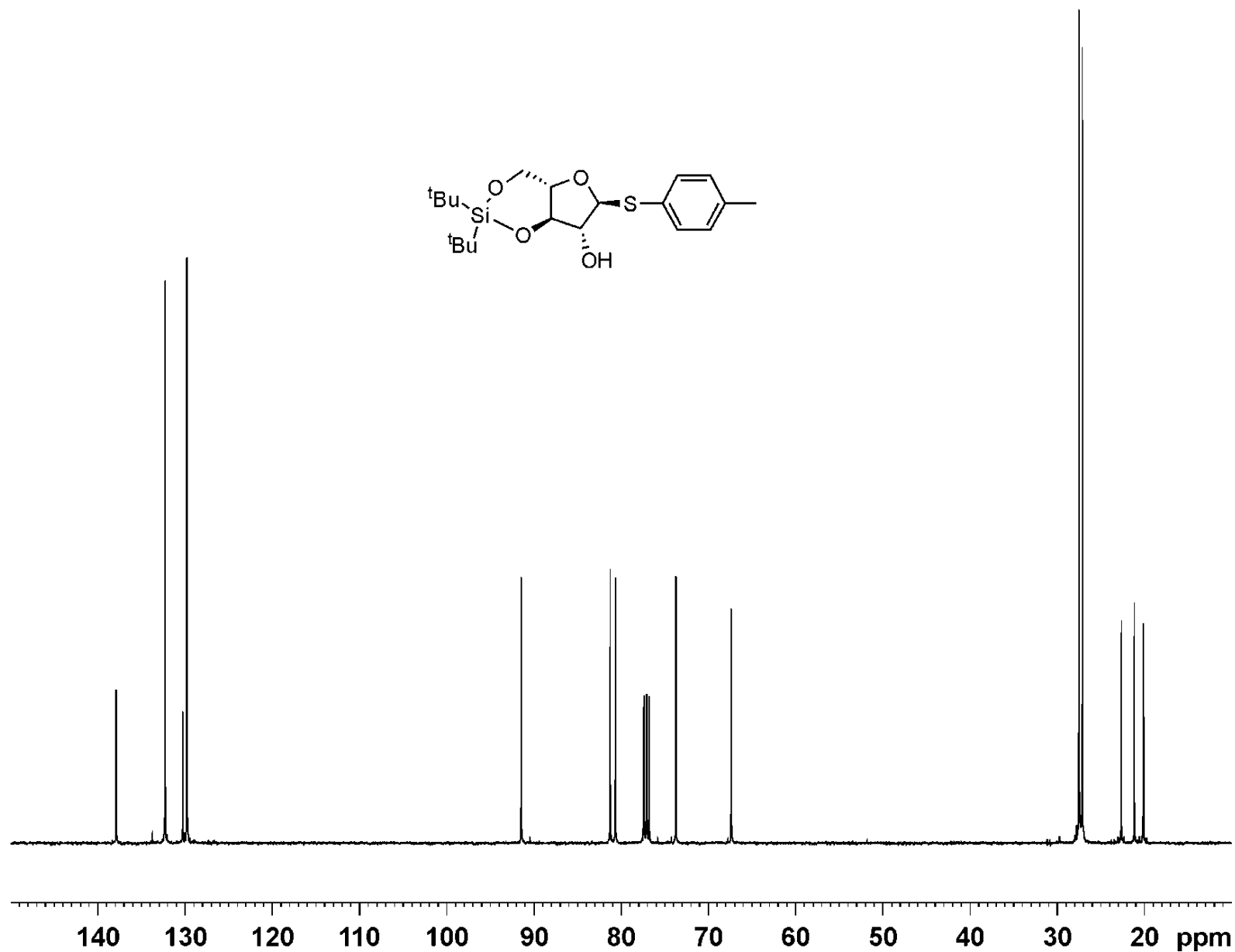


Compound **52** (Scheme 2.11) - ^1H NMR spectrum

silyl thioglycoside; 400 MHz; D Chloroform

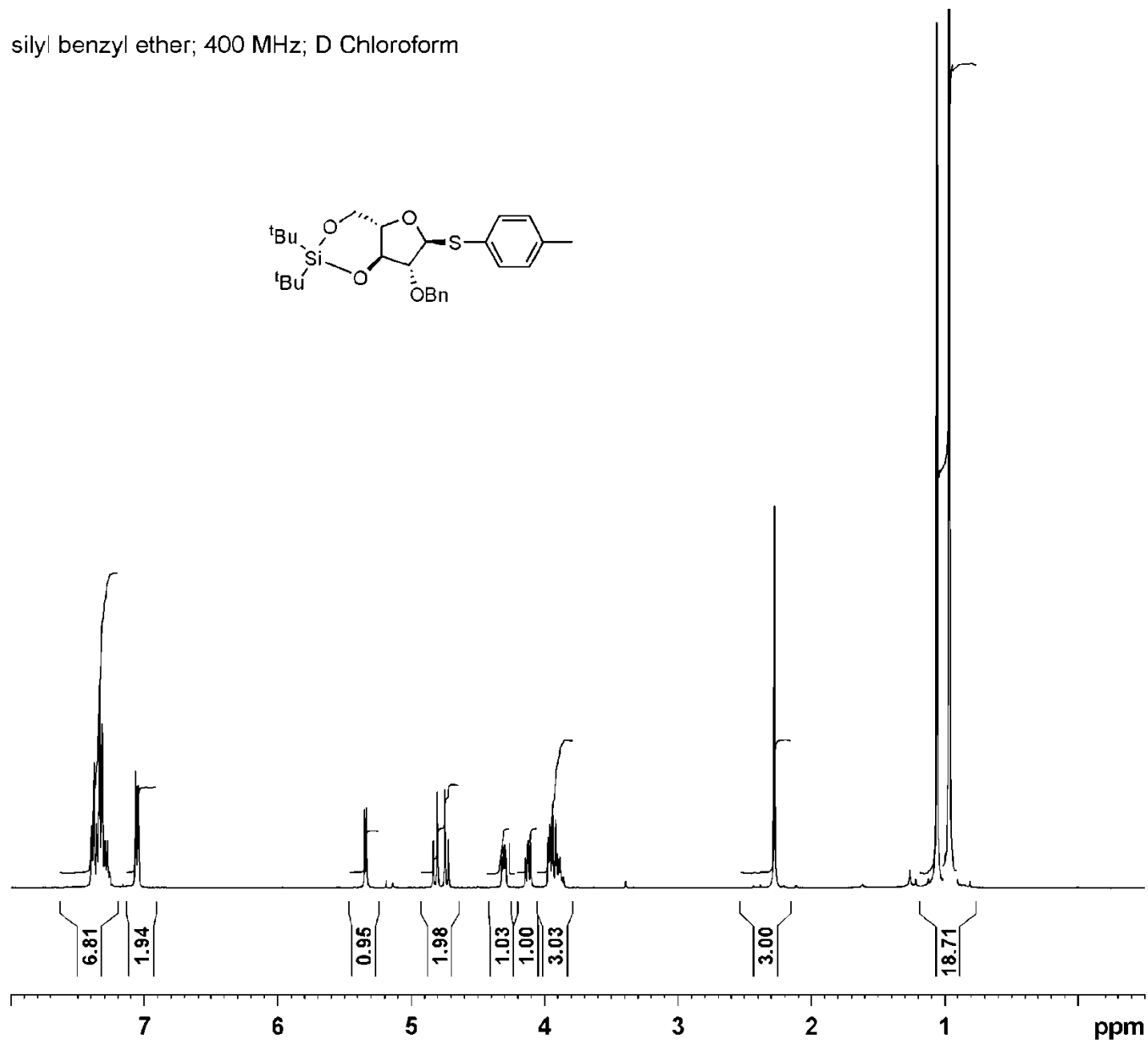
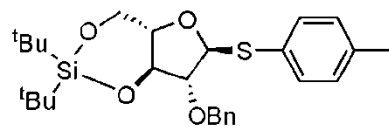


Compound **52** (Scheme 2.11) – ^{13}C NMR spectrum
silyl acetal thioglycoside; 100 Mhz; D Chloroform



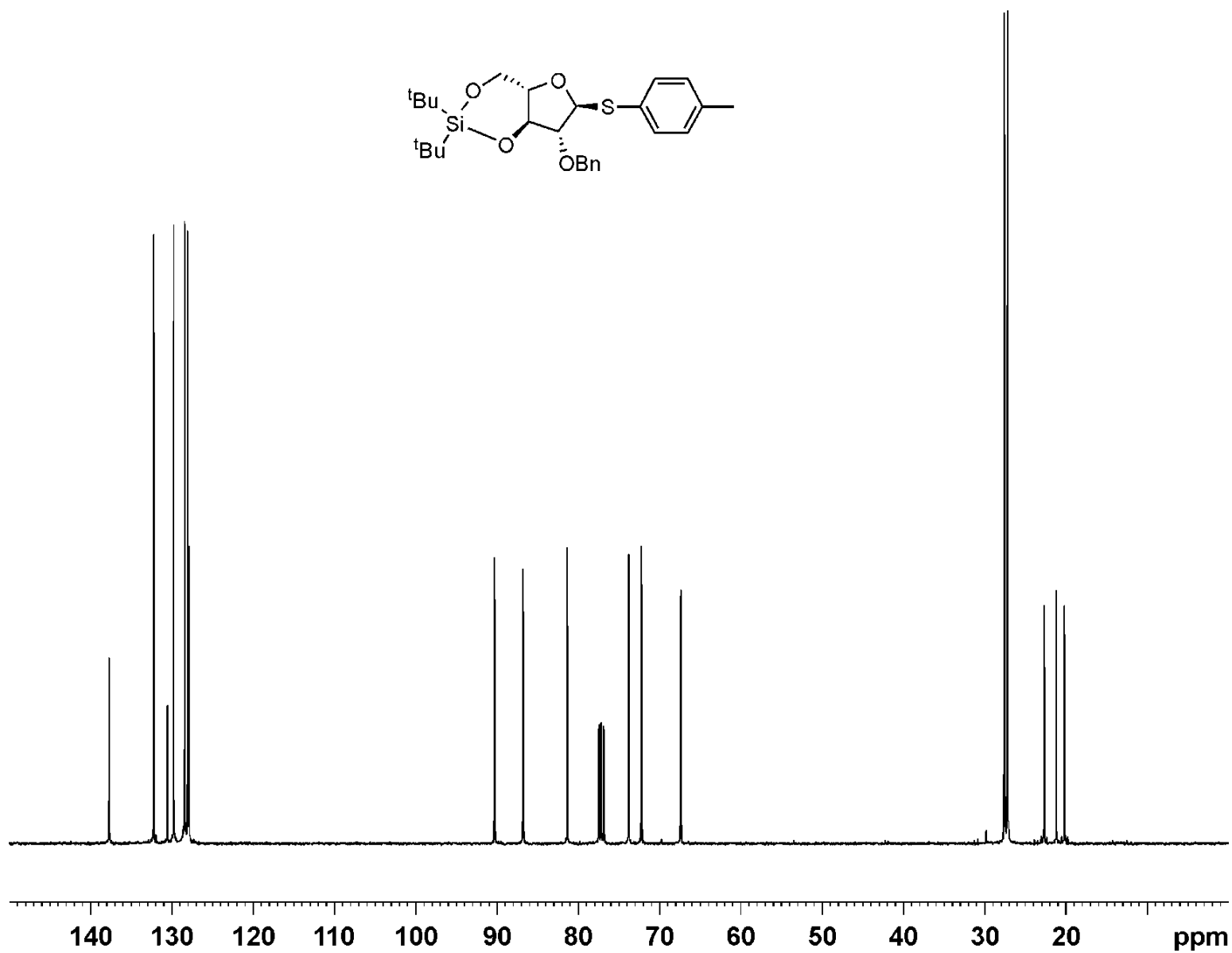
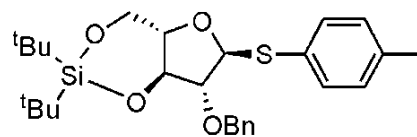
Compound **29** (Scheme 2.12) - ^1H NMR spectrum

silyl benzyl ether; 400 MHz; D Chloroform



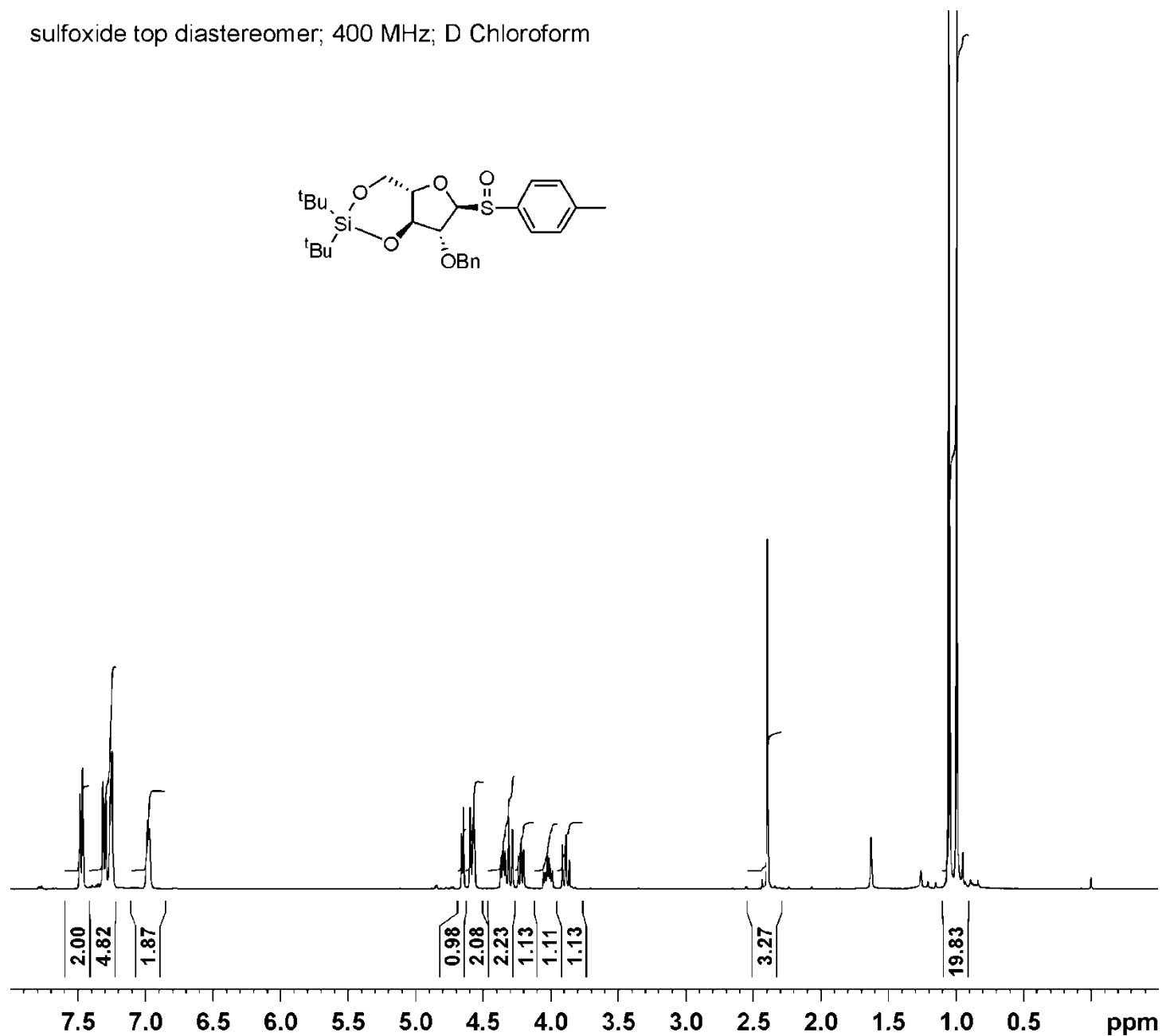
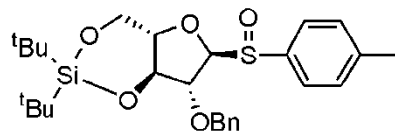
Compound **29** (Scheme 2.12) – ^{13}C NMR spectrum

silyl benzyl ether; 100 MHz; D Chloroform



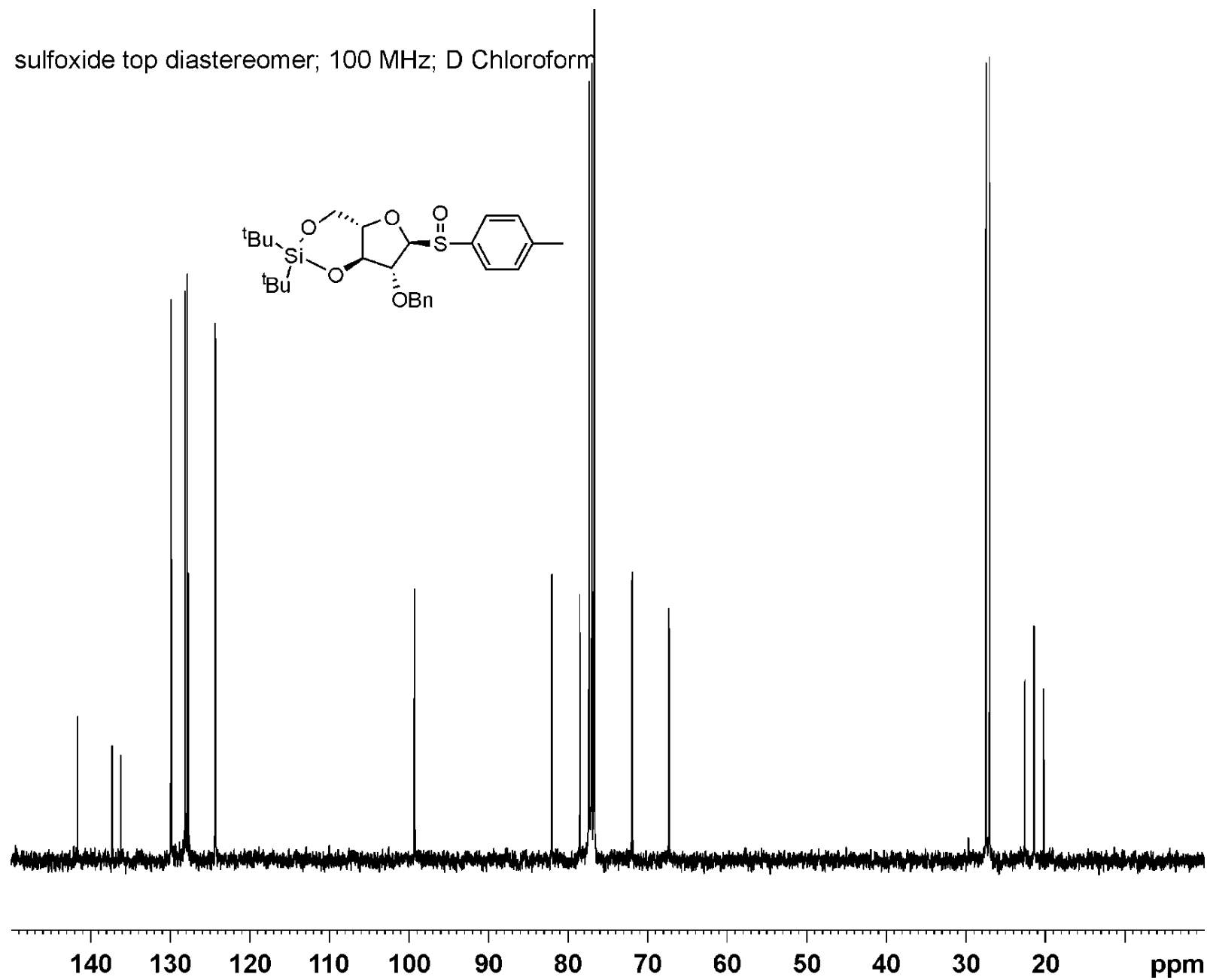
Compound **42a** (Scheme 2.15) - ^1H NMR spectrum

sulfoxide top diastereomer; 400 MHz; D Chloroform



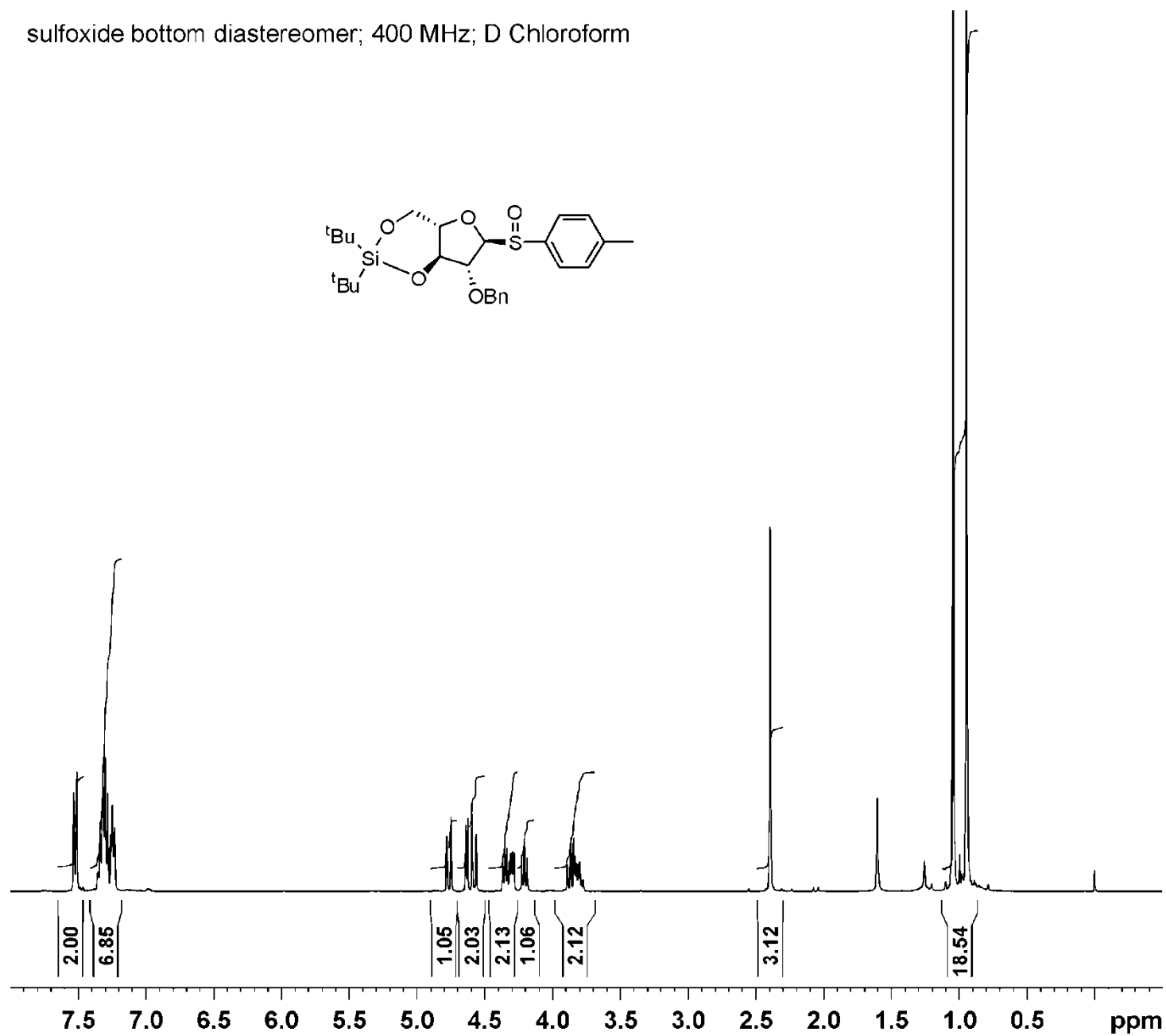
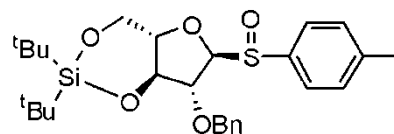
Compound **42a** (Scheme 2.15) – ^{13}C NMR spectrum

sulfoxide top diastereomer; 100 MHz; D Chloroform



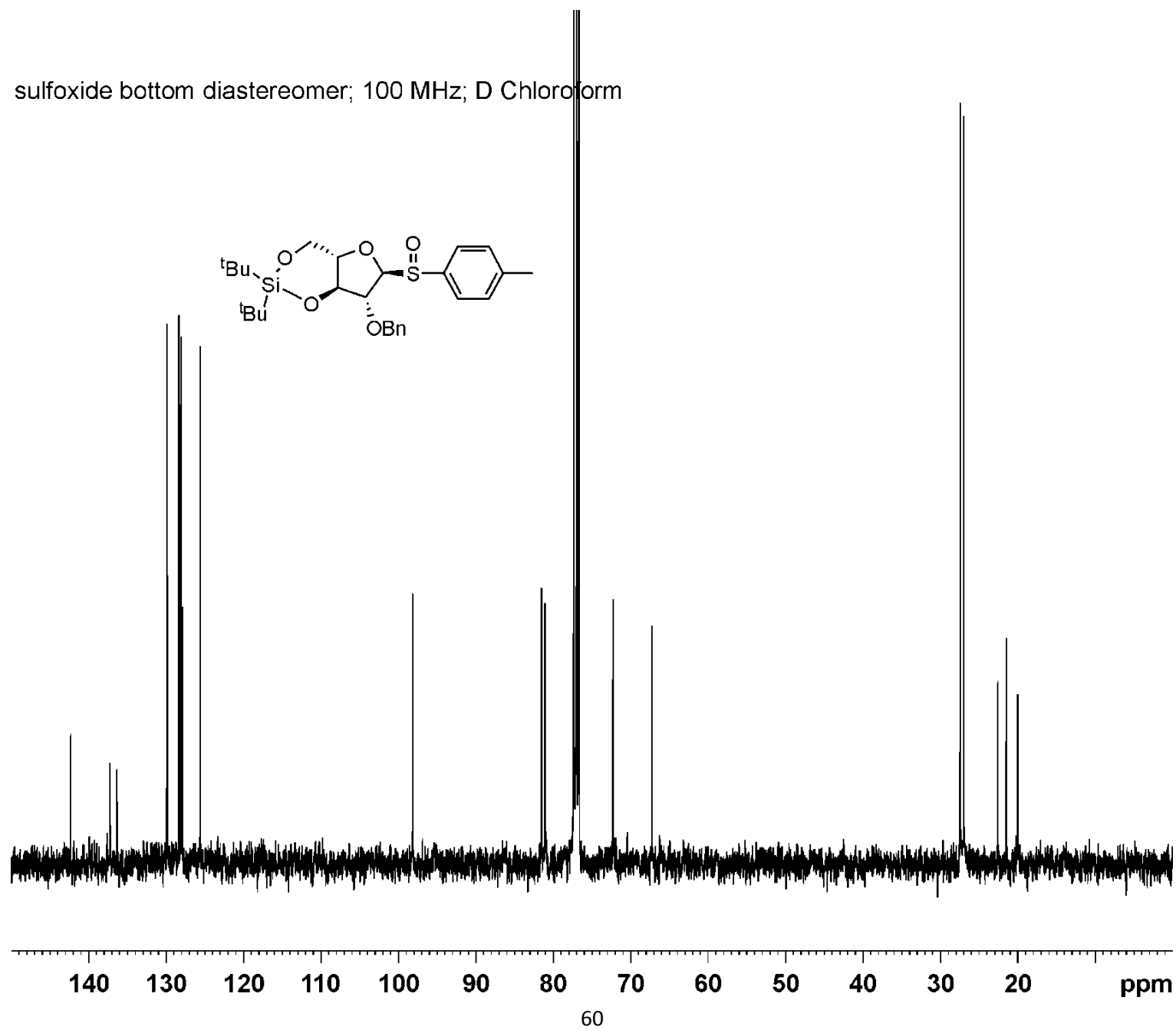
Compound **42b** (Scheme 2.15) - ^1H NMR spectrum

sulfoxide bottom diastereomer; 400 MHz; D Chloroform



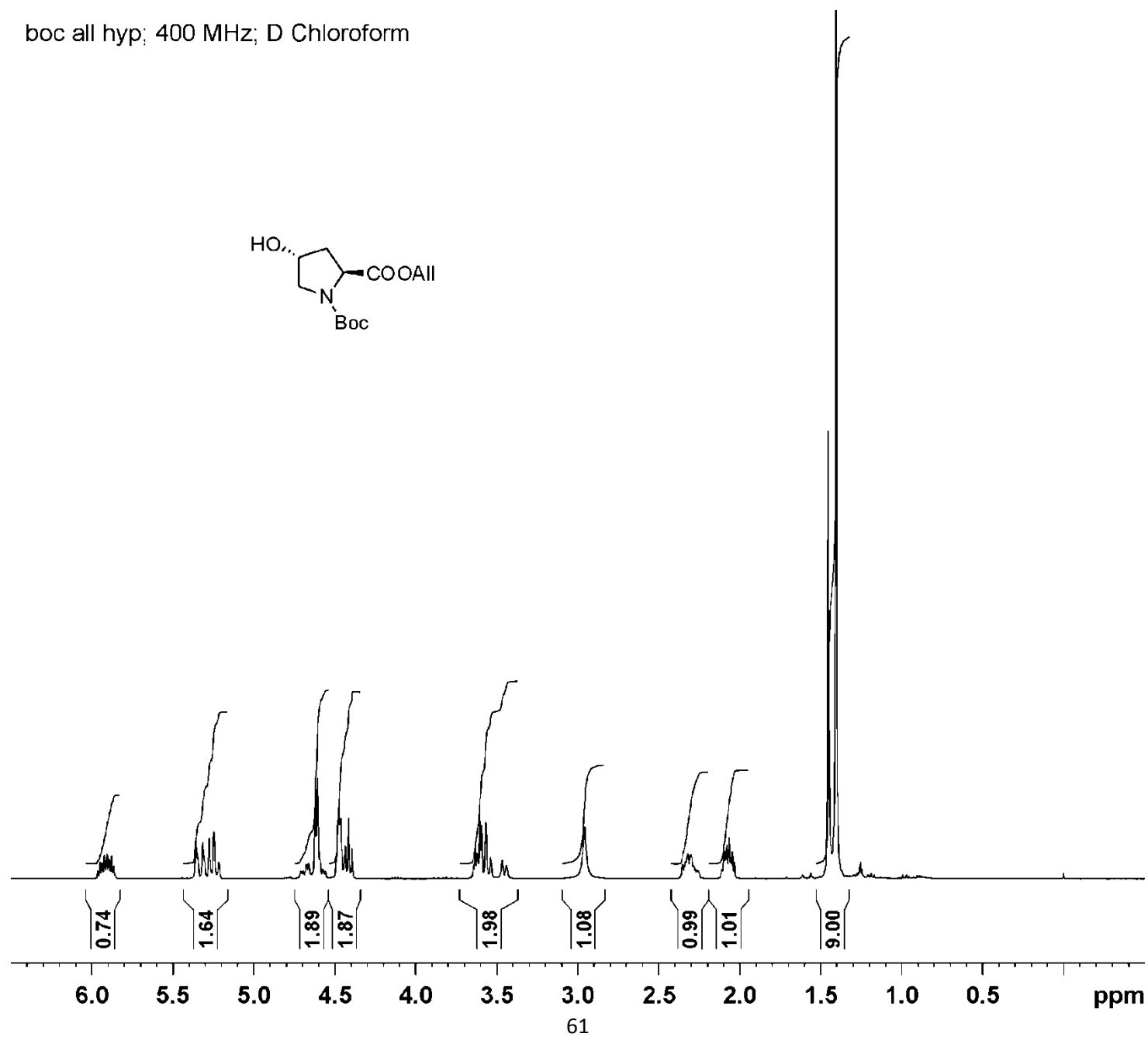
Compound **42b** (Scheme 2.15) – ^{13}C NMR spectrum

sulfoxide bottom diastereomer; 100 MHz; D Chloroform



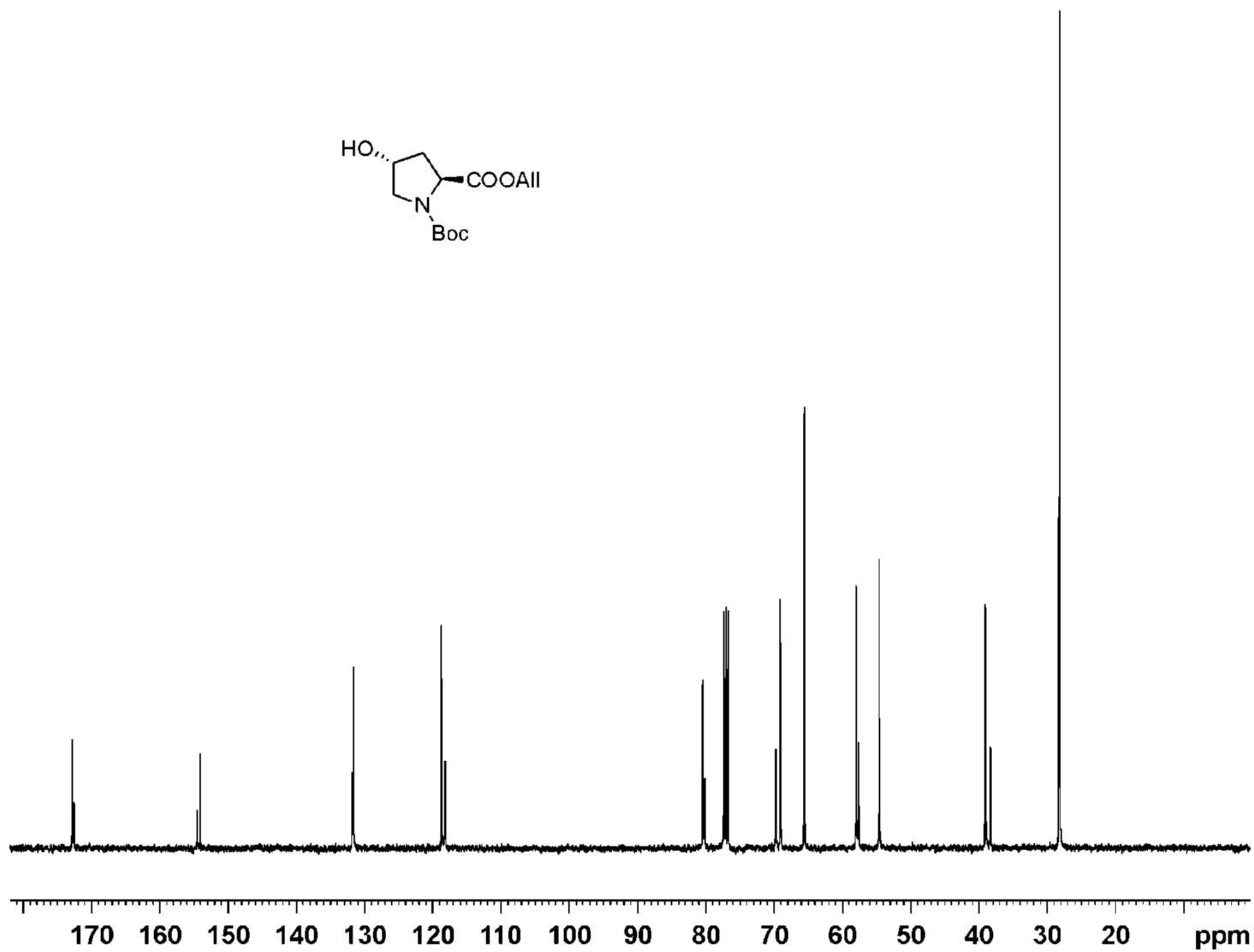
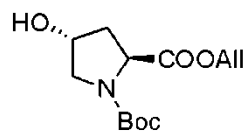
Compound **54** (Scheme 2.13) - ^1H NMR spectrum

boc all hyp; 400 MHz; D Chloroform



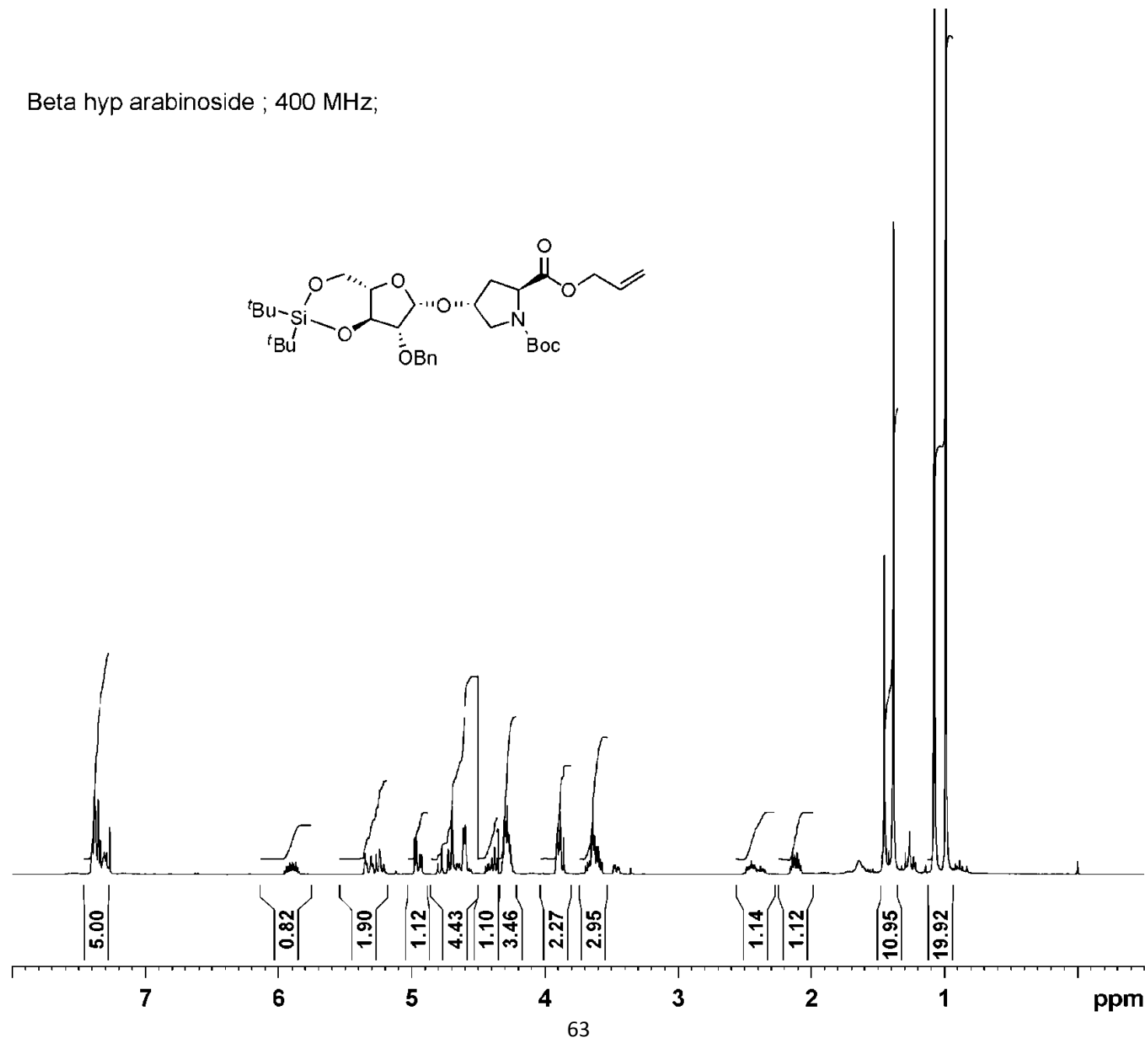
Compound **54** (Scheme 2.13) – ^{13}C NMR spectrum

Boc-Hyp-AlI; C NMR 100MHz; D Chloroform



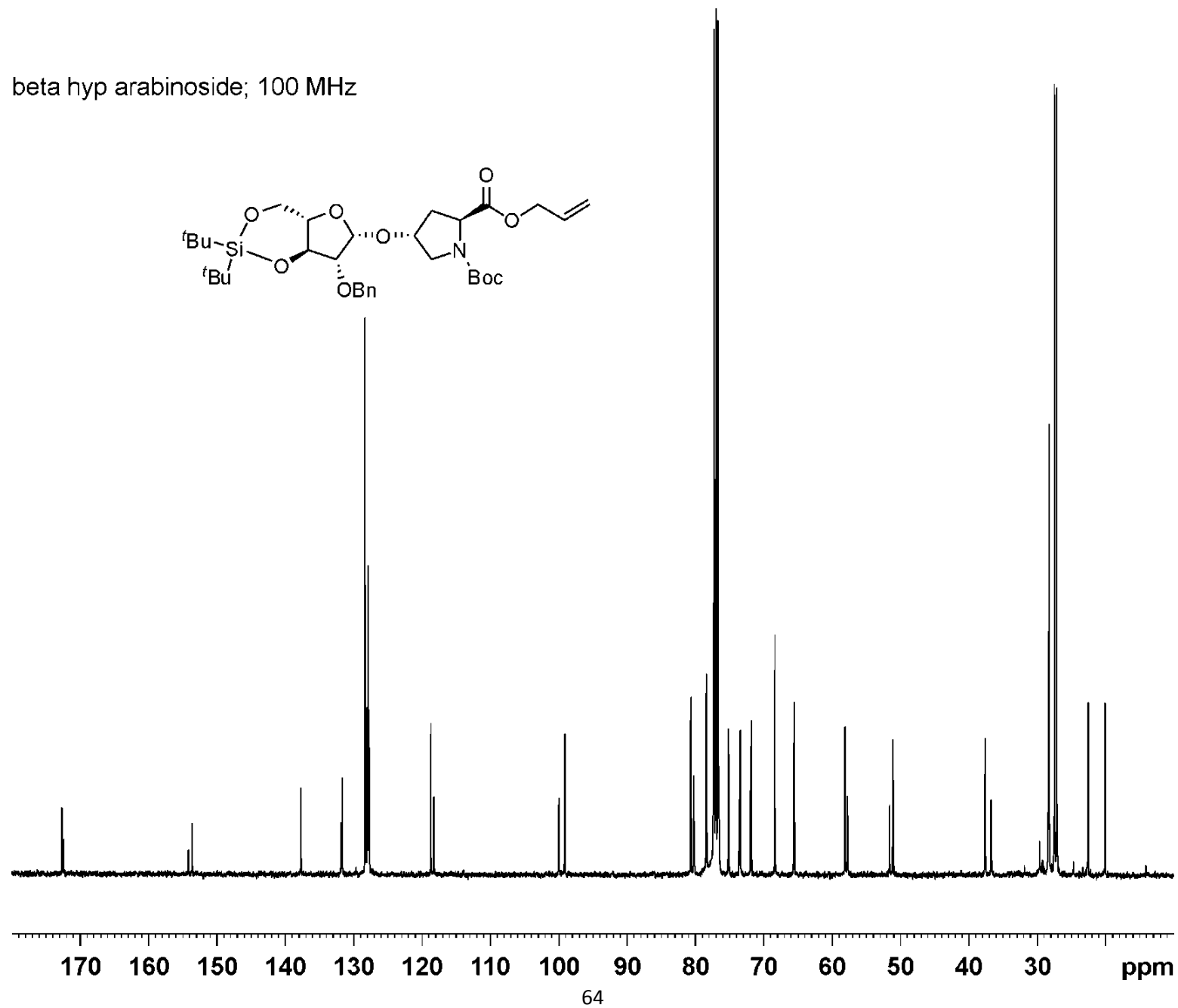
Compound **55 β** (Scheme 2.14) - ^1H NMR spectrum

Beta hyp arabinoside ; 400 MHz;



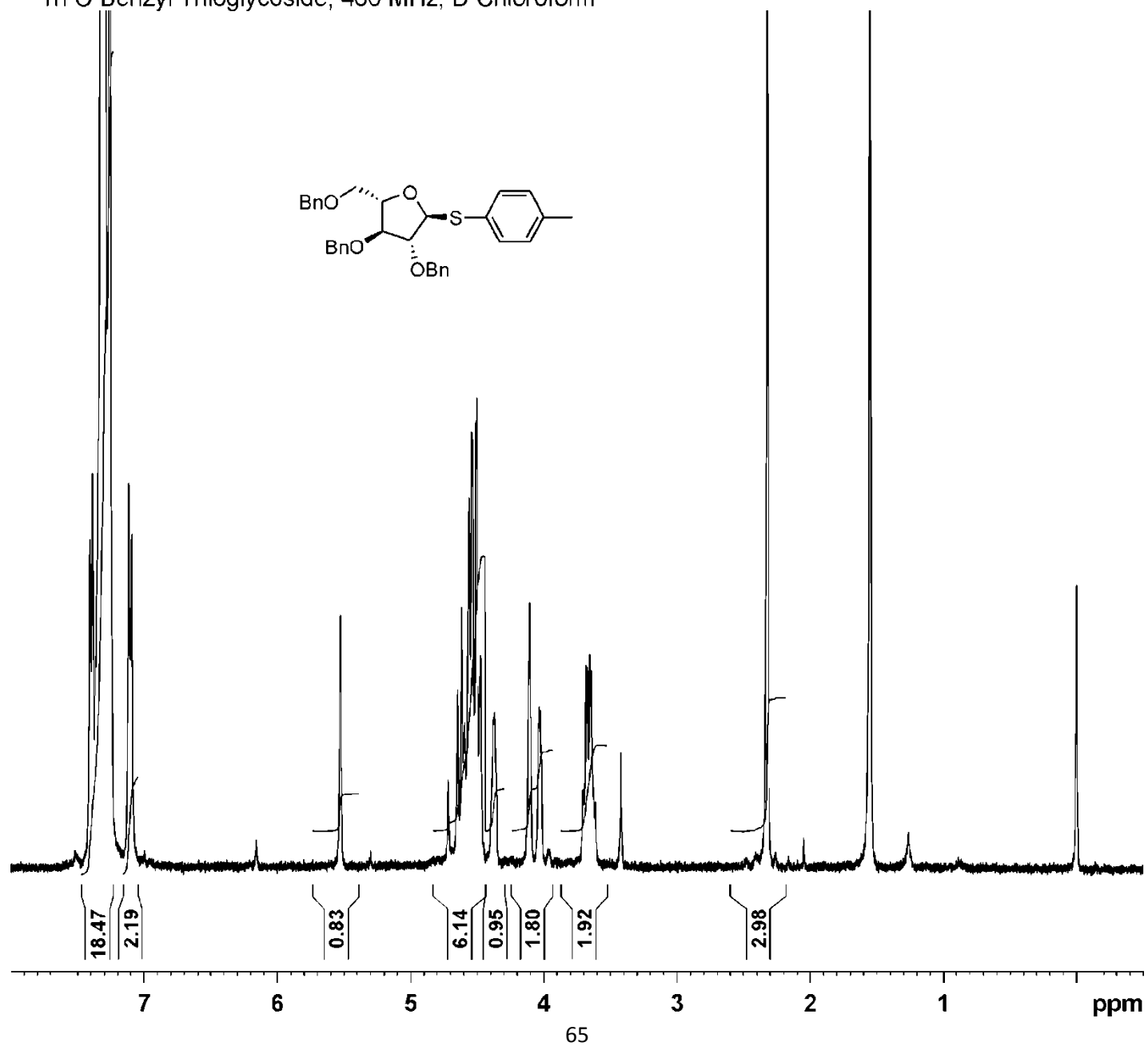
Compound **55β** (Scheme 2.14) – ^{13}C NMR spectrum

beta hyp arabinoside; 100 MHz



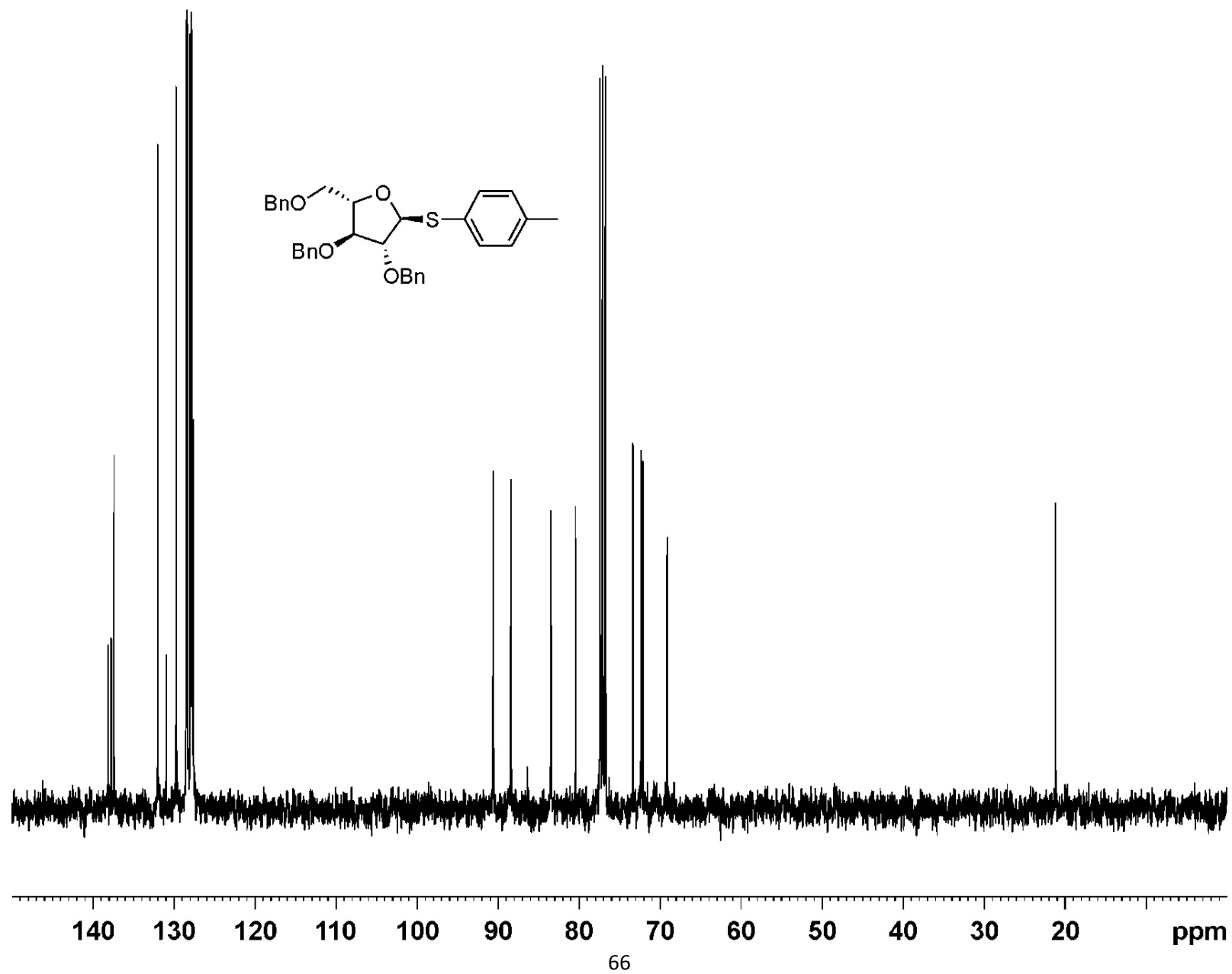
Compound **60** (Scheme 2.18) - ^1H NMR spectrum

Tri O Benzyl Thioglycoside; 400 MHz; D Chloroform



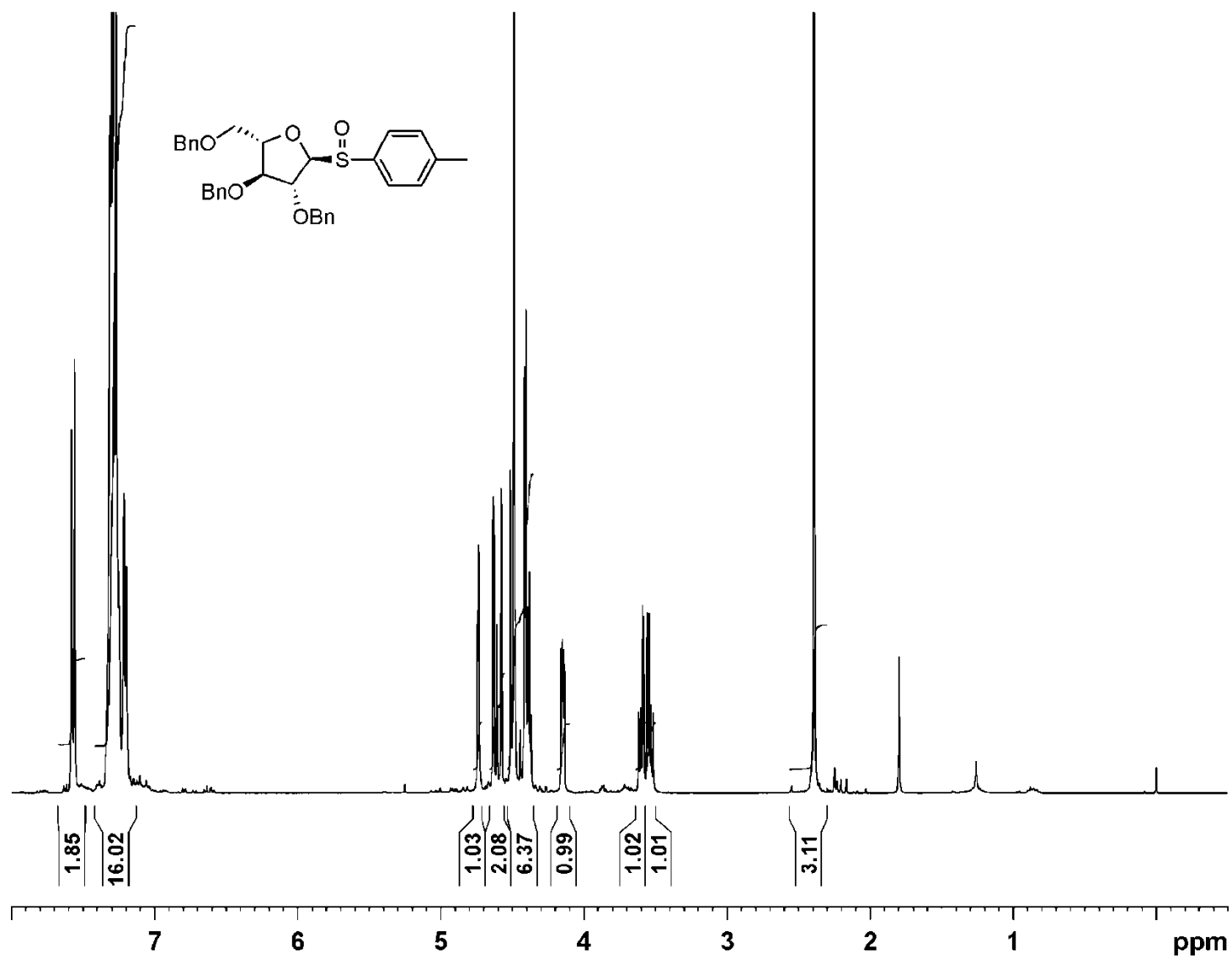
Compound **60** (Scheme 2.18) – ^{13}C NMR spectrum

Tri O Benzyl thioglycoside; 100 MHz; D Chloroform



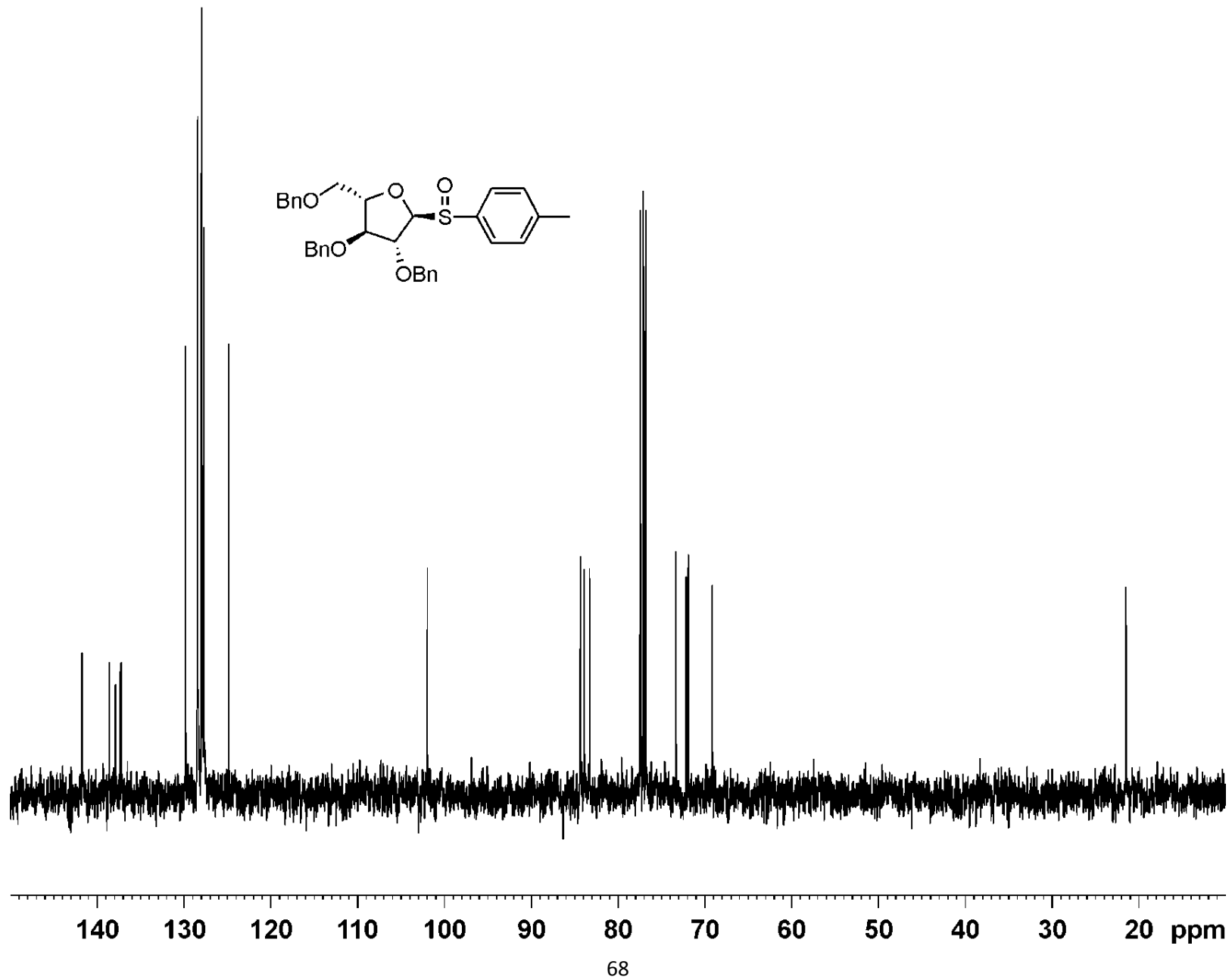
Compound **61** (Scheme 2.18) - ^1H NMR spectrum

tri o benzyl sulfoxide; 400 MHz; D Chloroform

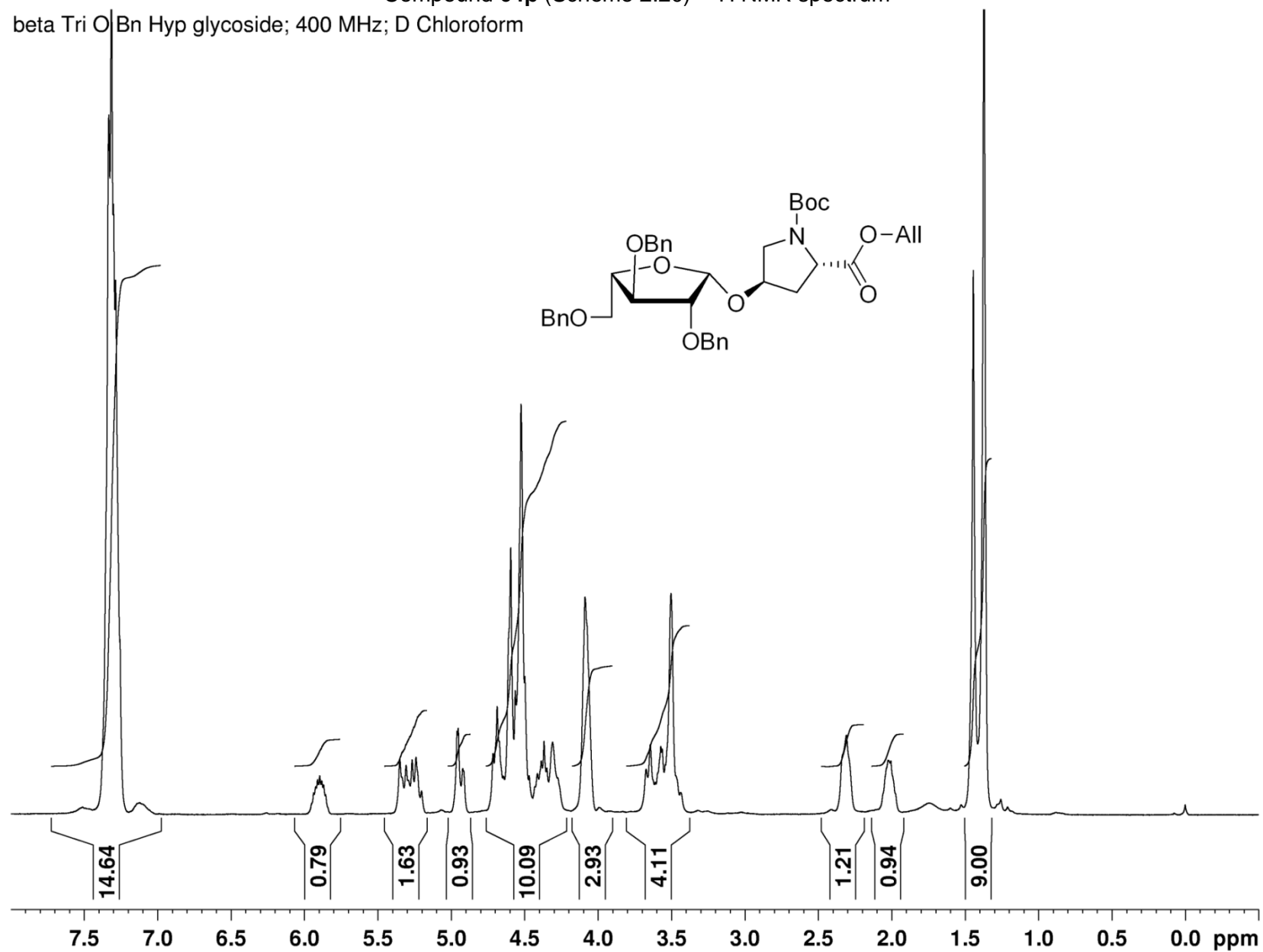


Compound **61** (Scheme 2.18) – ^{13}C NMR spectrum

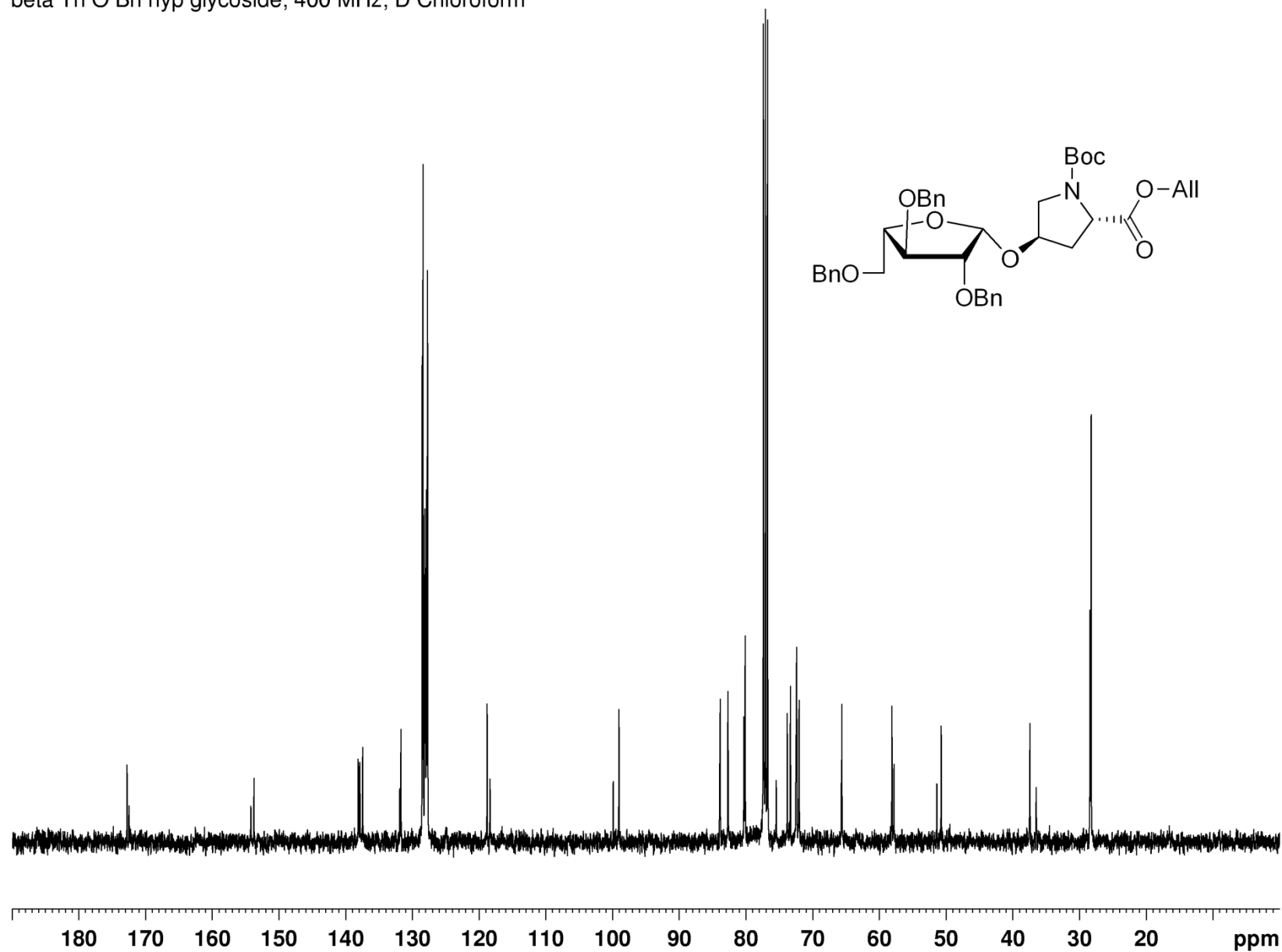
tri o benzyl sulfoxide; 100 MHz; D Chloroform



Compound **64β** (Scheme 2.20) - ^1H NMR spectrum
 beta Tri O Bn Hyp glycoside; 400 MHz; D Chloroform



Compound **64 β** (Scheme 2.20) – ^{13}C NMR spectrum
beta Tri O Bn hyp glycoside; 400 MHz; D Chloroform



CHAPTER 3: SYNTHESIS OF OLIGOMERS OF 4-O-[β -L-ARABINOFURANOSYL]-(2S,4R)-4-HYDROXYPROLINE

With the completion of the monomeric β -arabinoside of hydroxyproline in Chapter 2, we moved forward with the assembly of its oligomers. We expected the peptide bond formations to be increasingly difficult due to the gradual accumulation of size in the building blocks and the associated increase in steric demands. We considered a variety of peptide coupling reagents known for their efficiency in reactions involving prolyl amino components. There is an inherent challenge in the coupling of a sterically hindered proline amino component. Fortunately, proline carboxyl components are generally not expected to undergo racemization at C- α , which allowed us to broaden our scope in coupling reagent selection.

3.1 Previous Syntheses of Glycoclusters

There is an abundance of literature detailing synthetic glycocluster peptides.⁶³ A glycocluster is an array of carbohydrate groups that are present in close proximity as a result of primary sequence or backbone conformation. The “glycoside cluster effect” was introduced by Lee’s group to describe the clustering effect that carbohydrate groups exhibit when interacting with protein receptors.⁶⁴ While many types of carbohydrate clusters exist, it is the contiguous O-glycosylated amino acid cluster that is the focus of the present work. From our perspective, the most relevant solution phase synthesis of these glycoclusters has been in the area of mucins.

The mucin MUC1, a cancer biomarker, is a highly O-glycosylated molecule found on the epithelial cells of the stomach, lungs, eyes, and other major organs.⁶⁵ In 1998, the Kunz group reported the synthesis of a diglycohexapeptide and a diglycodecapeptide in the investigation of the MUC1 core related glycopeptides (Figure 3.1).⁶⁶ These glycopeptides represent two sequences that are prominently found in MUC1 and which are repeated throughout the molecule. Both glycopeptides feature adjacent serine and threonine residues O-glycosylated by α -N-acetyl galactosamine. The clustered glycopeptide fragment **69** was synthesized by

fragment condensation of Fmoc-[O-(2-azido-3,4,6-tri-*O*-acetyl-2-deoxy- α -D-galactopyranosyl)]-*L*-Ser-OH (**67**) and H-[O-(2-azido-3,4,6-tri-*O*-acetyl-2-deoxy- α -D-galactopyranosyl)]-*L*-Thr-Ala-OHep (**68**) (Scheme 3.1).⁶⁷ *N*-Hydroxybenzotriazole (HOBt) and 1-ethyl-3-(3-dimethylaminopropyl)carbodiimide hydrochloride (EDC) were employed to give the resulting tripeptide in 48% yield.

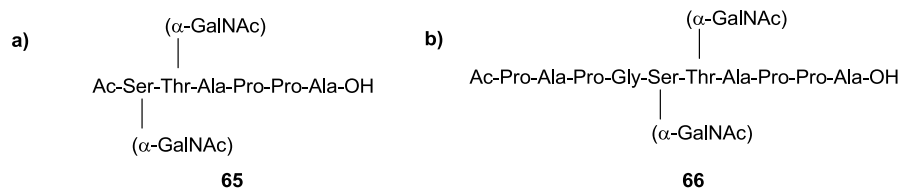
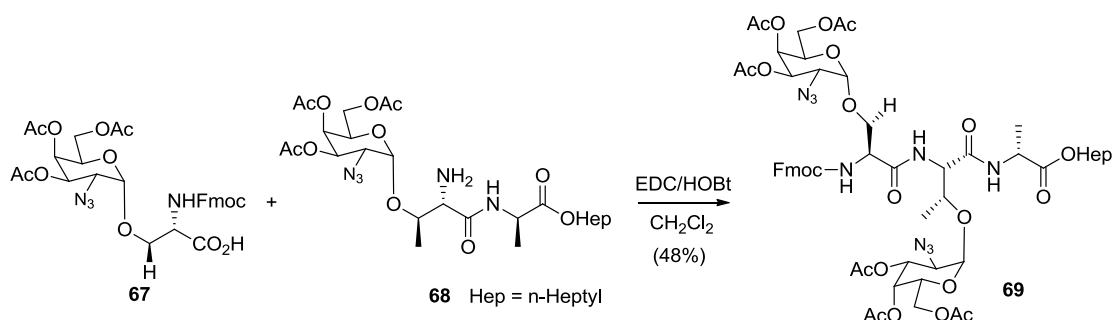


Figure 3.1 MUC1 core related diglycohexapeptide and diglycodecapeptide



Scheme 3.1 Fragment condensation using HOBt and EDC

The Danishefsky group published a paper in 1998 detailing the synthesis of a glycocluster in the T_N and TF (Thomsen-Friedenreich) tumor-associated antigens (Figure 3.2) where the *N*-acetyl galactosamine moiety is α -linked to a serine or threonine residue.⁶⁸ The glycosylated amino acids were each unmasked at the *N*- or *C*-terminus and condensed to obtain the diglycodipeptide (**74/75**) and, subsequently, the triglycotripeptide cluster (**78/79**) (Scheme 3.2). The use of *N*-isobutyloxyl-carbonyl-2-isobutyloxy-1,3,-dihydroquinone (IIDQ) gave great yields in the synthesis of the T_N cluster. However, the bulkier residues, glycosylated by disaccharides in the TF antigen, required the use of HATU/HOAt as the reactions were reported as being “sluggish” with IIDQ.⁶⁸ This observation was pertinent to us as the

serine/threonine galactosides have the advantage of being primary amine nucleophiles, thus providing steric advantages in peptide coupling relative to our hydroxyproline arabinosides. In light of this precedent for addressing the steric challenges, we considered that HATU was a strong candidate for the formation of our oligomers.

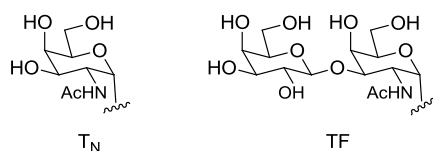
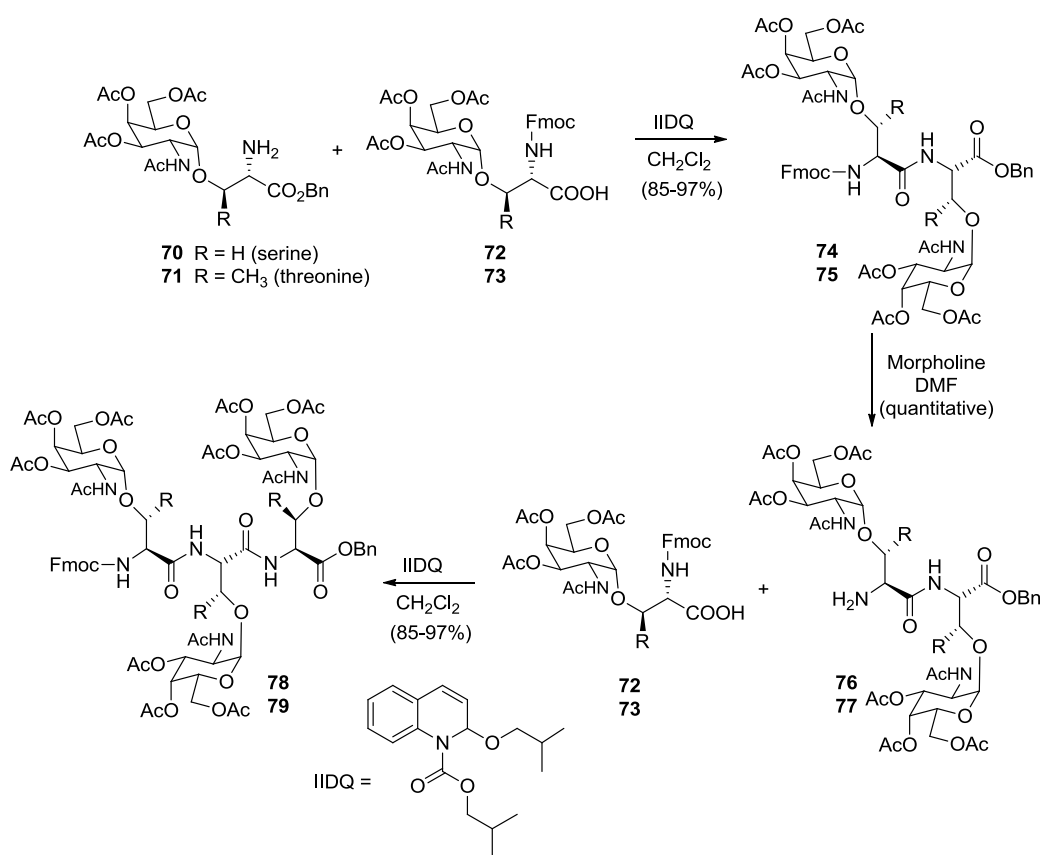


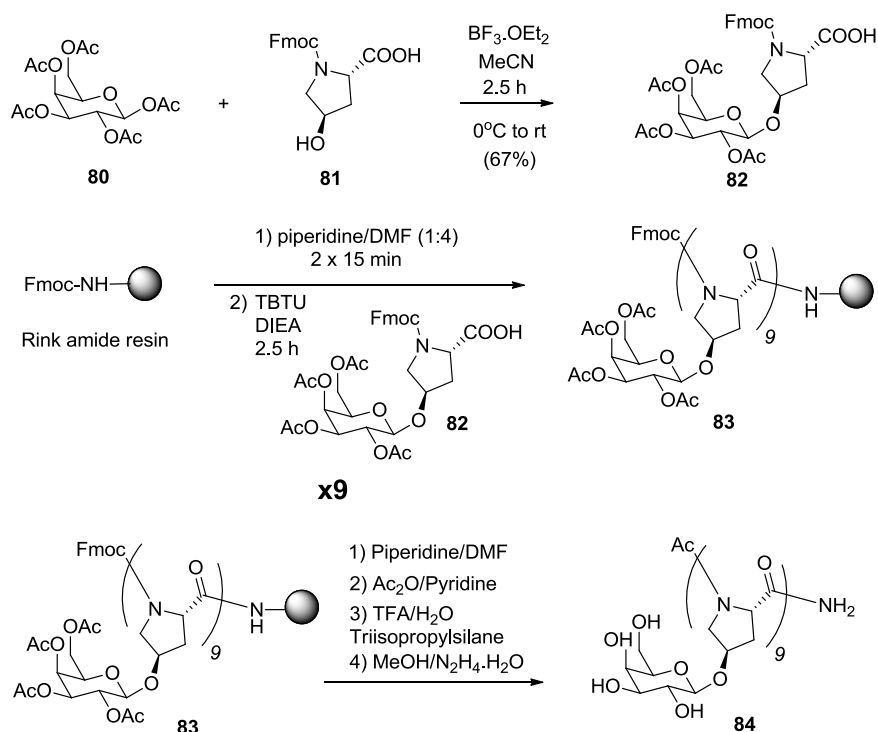
Figure 3.2 T_N and TF antigen



Scheme 3.2 Synthesis of a triglycotriptide cluster (T_N only)

Contiguous *O*-glycosylated amino acid motifs have also been synthesized using solid phase peptide synthesis (SPPS) by the Barany group to prepare mucin-like glycopeptides⁶⁹ and glycopeptide sequences from α -dystroglycan,⁷⁰ an extracellular glycoprotein that controls

muscle function. However, the most relevant SPPS study was reported by the Schweizer group.⁷¹ Owens *et al.* investigated the conformational effects of contiguous *O*-galactosylation of *trans*-L-hydroxyproline (details will be more closely examined in Chapter 4). A per-galactosylated nonapeptide (**83**) was prepared by solid phase synthesis using Fmoc-Rink Amide resin; when the peptide is cleaved from the resin it affords a *C*-terminal amide (**84**) (Scheme 3.3). The hydroxyproline galactoside donor was reportedly prepared in one step from commercially available β -D-galactose pentaacetate (**80**) and Fmoc-Hyp-OH (**81**) giving the 1,2-*trans*-glycoside as the only product. For each on-resin peptide coupling, three equivalents of acid **82** was used in combination with four equivalents of *O*-(benzotriazol-1-yl)-*N,N,N,N*-tetramethyluronium tetrafluoroborate (TBTU) and eight equivalents of diisopropylethyl amine (DIEA). The authors were able to prepare the nonaglycopeptide (**84**) for their structural studies. However, no yields were reported.

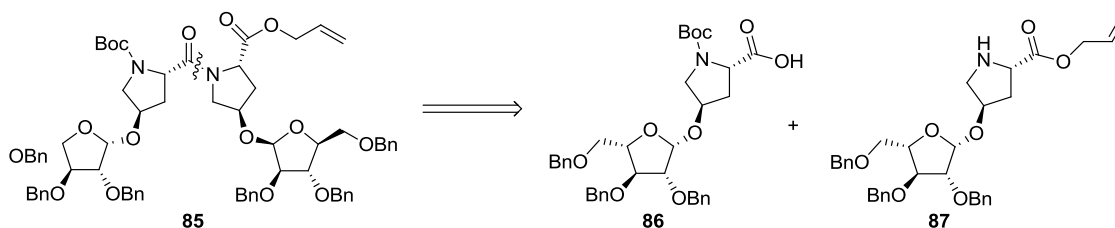


Scheme 3.3 Solid phase peptide synthesis of a nonaglycopeptide

We concluded at the outset that solid phase synthesis was not a realistic route for us due to the high stoichiometry of monomer necessary to carry out each of the cycles. While the galactose pentaacetate donor used by Schweitzer *et al.* is commercially available, our arabinofuranoside donor is not. The difficulty of synthesizing β -L-arabinosides of hydroxyproline, as outlined in Chapter 2, rendered us unwilling to sacrifice the precious material in these excess quantities. Our plan was to utilize the latest advances in solution phase peptide coupling strategies in order to obtain these synthetically challenging glycopeptide clusters in optimal yield and purity.

3.2 Dimer Synthesis

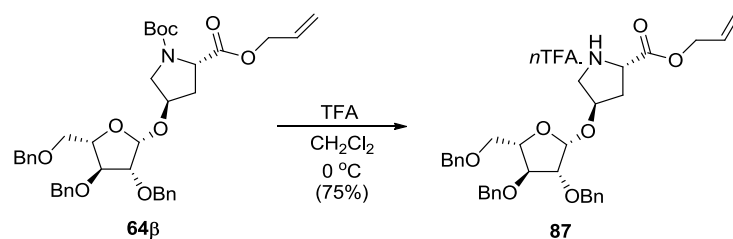
Retrosynthetically, it is obvious that we must derive the free carboxylic acid (**86**) and prolyl amine (**87**) from our hydroxyproline arabinoside monomer for diglycodipeptide (**85**) assembly (Scheme 3.4). Our choice of deprotection methods should look to leave the non-targeted protecting groups unaffected, as well as preserving the ever important O-glycosidic linkage.



Scheme 3.4 Retrosynthetic analysis of dimer

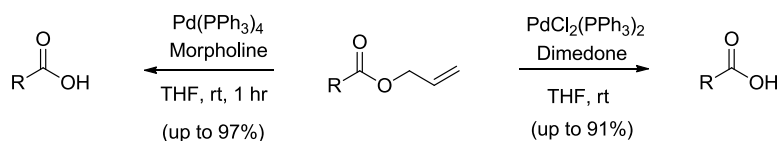
Treatment of compound **64b** (Scheme 3.5) with trifluoroacetic acid afforded the secondary amine **87**. When the reaction was carried out at room temperature, we isolated small amounts of a prolyl species lacking the carbohydrate moiety. To minimize cleavage of the O-glycosidic linkage, we therefore removed the Boc-carbamate at 0 °C. While the amine salt is typically not purified any further due to its high polarity, we found it beneficial to submit the

residue to flash chromatography prior to the coupling reaction. Proton and ^{13}C NMR spectra of compound **87** saw the disappearance of the second set of peaks present in the spectra of **64 β** as a consequence of rotational isomerization, thus confirming that the two species observed in the spectra of **64 β** were indeed assignable to carbamate rotamers.

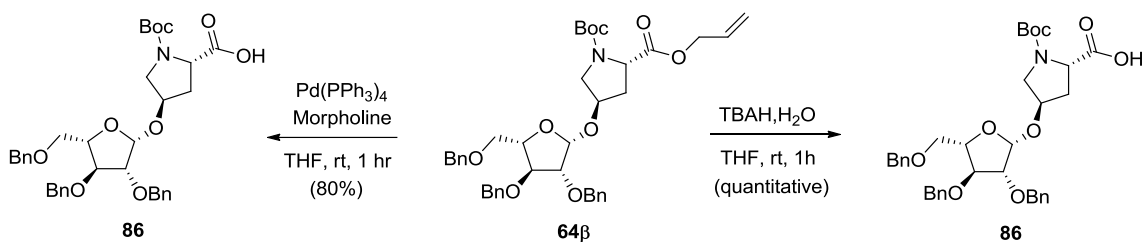


Scheme 3.5 Boc deprotection of monomer

Our initial motivation to mask the acid as an allyl ester was the established ease of deprotection under mild or neutral conditions (Scheme 3.6). Deallylation of the allyl ester with 10 mol % of palladium (0) and an allyl scavenger could be achieved in excellent yield as shown by the groups of Zhang and Kunz.⁷² We chose *tetrakis*(triphenylphosphine)palladium(0) and morpholine as the reaction conditions because the scavenger and its allylated counterpart could be purified from the product through simple extraction using dilute HCl. The product, however, could not be rendered free from residual catalyst, as evidenced by the distinct gold color which carried into the dimeric product of coupling. The high polarity of the free acid also made purification by flash chromatography difficult. In search of an ester cleavage protocol free of byproducts, we decided to try mild basic hydrolysis using aqueous tetrabutylammonium hydroxide (TBAH) in THF (Scheme 3.7).⁷³ The product of this reaction was colorless and was not subjected to flash chromatography despite it being not completely free of byproducts.

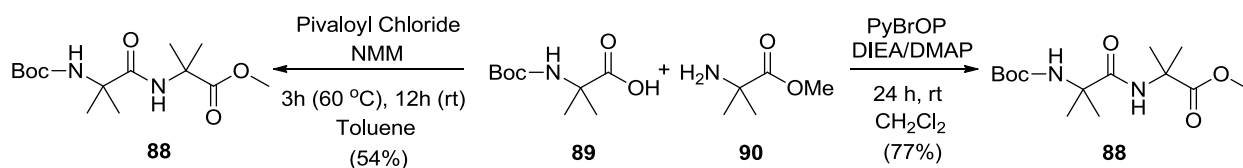


Scheme 3.6 Known methods of allyl ester deprotection



Scheme 3.7 Deallylation of monomer

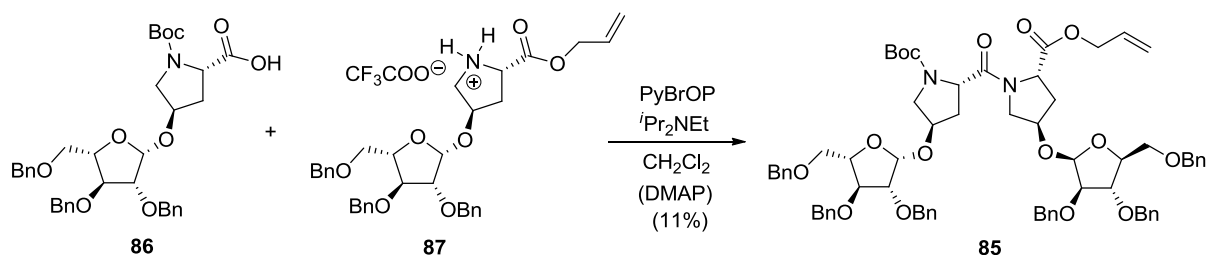
We tried a variety of coupling reagents in the synthesis of the clustered diglycodipeptide. We first looked at bromo-*tris*-pyrrolidinophosphoniumhexafluorophosphate (PyBrOP) for our coupling due to its efficiency in the difficult coupling of the dipeptide of α -aminoisobutyric acid (Aib) (**88**) (Scheme 3.8).⁷⁴ Aib is a sterically hindered α -methylalanyl residue that can affect the conformation⁷⁵ of a peptide as well as its pharmacological activity. The coupling of Boc-Aib-OH (**89**) and H₂N-Aib-OMe (**90**) was carried out using PyBrOP and 4-dimethylaminopyridine (DMAP) to give a 77% yield of the hindered dipeptide **88**. Previous methods using pivaloyl chloride and NMM, which constructed the dipeptide by way of a mixed anhydride, gave only 54% of product.⁷⁶ Considering that both our nucleophile and carboxylate are also fairly hindered, we chose PyBrOP as our first coupling reagent.



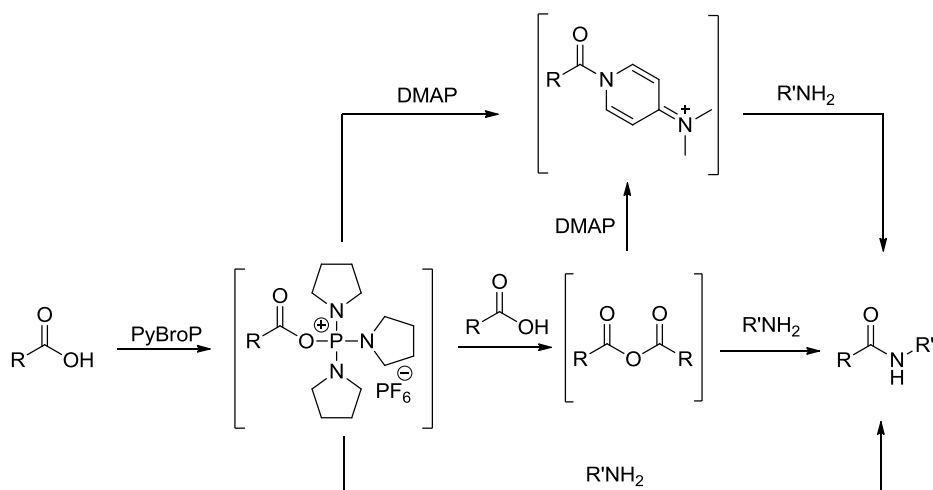
Scheme 3.8 Difficult coupling of a dipeptide of aminoisobutyric acid

Coupling of acid **86** and amine **87** with PyBrOP (Scheme 3.9) yielded unsatisfactory results. Thin layer chromatography (TLC) showed an array of products and the diglycodipeptide (**85**) was isolated in only 11% yield. Unreacted amine and acid starting materials were evident by TLC. Frerot *et al.* showed that addition of DMAP to peptide coupling reactions can improve yields when used in combination with PyBrOP.⁷⁴ PyBrOP is known to facilitate the formation of

anhydrides⁷⁷ while DMAP promotes the aminolysis of these anhydrides (Scheme 3.10). Unfortunately, the isolated yields of **85** were not much better than coupling without DMAP.



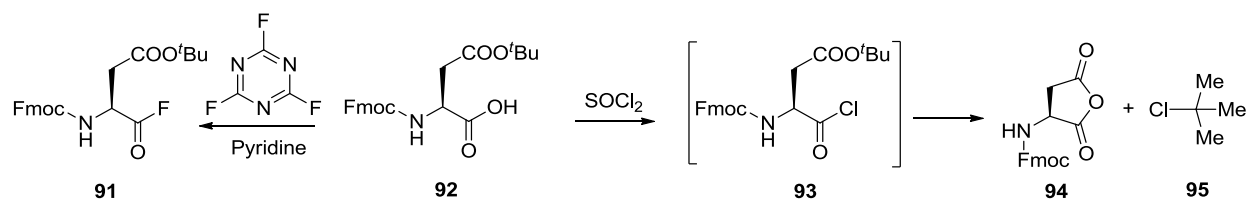
Scheme 3.9 Fragment condensation of dimer with PyBrOP



Scheme 3.10 Mechanism of PyBrOP/DMAP mediated coupling

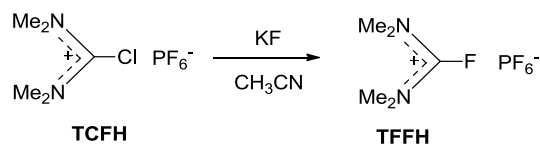
Given the inefficiency of PyBrOP, we moved to a coupling reagent that would generate a less sterically hindered activated species. Carpino and coworkers published a paper in 1990 detailing a new peptide coupling strategy involving the use of stable amino acid fluorides (e.g., **91**) as key intermediates (Scheme 3.11).⁷⁸ An amino acid fluoride has an advantage over its chloride counterpart due to the smaller size of the leaving halide. Moreover, amino acid chlorides have shown lability in reactions involving acid side chains containing *tert*-butyl esters wherein formation of the cyclic anhydride **94** and *tert*-butyl chloride (**95**) side products are observed.⁷⁹ This instability is not limited to *tert*-butyl esters, however, as β -1-adamantyl ester,

N-Boc-lysine, and *tert*-butyl ethers of hydroxyl-bearing amino acids also undergo unwanted transformations under coupling conditions involving acid chloride intermediates. Amino acid fluorides do not undergo this process, most likely due to the stronger C-F bond character as compared to its C-Cl counterpart,⁸⁰ while being comparable in reactivity toward amine nucleophiles.⁸¹



Scheme 3.11 Classical preparation of acid fluorides; acid chloride side reactions

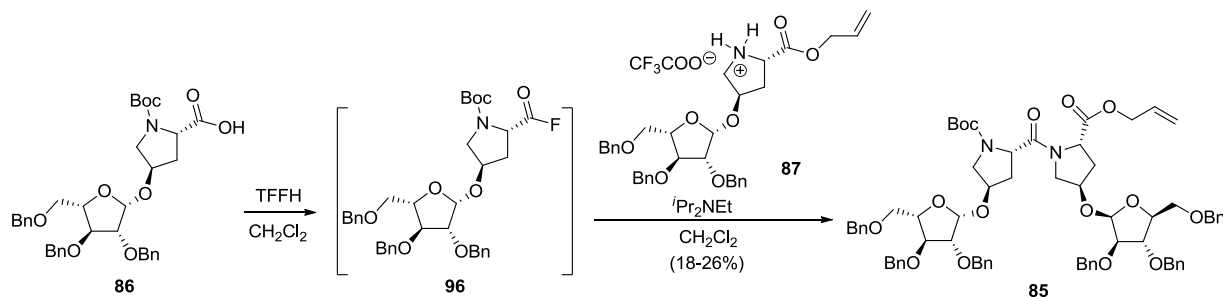
Amino acid fluorides were classically synthesized using cyanuric fluoride in pyridine (Scheme 3.11).⁸² More recently, tetramethylfluoroformamidinium hexafluorophosphate (TFFH) (Scheme 3.12), a much milder reagent relative to cyanuric fluoride, was used to convert Fmoc amino acids to acid fluorides.⁸³ Acid fluorides can be generated by treatment of the corresponding acid with TFFH within 15 minutes, with more hindered amino acids taking up to two hours. While these compounds are stable enough to be isolated, peptide coupling reactions can be subsequently carried out in one pot by adding the amine nucleophile and a hindered amine base after formation of the acid fluoride.



Scheme 3.12 Preparation of TFFH

Initial use of TFFH in generating the acyl fluoride of our acid **86** for coupling with the amine monomer **87** gave an increased yield when compared to coupling with PyBroP (Scheme 3.13). Chemical yields ranging from 18-26% were obtained using TFFH. Thin layer chromatography showed that significant amounts of unreacted acid and amine monomers were

present, in common with couplings using PyBrOP. This led us to believe that not all acid monomer was converted to the acyl fluoride **96** or, perhaps once formed, the intermediate underwent hydrolysis by adventitious water. While reaction with TFFH gave yields significantly better than PyBrOP, the results were still unsatisfactory.



Scheme 3.13 Fragment condensation to produce dimer with TFFH

Peptide coupling reagent O-(7-azabenzotriazol-1-yl)-1,1,3,3-tetramethyluronium hexafluorophosphate (HATU) has been widely used for amide formation in biologically interesting, complex molecules.⁸⁴ HATU has proven to be superior to its HBTU counterpart⁸⁵ due to the neighboring group effect of the aromatic nitrogen (Figure 3.3b).⁸⁶ Carpino has shown that the true form of HATU/HBTU to be the guanidinium salts (*N*-form) as opposed to the uronium salts (*O*-form),⁸⁷ which was previously believed to be the case. The *O*-isomers have been shown to be more reactive than the *N*-form.

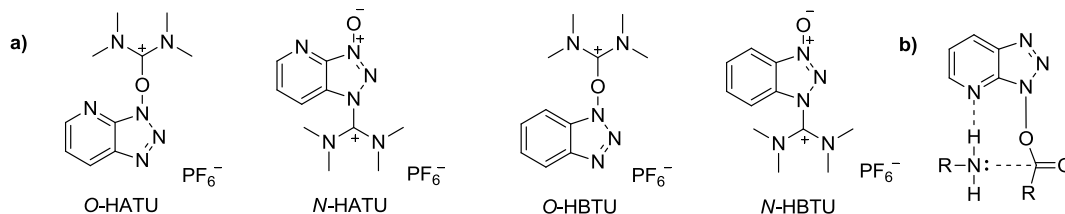
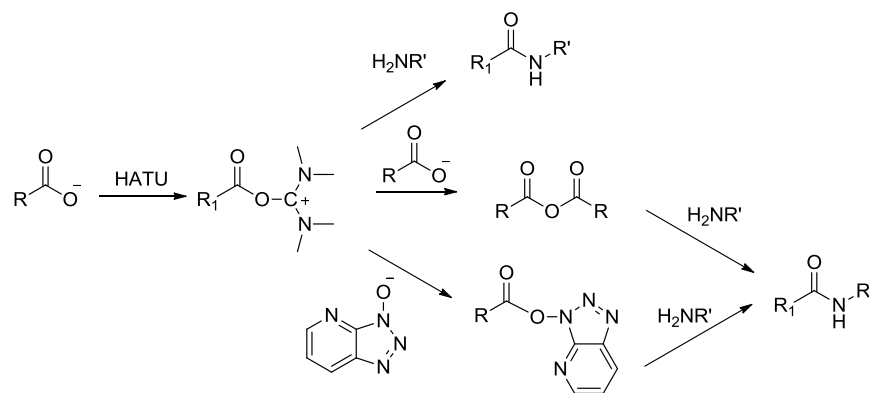


Figure 3.3 a) Guanidinium and uronium salts of HATU and HBTU, b) Neighboring group effect

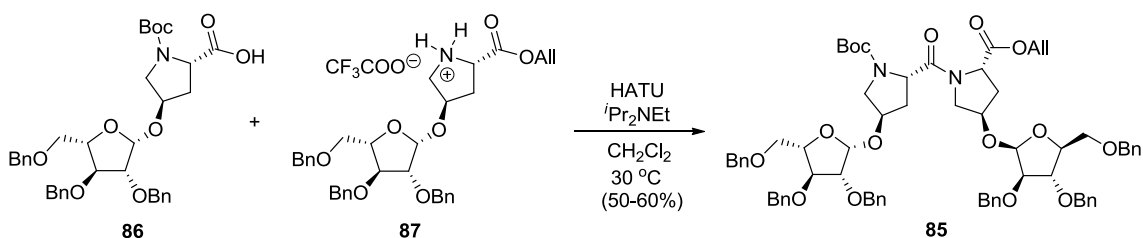
Scheme 3.14 shows the possible pathways of peptide coupling using HATU. Initially, the deprotonated acid nucleophile attacks the electrophilic carbon to form the *O*-acyl urea,

which can immediately couple with the amine nucleophile to give the resulting peptide and urea by-product. At least two other pathways can transpire after initial activation: 1) the *O*-acyl urea can be displaced by another molecule of the carboxylate to form a symmetrical anhydride, 2) formation of the activated ester. The leaving group of either of the intermediates can be displaced by the amine nucleophile to give the desired peptide product.



Scheme 3.14 Pathways of amide formation using HATU

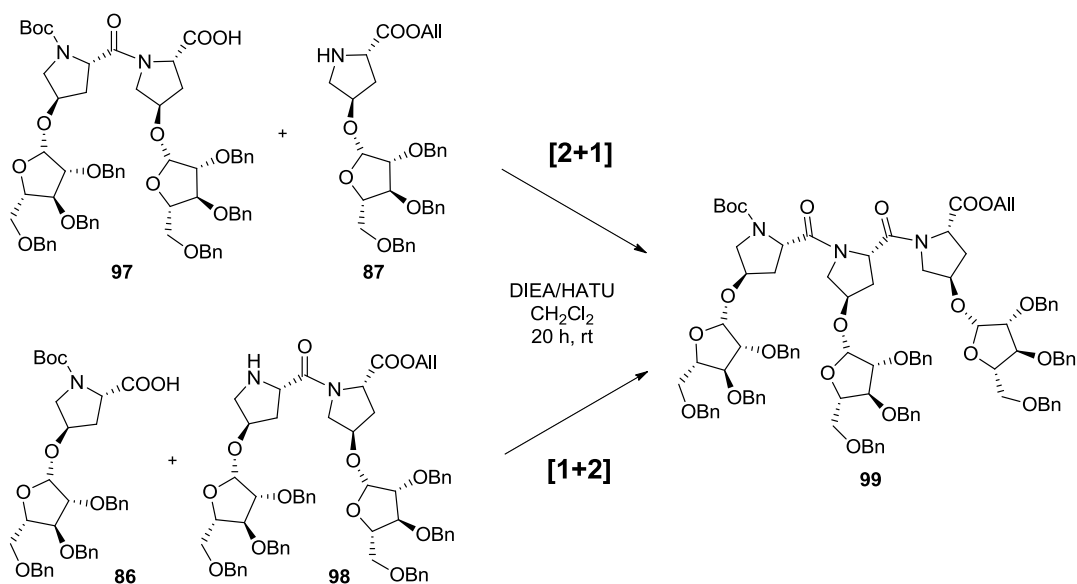
Chemical yields of diglycodi-peptide (**85**), obtained using HATU as the coupling reagent (Scheme 3.15), were immediately better than any reagent we have used previously. Yields of 45-50% were achieved when the reaction was run at room temperature. When the reaction was initiated in an ice bath, then allowing the mixture to warm to room temperature overnight as the ice melted, the percent yield was reduced (~25%). This prompted us to investigate the effects that increasing the temperature might have on this coupling reaction. Interestingly enough, mild heating of the reaction vessel (30 °C) gave higher percent yields (50-60%). Further increase in temperature did not show any improvement in chemical yield. Optimization of this reaction condition has allowed us to obtain the dimer in amounts practical for the further synthesis of larger oligomers. The diglycodi-peptide has been fully characterized by mass spectrometry, ^1H and ^{13}C NMR, and 2-D NMR experiments. Structural studies will be elaborated in Chapter 4.



Scheme 3.15 Fragment condensation to produce dimer using HATU

3.3 Oligomer Synthesis

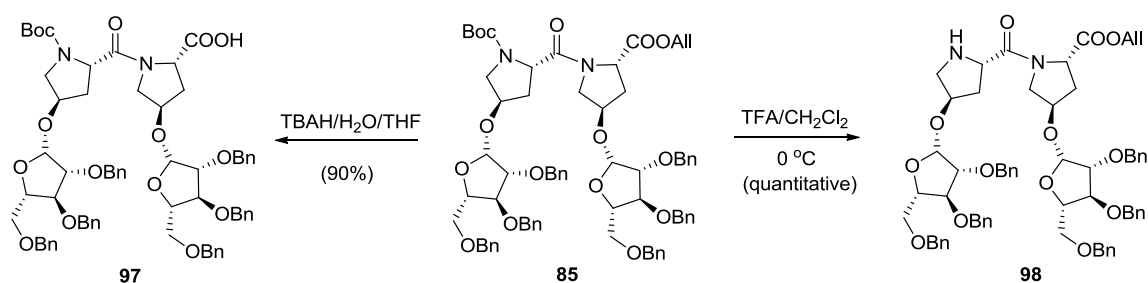
In the preparation of the trimer **99**, we were faced with two possible paths to reach the glycopeptide: a [2+1] or a [1+2] coupling strategy. The [2+1] coupling would place the steric bulk of an extra hydroxyproline arabinoside residue on the free acid **97** in favor of a less sterically hindered amine nucleophile **87**, while the [1+2] strategy would feature a bulkier prolyl nucleophile **98** coupling to a less sterically hindered acid **86** (Scheme 3.16).



Scheme 3.16 [2+1] and [1+2] Trimer coupling strategy

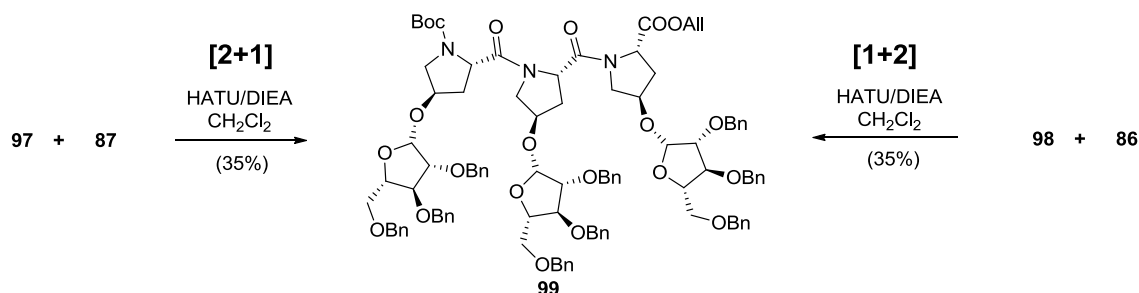
Free acid **97** and amine **98** were prepared from diglycodipeptide **85** (Scheme 3.17). Tetrabutylammonium hydroxide was again used to hydrolyze the allyl ester to avoid the need for

chromatography as the polarity of free dimer acid **97** is higher than that of its monomer counterpart. The heightened polarity likely also accounts for the less than quantitative yields as the dimer acid has a higher affinity for the aqueous layer during work-up. The free amine **98** could still be obtained quantitatively with 50% TFA in dichloromethane at 0 °C.



Scheme 3.17 Preparation of dimer building blocks

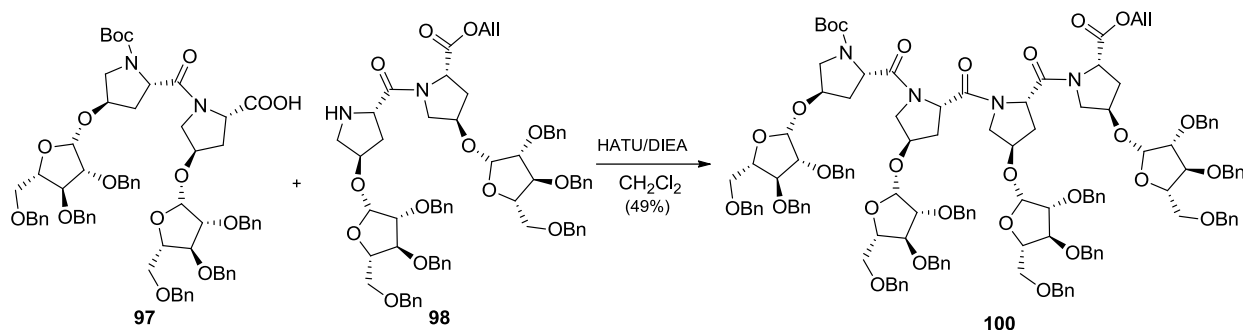
The [2+1] coupling of dimer acid **97** and monomer amine **87** gave the triglycotriptide **99** in ~35% yield (Scheme 3.18). Alternatively, the [1+2] coupling of monomer acid **86** and dimer amine **98** gave a similar yield. In this instance, raising the temperature slightly did not improve the yield in a noticeable fashion.



Scheme 3.18 Fragment condensation to produce trimer

Confronted with low yields for the construction of the triglycotriptide, we chose not to use it as a precursor to the tetramer. Instead, the alternate path of a [2+2] coupling, utilizing two dimer building blocks which could be synthesized in reasonable quantities, was pursued. Thus, free acid dimer **97** was coupled to dipeptide amine **98** to afford the glycotetrapeptide in 49%

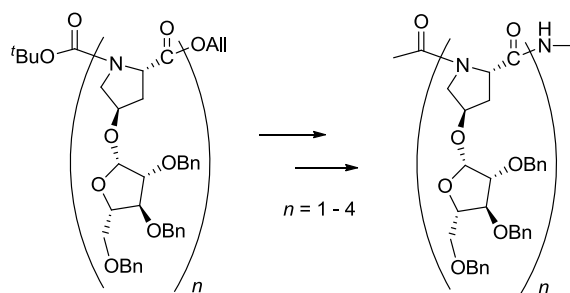
yield (Scheme 3.19). Mass spectrometry, proton, and carbon NMR confirmed the formation of the tetramer (**100**).



Scheme 3.19 Fragment condensation to produce tetramer

3.4 Oligomer End-Capping

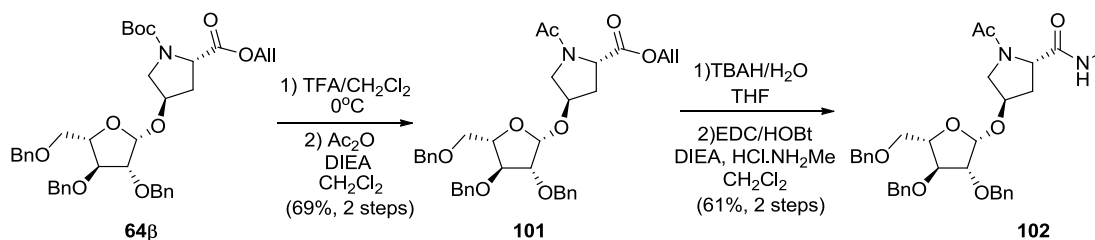
With monomer, dimer, trimer, and tetramer in hand, we began preparations to “end-cap” the glycopeptides. At this stage, the *N*- and *C*-termini were masked as a Boc carbamate and an allyl ester respectively. In order to better mimic the extended peptide, we sought to cap both termini as amides before committing to the global deprotection of the benzyl ethers of the carbohydrate moieties (Scheme 3.20).



Scheme 3.20 End-capping of glycopeptides

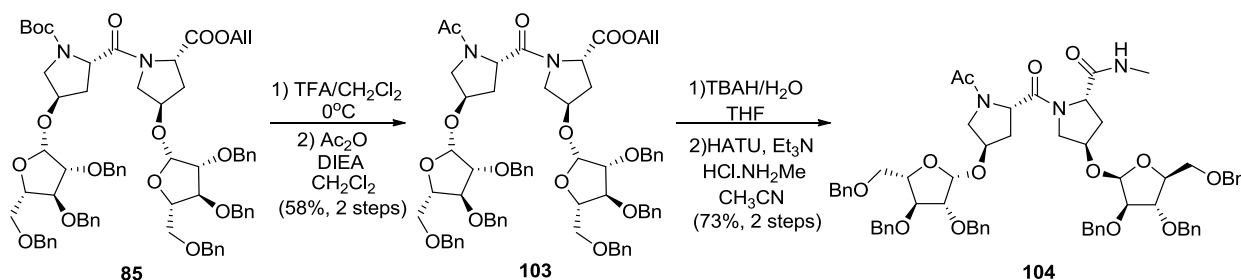
Starting with monomer **64β**, the carbamate was deprotected, as before, using TFA in dichloromethane (Scheme 3.21). Installation of the acetamide with acetic anhydride and diisopropylethyl amine gave compound **101** in 69% yield over two steps. Subsequent deprotection of the allyl ester was carried out under the hydrolysis conditions described

previously. The C-terminal methyl amide was formed using 1-ethyl-3-(3-dimethylaminopropyl) carbodiimide (EDC)/HOBt and methylamine hydrochloride under basic conditions to afford the fully end-capped monomer **102** in satisfactory yield.



Scheme 3.21 Monomer end-capping

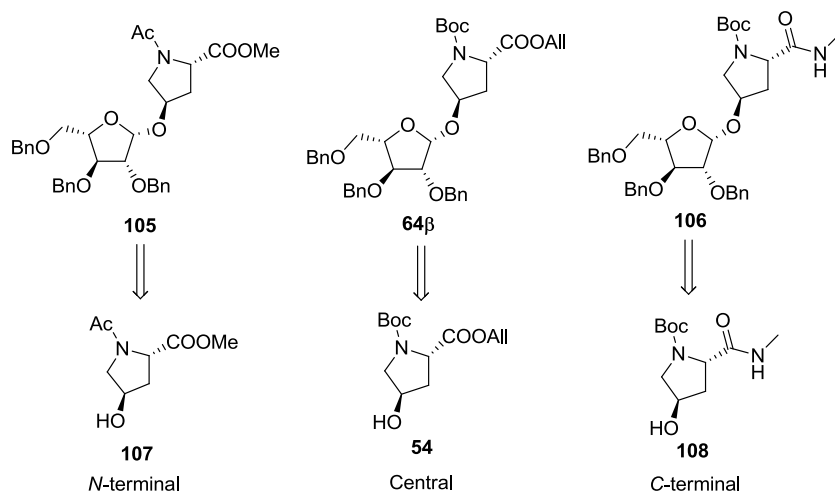
Dimer **85** was treated in a similar fashion to form acetamide **103**, albeit in slightly lower yield, over two steps (Scheme 3.22). Upon deallylation of the free acid, however, we saw a significant drop in yield when using EDC/HOBt as the coupling reagent in the formation of the *N*-methyl amide (**104**). Furthermore, NMR showed that the products obtained were of much lower purity. This problem was rectified by using HATU as the coupling reagent and acetonitrile as the solvent. Quality fully end-capped dimer **104** could be obtained in 73% yield over two steps.



Scheme 3.22 Dimer end-capping

Installation of the *N*- and C-terminal amides on the trimer and tetramer proved not to be trivial. Poor yields (trimer: 18% over 4 steps; tetramer: not obtained) forced us to modify our strategy to include end-caps prior to peptide coupling and/or glycosylation. This strategy has the potential to be more convergent, decreasing four linear steps in the overall oligomer

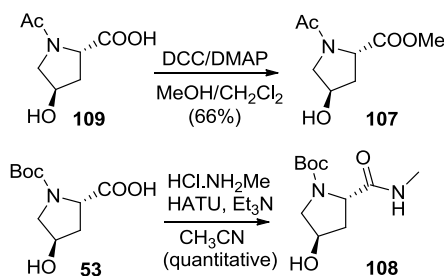
synthesis. This approach called for the preparation of oligomer-specific glycosidic building blocks (Scheme 3.23, **105** and **106**), as well as two new glycosyl acceptors (**107** and **108**).



Scheme 3.23 Oligomer-specific glycosidic building blocks

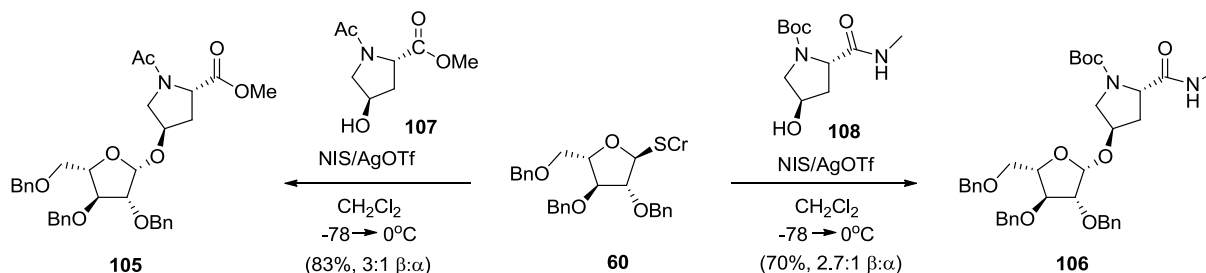
3.5 Pre-End-Capped Glycosides

Glycosyl acceptors **107** and **108** can both be constructed in one step from commercially available *N*-acetyl *trans*-4-hydroxyproline (**109**) and *N*-Boc-*trans*-4-hydroxyproline (**53**) respectively (Scheme 3.24). Treatment of Ac-Hyp-OH with dicyclohexylcarbodiimide (DCC) and 4-DMAP in methanol/dichloromethane affords acceptor **107** in 66% yield. The *N*-methyl amide acceptor **108** could be obtained in quantitative yield using freshly recrystallized methylamine hydrochloride, HATU, and triethylamine in acetonitrile (Scheme 3.24).



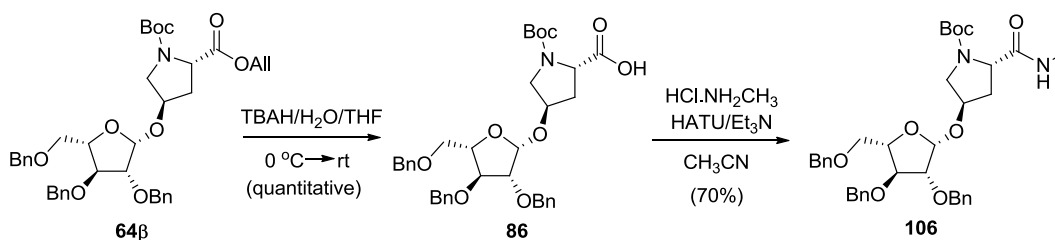
Scheme 3.24 Pre-end-capped glycosyl acceptors

Glycosylation of Ac-Hyp-OMe (**107**) with thioarabinoside donor **60** proved to be high-yielding relative to Boc-Hyp-OAll (Scheme 3.25). While the β : α ratio suffered slightly (3:1 as opposed to 4:1), the overall yield of the target β -glycoside was significantly higher (83% vs 60%). The compromise in selectivity *in lieu* of percent yield did lead to a higher overall yield for the β -glycoside.



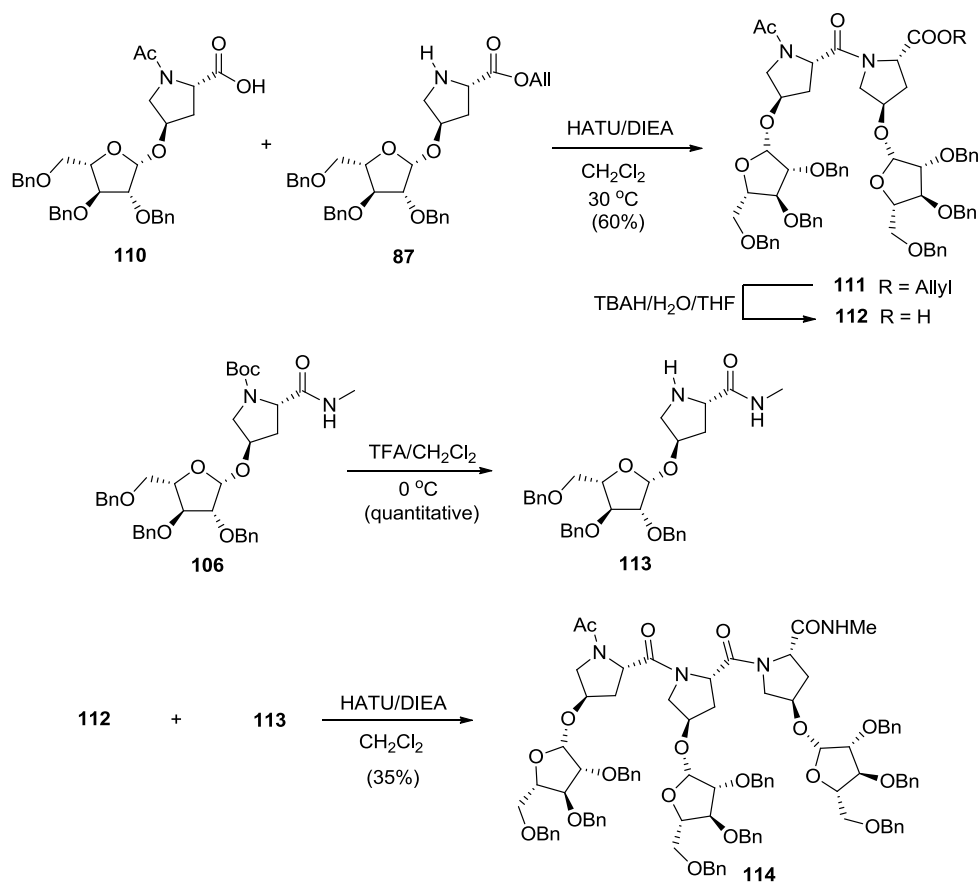
Scheme 3.25 Preparation of pre-end-capped monomers

Glycosylation of Boc-Hyp-NHMe (**108**) with donor **60** under standard conditions gave the methylamide building block **106** in 70 % yield, 2.7:1 β : α ratio. A huge drawback of this reaction is the insufficient polarity differences between the α - and β -anomers. The R_f values of the two diastereomers were nearly indistinguishable, which made separation by flash chromatography all but impossible. We require these building blocks to be synthesized on gram-scale, thus the tedious separation of the anomers by HPLC was impractical. Hence, for this particular building block, we chose to install the methyl amide post-glycosylation on the β -monomer **86** (Scheme 3.26). This transformation can be carried out in two steps from **64 β** to give **106** in good yield.



Scheme 3.26 Alternate strategy for preparation of C-terminal amide glycoside

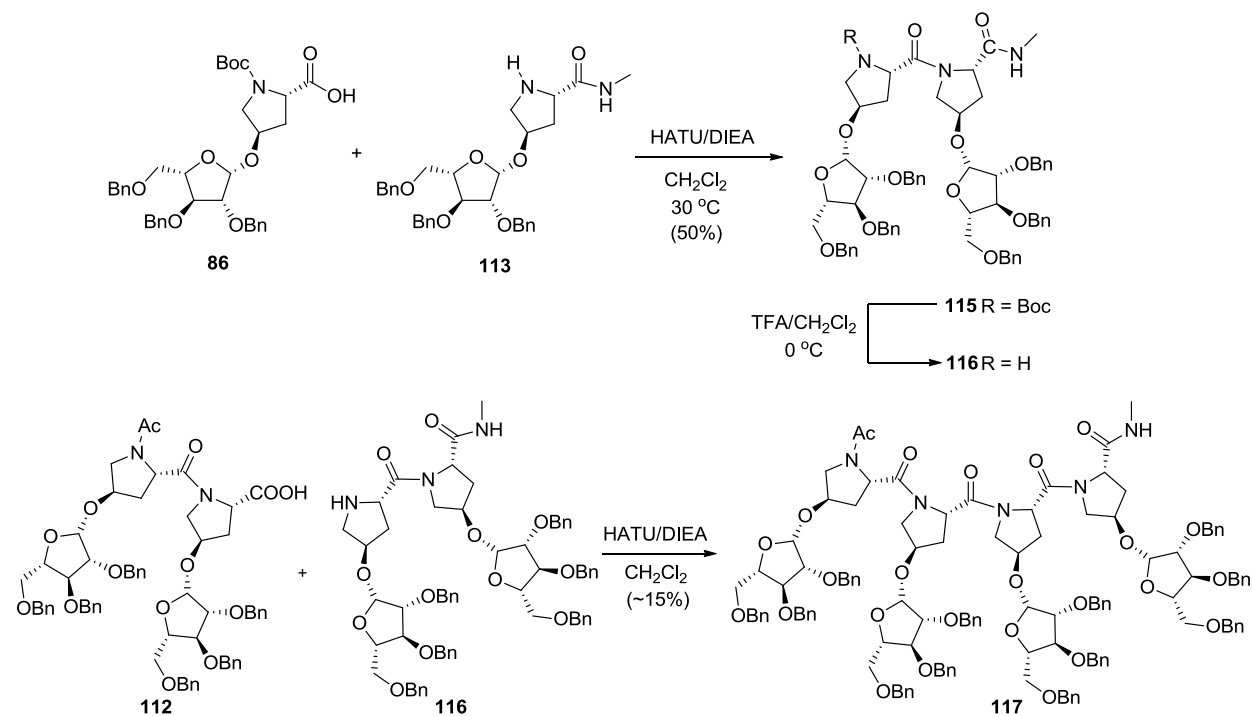
Synthesis of the end-capped triglycotriptide began with coupling of compound **110** and **87** to give the glycodipeptide building block **111** in 60% yield (Scheme 3.27). The allyl ester of the diglycodipeptide was hydrolyzed to reveal the free acid dimer **112**. The *N*-methyl amide monomer **106** was cleaved of its Boc carbamate by TFA in dichloromethane to afford the end-capped free amine **113**. Compounds **112** and **113** were coupled under standard conditions to give the fully end-capped trimer **114** in 35% yield.



Scheme 3.27 Pre-end-capped trimer synthesis

For the synthesis of the fully end-capped tetramer, we chose again to pursue a [2+2] route. The *N*-terminus-capped dimer building block could be formed by the coupling of compounds **86** and **113** under standard conditions (Scheme 3.28). The Boc carbamate (**115**) is

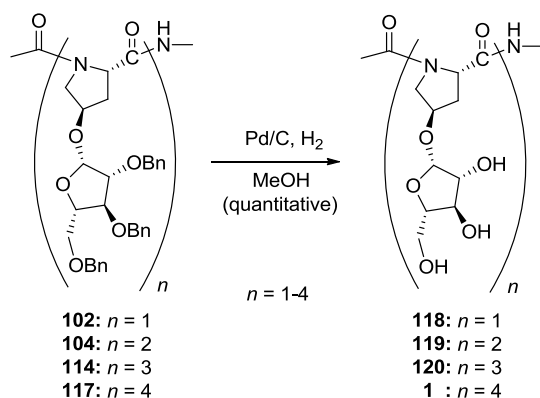
subsequently removed to give the free amine **116**) which is then coupled to free acid dimer **112** with HATU to give the fully end capped tetramer product **117**.



Scheme 3.28 Pre-end-capped tetramer synthesis

3.6 Global Deprotection

Global debenzoylation of all end-capped compounds was carried out using palladium on carbon (Pd/C) and hydrogen gas in methanol (Scheme 3.29). This process gave quantitative yields for all oligomers in an overnight reaction. For the larger oligomers, higher loadings of Pd/C were useful. After filtering off the catalyst, small impurities could be washed away by dissolving the highly polar products in water and extracting with immiscible organic solvents (ethyl acetate, chloroform, dichloromethane). Lyophilization of the aqueous layer overnight afforded the end-capped glycopeptides with fully deprotected arabinoside domains as amorphous solids.

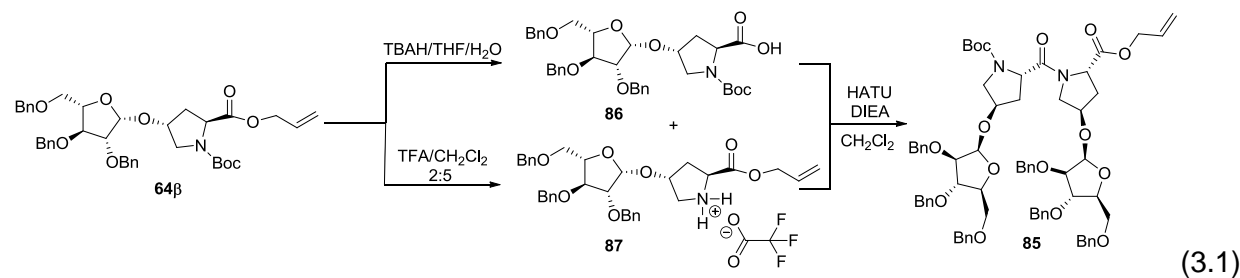


Scheme 3.29 Global debenzylation

3.7 Experimental Section

General methods: as stated in chapter 2.

3.7.1 Experimental procedures



Na-tert-Butyloxycarbonyl-trans-4-hydroxy-4-O-[2,3,5-O-Benzyl-L-arabinofuranosyl]-L-proline

(86) A solution of compound **64β** (662 mg, 1.0 mmol, 1.0 equiv.) in THF (8 mL) was treated with 40% aqueous tetrabutylammonium hydroxide (2.0 mL, 796 mg, 3.0 mmol, 3.0 equiv.) and stirred at RT for 1.5 h. The solvent was evaporated and the residue dissolved in EtOAc (45 mL) and washed with 1M HCl (50 mL). The aqueous portion was back extracted with EtOAc (3 x 25 mL). Organic portions were combined, filtered through MgSO₄, and concentrated. The crude acid **86** (quantitative) was used in the next reaction without further purification.

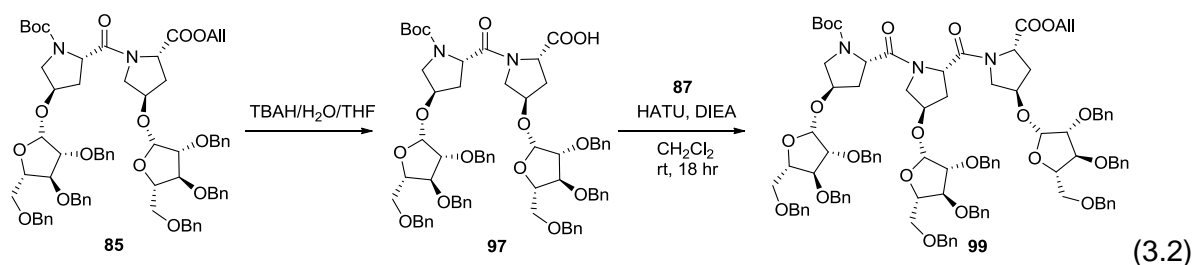
trans-4-Hydroxy-4-O-[2,3,5-O-Benzyl-L-arabinofuranosyl]-L-proline Allyl Ester (87).

Compound **64β** (144 mg, .21 mmol, 1 equiv.) was dissolved in dry CH₂Cl₂ (2.5 mL) and stirred

under N₂. The mixture was cooled to 0 °C and treated with TFA (1 mL) and thioanisole (25 µL, 27 mg, 0.21 mmol, 1.0 equiv.). The mixture was stirred at 0 °C for 30 min, warmed to RT over the next 2.5 h, and concentrated. The residue was purified by flash column chromatography, starting with 2:1 EtOAc/Hex and flushing with 4:1 CH₂Cl₂/MeOH to give **87** as a light brown oil (107 mg, 73%).

Diglycodipeptide (**85**). **87** (56 mg, .08 mmol, 1 equiv.) and **86** (62 mg, 0.10 mmol, 1.2 equiv.) were suspended in dry CH₂Cl₂ (3 mL). The mixture was cooled to 0 °C and DIEA (53 µL, 40 mg, 0.30 mmol, 3.7 equiv.) and HATU (48 mg, 0.13 mmol, 1.5 equiv.) were added successively. The reaction was heated to 30 °C while stirring under N₂ overnight. Upon completion, the mixture was diluted with CH₂Cl₂ to 25 mL total volume, washed with 1M HCl (2 x 20 mL), sat'd NaHCO₃ (20 mL), and brine (20 mL). The organic layer was filtered through MgSO₄ and concentrated. The residue was purified by flash column chromatography, eluting with 1.5:1 Hex/EtOAc → 1.5:1 EtOAc/Hex to give title compound **85** as a light oil (58 mg, 60%). *R*_f 0.56 (2:1 EtOAc/Hex). [α]_D²⁵ +30.1 (*c* 1.0, CH₂Cl₂). ¹H NMR (400 MHz, CDCl₃) δ 1.35 (1.30)* (s, 9H), 1.96-2.13 (m, 2H), 2.17-2.37 (m, 2H), 3.40-3.75 (m, 8H), 3.90-4.27 (m, 6H), 4.38-4.72 (m, 18H), 4.88 (5.08) (s {d, *J* = 4.0 Hz}, 1H), 4.99 (app. t, *J* = ~4.3 Hz, 1H), 5.20 (app. d, *J* = 10.4 Hz, 1H), 5.29 (app. d, *J* = 16.9 Hz, 1H), 5.82-5.91 (m, 1H), 7.25-7.33 (m, 30H); ¹³C NMR (100 MHz, CDCl₃) δ *t*-Boc (28.4, 28.5)*, C-β (35.3, 35.5, 36.0, 36.6), C-δ (50.3, 51.0, 51.6, 51.7), C-α (56.6, 56.8, 57.8, 58.0), CH₂CH=CH₂ (65.7, 65.9), OCH₂Ph (72.0-72.8, 73.4, 73.5), furanose C5 73.3, C-γ (73.8, 74.3), (CH₃)₃C- (75.5, 76.8), furanose C2,3,4 (79.8-84.2), furanose C1 (98.5, 99.3, 98.9, 101.3), CH₂CH=CH₂ (118.4, 118.7), aromatic CH (127.7-128.6), CH₂CH=CH₂ (131.8, 131.9), aromatic -C- (137.4-138.2), NCOOR (153.7, 154.2), COR (171.4, 171.6, 171.4, 171.5); HRMS (ESI) calcd C₇₀H₈₀N₂O₁₅Na for (M+Na)⁺: 1211.5456; obsd: 1211.5412.

*signals in parentheses signify pairs of rotamers.

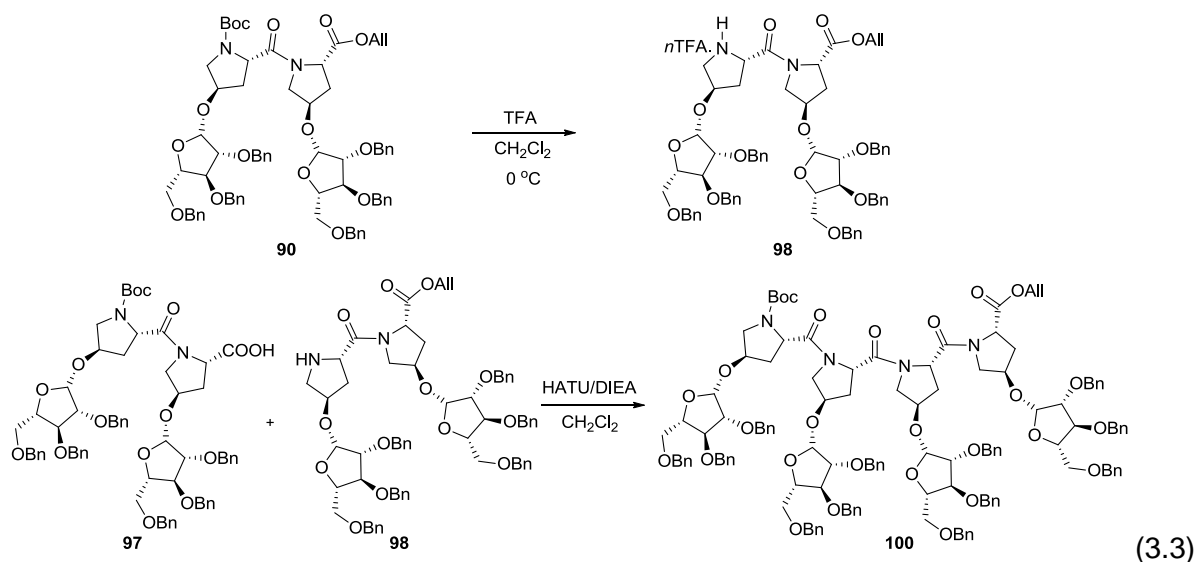


Dimer acid (97). A solution of compound **85** (180 mg, 0.15 mmol, 1.0 equiv.) in THF (3 mL) was treated with a 40% aq. solution of tetrabutylammonium hydroxide (296 μ L, 160 mg, 0.45 mmol, 3.0 equiv.) and stirred at RT under N₂ for 2 h. The solvent was evaporated, the residue dissolved in EtOAc (20 mL) and washed with 1M HCl (15 mL). The aqueous layer was back-extracted with EtOAc (3 x 10 mL). The organic portions were combined, filtered through MgSO₄ and concentrated. The crude acid **97** was obtained in quantitative yield and submitted to the next step without further purification.

Triglycotriptide (99). Compounds **87** (48 mg, 0.07 mmol, 1.0 equiv.) and **97** (81 mg, 0.07 mmol, 1.0 equiv.) were suspended in dry CH₂Cl₂ (3 mL). Diisopropylethylamine (37 μ L, 30 mg, .21 mmol, 3.0 equiv.) and HATU (40 mg, 0.1 mmol, 1.5 equiv.) were added successively. The reaction mixture was stirred for 21 h under N₂. The mixture was diluted with CH₂Cl₂ to a total volume of 25 mL, washed with 1M HCl (2 x 20 mL), sat'd NaHCO₃ (20 mL), and brine (20 mL). The organic layer was filtered through MgSO₄ and concentrated. The residue was purified by flash column chromatography, eluting with 1.5:1 Hex/EtOAc \rightarrow 1.5:1 EtOAc/Hex \rightarrow 1:2 EtOAc/Hex to give the title compound **99** as a light oil (42 mg, 35%). *R*_f 0.62 (2:1 EtOAc/Hex). $[\alpha]_D^{25}$ 42.6 (c 1.0, CH₂Cl₂). ¹H NMR (400 MHz, CDCl₃) δ 1.34 (1.33)* (s, 9H), 1.75-1.80 (m, 1H), 1.90-2.00 (m, 1H), 2.04-2.34 (m, 4H), 3.06-3.67 (m, 8H), 3.84-4.13 (m, 12H), 4.38-4.72 (m, 27H), 4.84 (d, *J* = 4.2 Hz, 0.5H), 4.87 (d, *J* = 4.1 Hz, 0.5H), 4.92 (d, *J* = 3.8, 0.5H), 5.09 (d, *J* = 2.8 Hz, 0.5H), 5.15 (d, *J* = 2.1 Hz, 0.5H), 5.16 (d, *J* = 4.0 Hz, 0.5H), 5.19-5.30 (m, 2H), 5.81-5.91 (m, 1H), 7.28-7.33 (m, 45H); ¹³C NMR (100 MHz, CDCl₃) δ 28.5 (*t*-Boc CH₃), (34.9, 35.1,

35.5, 35.7, 36.0, 36.3) (C-β), (50.0, 50.1, 50.5, 50.7, 51.6, 51.9) (C-δ), (56.6, 56.8, 56.9, 57.0, 57.9, 58.1) (C-α), 65.7 (CH₂CH=CH₂), (72.0-72.7) (OCH₂Ph), (73.1, 73.3) (furanose C5), (73.61, 73.7, 74.5) (C-γ), (79.6, 79.7) (Boc (CH₃)₃C-), (79.9-84.2) (furanose C2,3,4), (98.2, 98.6, 98.9, 101.0) (furanose C1), 118.4 (CH₂CH=CH₂), (127.8-128.4) (Ar 3° CH), 131.8 (CH₂CH=CH₂), (137.5-138.2) (Ar 4° -C-), (153.8, 154.2) (NCOO^tBu), (170.8, 170.8, 171.0, 171.1, 171.4, 171.5) (COR); HRMS (ESI) calcd C₁₀₁H₁₁₂N₃O₂₁Na for (M+Na)⁺: 1726.7759; obsd: 1726.7750.

*Signals in parentheses refer to the minor conformation arising from restricted rotation about the prolyl peptide bond

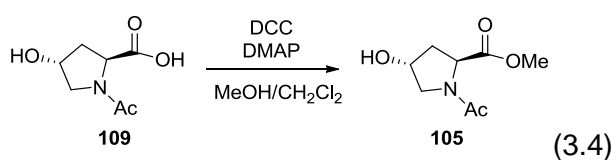


Dimer amine 98. Diglycodipeptide **85** (168 mg, .14 mmol, 1 equiv.) was dissolved in dry CH₂Cl₂ (3 mL) and stirred under N₂. The mixture was cooled to 0 °C and treated with TFA (1.5 mL). The mixture was stirred at 0 °C for 3 h and concentrated to give compound **98** in quantitative yield. The residue was submitted to the next step without further purification.

Tetraglycotetrapeptide 100. Compounds **97** (145 mg, 0.13 mmol, 1 equiv.) and **98** (170 mg, 0.14 mmol, 1.1 equiv.) were suspended in dry CH₂Cl₂ (5 mL). HATU (50 mg, 0.13 mmol, 1.0 equiv.) and DIEA (110 μL, 82 mg, 0.63 mmol, 5.0 equiv.) were added successively. The mixture

was stirred for 18 h under N₂. Upon completion, the solvent was evaporated and the residue diluted with EtOAc (30 mL), washed with 1M HCl (30 mL), sat'd NaHCO₃ (30 mL), and brine (30 mL). The organic layer was filtered through MgSO₄ and concentrated. The residue was purified by flash column chromatography, eluting with 1.5:1 Hex/EtOAc → 1:1 Hex/EtOAc → 1:1.5 Hex/EtOAc → 1:2 Hex/EtOAc to give the title compound **100** as a light oil (138 mg, 49%). *R*_f 0.80 (2:1 EtOAc/Hex). [α]_D²⁵ +42.2 (*c* 1.0, CH₂Cl₂). ¹H NMR (400 MHz, CDCl₃) δ 1.30 [1.26]* (s, 9H), 1.70-2.30 (m, 8H), 3.08-3.66 (m, 16H), 3.76-4.20 (m, 15H), 4.23-4.67 (m, 31H), 4.76-5.10 (anomeric signals, 4H), 5.18 (d, *J* = 10.4 Hz, 1H), 5.27 (d, *J* = 17.3 Hz, 1H), 5.78-5.88 (m, 1H), 7.26-7.31 (m, 60H); ¹³C NMR (100 MHz, CDCl₃) δ (28.5, 29.7) (Boc CH₃), (34.8, 35.0, 35.1, 35.3, 35.4, 35.9, 36.2) (C-β), (50.0, 50.1, 50.2, 50.4, 50.5, 50.8, 51.6, 52.1) (C-δ), (56.7, 56.8, 57.0, 57.1, 57.2, 57.9) (C-α), (65.8) (CH₂CH=CH₂), (72.0-72.6) (OCH₂Ph), (73.2, 73.3, 73.4) (furanose C5), (73.8, 74.0, 74.1, 74.3) (C-γ), (79.6, 79.7) (Boc (CH₃)₃C-), (79.9-84.3) (furanose C2,3,4), (98.0, 98.1, 98.3, 98.6, 98.9, 99.2, 99.4, 100.8) (furanose C1), (118.5, 118.6) (CH₂CH=CH₂), (127.8-128.7) (Ar CH), 131.8 (CH₂CH=CH₂), (137.5-138.2) (Ar -C-), (153.9, 154.2) (NCOO^tBu), (170.4, 170.5, 170.7, 170.9, 171.4) (COR); HRMS (ESI) calcd C₁₃₂H₁₄₅N₄O₂₇Na for (M+Na)⁺: 2242.0067; obsd: 2243.0072.

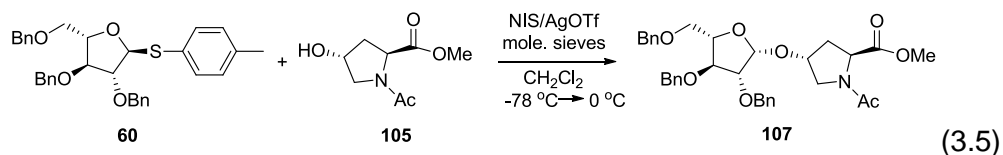
*signals in parentheses refer to the minor conformation arising from restricted rotation about the prolyl peptide bond.



N-Acetyl-*L*-trans-4-hydroxy-*L*-proline methyl ester (**105**). Dicyclohexylcarbodiimide (119 mg, 0.58 mmol, 1.0 equiv.) and 4-DMAP (18 mg, 0.15 mmol, 0.25 equiv.) were added sequentially to a suspension of Ac-Hyp-OH (**109**) (100 mg, 0.58 mmol, 1.0 equiv.) in dry MeOH (2 mL) and CH₂Cl₂ (2 mL). The mixture was stirred overnight under N₂ after which the solvent was

evaporated. The residue was triturated with CH_2Cl_2 and filtered to remove dicyclohexylurea. The filtrate was concentrated and purified by flash column chromatography, eluting with $\text{CH}_2\text{Cl}_2/\text{MeOH}$ (14:1 \rightarrow 10:1) to give compound **105** as an amorphous solid (71 mg, 66%). R_f 0.33 (10:1 $\text{CH}_2\text{Cl}_2/\text{MeOH}$). $[\alpha]_D^{25}$ -89.9 (c 1.0, CH_2Cl_2). ^1H NMR (400 MHz, CDCl_3) δ 2.03-2.10 (2.15-2.23) (m, 1H), 2.07 (1.96)* (s, 3H), 2.26-2.32 (2.41-2.47) (m, 1H), 3.51 (app. d, J = 11.2 Hz, 1H), 3.72 (3.77) (s, 3H), 3.74-3.79 (m, 1H), 4.52-4.57 (4.45) (m, 2H); ^{13}C NMR (100 MHz, CDCl_3) δ 22.2 (21.6), 38.0 (39.7), 52.3 (52.7), 55.9 (54.5), 57.5 (58.8), 70.1 (68.5), 170.0 (170.7), 173.0 (172.7); HRMS (ESI) calcd for $\text{C}_8\text{H}_{14}\text{NO}_4$ ($\text{M}+\text{H}$) $^+$: 188.0917, obsdd: 188.0919.

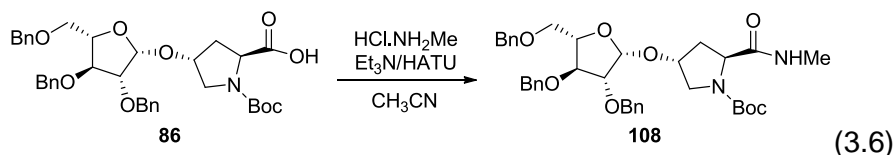
*signals in parentheses refer to the minor conformation arising from restricted rotation about the prolyl peptide bond.



N-Acetyl-trans-4-hydroxy-4-O-[2,3,5-O-benzyl-L-arabinofuranosyl]-L-proline Methyl Ester. A solution of compounds **60** (342 mg, 0.65 mmol, 1.0 equiv.) and **105** (124 mg, 0.66 mmol, 1.0 equiv.) in dry CH_2Cl_2 (40 mL) was stirred with activated powdered 4Å molecular sieves (1.0 g) under N_2 for ~30 min at RT. The suspension was cooled to -78 °C (acetone/dry ice) and then NIS (231 mg, 1.0 mmol, 1.5 equiv.) and AgOTf (83 mg, 0.32 mmol, 0.5 equiv.) were added. The reaction was allowed to gradually reach 0 °C over 1.5 h, at which time it was quenched with Et_3N (2 mL) and filtered. The filtrate was diluted with EtOAc (50 mL) and washed with 10% aqueous $\text{Na}_2\text{S}_2\text{O}_3$ (50 mL) and brine (50 mL). The organic layer was filtered through MgSO_4 and concentrated. The residue, determined to be a 3:1 β : α ratio by NMR, was purified by column chromatography, eluting with 3:1 Hex/EtOAc to afford **107** (317 mg, 83%) as an orange oil. R_f 0.34 (8:1 EtOAc/Hex). $[\alpha]_D^{25}$ 39.2 (c 0.5, CH_2Cl_2). ^1H NMR (400 MHz, CDCl_3) δ 2.02-2.08 (2.10-2.17)* (m, 1H), 2.03 (1.84) (s, 3H), 2.31-2.40 (m, 1H), 3.41 (dd, J = 10.6, 3.6 Hz, 1H),

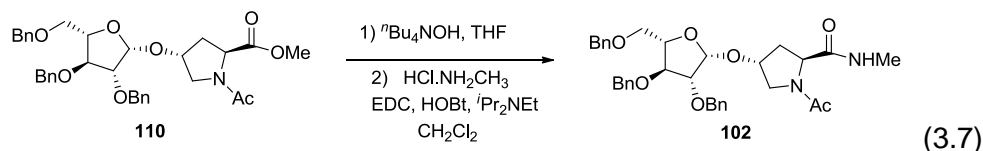
3.49-3.52 (m, 2H), 3.71 (3.75) (s, 3H), 3.72-3.74 (m, 1H), 4.07-4.14 (m, 3H), 4.29-4.43 (m, 1H), 4.48-4.73 (m, 7H), 4.90 (4.98) (d, $J = 3.6$ (4.0) Hz, 1H), 7.27-7.36 (m, 15H); ^{13}C NMR (100 MHz, CDCl_3) δ 22.3 (21.5), 36.0 (38.0), 52.3 (52.7), 52.8 (50.6), 57.5 (58.8), 71.9 (72.2), 72.5 (72.4), 72.7 (73.1), 73.4 (73.3), 76.3, 80.1, 82.4, 84.2 (83.9), 100.5 (99.1), 127.8, 127.9, 128.0, 128.1 (2c), 128.4, 128.5, 128.6, 137.6, 137.8 (137.9), 138.1 (2c), 169.3, 172.7 (172.6); HRMS (ESI) calcd for $\text{C}_{34}\text{H}_{40}\text{NO}_8$ ($\text{M}+\text{H}$) $^+$: 590.2748, obsd: 590.2758.

*signals in parentheses refer to the minor conformation arising from restricted rotation about the prolyl peptide bond



HATU (50 mg, 0.13 mmol, 1.5 equiv) and triethylamine (62 μL , 45 mg, 0.45 mmol, 5 equiv.) were added to a solution of compounds **86** (56 mg, 0.09 mmol, 1 equiv.) and methylamine hydrochloride (12 mg, 0.18 mmol, 2 equiv.) in acetonitrile under an atmosphere of N_2 . The mixture was stirred for 18 h and the solvent evaporated. The residue was diluted with EtOAc (30 mL), washed with 1 M HCl (30 mL) and aq. NaHCO_3 (30 mL), filtered through MgSO_4 , and concentrated. The residue was purified by flash column chromatography, eluting with 8:1 EtOAc/Hex to give the amide product **108** as a light oil (40 mg, 70%). R_f 0.32 (8:1 EtOAc/Hex). $[\alpha]_{\text{D}}^{25}$ 19.6 (c 1.0, CH_2Cl_2). ^1H NMR (400 MHz, CDCl_3) δ 1.44 (1.38)* (s, 9H), 2.08 (br s, 1H), 2.43 (2.32) (br s, 1H), 2.78 (2.77) (s, 3H), 3.43-3.47 (3.75-3.78) (m, 2H), 3.52 (app d, $J = 3.3$ Hz, 2H), 4.06-4.31 (m, 5H), 4.50-4.70 (m, 6H), 4.97 (s, 1H), 6.57 (5.74) (s, 1H), 7.26-7.36 (m, 15H); HRMS (ESI) calcd for $\text{C}_{37}\text{H}_{46}\text{N}_2\text{O}_8$ ($\text{M}+\text{H}$) $^+$: 647.3327, obsd: 647.3323.

*signals in parentheses refer to the minor conformation arising from restricted rotation about the prolyl peptide bond.

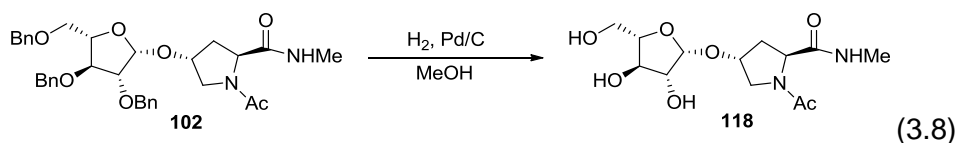


N-Acetyl-*trans*-4-hydroxy-4-*O*-[2,3,5-*O*-benzyl-*L*-arabinofuranosyl]-*L*-proline Methyl Amide (**102**). A solution of compound **110** (121 mg, 0.21 mmol, 1.0 equiv.) in dry THF (4 mL) was treated with a 40% aq. solution of tetrabutylammonium hydroxide (401 μ L, 160 mg, 0.62 mmol, 3.0 equiv.) and stirred at RT under N₂ for 1.5 h. The solvent was evaporated and the residue dissolved in EtOAc (25 mL), washed with 1M HCl (25 mL). The aqueous layer was back-extracted with EtOAc (10 mL). The organic portions were combined, filtered through MgSO₄ and concentrated. The crude acid was obtained in quantitative yield and submitted to next step without further purification.

A suspension of the free acid (56 mg, 0.10 mmol, 1.0 equiv.) and methylamine hydrochloride (8 mg, 0.10 mmol, 1.0 equiv.) in dry CH₂Cl₂ was cooled to 0 °C while stirring under N₂. Diisopropylethylamine (19 μ L, 14 mg, 0.11 mmol, 1.1 equiv.) was added, followed by EDC (21 mg, 0.11 mmol, 1.1 equiv.) and HOBT (17 mg, 0.13 mmol, 1.3 equiv.). The ice bath was then removed and the reaction was left to stir overnight. The mixture was diluted with CH₂Cl₂ (25 mL) and washed with 1 M HCl (25 mL), sat'd NaHCO₃ (aq.) (25 mL), and brine (25 mL). The organic layer was filtered through MgSO₄ and concentrated. The residue was purified by flash column chromatography, eluting with 19:1 CH₂Cl₂/MeOH to give compound **102** (35 mg, 61%) as an oil. *R*_f 0.49 (10:1 CH₂Cl₂/MeOH). [α]_D²⁵ 20.6 (c 1.0, CH₂Cl₂). ¹H NMR (400 MHz, CDCl₃) δ 2.02 (1.84)* (s, 3H), 2.04-2.07 (m, 1H), 2.53 (dt, *J* = 13.0, 5.1 Hz, 1H), 2.72 (2.77) (d, *J* = 4.8 Hz, 3H), 3.36 (3.43) (dd, *J* = 11.6 (12.7), 4.6 (4.1) Hz, 1H), 3.53-3.56 (m, 2H), 3.61 (dd, *J* = 10.7, 5.8 Hz, 1H), 4.07-4.11 (m, 3H), 4.39-4.44 (app. p, *J* = 5.4 Hz, 1H), 4.48-4.73 (m, 7H), 4.94 (4.99) (d, *J* = 3.8 Hz, 1H), 7.26-7.35 (m, 15H); ¹³C NMR (100 MHz, CDCl₃) δ 22.5, 26.2, 34.2, 52.9, 58.37, 72.1, 72.5, 72.7, 73.3, 76.3, 80.1, 82.7, 84.2, 127.7, 127.9, 128.0, 128.1, 128.4,

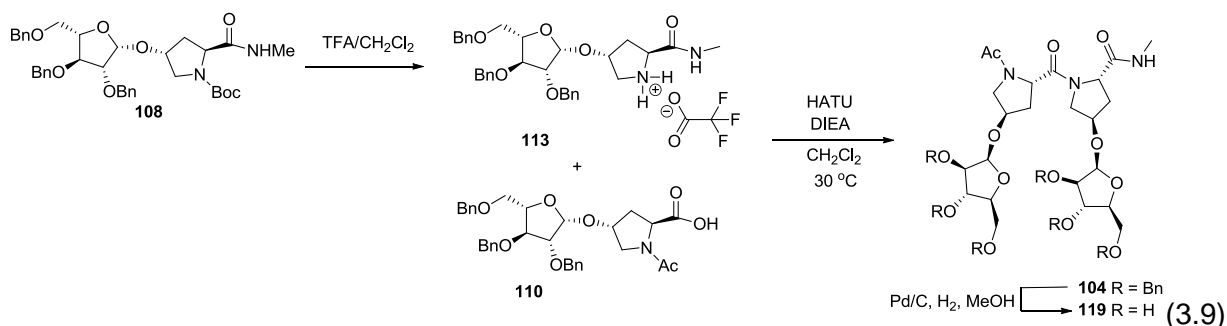
128.5, 128.5, 137.6, 137.9, 138.1, 170.5, 171.4; HRMS (ESI) calcd for C₃₄H₄₁N₂O₇ (M+H)⁺: 589.2908, obsd: 589.2913.

*Signals in parentheses refer to the minor conformation arising from restricted rotation about the prolyl peptide bond. Interestingly, the ¹³C spectrum only displayed signals for one species.



N-Acetyl-4-*O*-[*L*-arabinofuranosyl]-*trans*-4-hydroxy-*L*-proline Methyl Amide (**118**). Palladium on carbon (10% w/w, 45 mg) was added to a solution of compound **102** (35 mg, 0.06 mmol) in MeOH (2 mL). The suspension was stirred under an atmosphere of H₂ gas for 18 h. Upon completion, the mixture was filtered through Celite® and concentrated to give the triol **118** (19 mg, quantitative). [α]_D²⁵ 25.6 (c 0.5, MeOH). ¹H NMR (400 MHz, CD₃OD) δ 2.08 (1.93)* (s, 3H), 2.03-2.10 (2.13-2.19) (m, 1H), 2.47-2.53 (2.59-2.64) (m, 1H), 2.73 (2.77) (s, 3H), 3.34 (s, 1H), 3.56 (dd, *J* = 11.6, 7.1 Hz, 1H), 3.68-3.78 (m, 3H), 3.85-3.91 (m, 1H), 3.96 (dd, *J* = 7.8, 4.6 Hz, 1H), 4.41 (4.51) (t, *J* = 8.0 (7.7) Hz, 1H), 4.45-4.47 (m, 1H), 4.99 (4.95) (d, *J* = 4.6 (4.5) Hz, 1H); ¹³C NMR (100 MHz, CD₃OD) δ 21.0 (20.2), 25.0 (25.1), 36.5 (38.4), 53.5 (51.7), 59.0 (60.1), 63.9 (63.8), 75.0 (74.4), 76.4, 77.2, 83.0, 101.2 (100.7), 171.2 (171.6), 173.7 (173.5); HRMS (ESI) calcd for C₁₃H₂₃N₂O₇ (M+H)⁺: 319.1500, obsd: 319.1486.

*Signals in parentheses refer to the minor conformation arising from restricted rotation about the prolyl peptide bond.



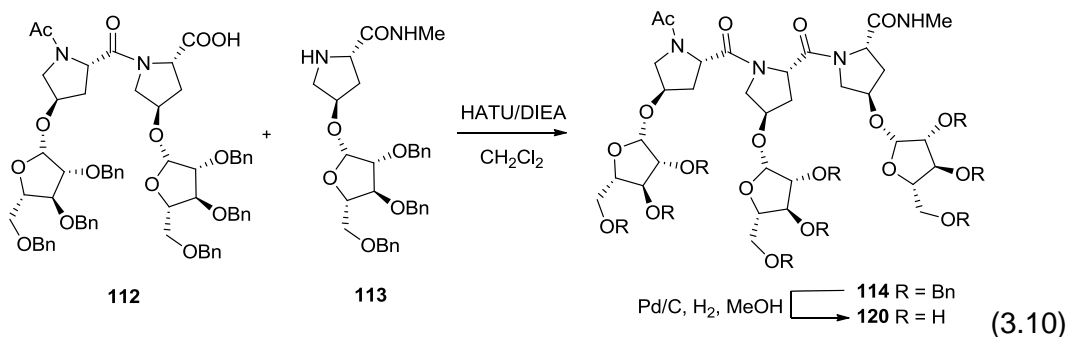
Fully deprotected diglycodipeptide 104. The methyl amide **108** (199 mg, 0.31 mmol, 1 equiv.) was dissolved in dry CH_2Cl_2 (5 mL) and cooled to 0 °C under an atmosphere of N_2 . Trifluoroacetic acid (1.6 mL) was then added and the mixture stirred for 3 h at 0 °C and concentrated. The free amine was submitted to the next reaction without further purification.

The acid **110** (94 mg, 0.14 mmol, 1 equiv.) and amine **113** (104 mg, 0.14 mmol, 1 equiv.) were dissolved in dry CH_2Cl_2 and stirred under N_2 . The coupling reagent HATU (93 mg, 0.21 mmol, 1.5 equiv.) was added and the reaction stirred for 15 min, after which DIEA (102 mg, 137 μL , 0.79 mmol, 5.5 equiv.) was added to the mixture. The reaction was (mildly) heated to 30 °C and stirred for 18 h. The mixture was diluted with CH_2Cl_2 (25 mL), washed with 1 M HCl (25 mL) and brine (25 mL), filtered through MgSO_4 , and concentrated. The residue was purified by flash column chromatography, eluting with 14:1 $\text{CH}_2\text{Cl}_2/\text{MeOH}$ to give the dimer **104** as a cloudy oil (86 mg, 55%).

Palladium on carbon (20 mg, 10% w/w) was added to a solution of compound **104** (19 mg, 0.018 mmol) in MeOH (1 mL). The suspension was stirred under an atmosphere of H_2 gas for 18 h. Upon completion, the mixture was filtered through Celite® washing well with MeOH, and concentrated. The residue was dissolved in H_2O (10 mL) and washed with CH_2Cl_2 (3 x 10 mL) to remove organic impurities. The aqueous layer was lyophilized to give the fully deprotected dimer **119** (10 mg, quantitative) as an amorphous solid. $[\alpha]_D^{25} +30.8$ (c 0.5, MeOH). ^1H NMR (400 MHz, CD_3OD) δ 2.00-2.11 (m, 2H)*, 2.06 (s, 3H), 2.44-2.49 (m, 1H), 2.58-2.63 (m, 1H), 2.73 (s, 3H), 3.55-3.61 (m, 2H), 3.69-3.78 (m, 7H), 3.89-3.99 (m, 4H), 4.12 (d, $J = 11.1$ Hz, 1H),

4.46 (t, $J = 8.1$ Hz, 1H), 4.52 (br s, 1H), 4.76 (t, $J = 8.1$ Hz, 1H), 5.01 (d, $J = 4.2$ Hz, 1H), 5.04 (d, $J = 4.4$ Hz, 1H); ^{13}C NMR (100 MHz, CD_3OD) δ 20.8, 25.0, 35.6, 36.1, 52.4, 53.5, 56.9, 59.4, 74.9, 75.2, 76.2, 76.7, 77.3, 77.4, 83.0, 83.1, 100.9, 101.0, 170.7, 171.9, 173.4; HRMS (ESI+) calcd for $\text{C}_{23}\text{H}_{38}\text{N}_3\text{O}_{13}$ ($\text{M}+\text{H}$) $^+$: 564.2399, obsd: 564.2390.

*Product is predominantly a single species in solution thus minor rotamer not reported.

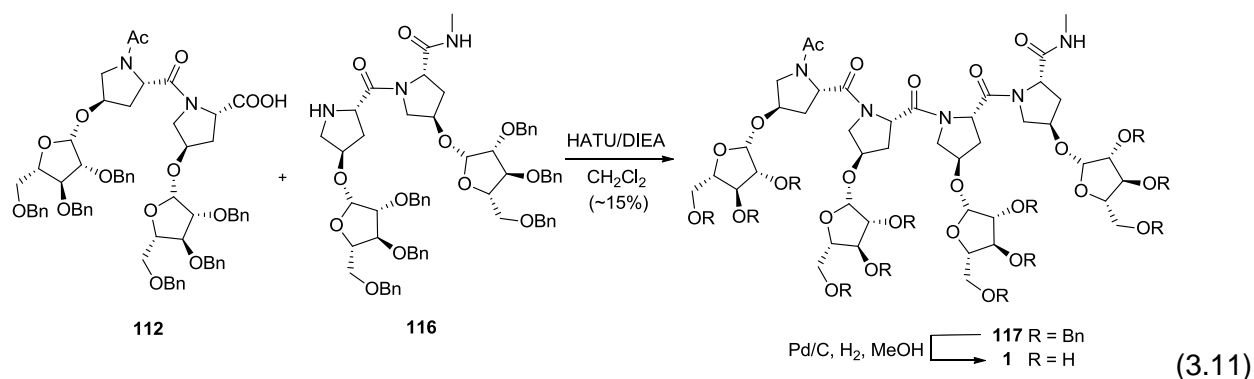


Fully deprotected triglycotriptide 120. The acid **112** (156 mg, 0.14 mmol, 1.0 equiv.) and amine **113** (94 mg, 0.14 mmol, 1.0 equiv.) were dissolved in dry CH_2Cl_2 (5 mL) and stirred under N_2 . The coupling reagent HATU (82 mg, 0.22 mmol, 1.5 equiv.) was added and the reaction stirred for 15 min, after which DIEA (124 μL , 92 mg, 0.71 mmol, 5.0 equiv.) was added to the mixture. The reaction was stirred at rt for 21 h. The mixture was diluted with EtOAc (25 mL), washed with 1 M HCl (25 mL), sat'd NaHCO_3 (25 mL) and brine (25 mL), filtered through MgSO_4 and concentrated. The residue was purified by flash column chromatography, eluting with 19:1 $\text{CH}_2\text{Cl}_2/\text{MeOH}$ to give the protected trimer **114** as a light oil (81 mg, 35%).

Palladium on carbon (100 mg, 10% w/w) was added to a solution of compound **114** (11 mg, 6.8 μmol) in MeOH (1.5 mL). The suspension was stirred under an atmosphere of H_2 gas for 24 h. The mixture was filtered through Celite[®], washing well with MeOH, and concentrated. The residue was dissolved in H_2O (10 mL) and washed with CH_2Cl_2 (3 x 10 mL) to remove organic impurities. The aqueous layer was lyophilized to give the fully deprotected trimer **120** in quantitative yield (5.5 mg). $[\alpha]_{\text{D}}^{25}$ -17.4 (c 0.1, MeOH). ^1H NMR (400 MHz, CD_3OD) δ 2.01-2.17

(m, 3H), 2.11 (s, 3H), 2.47-2.66 (m, 3H), 2.75 (s, 3H), 3.58-3.66 (m, 3H), 3.69-3.78 (m, 10H), 3.86-4.01 (m, 6H), 4.15 (d, $J = 11.5$ Hz, 1H), 4.26 (d, $J = 11.1$ Hz, 1H), 4.48 (t, $J = 8.5$ Hz, 2H), 4.53 (br s, 2H), 4.60 (br s, 1H), 4.79 (t, $J = 8.3$ Hz, 1H), 5.02 (d, $J = 4.4$ Hz, 1H), 5.04 (app t, $J = 4.8$ Hz, 2H); ^{13}C NMR (100 MHz, CD_3OD) δ 24.1, 28.6, 37.5, 37.7, 38.5, 55.4, 55.5, 56.4, 59.6, 60.2, 62.4, 63.2, 65.9, 65.9(5), 66.0, 72.5, 74.4, 77.1, 77.1(5), 77.2, 78.8, 78.8(2), 78.9, 79.0, 79.0(3), 79.3, 84.6, 84.6(7), 84.7, 102.7, 102.8, 102.9, 173.8, 174.6, 174.8, 175.5, 176.5; HRMS (ESI+) calcd for $\text{C}_{33}\text{H}_{52}\text{N}_4\text{O}_{19}$ ($\text{M}+\text{H}$) $^+$: 809.3299, obsd: 809.3314.

*Product is predominantly a single species in solution thus minor rotamer not reported.



Fully deprotected tetraglycotetrapeptide 1. The acid **112** (47 mg, 0.04 mmol, 1.0 equiv.) and amine **116** (71 mg, 0.06 mmol, 1.4 equiv.) were dissolved in dry CH_2Cl_2 (1.75 mL) and stirred under N_2 . The coupling reagent HATU (17 mg, 0.04 mmol, 1.0 equiv.) was added and the reaction stirred for 15 min, after which DIEA (124 μL , 92 mg, 0.16 mmol, 4.0 equiv.) was added to the mixture. The reaction was stirred at rt for 20 h. The mixture was diluted with EtOAc (25 mL), washed with 1 M HCl (25 mL) and brine (25 mL), filtered through MgSO_4 and concentrated. The residue was purified by flash column chromatography, eluting with 19:1 $\text{CH}_2\text{Cl}_2/\text{MeOH}$ to give the protected tetramer **117** as a light oil (14 mg, 15%).

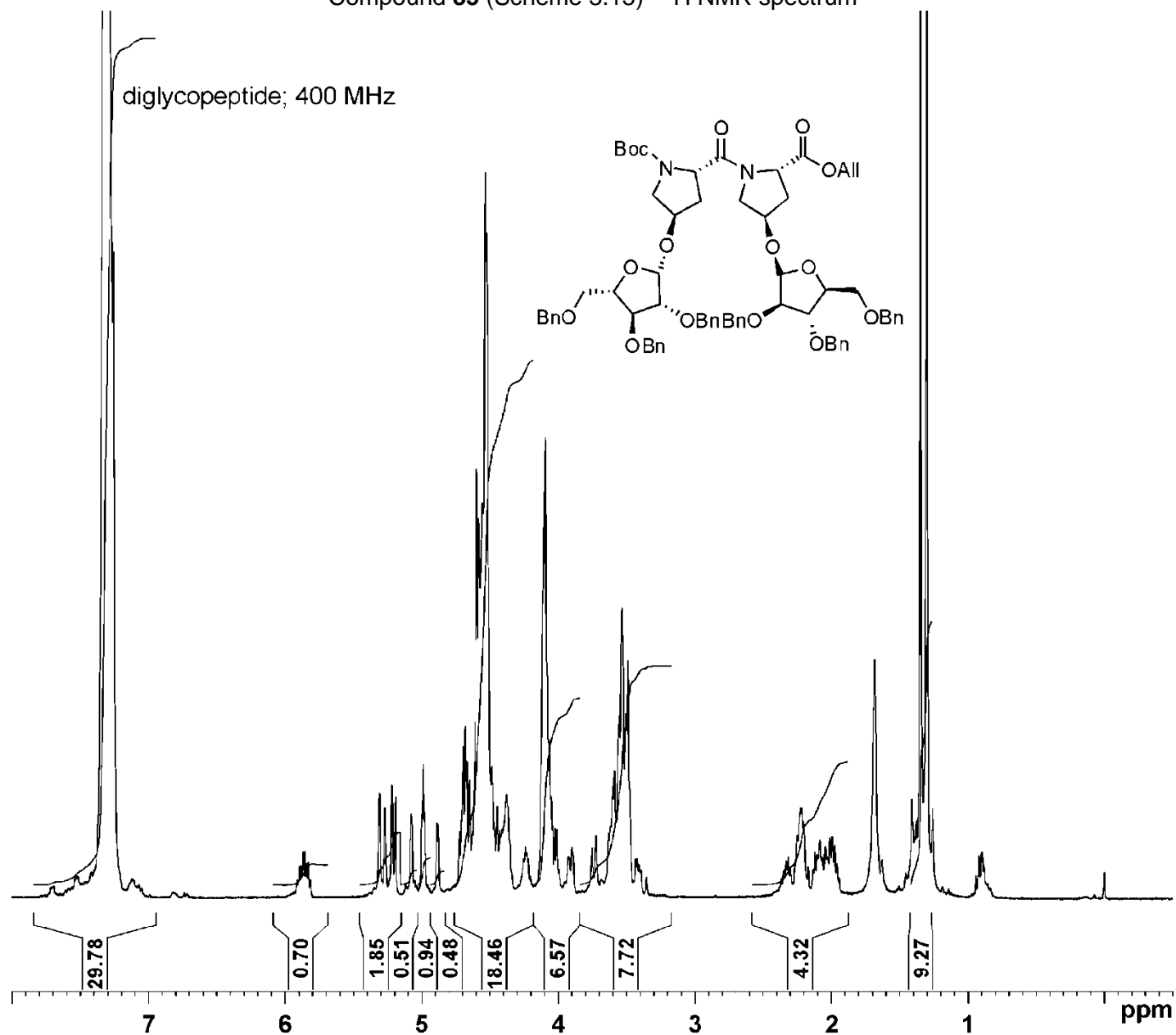
Palladium on carbon (25 mg, 10% w/w) was added to a solution of compound **117** (3 mg, 1.4 μmol) in MeOH (0.6 mL). The suspension was stirred under an atmosphere of H_2 gas for 24 h.

The mixture was filtered through Celite[®], washing well with MeOH, and concentrated. The residue was dissolved in H₂O (10 mL) and washed with CH₂Cl₂ (3 x 10mL) to remove organic impurities. The aqueous layer was lyophilized to give the fully deprotected tetramer **1** in quantitative yield (1.5 mg). $[\alpha]_D^{25} +60.8$ (c 0.075, MeOH). ¹H NMR (400 MHz, CD₃OD) δ 2.04-2.19 (m, 4H), 2.09 (s, 3H), 2.47-2.67 (m, 4H), 2.76 (s, 3H), 3.59-3.65 (m, 4H), 3.73-3.79 (m, 12H), 3.86-4.01 (m, 8H), 4.15 (app d, $J = 11.5$ Hz, 3H), 4.50 (t, $J = 8.0$ Hz, 4H), 4.56 (br s, 4H), 5.04 (d, $J = 4.5$ Hz, 2H), 5.04 (d, $J = 4.3$ Hz, 4H); HRMS (ESI+) calcd for C₄₃H₆₇N₅O₂₅Na (M+Na)⁺: 1076.4017, obsd: 1076.3992.

*Product is predominantly a single species in solution thus minor rotamer not reported.

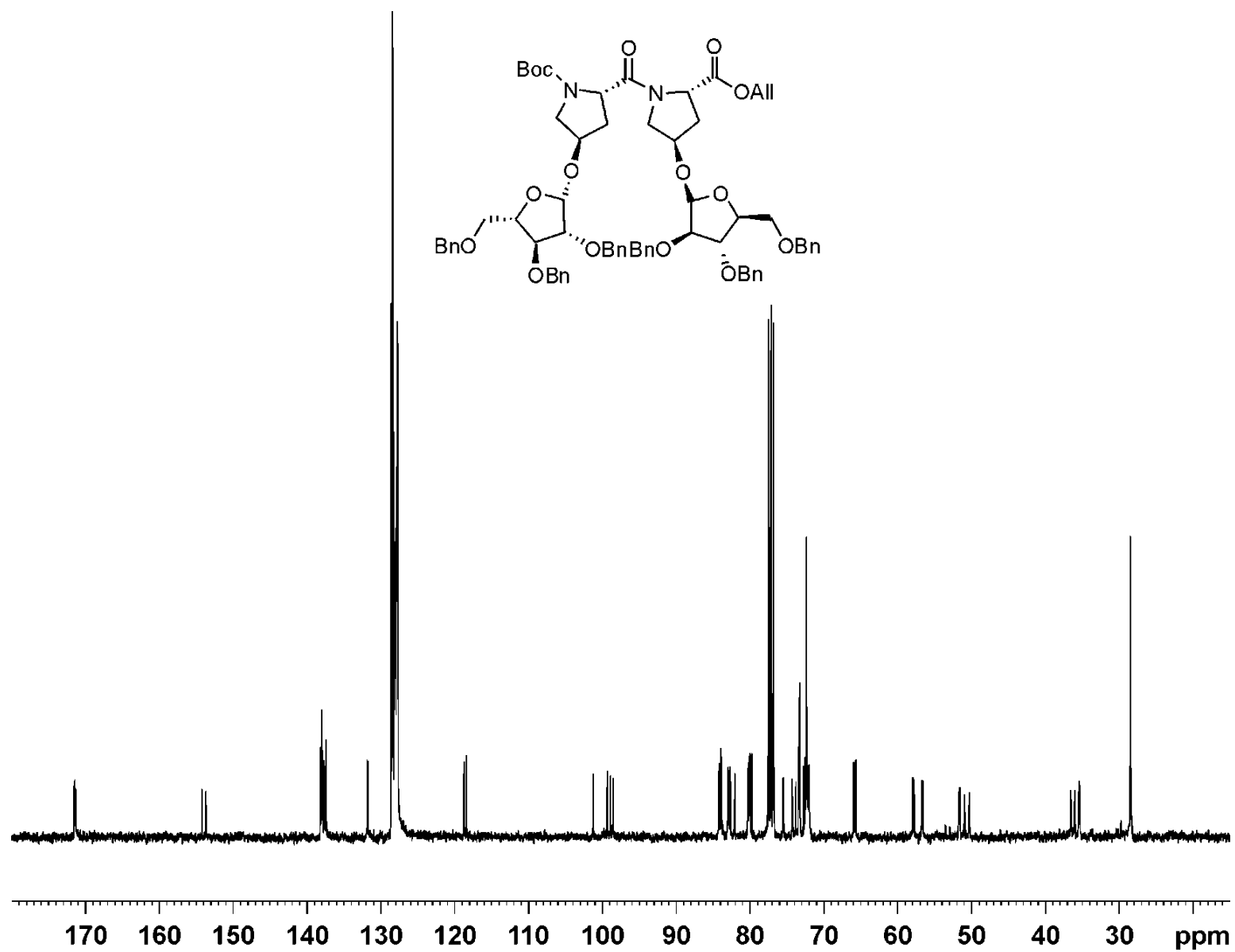
3.7.2 Spectra

Compound **85** (Scheme 3.15) - ^1H NMR spectrum



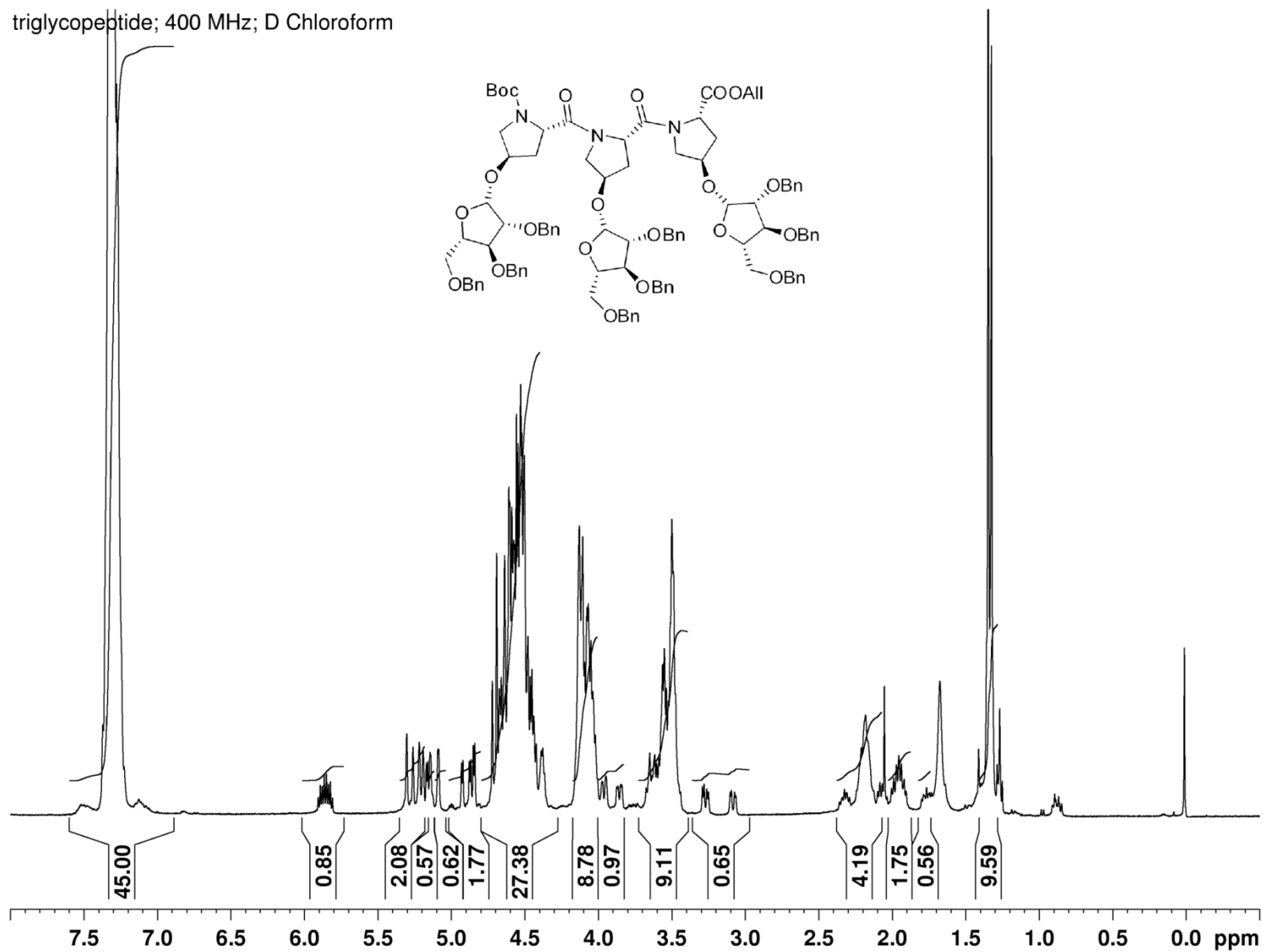
Compound **85** (Scheme 3.15) – ^{13}C NMR spectrum

diglycopeptide; 400 MHz; D Chloroform



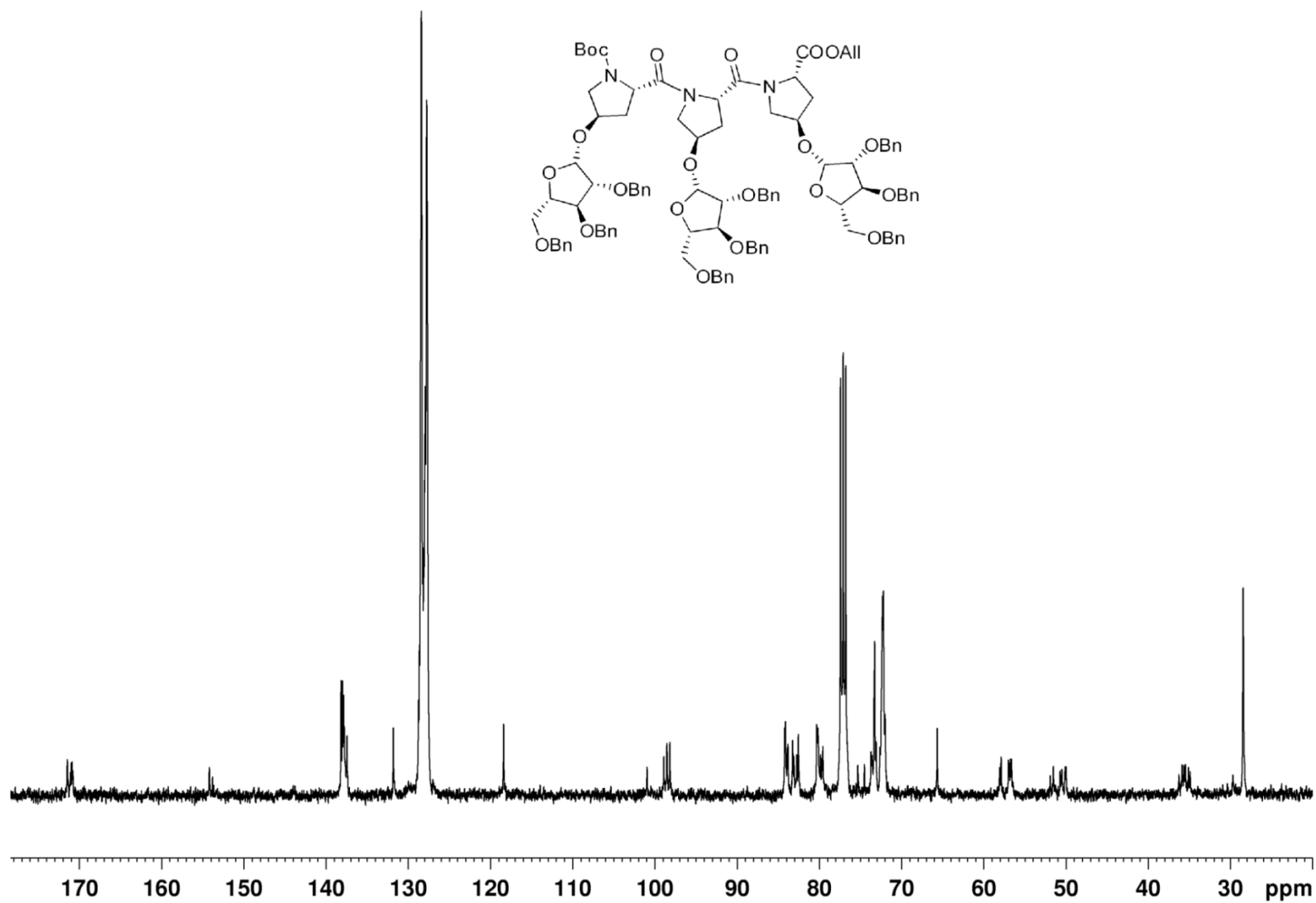
Compound **99** (Scheme 3.18) - ^1H NMR spectrum

triglycopeptide; 400 MHz; D Chloroform



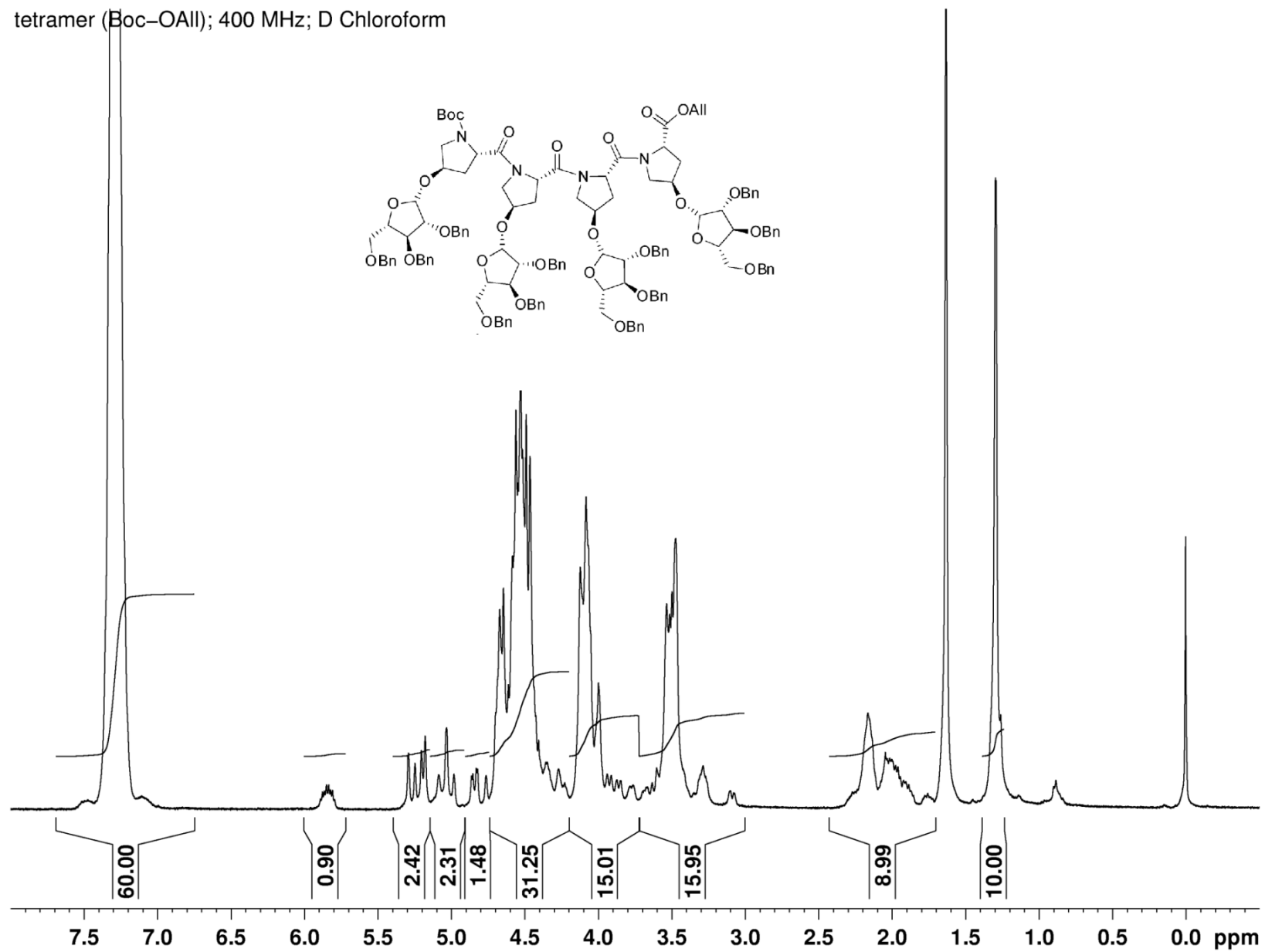
Compound **99** (Scheme 3.18) – ^{13}C NMR spectrum

Triglycopeptide; 400 MHz; D Chloroform



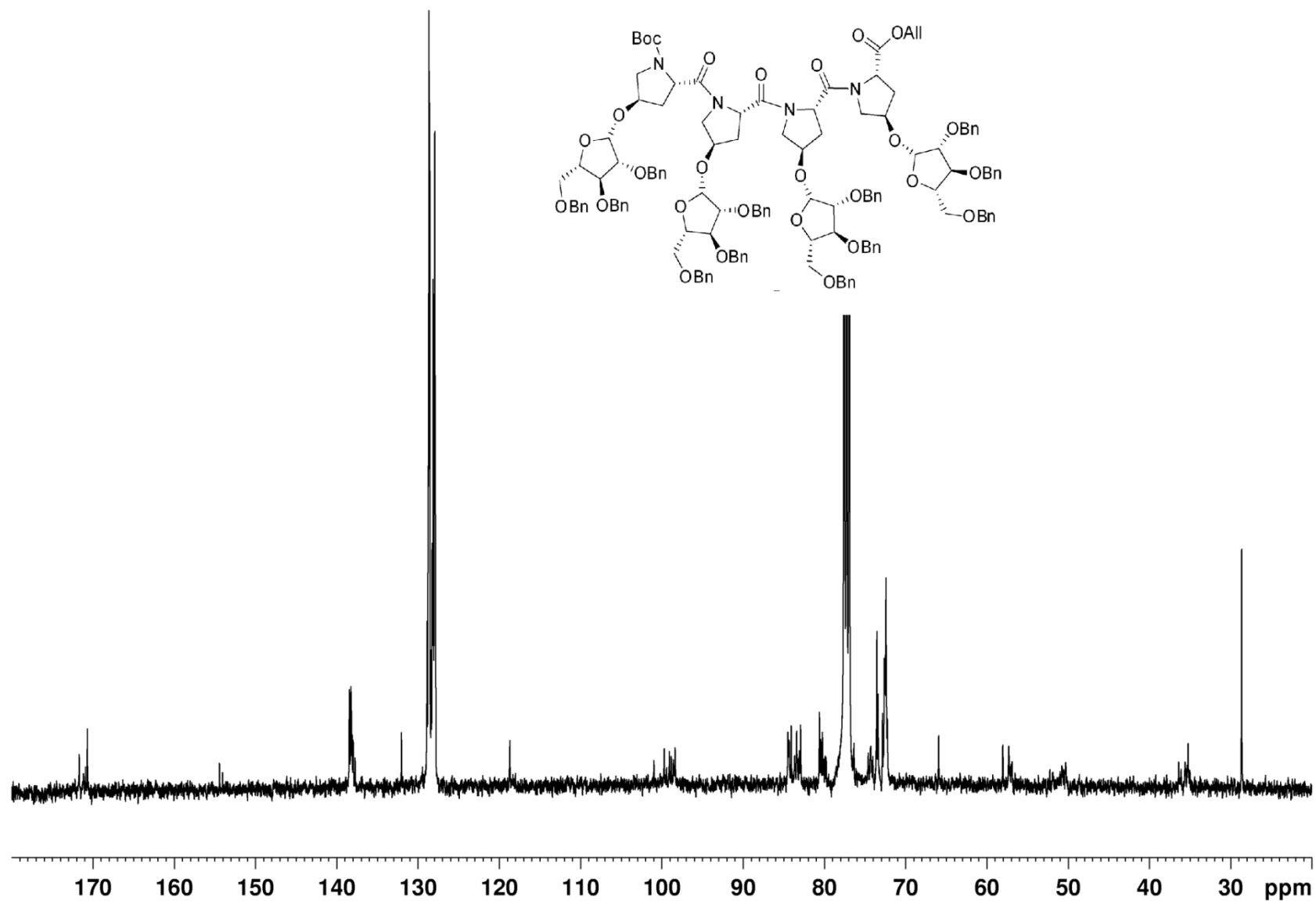
Compound **100** (Scheme 3.19) - ^1H NMR spectrum

tetramer (Boc-OAll); 400 MHz; D Chloroform



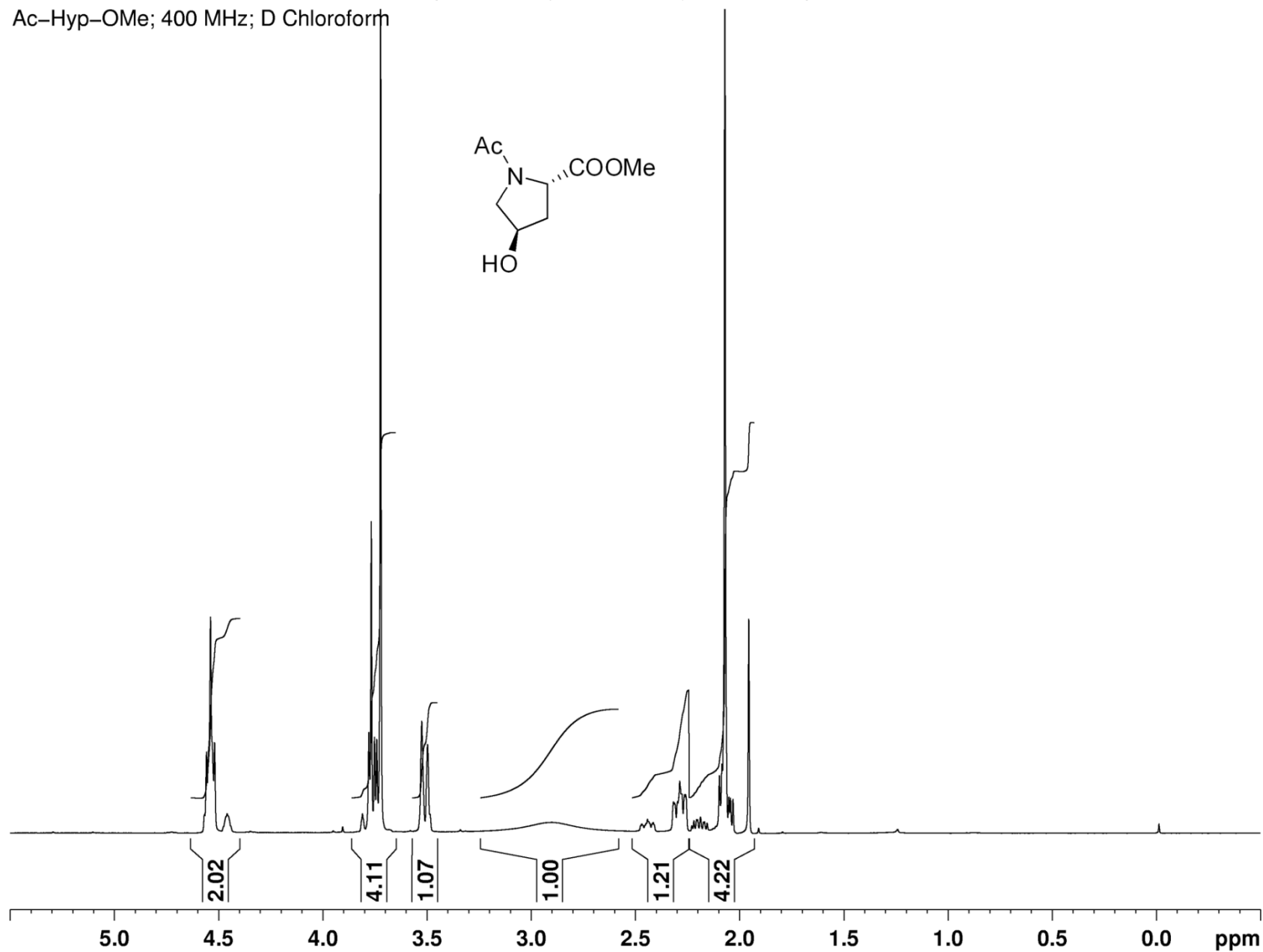
Compound **100** (Scheme 3.19) – ^{13}C NMR spectrum

Tetramer (Boc–OAll); 400 MHz; D Chloroform



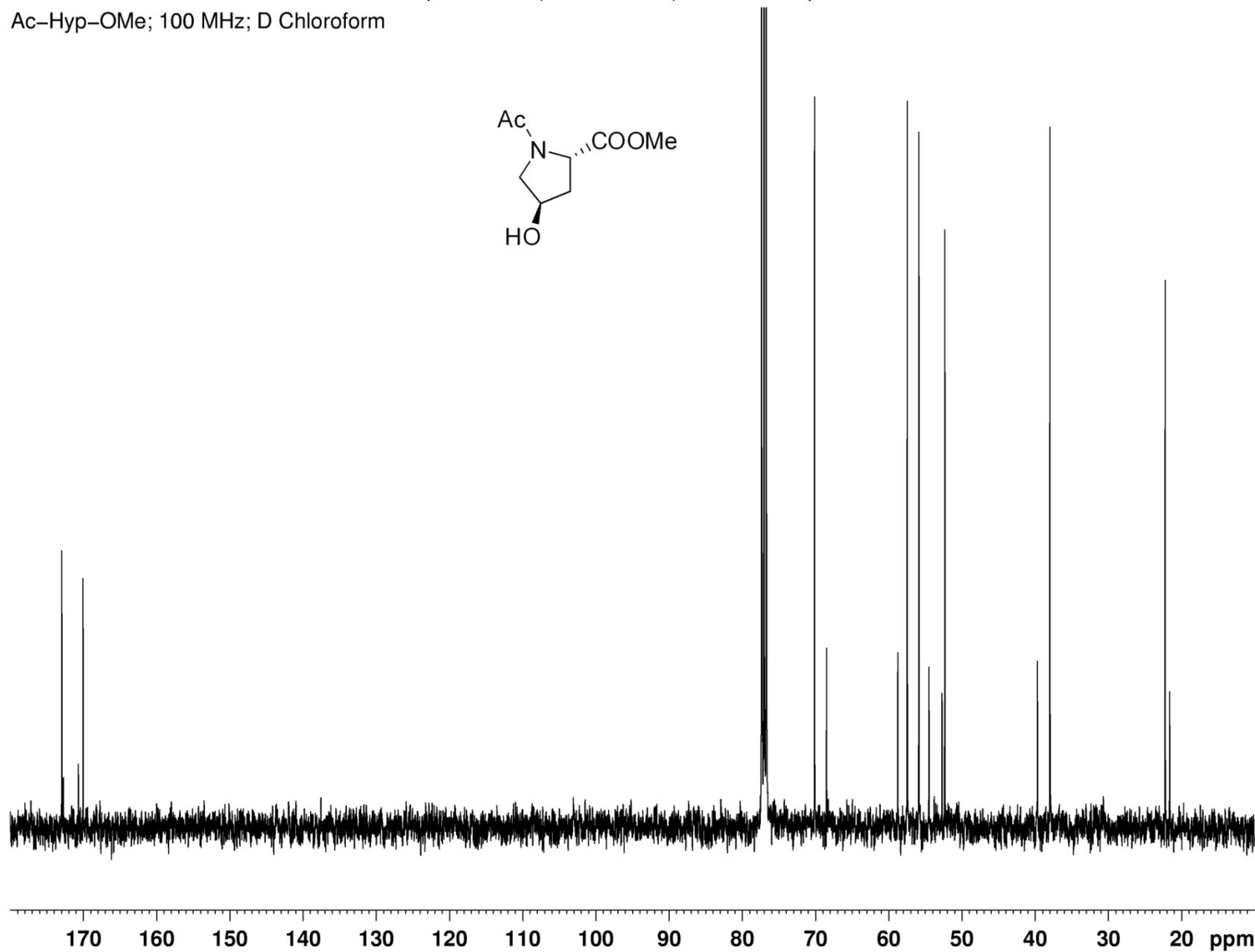
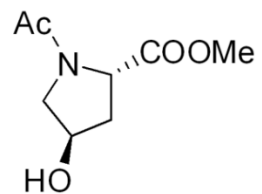
Compound **105** (Scheme 3.24) - ^1H NMR spectrum

Ac-Hyp-OMe; 400 MHz; D Chloroform



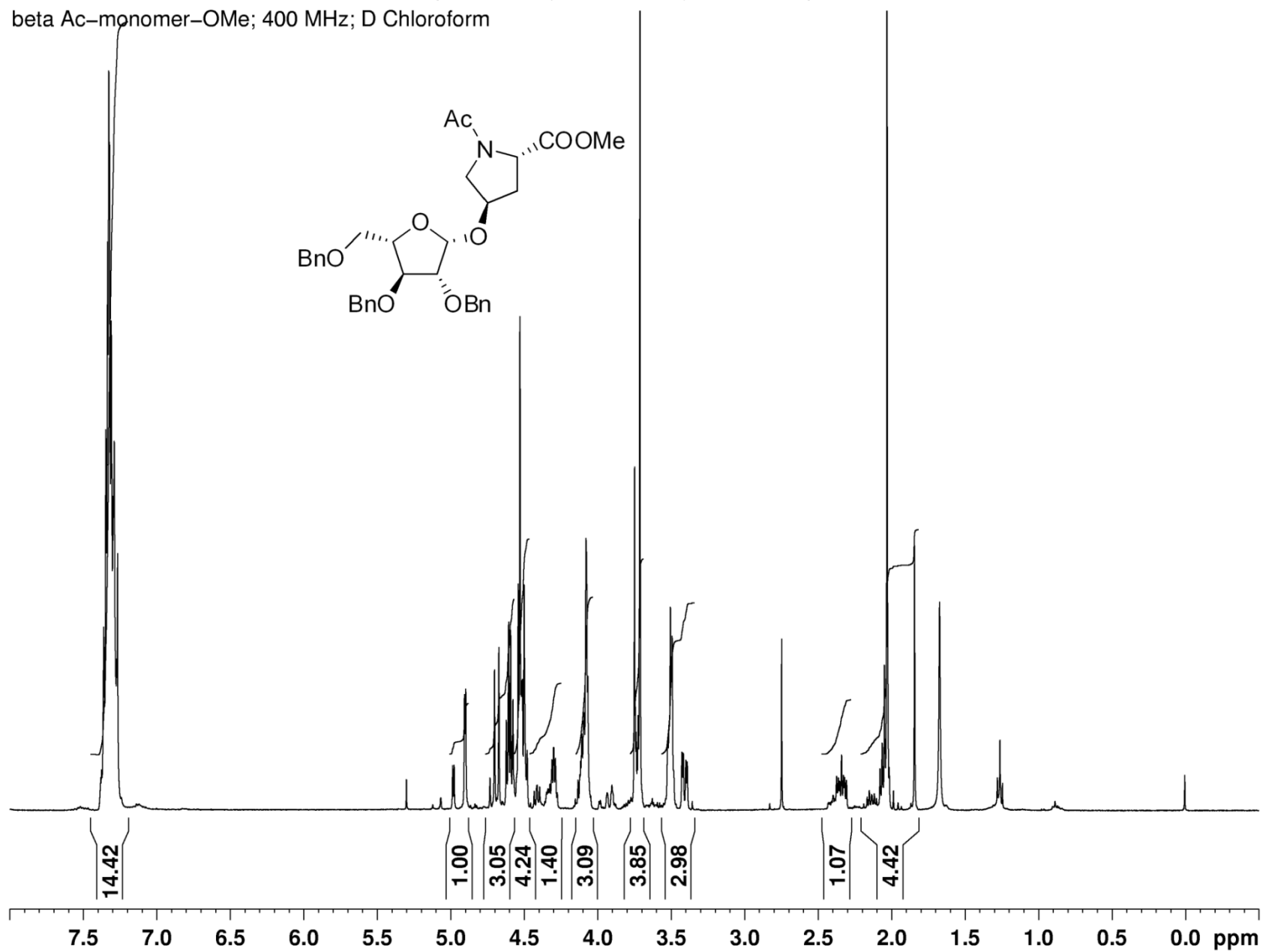
Compound **105** (Scheme 3.24) – ^{13}C NMR spectrum

Ac-Hyp-OMe; 100 MHz; D Chloroform

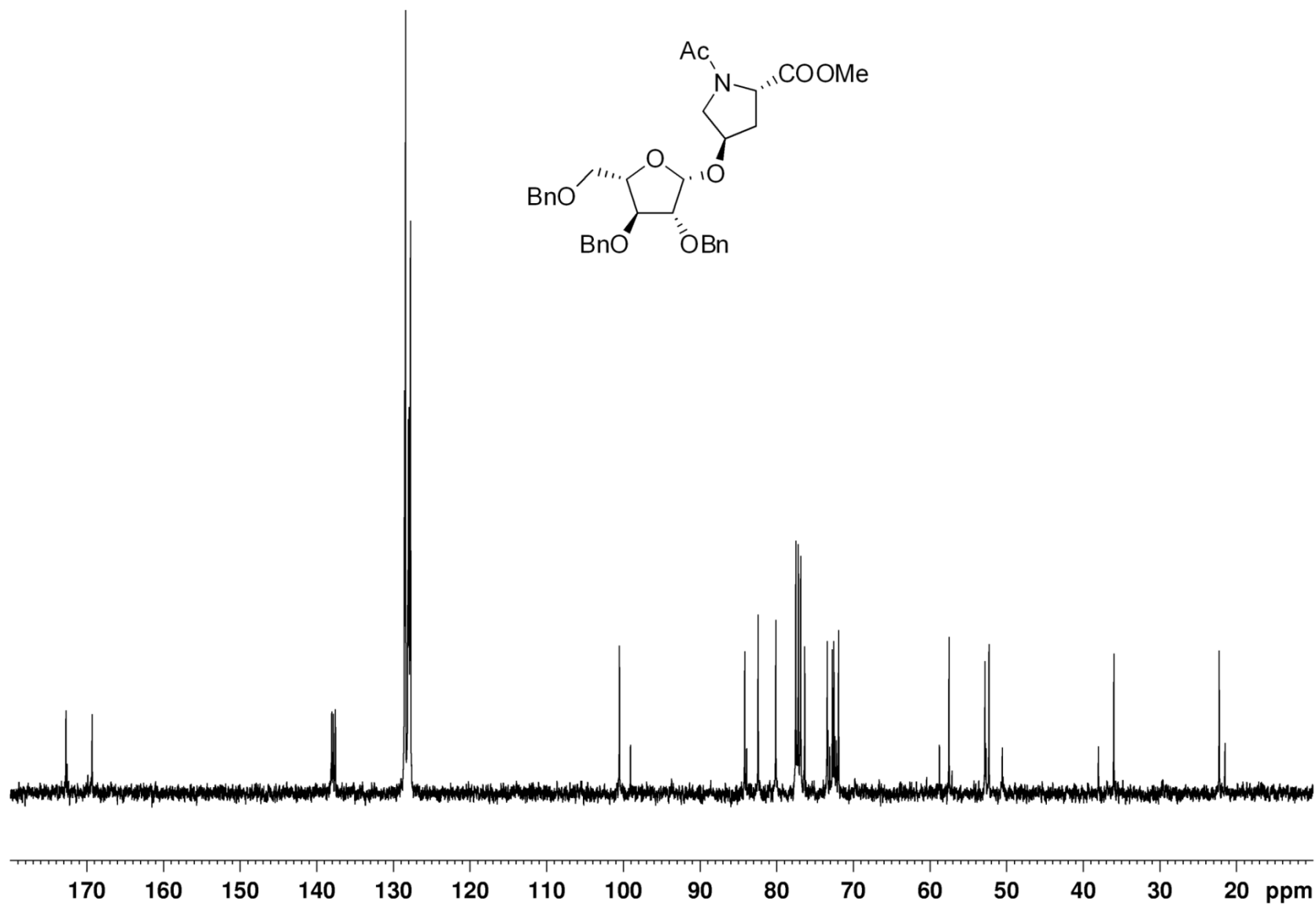


Compound **107** (Scheme 3.25) - ^1H NMR spectrum

beta Ac-monomer-OMe; 400 MHz; D Chloroform

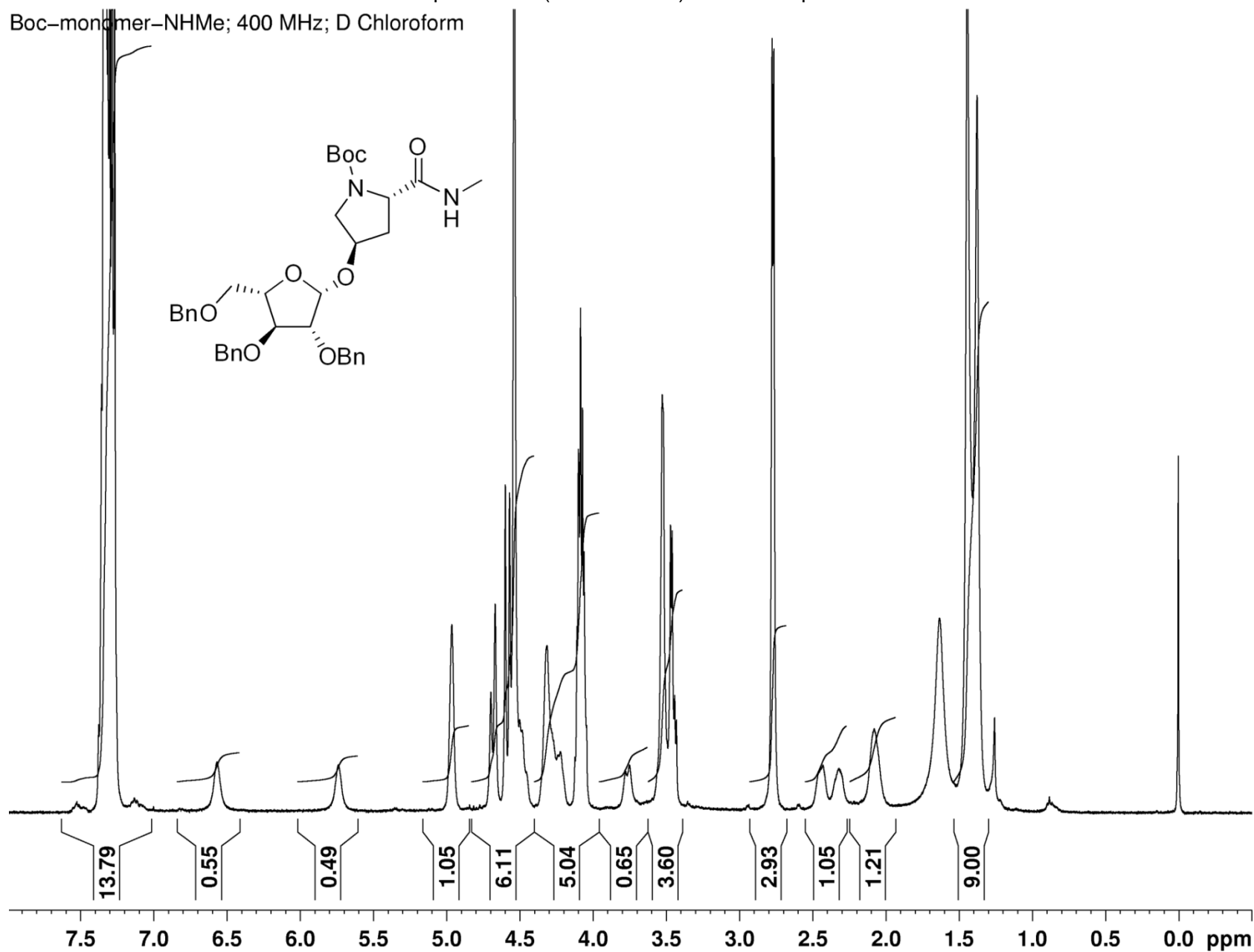


Compound **107** (Scheme 3.25) – ^{13}C NMR spectrum
beta Ac–monomer–OMe; 100 MHz; D Chloroform



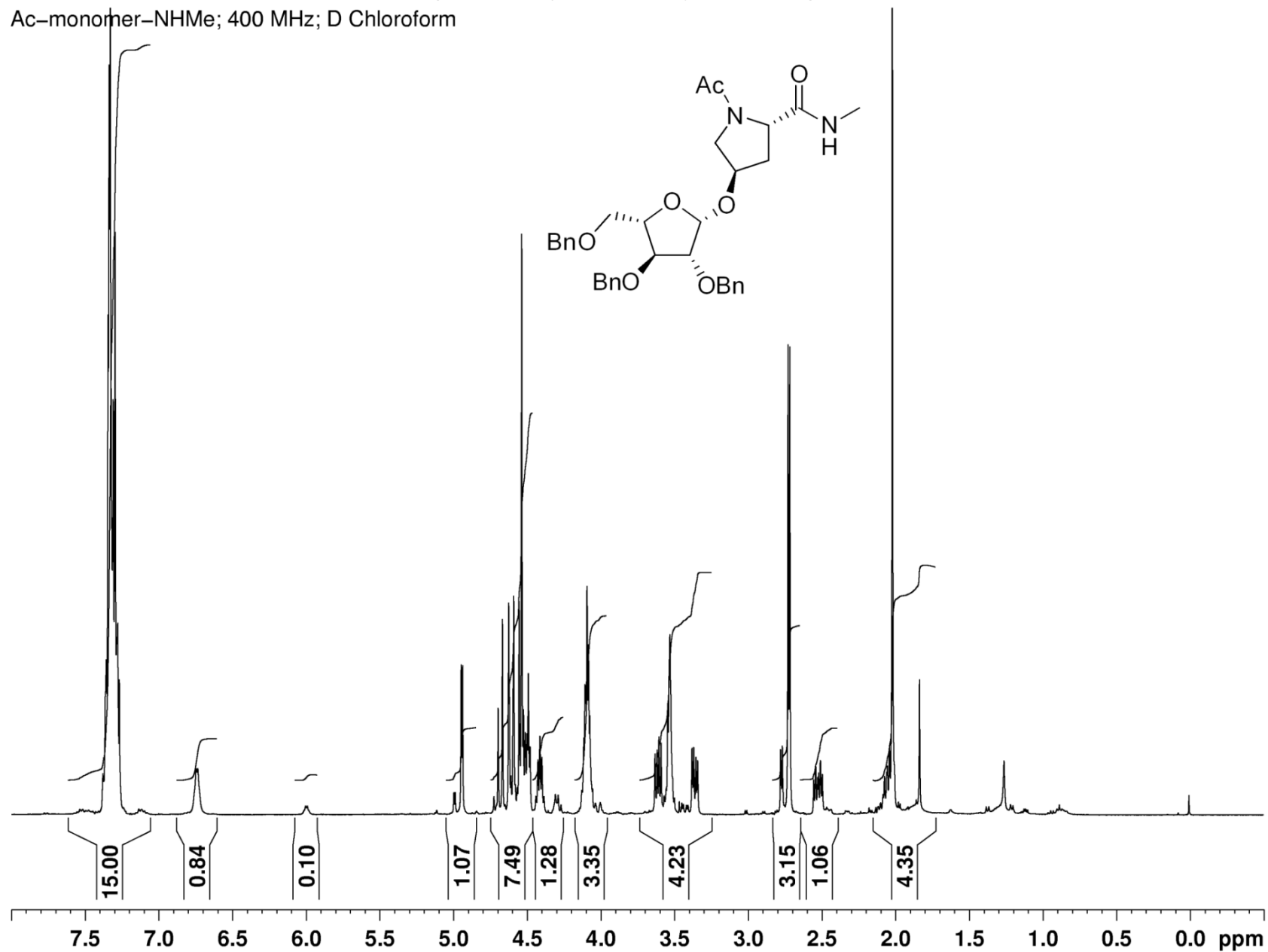
Compound **108** (Scheme 3.25) - ^1H NMR spectrum

Boc-monomer-NHMe; 400 MHz; D Chloroform



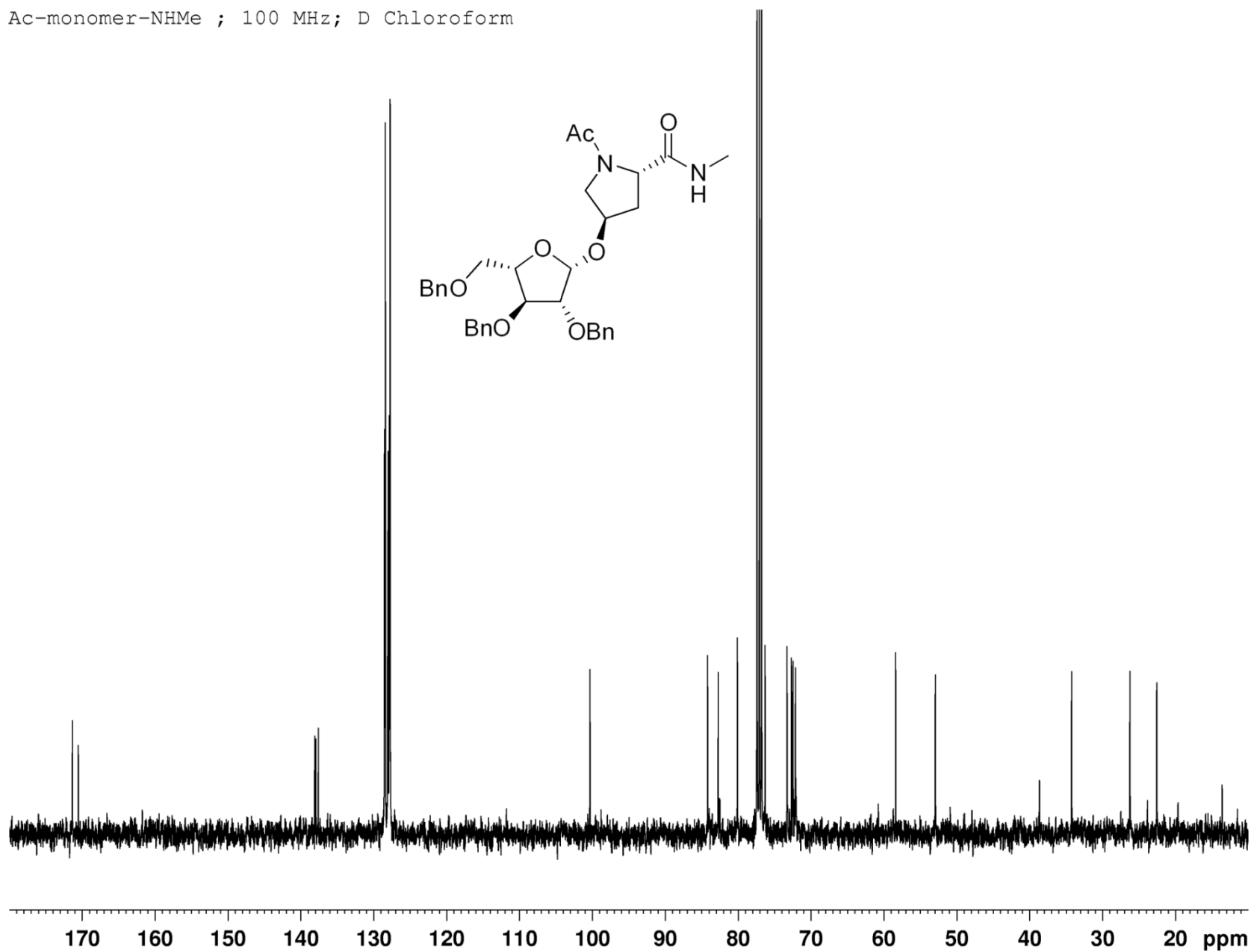
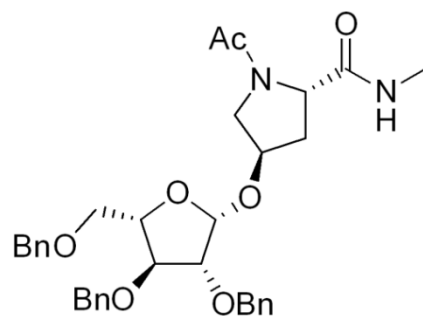
Compound **102** (Scheme 3.21) - ^1H NMR spectrum

Ac-monomer-NHMe; 400 MHz; D Chloroform



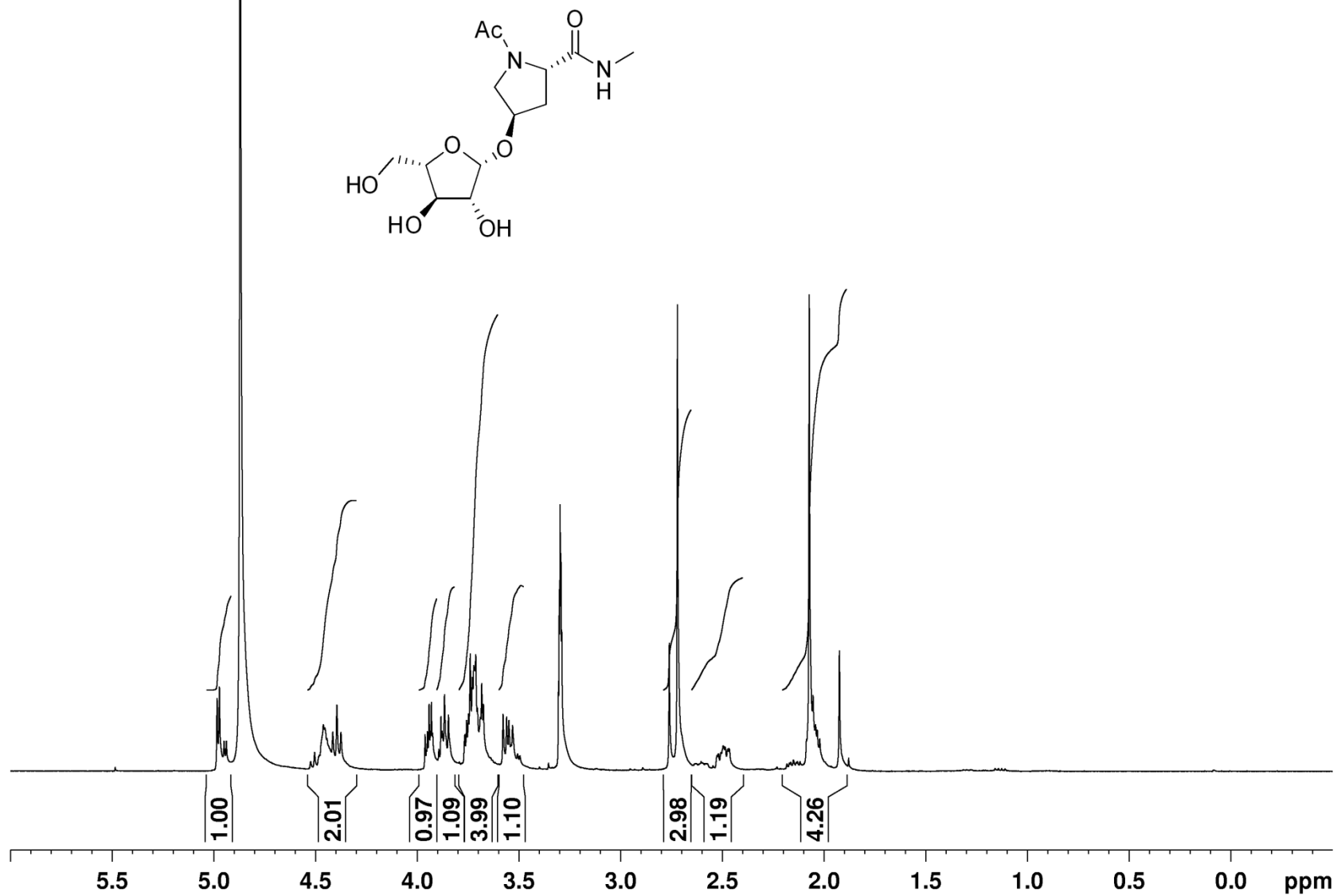
Compound **102** (Scheme 3.21) – ^{13}C NMR spectrum

Ac-monomer-NHMe ; 100 MHz; D Chloroform



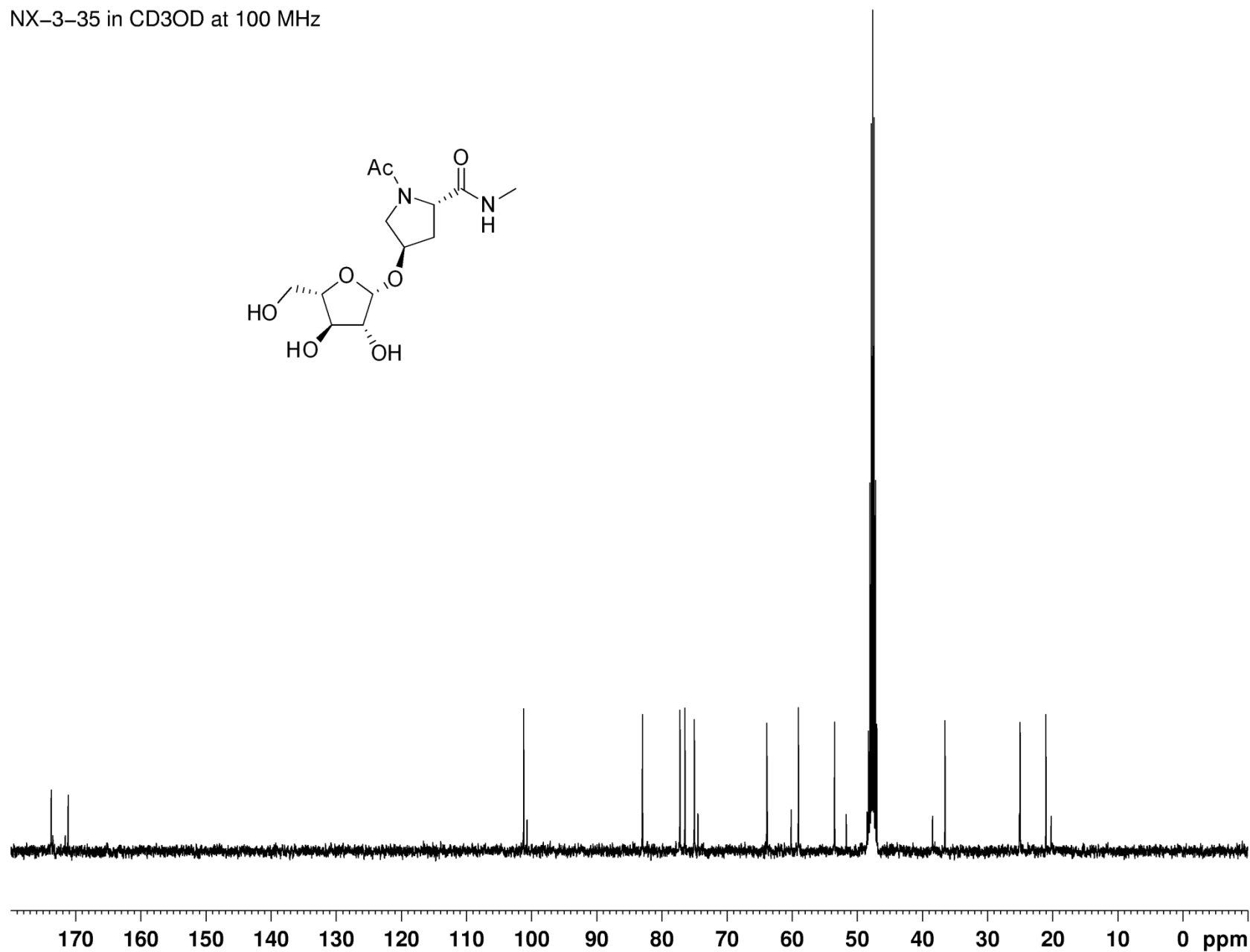
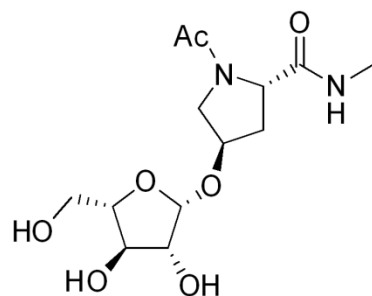
Compound **118** (Scheme 3.29) - ^1H NMR spectrum

NX-3-35 in CD_3OD at 400 MHz



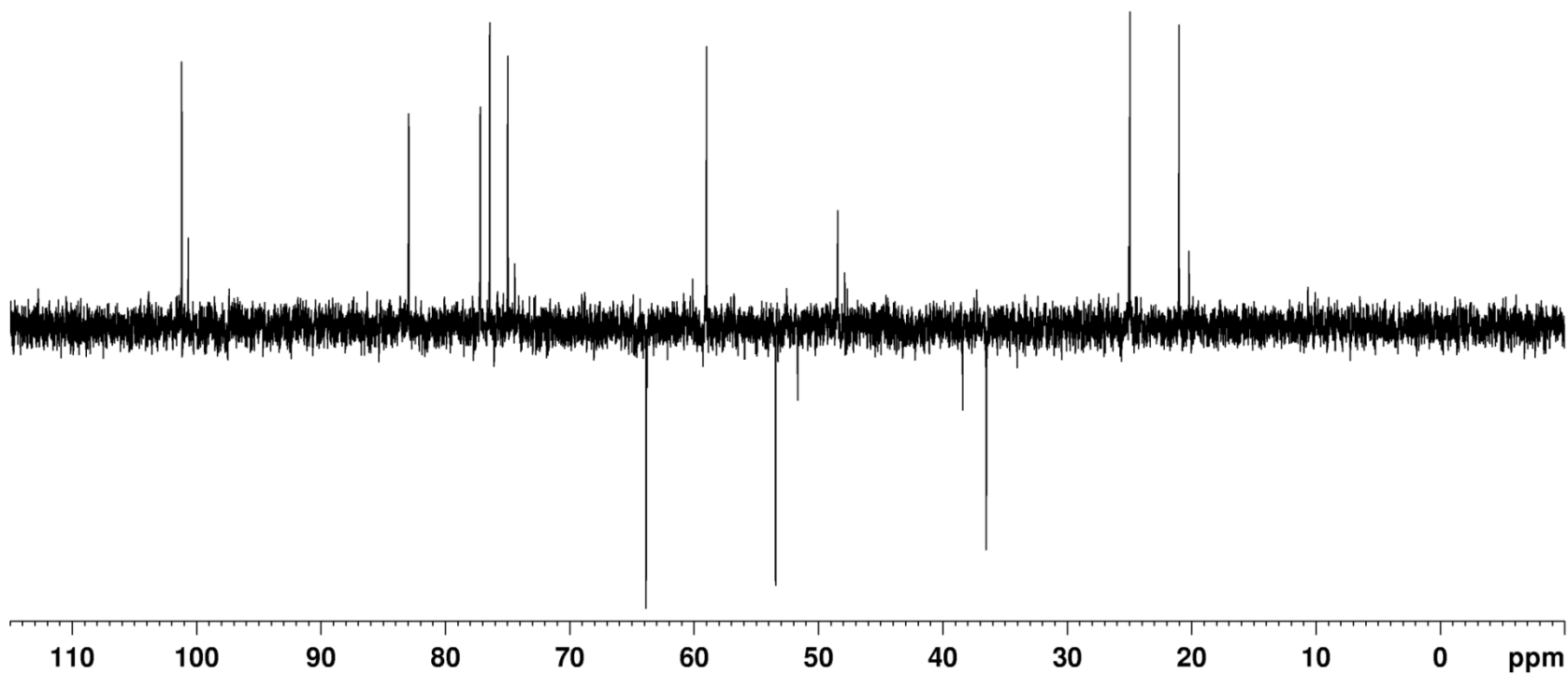
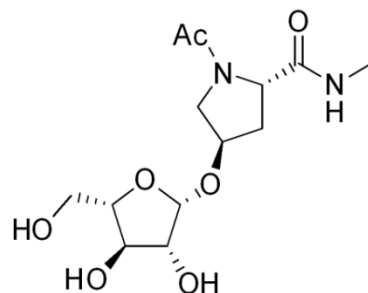
Compound **118** (Scheme 3.29) – ^{13}C NMR spectrum

NX-3-35 in CD_3OD at 100 MHz



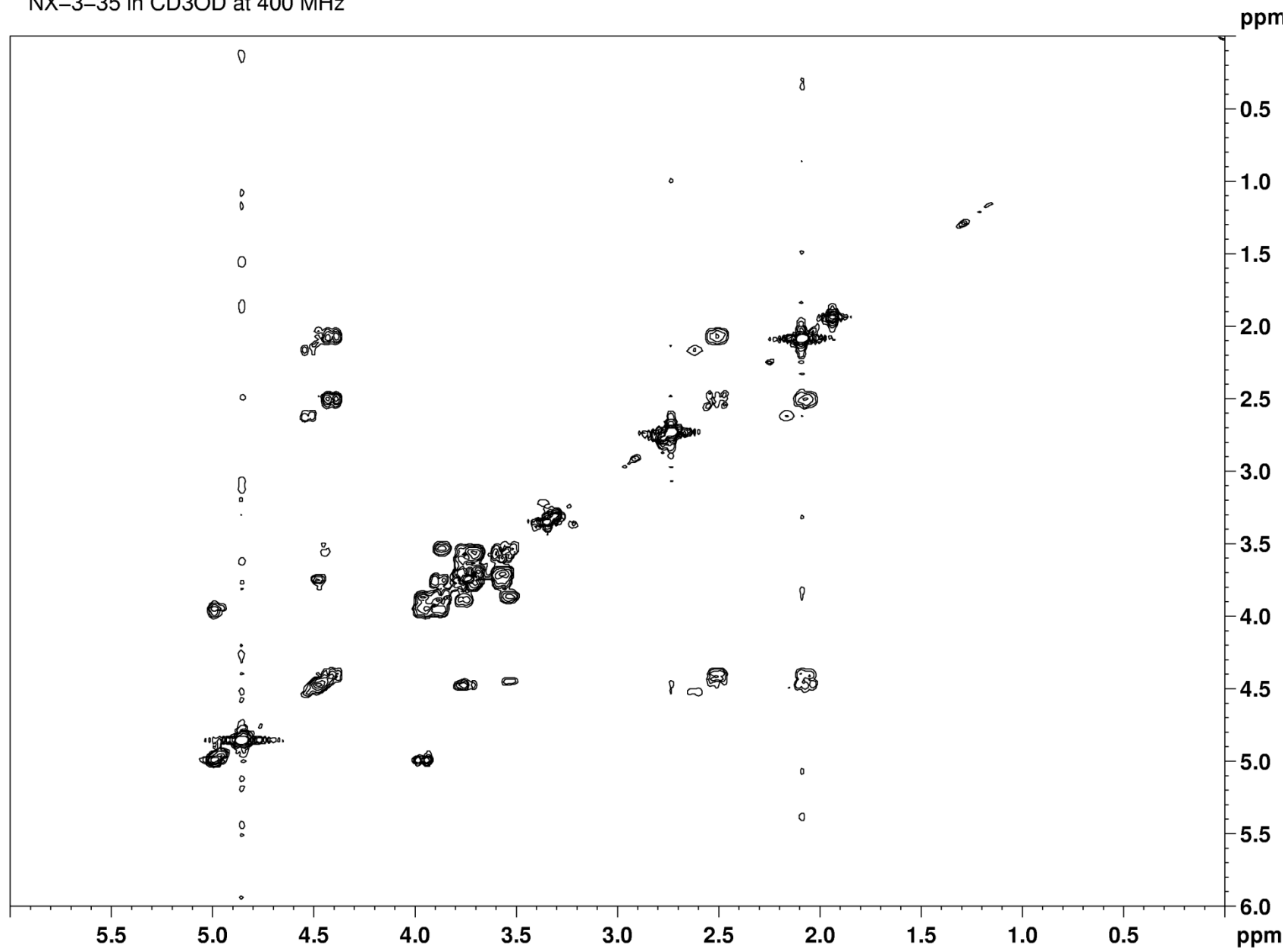
Compound **118** (Scheme 3.29) – Dept 135 NMR spectrum

NX-3-35 in CD₃OD at 100 MHz



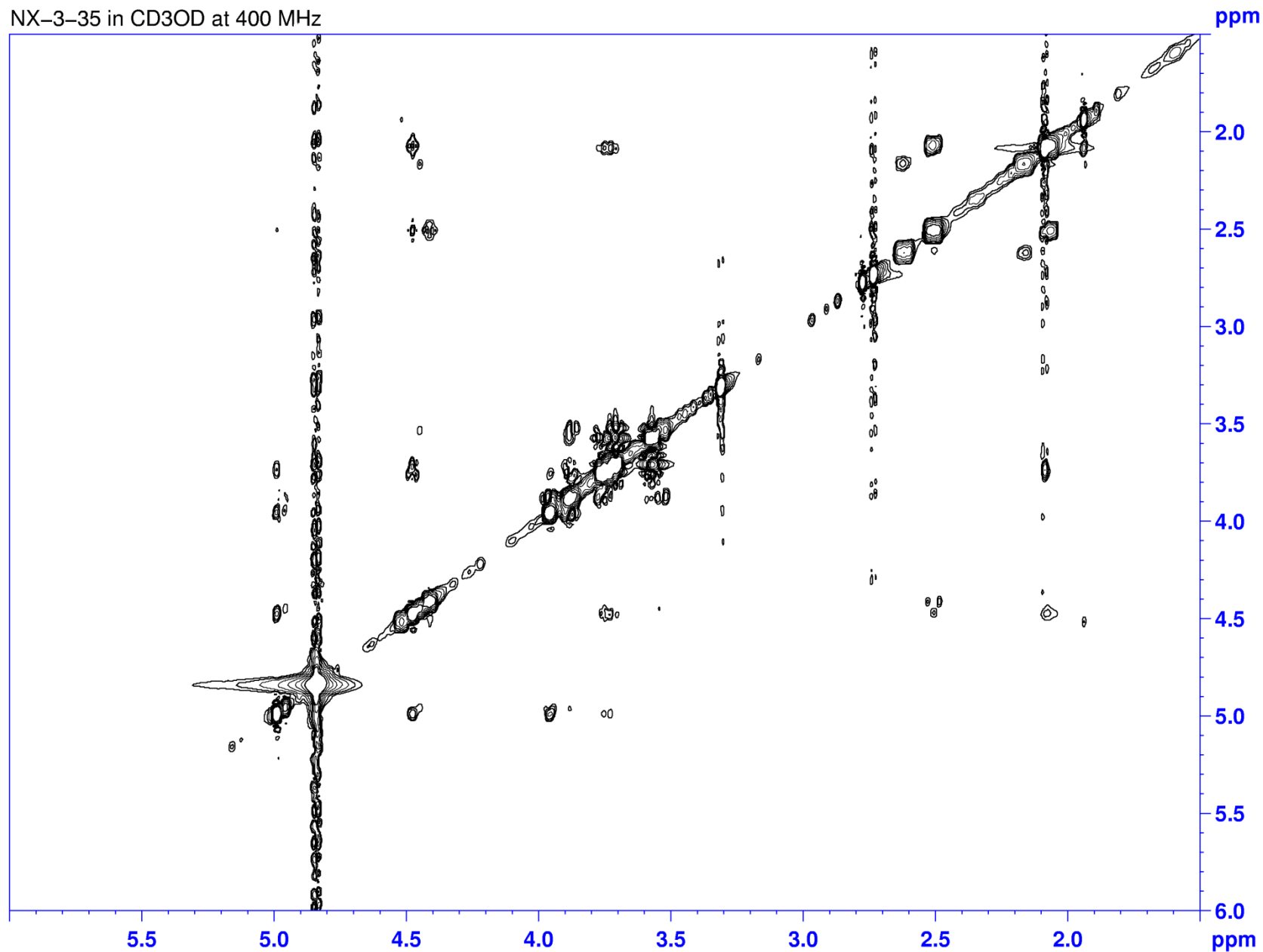
Compound **118** (Scheme 3.29) – COSY NMR spectrum

NX-3-35 in CD₃OD at 400 MHz

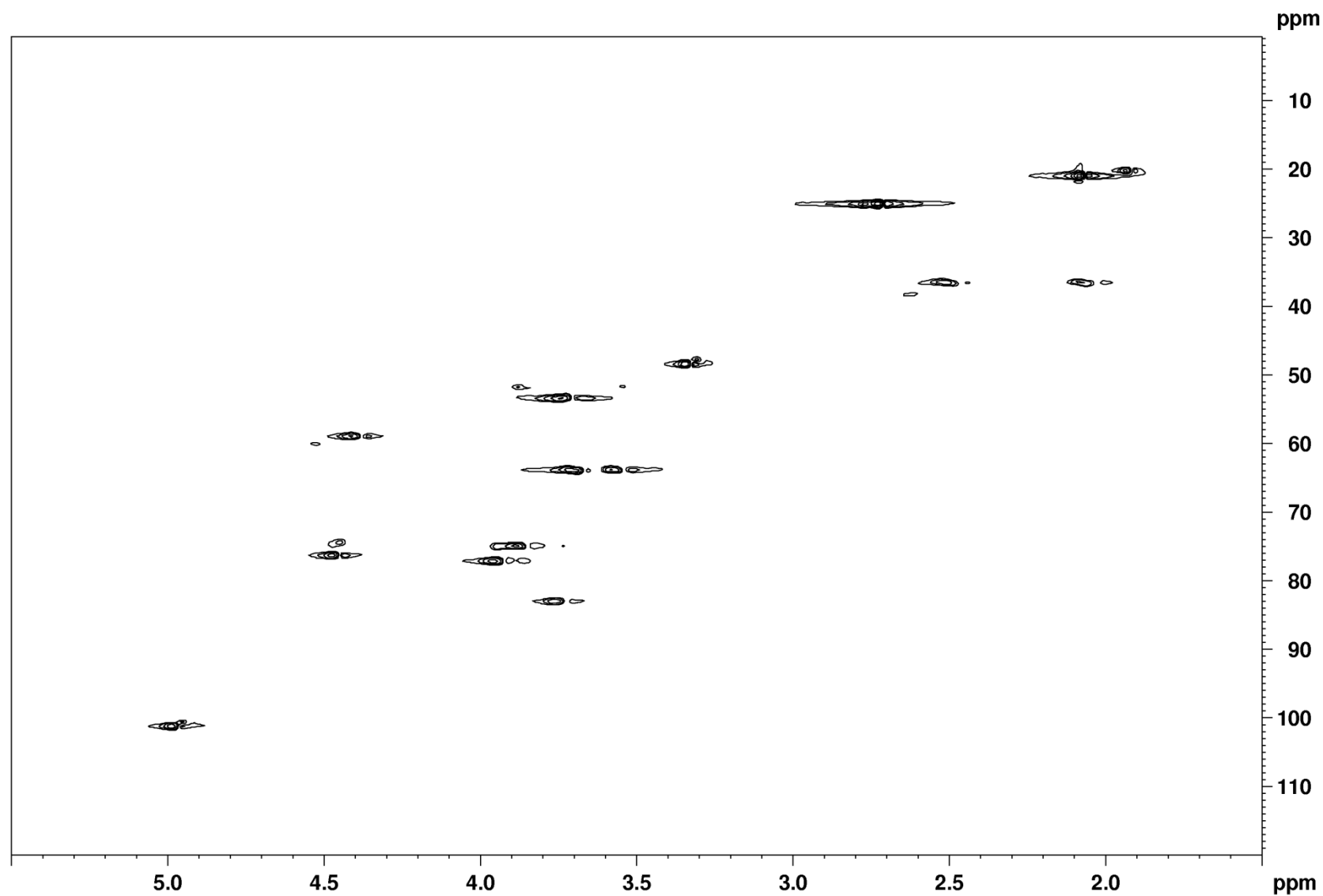


Compound **118** (S cheme 3.29) - NOSEY spectrum

NX-3-35 in CD3OD at 400 MHz

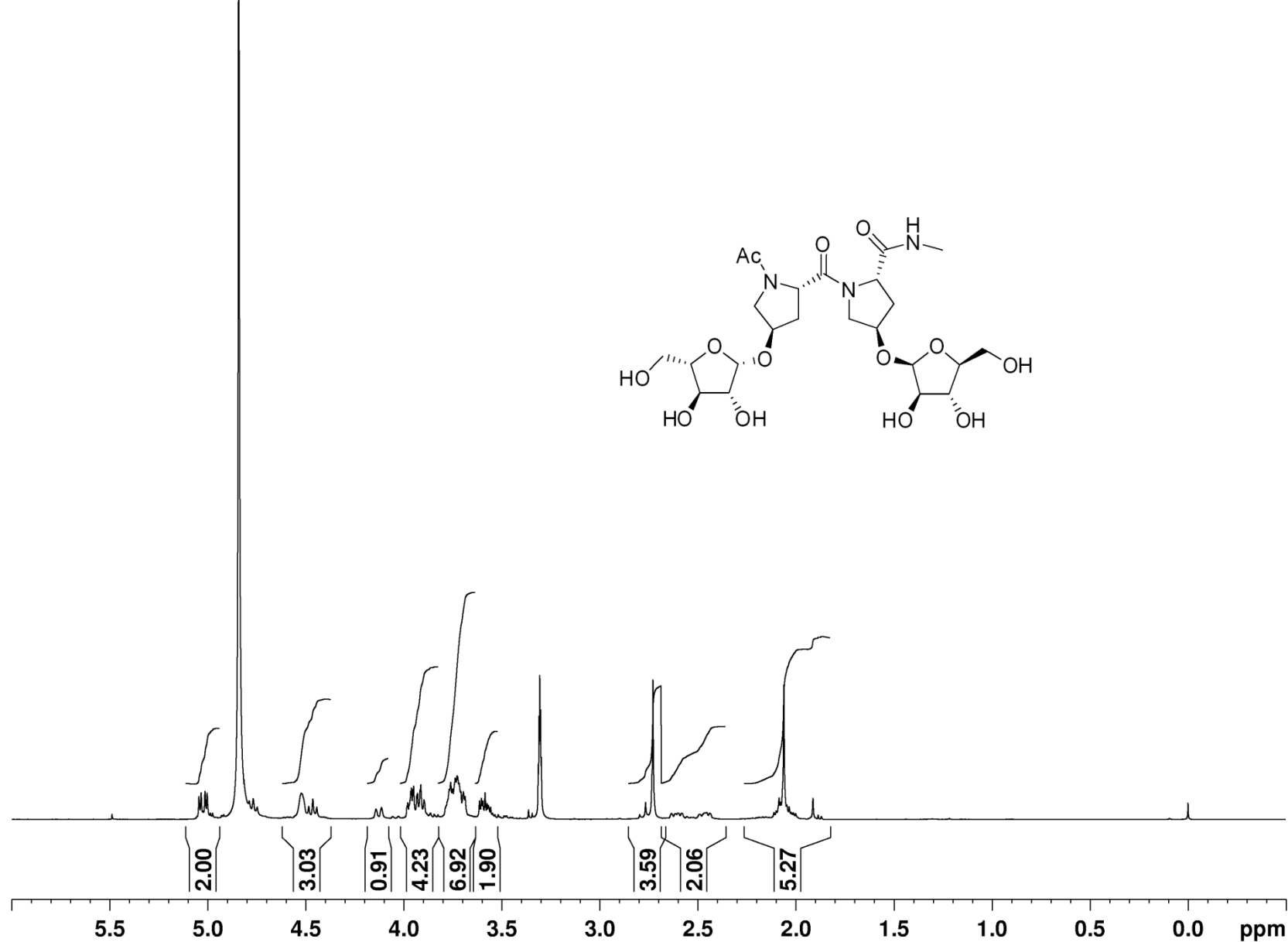


Compound **118** (Scheme 3.29) - HSQC spectrum
Ac-([beta-L-Araf]Hyp)-NHMe Triol in CD3OD at 400 MHz



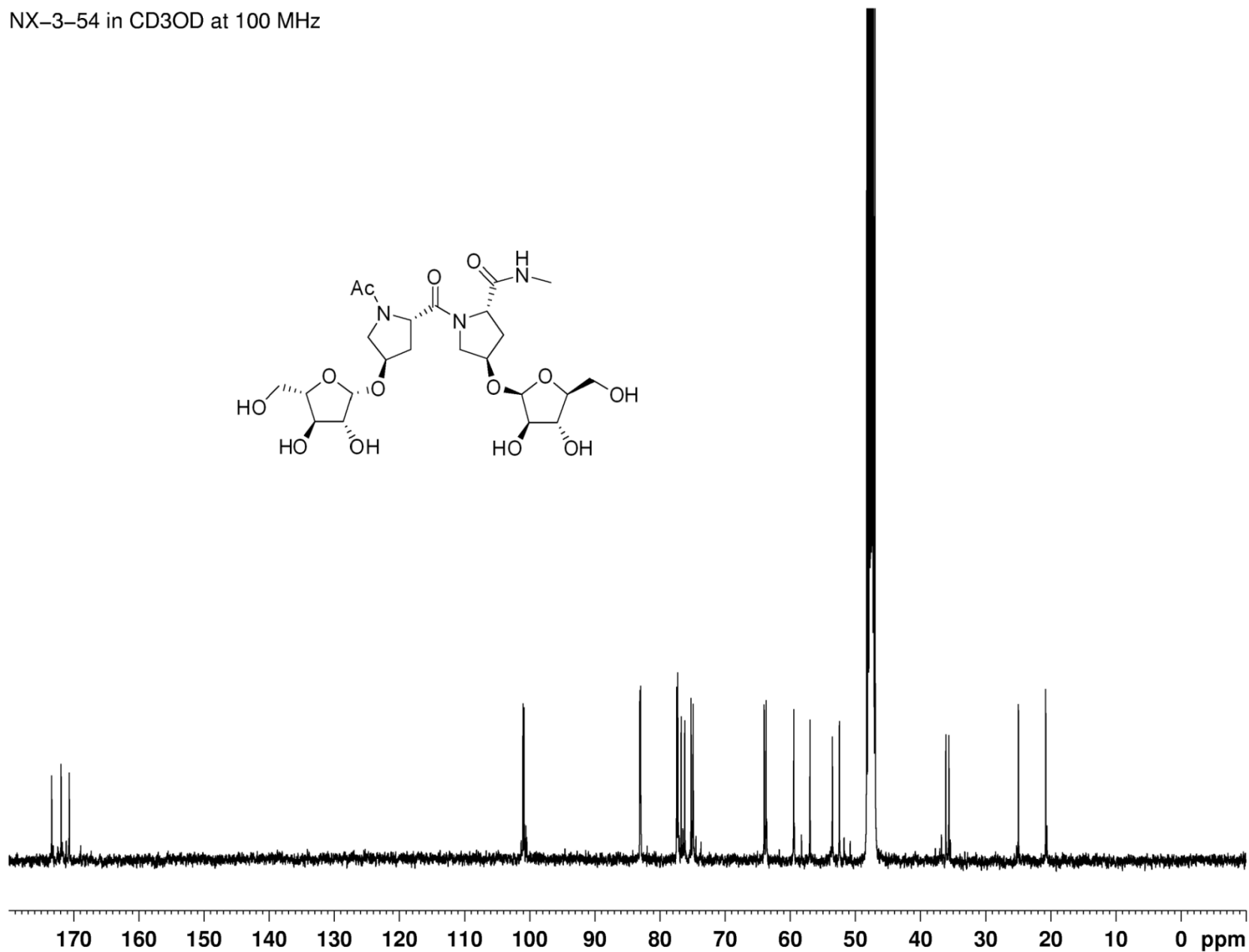
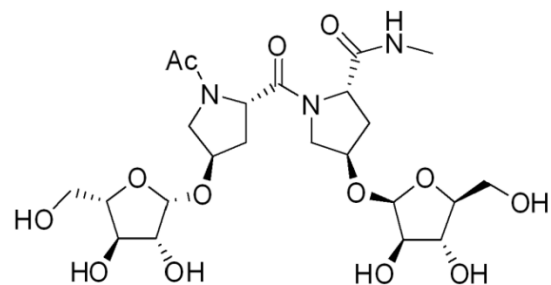
Compound **119** (Scheme 3.29) - ^1H NMR spectrum

NX-3-54 in CD_3OD at 400 MHz



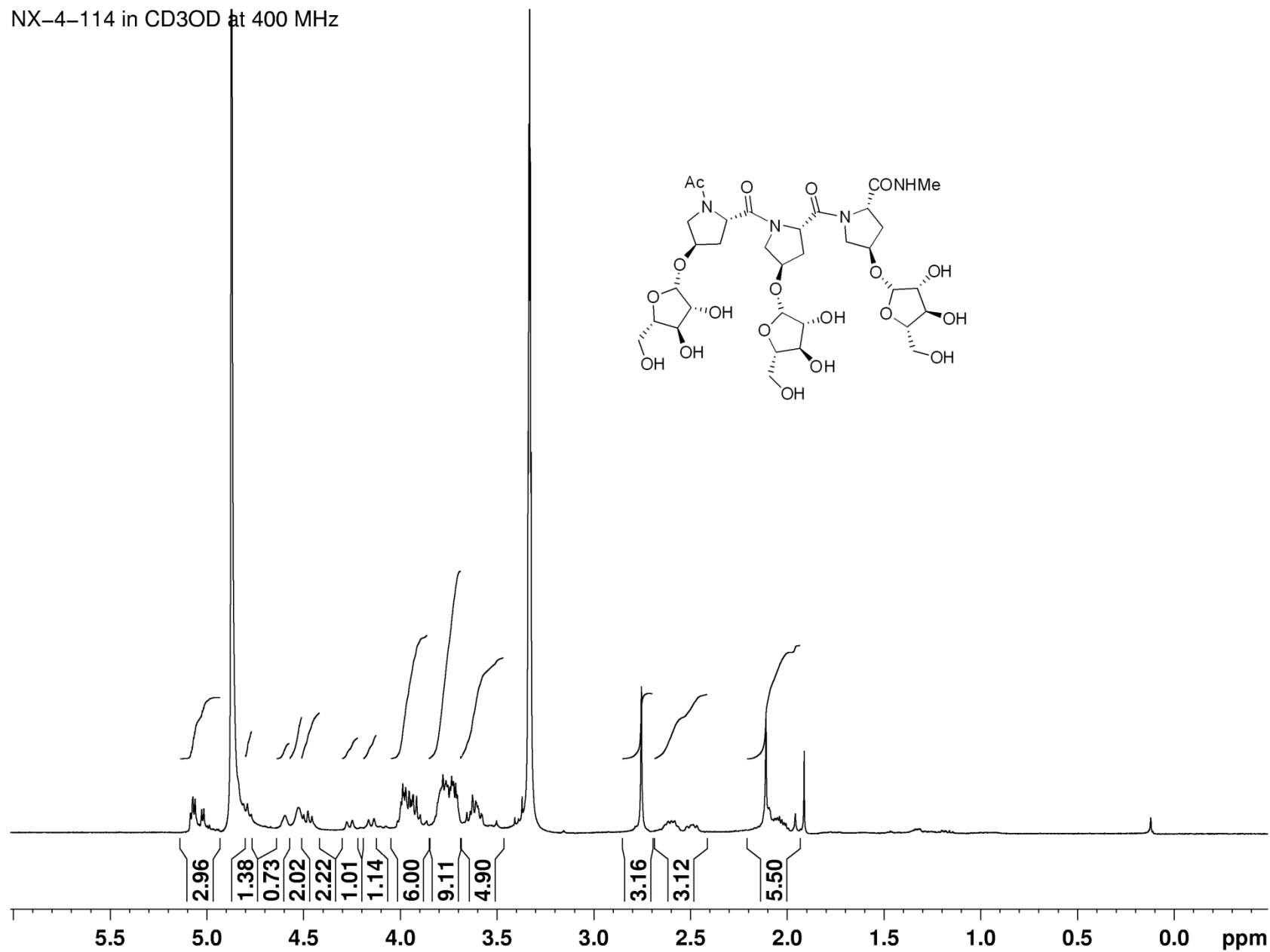
Compound **119** (Scheme 3.29) – ^{13}C NMR spectrum

NX-3-54 in CD_3OD at 100 MHz



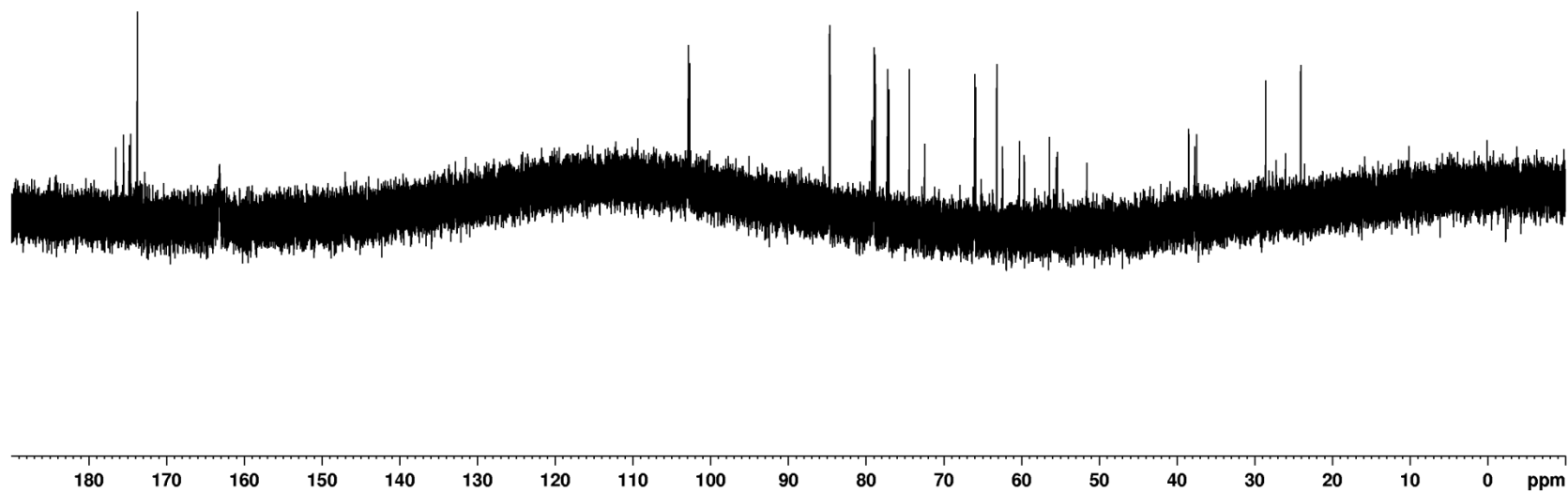
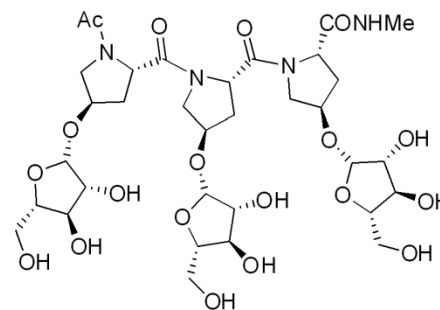
Compound **120** (Scheme 3.29) - ^1H NMR spectrum

NX-4-114 in CD_3OD at 400 MHz



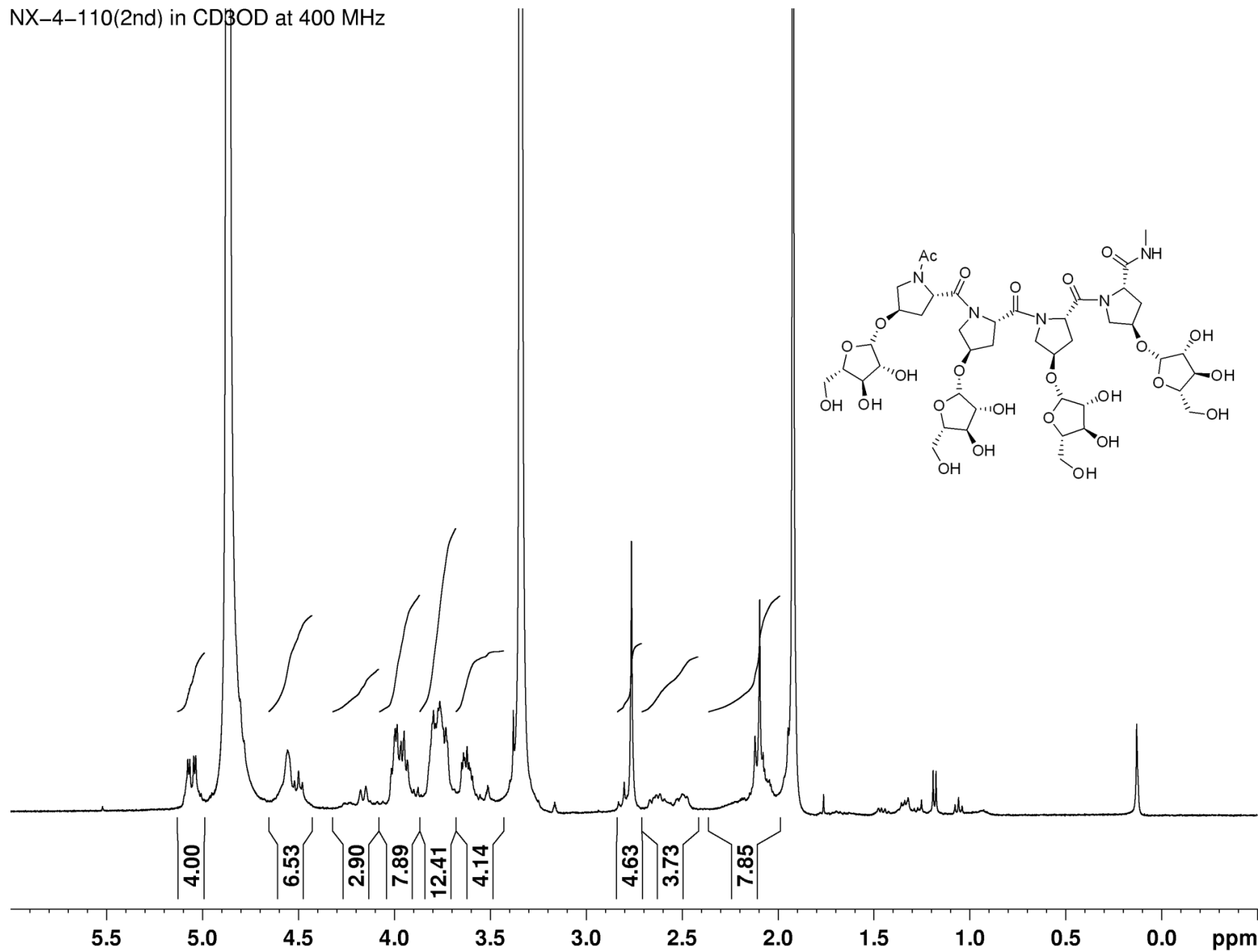
Compound **120** (Scheme 3.29) – ^{13}C NMR spectrum

NX-4-114 in D₂O at 175 MHz



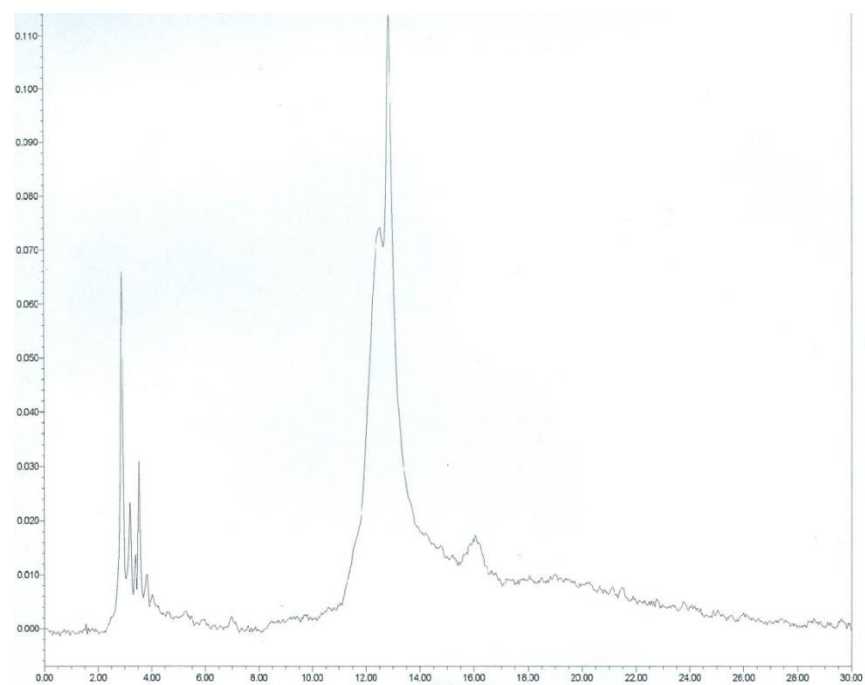
Compound **1** (Scheme 3.29) - ^1H NMR spectrum

NX-4-110(2nd) in CD₃OD at 400 MHz



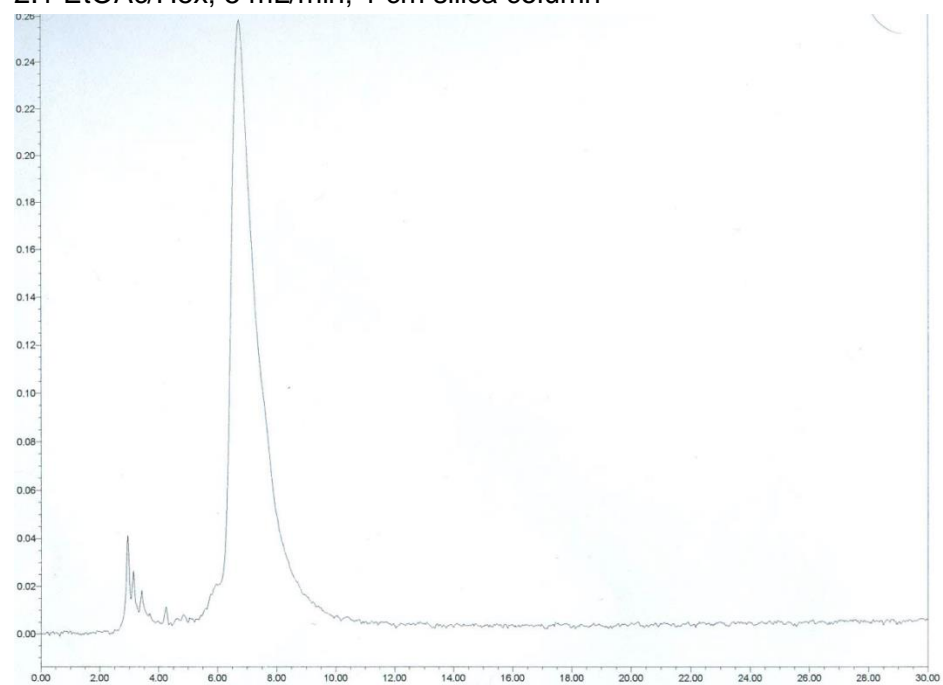
Triglycotriptide 99

1:1 EtOAc/Hex; 5 mL/min; 1 cm silica column



Tetraglycotetraptide 100

2:1 EtOAc/Hex; 5 mL/min; 1 cm silica column



CHAPTER 4: STRUCTURAL STUDIES OF POLYPROLINE GLYCOSIDES

4.1 Circular Dichroism

4.1.1 Polyproline helices

Circular dichroism is a light absorption spectroscopy that gives information about the secondary structure composition of polypeptides and proteins.⁸⁸ One such secondary structure found in proteins with recurring proline residues is the polyproline helix (Figure 4.1). A polyproline type I (PPI) helical conformation is a right handed helix having *cis* prolyl amide bonds ($\omega = 0^\circ$). The PPI helix features 3.3 residues per turn with dihedral angles of $\Phi = -75^\circ$ and $\Psi = +160^\circ$ (Figure 4.2). A polyproline type II (PPII) helical conformation is a left handed helix featuring all *trans*-amide bonds ($\omega = 180^\circ$) and three amino acid residues per turn.⁸⁹ Each residue in the PPII helix has dihedral angles of $\Phi = -75^\circ$ and $\Psi = +145^\circ$.⁹⁰

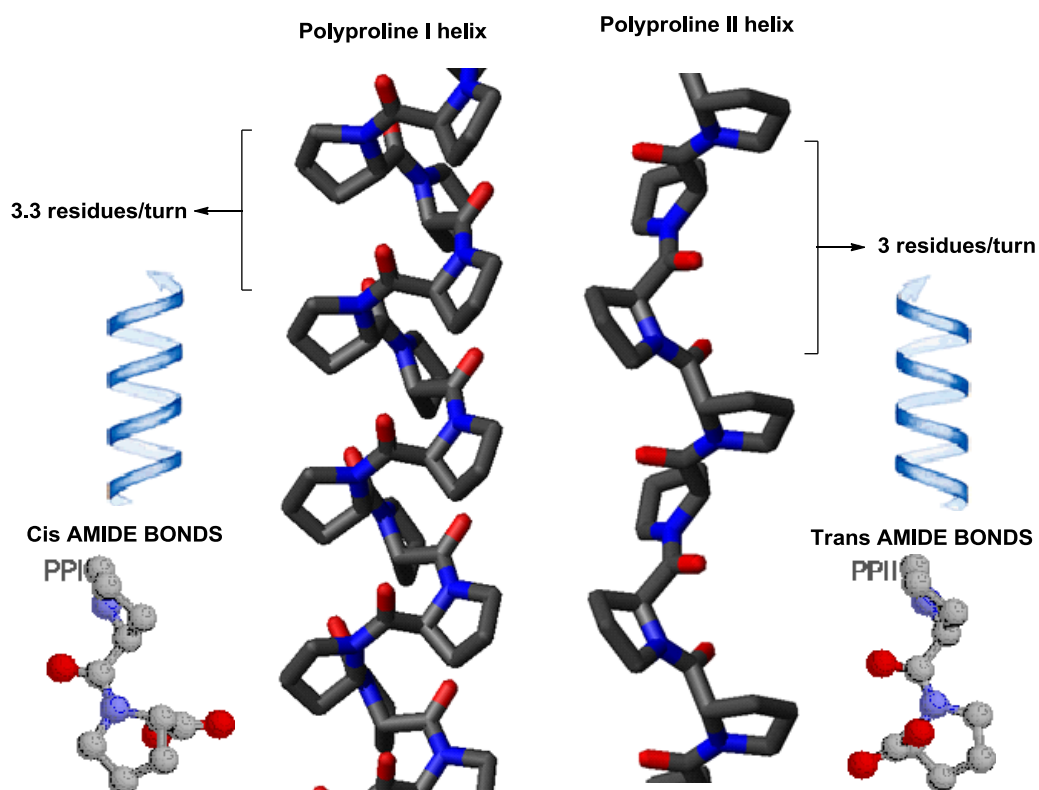


Figure 4.1 Polyproline type I and II helices

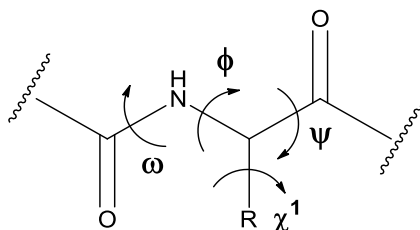


Figure 4.2 Phi (Φ), psi (Ψ), and omega (ω) backbone dihedral angles of peptides

Twenty five percent of all residues in the PPII helix participate in $n \rightarrow \pi^*$ interactions as reported by Bartlett *et al.*⁹¹ The $n \rightarrow \pi^*$ interaction arises when a lone pair of electrons on a carbonyl oxygen (n) donates into the empty electrophilic π^* orbital on the succeeding carbonyl carbon (Figure 4.3). This electron delocalization event plays a crucial role in the conformational stability of proteins. Proline is especially suited to be an acceptor in this interaction. The psi angle of the PPII conformation is 145° , favorable for $n \rightarrow \pi^*$ interaction (optimal $\Psi = 150^\circ$).⁹² This $n \rightarrow \pi^*$ interaction, coupled with the fact that the *trans*-amide bond conformation is lower in energy compared to the *cis*, renders the PPII helix more commonplace than the PPI. Sreerama and Woody estimated that 10% of all proteins may adopt the PPII conformation.⁹³ Circular dichroism spectroscopy has demonstrated that the PPII conformation has its own distinct elliptical shape (Figure 4.4).⁹⁴

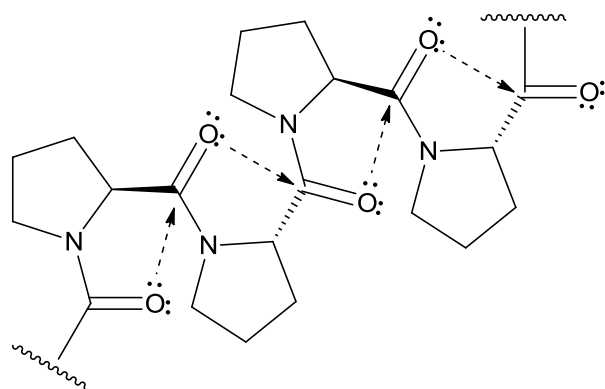


Figure 4.3 $n \rightarrow \pi^*$ interaction in a proline tetramer.

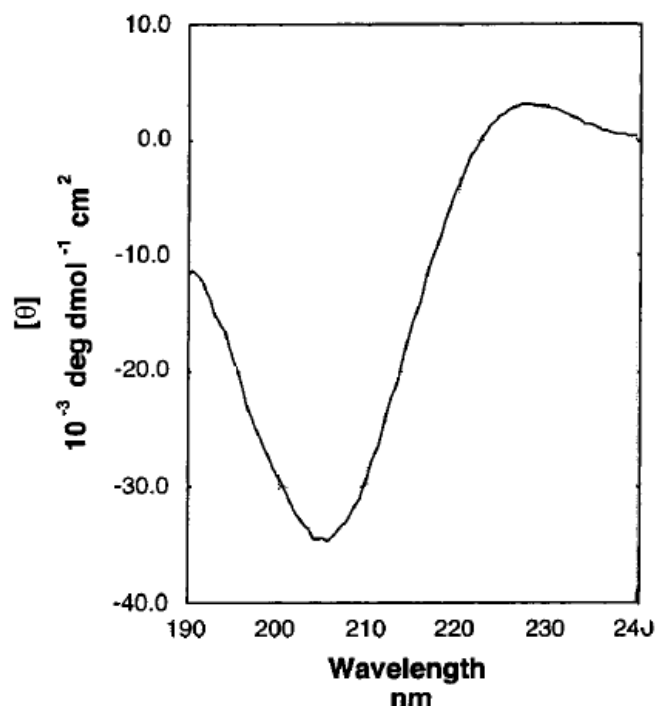


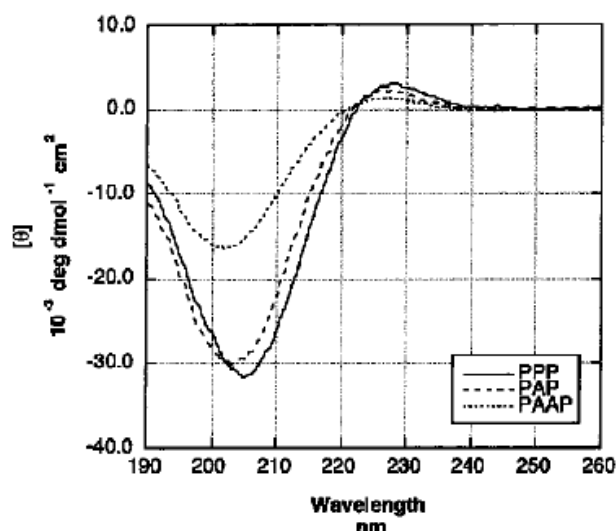
Figure 4.4 CD Spectrum of Ac-(Pro)₇-Gly-Tyr-NH₂ taken at 5 °C.⁹⁵ Reprint with permission from American Chemical Society.

The PPII structure plays a vital role in numerous biological processes. For example, in the plant kingdom, hydroxyproline-rich glycopeptides (HPRG) are responsible for a plant's growth and defense, among other functions,⁹⁶ and are known to adopt a PPII conformation in the cell wall.⁹⁷ In the animal kingdom, PPII helices are widely found in collagen, the main component of connective tissues found in vertebrates.⁹⁸ Interestingly, through use of computational protein modeling, Himly and coworkers predicted that the carboxyl terminal domain of Art v 1 would exhibit a left handed helical structure resembling collagen.¹⁷ Dedic *et al.* later confirmed that the CD spectra of Art v 1 was indeed similar to those of polyproline helices,⁹⁹ although no (further) details of the spectra were provided.

Proline-rich regions of peptides often contain many nonproline residues adjacent to one another.¹⁰⁰ Kelly *et al.* conducted a “host-guest” study on the effect a non-proline residue has on the CD spectra of short polyproline compounds.⁹⁵ “Guest” residues were inserted into a host

peptide known to adopt a PPII helix. Alanine was employed due to its inclination to be in a PPII helical conformation. The CD spectra of PPP, PAP, and PAAP were taken at 5 °C (Figure 4.5). The decrease in PPII helical content was found to be three percent between PPP and PAP and nine percent between PAP and PAAP. The nonlinearity of the decreasing helical content suggests that a more pronounced decrease in PPII helical content may be detected in stretches with three or even four non-proline residues in a proline rich region. Despite this decrease, it is

apparent from the CD spectra that PAAP still showed significant PPII character.



Ac-Pro-Pro-Pro-Xaa-Pro-Pro-Pro-Gly-Tyr-NH₂

PPP (Xaa = Pro)

PAP (Xaa = Ala)

PAAP (Xaa = Ala₂)

Figure 4.5 Host PPII helix sequence with insertion of guest amino acids. Reprint with permission from American Chemical Society

Figure 4.6 shows the circular dichroism spectra of various H-(Pro)_n-OH peptides as reported by Rothe *et al.*¹⁰¹ Synthetic oligomers of up to 40 unmodified proline residues were investigated. The authors note that three consecutive Pro residues are required for PPII characteristics to be observed. Moreover, the intensity of the maxima, namely the negative maxima at 206 nm, generally increased with the number of Pro residues.

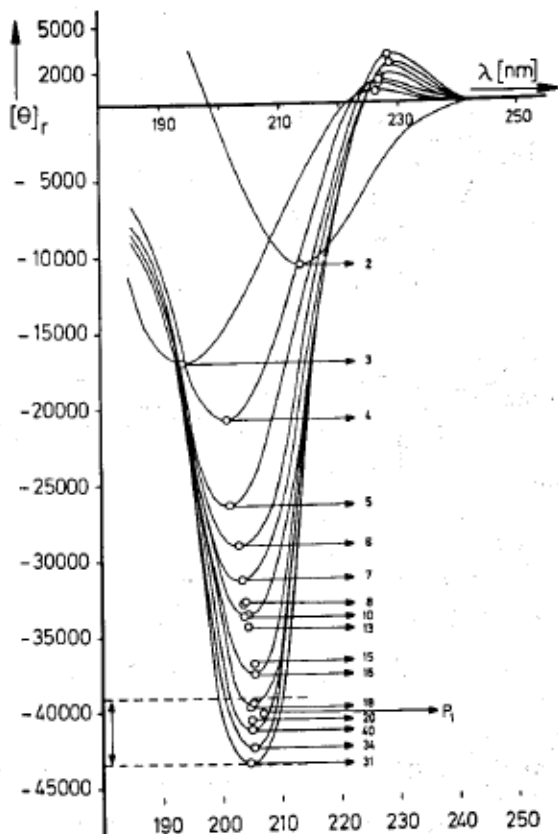


Figure 4.6 CD spectra of synthetic polyproline peptides $\text{H}-(\text{Pro})_n-\text{OH}$ ¹⁰¹

4.1.2 Effect of pH on peptide conformation

The pH of a solution can be highly influential in the *cis/trans* isomerization of X-Pro bonds where there are ionic functional groups.¹⁰² The *cis* conformation allows for an electrostatic interaction between amino and carboxylate groups in the zwitterion (Figure 4.7), while the *trans* conformation is favored in acidic medium due to hydrogen bonding. Thus, the impact of pH on the conformation of peptides having free termini would be measurable for short peptides (≤ 3 residues) being that the two types of polyproline helices favor differing conformations of proline.¹⁰³

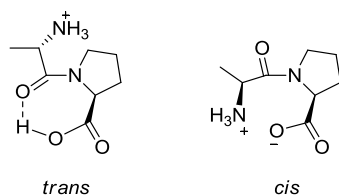


Figure 4.7 *Cis/Trans* isomerization of Alanylproline

This effect of pH, however, is not a factor with neutral glycopeptides that are end-capped with terminal amides. We hypothesized that the CD spectra of our monomer and dimer would demonstrate little or no secondary structure. Helbecque *et al.*, in their investigation of H-Gly-(Pro)_n-OH peptides, also noted that three proline residues were required for the PPII conformation ($n = 3$).¹⁰³ Thus, the emergence of helical character started with the tetrapeptide (H-Gly-(Pro)₃-OH). However, examination of the CD spectrum of their trimer (H-Gly-(Pro)₂-OH, Figure 4.8) shows some characteristics of the PPII elliptical curve, although not as intense as the larger oligomers. Hence, we might expect some PPII helical content in our own trimer (Ac-[(β -L-Araf)Hyp]₃-NHMe) as all of our amino acids involved are prolyl amides and PPII helical formation is a local folding event.¹⁰⁴ Being that the PPII conformation arises from the restricted set of the dihedral angles of an amino acid by the succeeding proline residue,¹⁰⁵ we therefore fully expect the tetramer to exhibit PPII helical character.

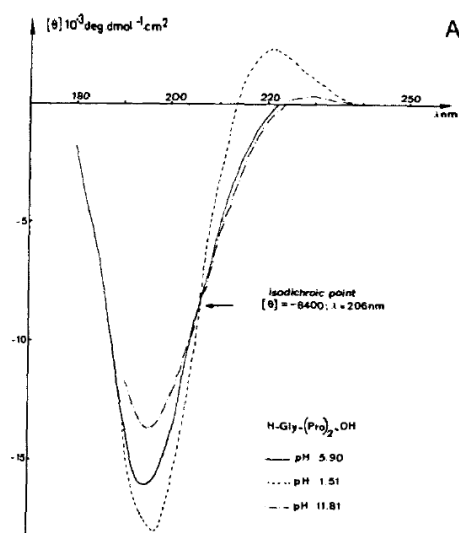


Figure 4.8 CD Spectra of H-Gly-(Pro)₂-OH. Reprint with permission from John Wiley and Sons.

4.1.3 Glycosylated oligomers of proline

The Schweizer group published a paper in 2010 detailing the conformation of contiguous β -O-galactosylated *trans*-4-hydroxyproline through analysis of far-ultraviolet circular dichroism spectra.⁷¹ As described in Chapter 3, model polyproline peptides were synthesized by solid phase peptide synthesis (Scheme 3.3). Far-ultraviolet circular dichroism spectra of peptides Ac-(Pro)₉-NH₂, Ac-(Hyp)₉-NH₂, and Ac-[(β -D-Gal)Hyp]₉-NH₂ (**121-123**) were recorded at 25 °C in water (Figure 4.9). All peptides exhibited spectra characteristic of the PPII conformation,¹⁰⁶ viz. positive maxima at 220-230 nm and negative maxima at 200-210 nm.⁹⁴ The hydroxylated nonamer **122** had a more accentuated positive maxima and a depreciated negative maxima relative to the proline nonamer **121**. The glycosylated nonamer **123** exhibited both a weaker positive and weaker negative band compared to its hydroxyproline counterpart **122**. Owens *et al.* speculated that while the lowered positive and negative maxima of compound **123** may be attributed to a possible distortion of the PPII conformation, much like the PAAP model peptide, glycopeptide **123** was still considered to have significant PPII character.

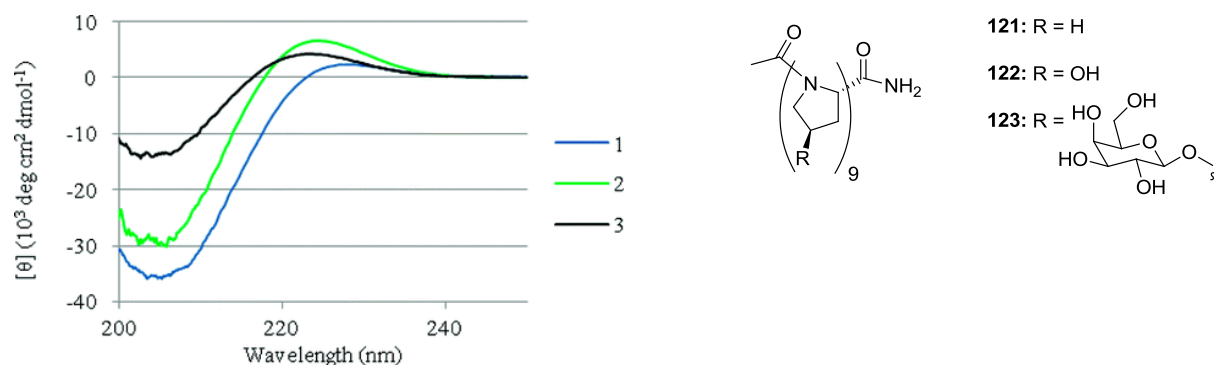


Figure 4.9 CD spectra of model peptides. Reprinted with permission from American Chemical Society.

The relative band strength (ρ) is defined as the ratio of the maximum positive ellipticity to the maximum negative ellipticity.¹⁰⁷ Pysh attributed the increase or decrease in ρ to conformational differences or changes to solvent and carbonyl backbone interactions.¹⁰⁶

Calculations show that a decreasing ρ value corresponds to an increasing solvent-carbonyl interaction. Owens reported the ρ values of Ac-(Pro)₉-NH₂, Ac-(Hyp)₉-NH₂, and Ac-[(β -D-Gal)Hyp]₉-NH₂ to be 0.06, 0.21, and 0.29 respectively.⁷¹ The consistent increase in ρ through the series of model peptides can be attributed to a decreasing solvation of the amide backbone. While the increase in ρ values can also indicate a destabilization of the PPII conformation, the authors hypothesized that hydration differences, or shielding of the amide carbonyl groups, was the primary reason for the significant differences in ρ values.

Naziga *et al.*, working in conjunction with the Schweizer group, recently reported that the conformation of glycosylated oligoprolines is highly influenced by solvent interactions.¹⁰⁸ Examining the same model peptides as Owens *et al.* (Figure 4.9, **121**, **122**, and **123**),⁷¹ Naziga and coworkers used molecular modeling techniques to investigate the increase in thermal stability of glycosylated oligoprolines and the effect of temperature on the polyproline conformation. Thermal melting experiments gave T_m values of 22, 38, and 70 °C for compounds **121**, **122**, and **123** respectively.⁷¹ While increased stability of the Hyp and glycosylated Hyp oligomers relative to the unmodified proline oligomer can be attributed to a higher population of the *trans* isomer,¹⁰⁹ it did not explain the T_m difference in Ac-(Hyp)₉-NH₂ and Ac-[(β -D-Gal)Hyp]₉-NH₂ as *trans* stabilization was not observed upon glycosylation of Ac-Hyp-NHMe as a model compound. Using molecular dynamics simulations, Naziga *et al.* reported that while sugar-sugar and sugar-backbone interactions may contribute to the stability of the PPII conformation, it was the interaction between the sugar and water molecules that was paramount to the increased stability of the glycosylated oligoprolines.¹⁰⁸ The free energy difference between the Hyp and glycosylated Hyp oligomers was found to be 26 kcal mol⁻¹ in explicit solvent (*c.f.*, no estimated difference in implicit solvent where hydrogen bonding is not accounted for).

4.1.4 CD Spectra of Ara-Hyp glycopeptides

Circular dichroism spectra of the monomer **118**, dimer **119**, trimer **120**, and tetramer (**1**) were taken in the far-ultraviolet region of the spectrum (190-240 nm). The aqueous solutions of monomer, dimer, trimer, and tetramer showed a pH reading of 6.80, 7.38, 8.79, and 9.48 respectively. Circular dichroism data was recorded in water at 20 °C at a concentration of ~0.4 mM.

Examination of the CD spectrum of our monomer showed that this compound is largely unordered, as we had expected (Figure 4.10). While there seems to be a negative maxima at 200 nm ($[\theta] = -3967 \text{ deg cm}^2 \text{ dmol}^{-1}$), there is no defined maxima. A PPII helix would feature a positive maxima around 220-230 nm, whereas the spectrum of the monomer never rises above zero $\text{deg cm}^2 \text{ dmol}^{-1}$. The CD spectrum of the monomer is akin to that of an unmodified proline dimer (Figure 4.9, $n = 2$) where $\text{H}-(\text{Pro})_2\text{-OH}$ exhibits a negative maxima at around 210 nm but no positive maxima.¹⁰¹ This is consistent with previous work reporting that peptides with less than three residues do not exhibit the PPII conformation.¹⁰¹

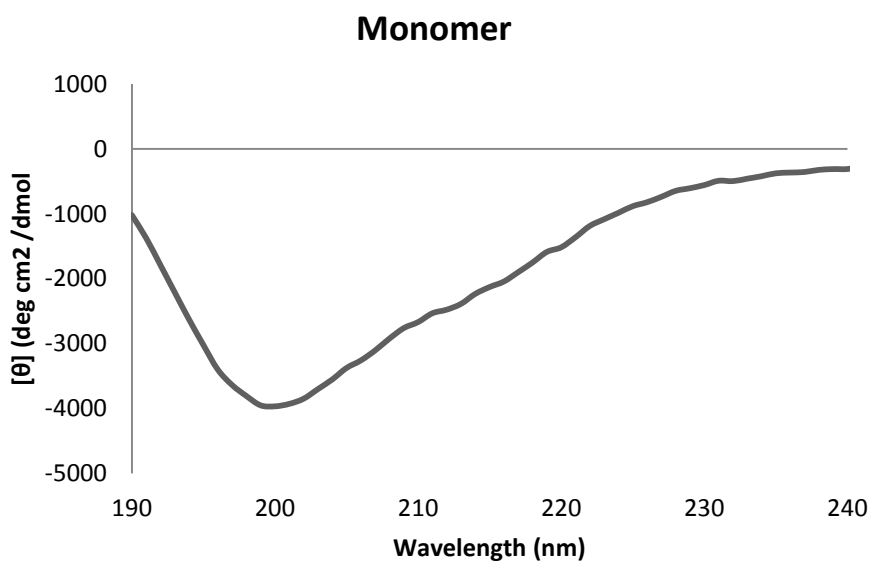


Figure 4.10 CD spectrum of $\text{Ac}-([\beta\text{-L-Araf}]\text{Hyp})\text{-NHMe}$

We fully expected that the CD spectrum of the dimer would be similar to that of the unordered monomer. Surprisingly, a cursory glance at Figure 4.11 shows that the dimer does indeed exhibit order in its elliptical curve. The peptide Ac-([β -L-Araf]Hyp)₂-NHMe displayed both a positive band ($\lambda_{\text{max}} = 220 \text{ nm}$, $[\theta] = 2905 \text{ deg cm}^2 \text{ dmol}^{-1}$) and a negative band ($\lambda_{\text{min}} = 199 \text{ nm}$, $[\theta] = -10423 \text{ deg cm}^2 \text{ dmol}^{-1}$) that is characteristic of the PPII conformation.⁹⁴ This is significant as previous studies on short polyproline peptides have shown that formation of the PPII helix began at three proline residues (H-Pro₃-OH) (Figure 4.9, $n = 3$).¹⁰¹ It is tempting to suggest that this difference is due to the carbohydrate residues acting as a restrictive medium, thus giving more order to the prolyl component of the molecule. Considering that polyproline helices are stabilized by the steric constraint of their pyrrolidine rings, we believe that the added bulk of the sugars might very well be contributing to their heightened structure.

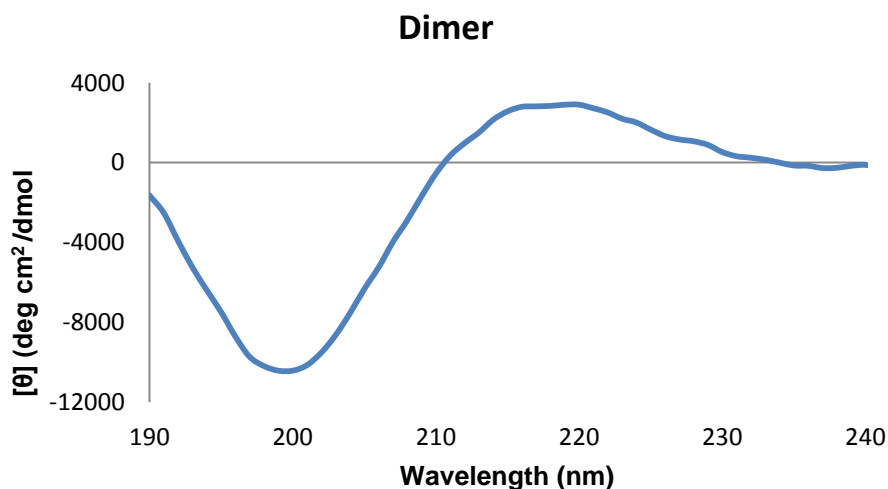


Figure 4.11 CD spectrum of Ac-([β -L-Araf]Hyp)₂-NHMe

The CD spectra of both trimer and tetramer showed typical PPII-type helical structure (Figure 4.12). Peptide Ac-([β -L-Araf]Hyp)₃-NHMe showed a positive band at 222 nm ($[\theta] = 4207 \text{ deg cm}^2 \text{ dmol}^{-1}$) and a negative maxima at 203 nm ($[\theta] = -13352 \text{ deg cm}^2 \text{ dmol}^{-1}$). Peptide Ac-

($[\beta\text{-L-Araf}]\text{Hyp}$)₄-NHMe exhibited a positive band at 220 nm ($[\theta] = 3704 \text{ deg cm}^2 \text{ dmol}^{-1}$) and a negative maxima at 200 nm ($[\theta] = -13816 \text{ deg cm}^2 \text{ dmol}^{-1}$).

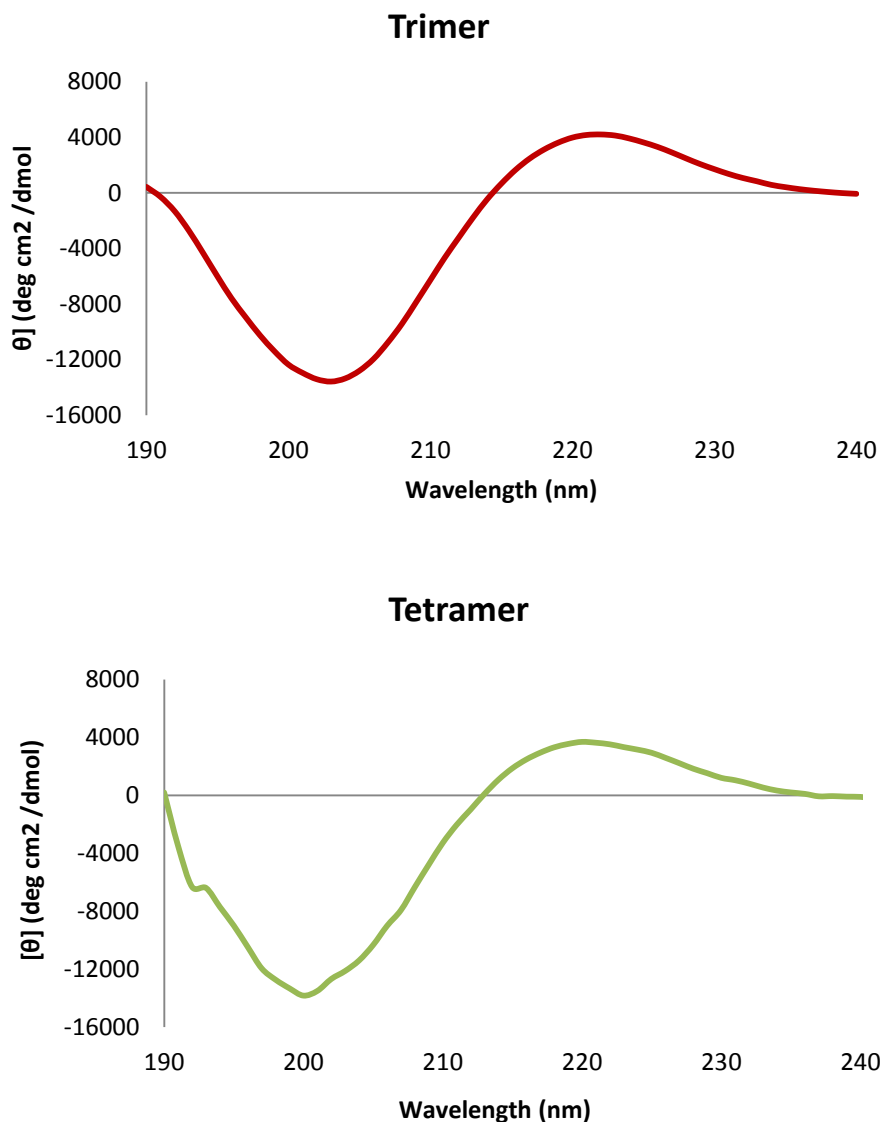


Figure 4.12 CD spectrum of Ac-([$\beta\text{-L-Araf}$]Hyp)₃-NHMe and Ac-([$\beta\text{-L-Araf}$]Hyp)₄-NHMe

Figure 4.13 shows an overlay of the CD spectra of all four synthetic glycopeptides relative to one another. Using the monomer as a baseline value, we can see that the intensity of the negative maxima increases with the length of the glycopeptide. This is consistent with the findings of Rothe.¹⁰¹ The trimer and tetramer, as expected, showed the most intense positive

and negative bands. This is likely due to the fact that the larger oligomers possess the necessary number of residues to form a proper PPII helix.

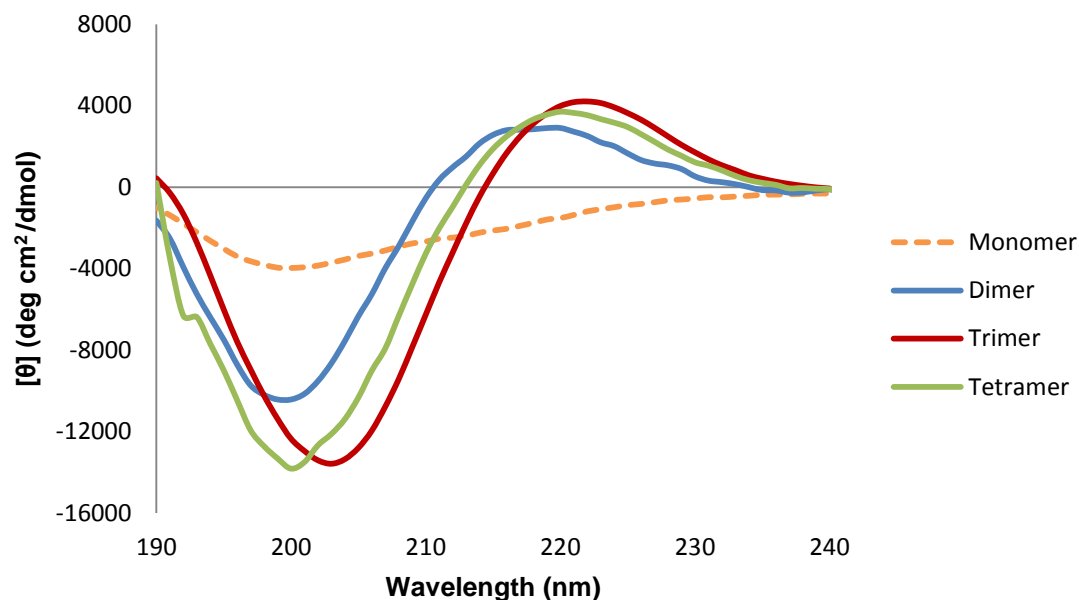


Figure 4.13 CD Spectra of all four synthetic glycopeptides

The relative band strength (ρ value) of dimer, trimer, and tetramer are 0.28, 0.30, and 0.27 respectively. While we anticipated a decrease in relative band strength with increasing residue count, this was not the case. Instead, the ρ value increased slightly from dimer to trimer, with tetramer having the lowest ρ value of all three peptides. However, we do not believe the differences in these values are significant. The discrepancies in the ρ values are most likely due to common experimental error and it is probable that the PPII helical content of the three compounds are quite comparable to one another. These values are also in agreement with the ρ value of the galactosylated hydroxyproline nonamer reported by Owens ($\rho = 0.29$).⁷¹

4.2 Nuclear Magnetic Resonance Spectroscopy

4.2.1 Characterization of Ara-Hyp glycopeptides of nArt v 1 by Leonard *et al.*

Nuclear magnetic resonance spectroscopy was conducted on α -arabinosidase-treated nArt v 1. Tables 4.1 and 4.2 show the chemical shifts for Hyp and β -Ara residues as reported by Leonard and coworkers.²² Three types of β -arabinoside residues were found for which distinct anomeric proton signals could be discerned around 5.10-5.12 ppm (Table 4.2). This is consistent with the occurrence of three residues per turn in the PPII helix. The ^{13}C NMR signal for the anomeric carbon, which could not be differentiated for the three types, was found at 100.9 ppm. For comparison, the C1 signal for α -Ara residues of nArt v 1 were found at 107-109 ppm. Typically, when substituents on C1 and C2 are *cis* to one another, as is the case for β -arabinosides, the C1 resonances can be found between 100 to 105 ppm.¹¹⁰ The ^{13}C chemical shifts are also in agreement with literature values reported from naturally occurring polysaccharide arabinans containing the β -Ara motif.¹¹¹ Nuclear Overhauser effect (nOe) correlations between the anomeric proton of β -Ara and the γ -proton of Hyp support the linkage of the arabinoside. Leonard *et al.* had reported the first ^1H and ^{13}C characterization of contiguous mono- β -arabinosides of hydroxyproline found in the carbohydrate region of nArt v 1.

Table 4.1 NMR resonances of Hyp in Art v 1 ²²

Hyp	Chemical Shift (ppm)					
	α	$\beta 1$	$\beta 2$	γ	$\delta 1$	$\delta 2$
Type 1 ^1H	4.837	2.547	2.000	4.581	4.035	3.729
Type 2 ^1H	4.844	2.552	2.005	4.574	4.012	3.758
Type 3 ^1H	4.831	2.531	2.001	4.580	4.028	3.722
^{13}C	58.6	35.7		77.5	53.8	

Table 4.2 NMR resonances of β -Ara in Art v 1²²

β -Ara	Chemical Shift (ppm)					
	1	2	3	4	5a	5b
Type 1 ^1H	5.120	4.10	4.012	3.848	3.744	3.600
Type 2 ^1H	5.108	4.069	3.991	3.840	3.734	3.577
Type 3 ^1H	5.105	4.089	3.972	3.840	3.734	3.572
^{13}C	100.9	77.2	75.3	82.8	64.1	

4.2.2 Characterization of synthetic Ara-Hyp glycopeptides

Various ^1H , ^{13}C , and 2-D NMR spectra of Ac-([β -L-Araf]Hyp)-NHMe (**118**) in CD_3OD were acquired. Due to the rotational isomerization of the prolyl acetamide, an approximate 4:1 ratio of rotamers is detected. Examination of the NOESY spectrum (Figure 4.14) shows a correlation between the acetamide CH_3 signal (2.08 ppm) of the major rotamer to the δ protons (3.73 ppm) of hydroxyproline, signifying that the preferred isomer is in the *trans* conformation. There is also correlation of the minor acetamide CH_3 signal (1.93 ppm) to the minor α proton (4.52 ppm) of the prolyl ring. For simplicity's sake, we will assign only the major rotamer from here forth.

The resonances at 4.99 ppm could be readily assigned to the anomeric proton of the arabinose residue, close to the ~ 5.11 ppm reported by Leonard,²² with the disparity between the numbers most likely due to the differing solvent used. The ^{13}C - ^1H correlation spectrum (Figure 4.15, HSQC) revealed that the anomeric proton was attached to a ^{13}C resonance at 101.2 ppm, indicating the substituents at C1 and C2 are *cis*.¹¹⁰ The J coupling constant of the anomeric signal was 4.6 Hz which is typical for β -arabinosides (*c.f.*, $J = 0\text{--}2$ Hz for α -arabinosides). The COSY spectrum (Figure 4.16, p 144) shows a correlation of the anomeric

proton signal to a doublet of doublets at 3.96 ppm which we label H2. Resonances at 3.88 and 3.76 can be readily assigned to H3 and H4 respectively. Two signals correlate to H4, which the HSQC spectrum reveals to be attached to the same carbon at 63.9 ppm (*c.f.*, 64.1 ppm as assigned by Leonard in Art v 1), and is assigned as the diastereotopic H5 protons of the arabinose ring.

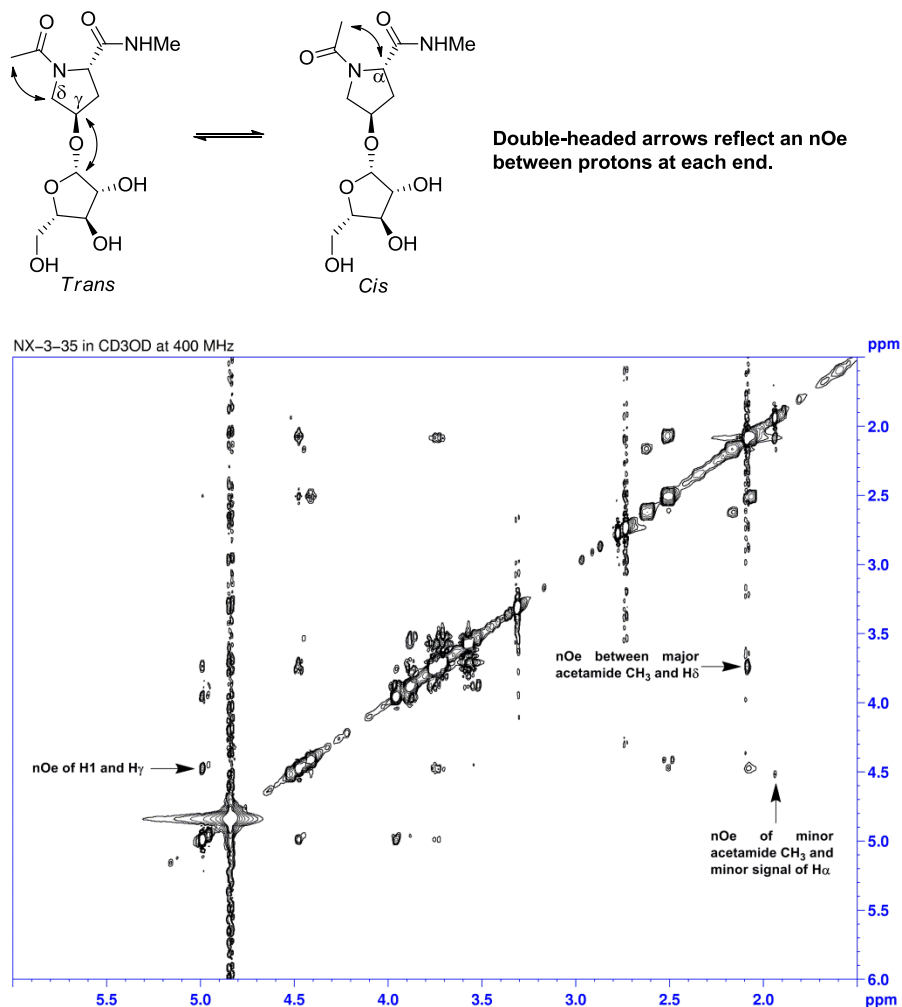


Figure 4.14 NOESY spectrum of Ac-([β-L-Araf]Hyp)-NHMe

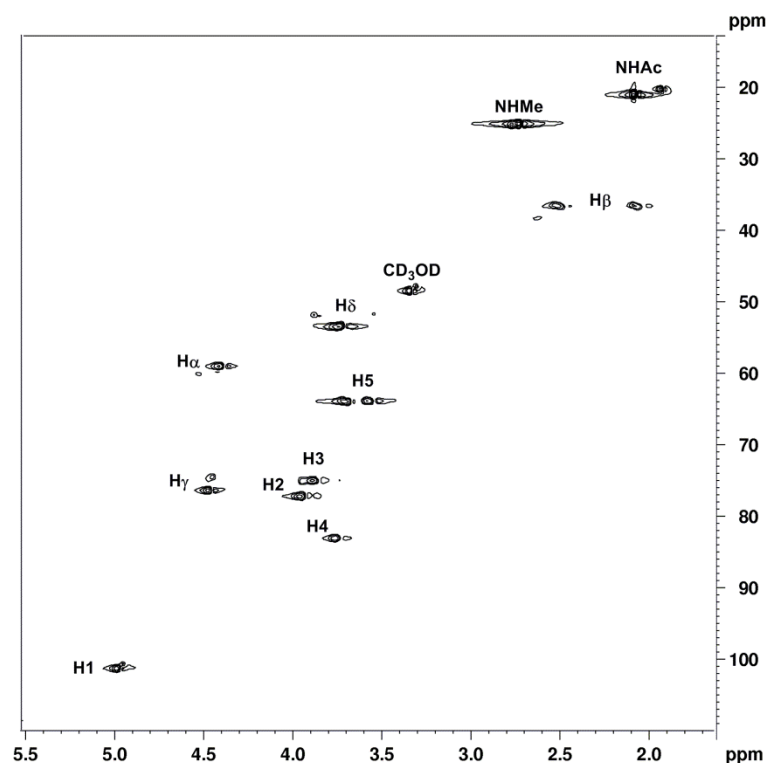


Figure 4.15 HSQC spectrum of Ac-([β-L-Araf]Hyp)-NHMe

Multiplets at 2.06 and 2.50 ppm can be assigned to a pair of diastereotopic protons attached to a carbon that resonates at 36.5 ppm as seen in the HSQC spectrum. These were assigned to H β of the proline ring, consistent with their chemical shifts. The H β signals show correlations with two other signals in the COSY spectrum. The first of the two signals was assigned to H α (4.41 ppm), as evidence by its splitting into a triplet. The second of these signals is H γ (4.46 ppm) which was split into a multiplet as expected from its environment. The H γ resonance showed further correlation with a pair of diastereotopic protons at 3.72 ppm which are the H δ signals. Finally, the glycosidic linkage of hydroxyproline and arabinose was confirmed by an nOe between H γ of Hyp (4.46 ppm) and the anomeric proton of β -Araf (4.99 ppm).

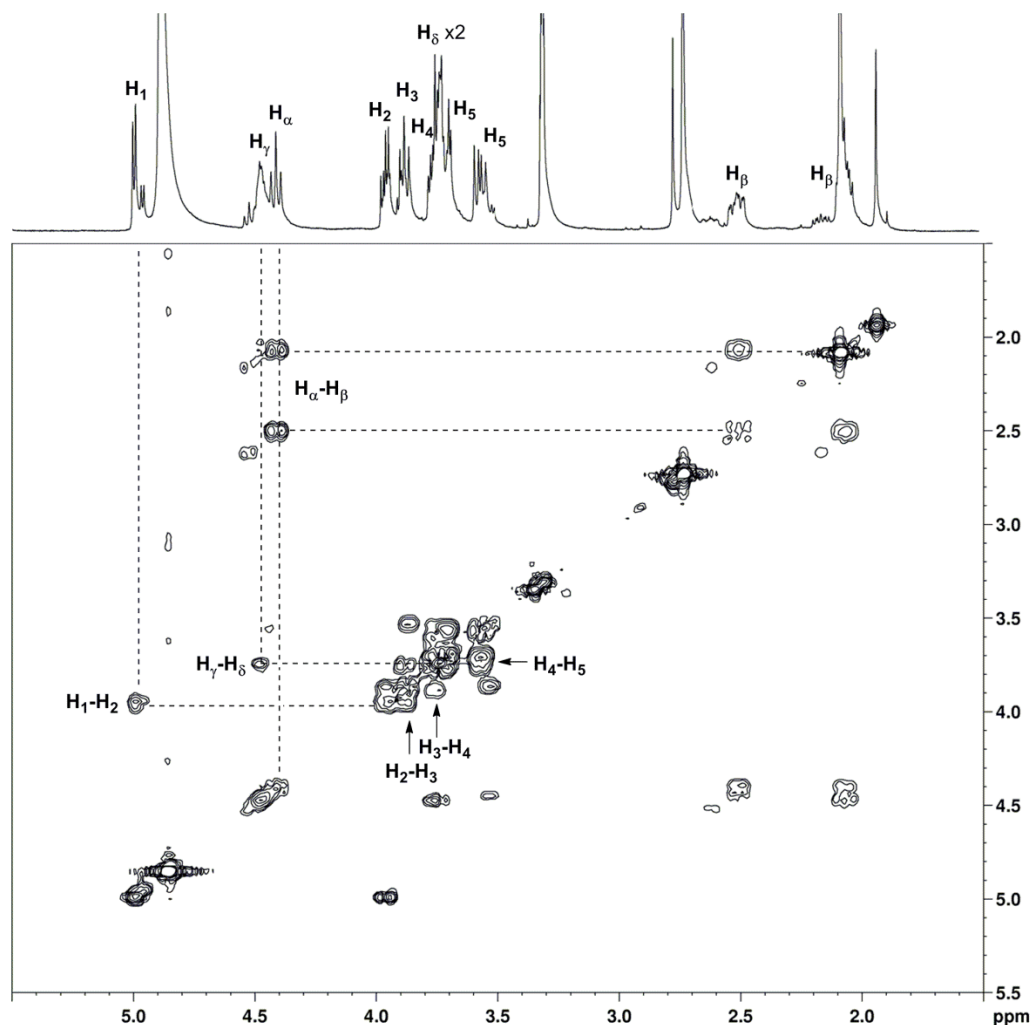


Figure 4.16 COSY spectrum of Ac-([β -L-Araf]Hyp)-NHMe

Nuclear magnetic resonance spectra were acquired for the oligomers. Figure 4.17 shows a comparison of the ^1H NMR spectra of the four compounds. We have fully characterized the monomer and dimer using ^1H , ^{13}C , and 2D NMR experiments. With each additional (β -L-Araf)Hyp residue added, however, the NMR spectra became increasingly more complex. The spectral assignments of trimer and tetramer were made with only 1-D NMR experiments and by extrapolation from spectral assignments of monomer and dimer.

To validate the number of residues, we compared the integration of C-terminal methyl amide (#H = 3 for all compounds, ~2.75 ppm) to the anomeric signal (#H = 1-4 for monomer,

dimer, trimer and tetramer, ~5.00 ppm). The *N*-terminal acetamide could also be employed for this comparison, albeit some overlap with H β signal made this less straightforward than using the methyl amide. Although the integration of the combined anomeric signals increased by one unit per added residue, additional anomeric peaks were not detected, signifying that all sugar residues are in a similar environment and conformation. In the larger oligomers, rotational isomeric signals were less prominent than that of the monomer. This is in contrast to the fully benzylated Boc-([β -L-Ara/Hyp] $_n$ -OAll peptides where each additional residue gave rise to a new pair of rotational isomeric signals, resulting in up to eight ^{13}C signals for C1 in the fully protected tetramer (**100**, Scheme 3.19). Our findings on the protected oligomers are in agreement with previous work on oligoprolines.¹¹² It is possible that the carbohydrate residues are contributing to the reduced number of species of these larger compounds in solution. Figure 4.17 shows the ^1H NMR spectra of **118**, **119**, **120**, and **1** in CD $_3$ OD at 400 MHz (Next Page).

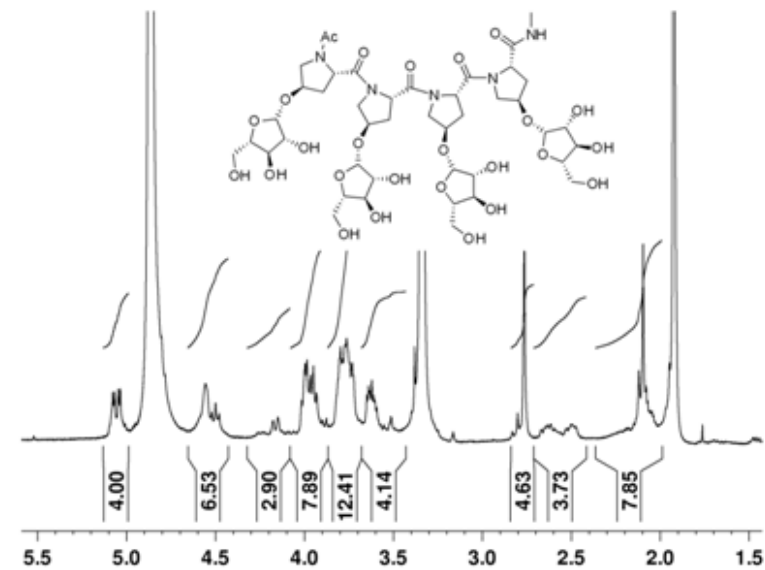
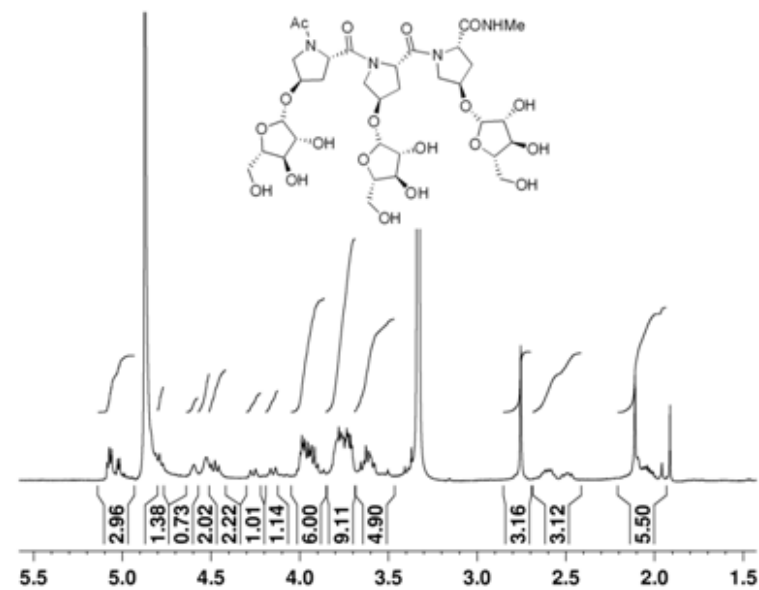
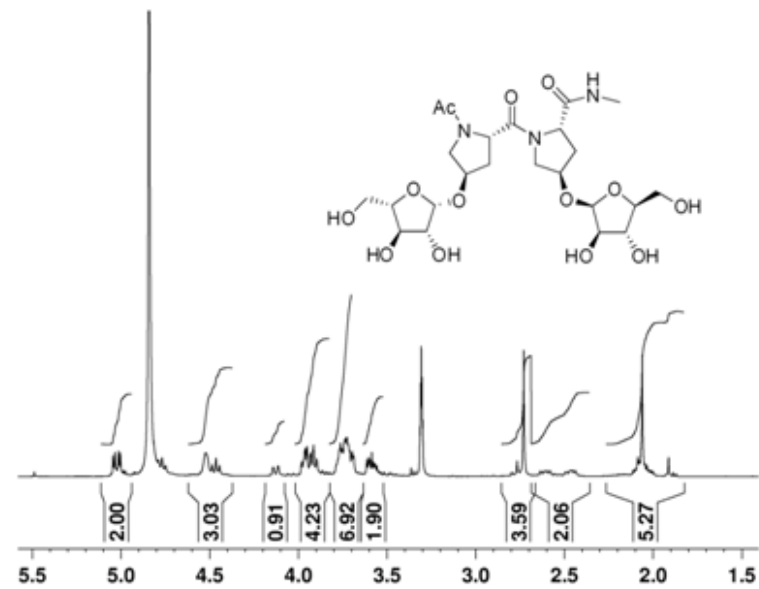
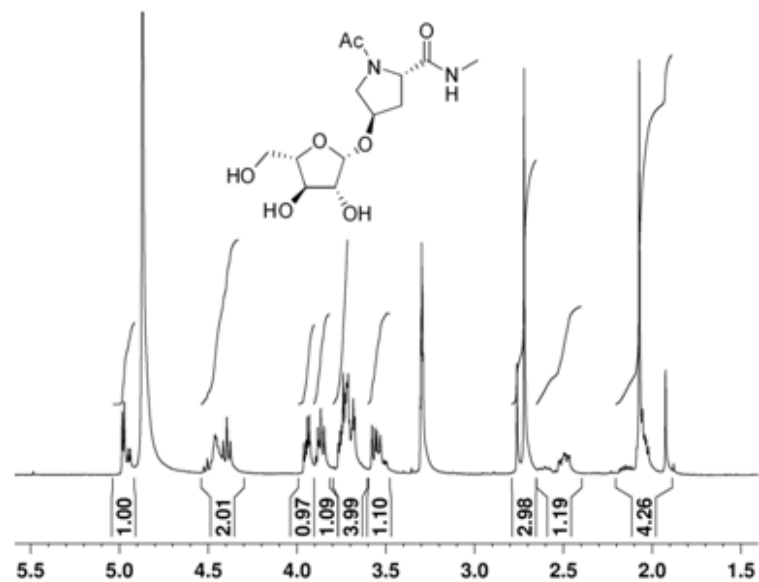


Figure 4.17 ^1H NMR of all four synthetic glycopeptides

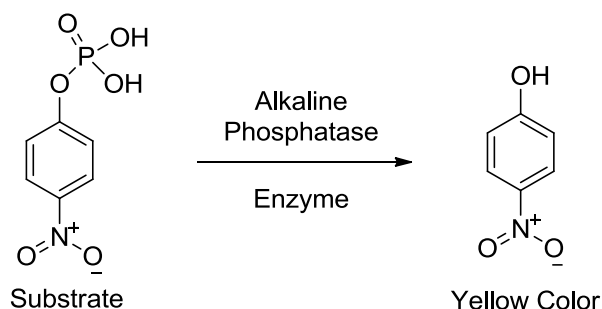
4.3 Enzyme Linked Immunosorbent Assays

In the spring of 2011, the first two synthetic glycopeptides were sent to the Altmann Group at BOKU in Vienna, Austria. Ten milligrams each of monomer **117** and dimer **118** were provided by the Taylor Group for biological testing against antibodies specific for the carbohydrate region of Art v 1. Enzyme linked immunosorbent assay (ELISA) experiments, used extensively for the detection of antibodies/antigens in serum samples, were employed to confirm the existence of glycan epitopes. The Altmann group conducted cross-inhibition ELISA experiments, also known as competitive ELISA, to determine the IgG binding properties of the synthetic glycopeptides.

First, various concentrations of monomer **117** and dimer **118** were incubated with rabbit serum containing only the anti-glycan IgGs. This serum was then added to a microtiter plate bound with natural Art v 1 to allow for possible competitive binding to the antibody. The plate was washed so that any unbound antibody was washed away. The amount of remaining antigen still bound to the surface of the plate correlates directly to the binding capacity of the synthetic glycopeptides to the antibody generated against the carbohydrate region of the natural allergen. The higher the percentage of antigen still present in the wells signifies a higher percentage of the synthetic glycopeptides binding to the antibody.

In order to measure this displacement, the remaining bound anti-glycan IgGs were treated with an alkaline phosphatase-conjugated goat anti-rabbit IgG that is specific for the bound antigen. The plate was washed again to remove any unbound antibody-enzyme conjugate. Upon activation of the enzyme with 0.1% p-nitrophenyl phosphate (Scheme 4.1), a chromogenic substrate, and a 0.1 M diethanolamine (pH 9.8) buffer, the plate was read immediately at 405/620 nm with an SLT-spectra plate reader to obtain quantitative results on

the amount of antigen remaining. Figure 4.18 shows the initial results of the ELISA inhibition experiment with the synthetic glycopeptides at millimolar concentration.



Scheme 4.1 Activation of ALP with *p*-nitrophenyl phosphate

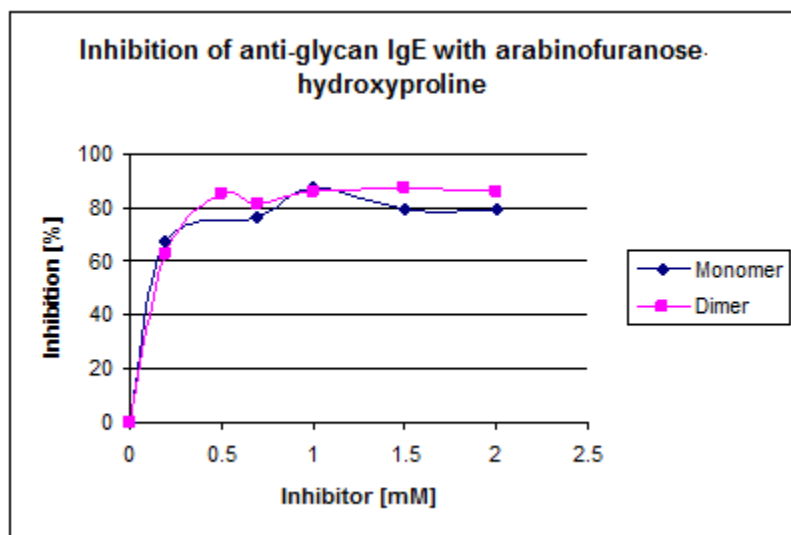


Figure 4.18 ELISA inhibition experiments of synthetic glycopeptides

At the highest of concentrations (2 mM), the % inhibition for both the monomer and dimer were similar to one another, reaching 80% at ~0.5 mM; these initial results were encouraging. Unfortunately, subsequent repeated assays with diluted samples showed inconsistencies (Figure 4.19). The inhibition potency of monomer and dimer varied in the experiments for unexplained reasons. However, in all three experiments presented here, monomer and dimer inhibit Art v 1 binding to a similar extent. The results reported herein are unpublished work from the Altmann Group.¹¹³

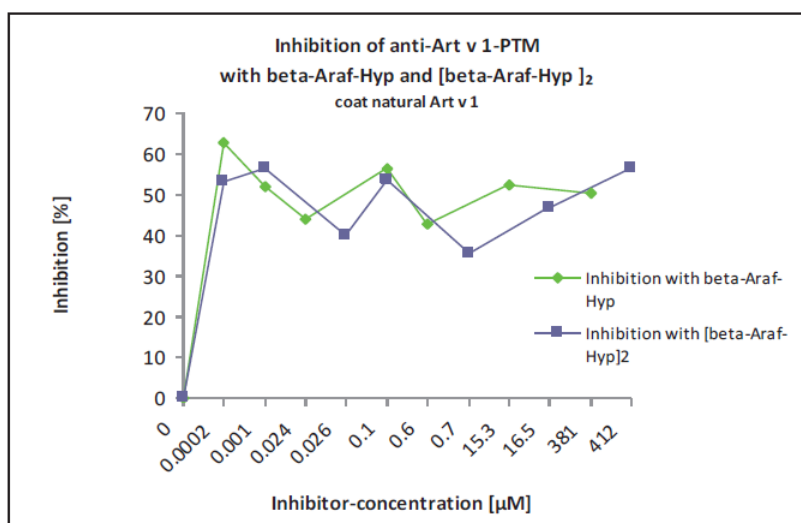
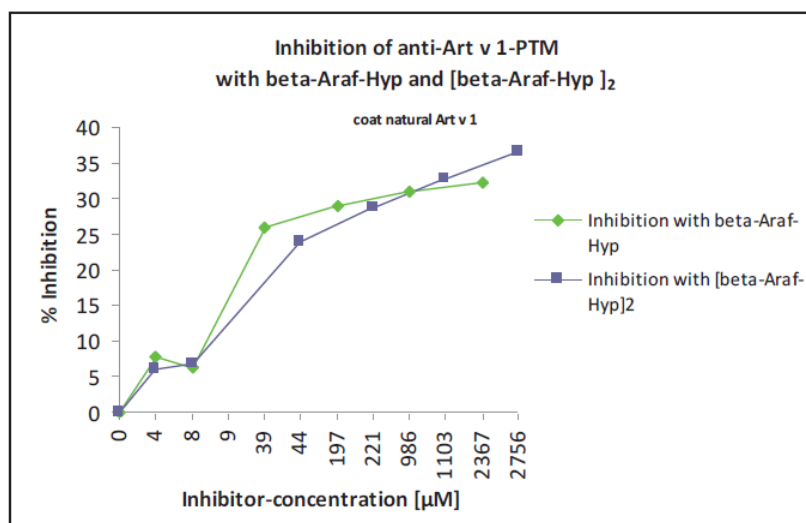
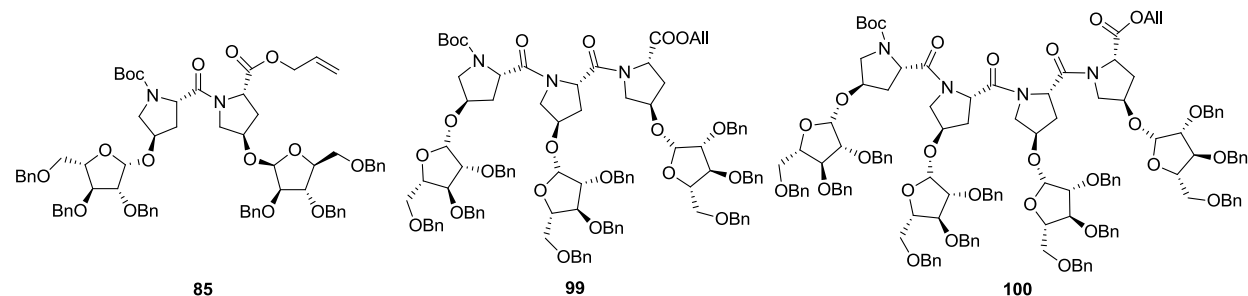


Figure 4.19 Varied concentrations of synthetic glycopeptides in inhibition experiments

4.4 Summary

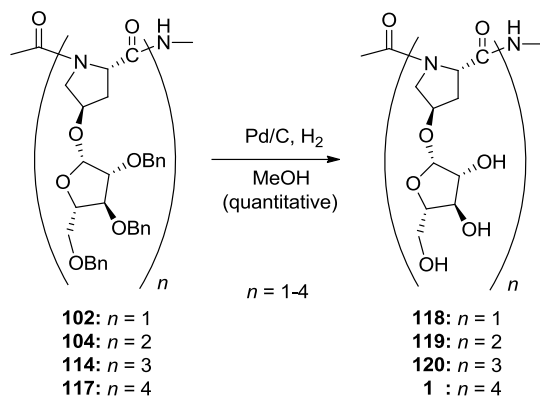
It was the goal of this dissertation to find the minimal carbohydrate epitope of the Art v 1 allergen. A key intermediate in the assembly of relevant oligomers was a β -arabinoside of hydroxyproline, a 1,2-*cis* glycoside that is a challenge to synthetic organic chemistry. Towards the synthesis of this intermediate, we prepared *N*-*tert*-butoxycarbonyl-trans-4-hydroxy-L-proline allyl ester (**54**) for glycosylation with p-cresyl 2-O-benzyl-3,5-O-(di-*tert*-butylsilylene)-1-thio- α -L-arabinofuranoside (**42**). Unfortunately, use of this conformationally restricted bicyclic donor **60**

In preparing the oligomers of hydroxyproline arabinosides, we unmasked the *N*- and C-termini of Boc-([β-L-Araf]Hyp)-OAll in independent experiments. Coupling of the free acid and amine with HATU gave the Boc-([β-L-Araf]Hyp)₂-OAll dimer (**85**) in 60% yield. The trimer **99** could be assembled by the coupling of Boc-([β-L-Araf]Hyp)-OH with H-([β-L-Araf]Hyp)₂-OAll [1+2] or Boc-([β-L-Araf]Hyp)₂-OH with H-([β-L-Araf]Hyp)-OAll [2+1], with each strategy affording chemical yields of ~35%. Coupling of a Boc-([β-L-Araf]Hyp)₂-OH and H-([β-L-Araf]Hyp)₂-OAll gave the tetramer **100** in 49%.



Installation of amide end-caps on Boc-([β-L-Araf]Hyp)-OAll gave Ac-([β-L-Araf]Hyp)-NHMe in 42% yield over 4 steps. Switching to a more convergent and higher yielding route, we chose to utilize pre-endcapped glycosidic building blocks for the preparation of end-capped oligomers. Position-specific glycosidic building blocks Ac-([β-L-Araf]Hyp)-OMe (*N*-terminal) and

Boc-([β-L-Araf]Hyp)-NHMe (C-terminal) were prepared. With this strategy, fragment condensation of end-capped building blocks afforded dimer **104**, trimer **114**, and tetramer **117** in 48%, 35%, and 15% respectively. Global debenzoylation of the end-capped glycopeptides gave the four deprotected compounds in quantitative yield.



Scheme 4.3 Global debenzoylation

Circular dichroism data were obtained for the synthetic glycopeptides. The monomer spectrum showed it to be unordered as expected. Analysis of the CD spectra showed that the glycosylated proline oligomers exhibited characteristic polyproline II helical conformation. However, to our surprise, the dimer displayed order in its elliptical curve ($\lambda_{\text{max}} = 220$ nm, $\lambda_{\text{min}} = 199$ nm). The trimer ($\lambda_{\text{max}} = 222$ nm, $\lambda_{\text{min}} = 203$ nm) and tetramer ($\lambda_{\text{max}} = 220$ nm, $\lambda_{\text{min}} = 200$ nm) both exhibited significant PPII helical conformation.

Nuclear magnetic resonance spectroscopy was used to characterize all target glycopeptides. ^1H , ^{13}C , and various 2-D NMR were used to identify key resonances in the comparison of the synthetic glycopeptides with glycoprotein isolated from the natural allergen.

In closing, the synthesis and oligomers described herein enable the further study of this important class of compounds. Our homogeneous compounds, characterized with the rigor of organic chemistry, lay the foundation for unambiguous biological studies that were not possible

with the trace amount of heterogeneous material available from degradation of the native Art v 1 protein.

4.5 Future Work

The obvious next step in the project is to conduct ELISA experiments on trimer and tetramer in varying concentrations. With the completion of the CD experiments, trimer and tetramer are ready to be sent to Vienna. Despite reproducibility issues, the fact that monomer and dimer have behaved similarly may suggest that the large oligomers will as well. The direction of the project thereafter will be conditional upon those results. In any event, we propose herein a plan for the continuation of the investigation of the carbohydrate epitope of Art v 1.

4.5.1 Incorporation of the β -Ara-Hyp motif into longer peptides

While we have synthesized the tetraproline component of the tail section of Art v 1, we do not yet know whether or not this is optimal, *vis-à-vis* biological response. While the monomer and dimer seemed to be at least partially effective, it is possible that increasing the length of the peptide chain may be beneficial to the activity of the glycopeptides. Table 4.3 shows the amino acid sequence of the carbohydrate domain of Art v 1. Note that the proline residues typically follow a serine or alanine residue. In fact, the amino acid sequence SPP is found thrice in this sequence and SPPPP twice. The sequences APP and APPP are also found. It is interesting as to whether or not an extended glycopeptide sequence, synthesized to include these serine and alanine residues, and perhaps more than one glycocluster, would have an effect on antibody binding. If so, will an even longer sequence of the tail section of Art v 1 be worth investigating?

Table 4.3 Amino acid sequence in the polyproline domain

56-60	61-70	71-80	81-90	91-100	100-108
SPPGA	TPAPPGAAPP	PAAGGSPSP	ADGGSPPPA	DGGSPPPVDGG	SPPPPSTH

4.5.2 Antibody generation

Glycosylated proteins have been known to have antigenic properties.¹¹⁴ Advances in carbohydrate research have further illuminated their potential as vaccines.¹¹⁵ However, the low immunogenicity of carbohydrate antigens continues to prove problematic. Polysaccharides are T-cell independent, meaning they do not induce immunological memory. To this end, carbohydrate antigens have been coupled to carrier proteins to heighten their immunogenicity.¹¹⁶

Avery and Goebel first introduced the technique to enhance the immunogenicity of polysaccharide antigens.¹¹⁷ More recently, this hapten-carrier protein conjugate strategy has been regularly employed for bacterial carbohydrates.¹¹⁸ The covalent linkage of the polysaccharide and the carrier protein has been achieved by various techniques (*i.e.*, carbodiimide coupling, reductive amination, etc).¹¹⁹

Covalent linkages to our synthetic glycopeptides can be made by *N*-terminal conjugation. The free amine will be modified for attachment via a spacer unit bearing a carboxylic acid which permits conjugation (Figure 4.21). The glycoprotein conjugate will then be used to raise a rabbit antiserum specific against the homogeneous, synthetic β -Ara-Hyp epitope. Monoclonal antibodies generated using the glycoprotein conjugate can potentially be useful in screening for cross-reactivity in other plant allergens. Finally, the glycoprotein conjugates can be used to determine binding affinities for rabbit and human IgG and IgE.

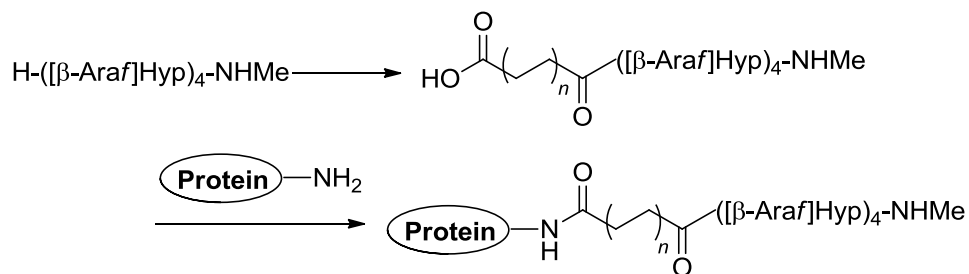
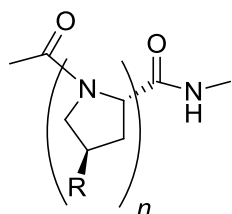


Figure 4.21 Proposed conjugation of synthetic glycopeptides to carrier proteins

4.5.3 Effect of glycosylation on oligoproline conformation

The Taylor group has made fundamental contributions to conformational determinates in proline-containing peptides.^{57, 120} This dissertation opens the door to studies on consecutive proline residues as well as modified proline oligomers. Molecular dynamics studies have shown the predominant conformation of end-capped oligoprolines to be *trans*,¹²¹ which indicates a PPII helix. Utilizing NMR and circular dichroism spectroscopy, investigation of the twelve compounds in Table 4.4 would allow us to see the changes in their conformation with regards to number of proline residues and degree of post-translational modification. This would give greater context to the results described in Section 4.14.

Table 4.4 Target oligoproline compounds



	124	125	126	127	128	129	130	131	118	119	120	1
<i>n</i>	1	2	3	4	1	2	3	4	1	2	3	4
R	H				OH				O-β-L-Araf			

4.5.4 Synthetic glycopeptides as diagnostic tools

The development of modern diagnostic tools has been paramount in the identification of allergies.¹²² Two of the most commonly used screening methods are the skin prick test (SPT) and allergy blood tests. In order to pinpoint the exact source of the allergen, investigations have focused on identifying cross-reactive pollens of the Asteraceae family.¹²³ Pollen from ragweed, chrysanthemum, and dandelion may share similar epitopes (β-Ara-Hyp) with mugwort pollen. Further related plants such as feverfew and sunflower may also contain the β-Ara-Hyp epitope as these species all produce a homolog of Art v 1. Most notably, the allergen of ragweed, Amb a 4, has 50% homology to Art v 1 and was found to contain small amounts of β-Ara-Hyp.³¹ Furthermore, natural Art v 1 was found to inhibit IgE binding of Amb a 4. In order to evaluate

the relevance of the β -Ara-Hyp epitope, we propose that a specific anti- β -Ara-Hyp serum be generated in order to screen a wide array of plant pollens.

4.6 Experimental Section

4.6.1 Circular dichroism spectroscopy

Sample compounds were lyophilized for 24 h prior to dilution to a concentration of 0.4 mM with water. The pH of the samples was determined at rt and found to be 6.80, 7.38, 8.79, and 9.48 for compounds **118**, **119**, **120**, and **1** respectively. Circular dichroism measurements were carried out using a JASCO J-815 spectrometer. For analysis, 175 μ L of the sample was loaded into a quartz cell with a path length of 0.1 cm. The CD spectra were recorded at a scan rate of 20 nm per min, data pitch of 1.0 nm, and bandwidth of 2.0 nm. The accumulation of three scans was averaged for each sample, after which a blank of the solvent was subtracted. The CD signal was converted to molar ellipticity per mean residue ($[\theta]$) and the data was smoothed by application of the Savitzky-Golay algorithm.

4.6.2 NMR spectroscopy

NMR spectra were obtained using a Bruker AV-400 or Varian 700 MHz spectrometer. Proton NMR data is reported in ppm downfield from TMS as an internal standard. Disodium 3-trimethylsilyl-1-propane-sulfonate (DSS) was used to reference ^1H NMR spectra run in D_2O . Minor rotational isomers are reported in parentheses when significant amount exist.

REFERENCES

1. Timmer, M. S. M.; Stocker, B. L.; Seeberger, P. H., Probing glycomics. *Current Opinion in Chemical Biology* **2007**, *11*, 59-65.
2. Sairam, M. R., Role of carbohydrates in glycoprotein hormone signal transduction. *Faseb Journal* **1989**, *3*, 1915-1926.
3. Avci, F. Y.; Kasper, D. L., How bacterial carbohydrates influence the adaptive immune system. *Annual Review of Immunology*, Vol 28 **2010**, *28*, 107-130.
4. Bishop, J. R.; Schuksz, M.; Esko, J. D., Heparan sulphate proteoglycans fine-tune mammalian physiology. *Nature* **2007**, *446*, 1030-1037.
5. (a) Zachara, N. E.; Hart, G. W., Cell signaling, the essential role of O-GlcNAc! *Biochimica Et Biophysica Acta-Molecular and Cell Biology of Lipids* **2006**, *1761*, 599-617; (b) Love, D. C.; Hanover, J. A., The hexosamine signaling pathway: deciphering the "O-GlcNAc code". *Sci STKE* **2005**, *2005*, re13.
6. Hart, G. W.; Housley, M. P.; Slawson, C., Cycling of O-linked beta-*N*-acetylglucosamine on nucleocytoplasmic proteins. *Nature* **2007**, *446*, 1017-1022.
7. Liu, F.; Iqbal, K.; Grundke-Iqbal, I.; Hart, G. W.; Gong, C. X., O-GlcNAcylation regulates phosphorylation of tau: A mechanism involved in Alzheimer's disease. *Proceedings of the National Academy of Sciences of the United States of America* **2004**, *101*, 10804-10809.
8. Oppenheimer, S. B.; Alvarez, M.; Nnoli, J., Carbohydrate-based experimental therapeutics for cancer, HIV/AIDS and other diseases. *Acta Histochemica* **2008**, *110*, 6-13.
9. Helling, F.; Shang, A.; Calves, M.; Zhang, S. L.; Ren, S. L.; Yu, R. K.; Oettgen, H. F.; Livingston, P. O., G(D3) Vaccines for melanoma - superior immunogenicity of Keyhole Limpet Hemocyanin conjugate vaccines. *Cancer Research* **1994**, *54*, 197-203.
10. Ada, G.; Isaacs, D., Carbohydrate-protein conjugate vaccines. *Clin Microbiol Infec* **2003**, *9*, 79-85.
11. Seeberger, P. H.; Werz, D. B., Synthesis and medical applications of oligosaccharides. *Nature* **2007**, *446*, 1046-1051.
12. World malaria situation 1990. *World health statistics quarterly* **1992**, *45*, 257-266.
13. Schofield, L.; Hewitt, M. C.; Evans, K.; Siomos, M. A.; Seeberger, P. H., Synthetic GPI as a candidate anti-toxic vaccine in a model of malaria. *Nature* **2002**, *418*, 785-789.
14. Lamport, D. T. A.; Clark, L., The isolation and partial characterization of hydroxyproline-rich glycopeptides obtained by enzymic degradation of primary cell walls. *Biochemistry-Us* **1969**, *8*, 1155-1163.
15. Sommer-Knudsen, J.; Bacic, A.; Clarke, A. E., Hydroxyproline-rich plant glycoproteins. *Phytochemistry* **1998**, *47*, 483-497.

16. Deepak, S.; Shailasree, S.; Kini, R. K.; Muck, A.; Mithofer, A.; Shetty, S. H., Hydroxyproline-rich Glycoproteins and Plant Defence. *Journal of Phytopathology* **2010**, *158*, 585-593.
17. Himly, M.; Jahn-Schmid, B.; Dedic, A.; Kelemen, P.; Wopfner, N.; Altmann, F.; van Ree, R.; Briza, P.; Richter, K.; Ebner, C.; Ferreira, F., Art v 1, the major allergen of mugwort pollen, is a modular glycoprotein with a defensin-like and a hydroxyproline-rich domain. *FASEB* **2002**, *16*, 106-108.
18. Spielsma, F. T. M.; Charpin, H.; Nolard, N.; Stix, E., City Spore Concentrations in the European Economic-Community (Eec) .4. Summer Weed Pollen(Rumex, Plantago, Chenopodiaceae, Artemisia), 1976 and 1977. *Clinical Allergy* **1980**, *10*, 319-329.
19. Beasley, R.; Keil, U.; von Mutius, E.; Pearce, N.; Ait-Khaled, N.; Anabwani, G.; Anderson, H. R.; Asher, M. I.; Bjorkstein, B.; Burr, M. L.; Clayton, T. O.; Crane, J.; Ellwood, P.; Lai, C. K. W.; Mallol, J.; Martinez, F. D.; Mitchell, E. A.; Montefort, S.; Robertson, C. F.; Shah, J. R.; Sibbald, B.; Stewart, A. W.; Strachan, D. P.; Weiland, S. K.; Williams, H. C.; Childhood, I. S. A. A., Worldwide variation in prevalence of symptoms of asthma, allergic rhinoconjunctivitis, and atopic eczema: ISAAC. *Lancet* **1998**, *351*, 1225-1232.
20. Gadermaier, G.; Jahn-Schmid, B.; Vogel, L.; Egger, M.; Himly, M.; Briza, P.; Ebner, C.; Vieths, S.; Bohle, B.; Ferreira, F., Targeting the cysteine-stabilized fold of Art v 1 for immunotherapy of *Artemisia* pollen allergy. *Molecular Immunology* **2010**, *47*, 1292-1298.
21. Razzera, G.; Gadermaier, G.; de Paula, V.; Almeida, M. S.; Egger, M.; Jahn-Schmid, B.; Almeida, F. C. L.; Ferreira, F.; Valente, A. P., Mapping the interactions between a major pollen allergen and human IgE antibodies. *Structure* **2010**, *18*, 1011-1021.
22. Leonard, R.; Petersen, B. O.; Himly, M.; Kaar, W.; Wopfner, N.; Kolarich, D.; van Ree, R.; Ebner, C.; Duus, J. O.; Ferreira, F.; Altmann, F., Two novel types of O-glycans on the mugwort pollen allergen Art v 1 and their role in antibody binding. *J Biol Chem* **2005**, *280*, 7932-7940.
23. Clarke, A. E.; Anderson, R. L.; Stone, B. A., Form and function of arabinogalactans and arabinogalactan-proteins. *Phytochemistry* **1979**, *18*, 521-540.
24. Anderson, R. L.; Clarke, A. E.; Jermyn, M. A.; Knox, R. B.; Stone, B. A., Carbohydrate-binding arabinogalactan-protein from liquid suspension cultures of endosperm from *Lolium multiflorum* *Australian Journal of Plant Physiology* **1977**, *4*, 143-158.
25. (a) Anderson, M. A.; Sandrin, M. S.; Clarke, A. E., A High proportion of hybridomas raised to a plant extract secrete antibody to arabinose or galactose. *Plant Physiology* **1984**, *75*, 1013-1016; (b) Willats, W. G. T.; Marcus, S. E.; Knox, J. P., Generation of a monoclonal antibody specific to (1→5)- α -l-arabinan. *Carbohydr Res* **1998**, *308* (1–2), 149-152.
26. (a) Haavik, S.; Paulsen, B. S.; Wold, J. K., Glycoprotein allergens in pollen of Timothy 4. Structural studies of a basic glycoprotein allergen. *International Archives of Allergy and Applied Immunology* **1987**, *83*, 225-230; (b) Haavik, S.; Paulsen, B. S.; Wold, J. K., Glycoprotein allergens in pollen of Timothy 5. Significance of the carbohydrate moiety for the immunological activity of a basic glycoprotein allergen. *International Archives of Allergy and Applied Immunology* **1987**, *83*, 231-237.

27. Oberhuber, C.; Ma, Y.; Wopfner, N.; Gadermaier, G.; Dedic, A.; Niggemann, B.; Maderegger, B.; Gruber, P.; Ferreira, F.; Scheiner, O.; Hoffmann-Sommergruber, K., Prevalence of IgE-binding to Art v1, Art v4 and Amb a1 in mugwort-allergic patients. *International Archives of Allergy and Immunology* **2008**, *145*, 94-101.
28. Jahn-Schmid, B.; Kelemen, P.; Himly, M.; Bohle, B.; Fischer, G.; Ferreira, F.; Ebner, C., The T cell response to Art v 1, the major mugwort pollen allergen, is dominated by one epitope. *Journal of Immunology* **2002**, *169*, 6005-6011.
29. Jahn-Schmid, B.; Fischer, G. F.; Bohle, B.; Fae, I.; Gadermaier, G.; Dedic, A.; Ferreira, F.; Ebner, C., Antigen presentation of the immunodominant T-cell epitope of the major mugwort pollen allergen, Art v 1, is associated with the expression of HLA-DRB1*01. *Journal of Allergy and Clinical Immunology* **2005**, *115*, 399-404.
30. Schmid-Grendelmeier, P.; Holzmann, D.; Himly, M.; Weichel, M.; Tresch, S.; Ruckert, B.; Menz, G.; Ferreira, F.; Blaser, K.; Wuthrich, B.; Cramer, R., Native Art v 1 and recombinant Art v 1 are able to induce humoral and T cell-mediated in vitro and in vivo responses in mugwort allergy. *Journal of Allergy and Clinical Immunology* **2003**, *111*, 1328-1336.
31. Leonard, R.; Wopfner, N.; Pabst, M.; Stadlmann, J.; Petersen, B. O.; Duus, J. O.; Himly, M.; Radauer, C.; Gadermaier, G.; Razzazi-Fazeli, E.; Ferreira, F.; Altmann, F., A new allergen from ragweed (*Ambrosia artemisiifolia*) with homology to Art v 1 from mugwort. *Journal of Biological Chemistry* **2010**, *285*, 27192-27200.
32. Ohyama, K.; Shinohara, H.; Ogawa-Ohnishi, M.; Matsubayashi, Y., A glycopeptide regulating stem cell fate in Arabidopsis thaliana. *Nature Chemical Biology* **2009**, *5*, 578-580.
33. Fletcher, J. C.; Meyerowitz, E. M., Cell signaling within the shoot meristem. *Current Opinion in Plant Biology* **2000**, *3*, 23-30.
34. Shinohara, H.; Matsubayashi, Y., Chemical synthesis of Arabidopsis CLV3 glycopeptide reveals the impact of hydroxyproline arabinosylation on peptide conformation and activity. *Plant and Cell Physiology* **2013**, *54*, 369-374.
35. Chatterjee, D., The mycobacterial cell wall: structure, biosynthesis and sites of drug action. *Curr. Opin. Chem. Biol.* **1997**, *1*, 579-588.
36. (a) Wende, G.; Fry, S. C., 2-O-beta-D-xylopyranosyl-(5-O-feruloyl)-L-arabinose, a widespread component of grass cell walls. *Phytochemistry* **1997**, *44*, 1019-1030; (b) Montes, R. A. C.; Ranocha, P.; Martinez, Y.; Minic, Z.; Jouanin, L.; Marquis, M.; Saulnier, L.; Fulton, L. M.; Cobbett, C. S.; Bitton, F.; Renou, J. P.; Jauneau, A.; Goffner, D., Cell wall modifications in Arabidopsis plants with altered alpha-L-arabinofuranosidase activity. *Plant Physiology* **2008**, *147*, 63-77.
37. Lowary, T. L., Synthesis and conformational analysis of arabinofuranosides, galactofuranosides and fructofuranosides. *Curr. Opin. Chem. Biol.* **2003**, *7*, 749-756.
38. Taylor, C. M.; Weir, C. A.; Jorgensen, C. G., Synthesis of D-galactopyranosides of trans-4-hydroxy-L-proline utilizing the sulfoxide glycosylation method. *Australian Journal of Chemistry* **2002**, *55*, 135-140.

39. Ellervik, U.; Magnusson, G., Anomeric Effect in Furanosides. Experimental Evidence from Conformationally Restricted Compounds. *J. Am. Chem. Soc.* **1994**, *116*, 2340-2347.
40. Houseknecht, J. B.; Lowary, T. L.; Hadad, C. M., Improved Karplus equations for ³J_{C1,H4} in aldopentofuranosides: Application to the conformational preferences of the methyl aldopentofuranosides. *Journal of Physical Chemistry A* **2003**, *107*, 372-378.
41. Glaudemans, C. P. J.; Fletcher, H. G. J., Syntheses with partially benzylated sugars. III. A simple pathway to a cis-nucleoside, 9-beta-D-arabinofuranosyladenine (Spongoadenosine). *Journal of Organic Chemistry* **1963**, *28*, 3004-3006.
42. Glaudemans, C. P. J.; Fletcher, H. G. J., The methanolysis of some D-arabinofuranosyl halides having a nonparticipating group at carbon 2. *Journal of the American Chemical Society* **1965**, *87*, 2456-2461.
43. Mootoo, D. R.; Konradsson, P.; Udodong, U.; Fraserreid, B., Armed and Disarmed N-Pentenyl Glycosides in Saccharide Couplings Leading to Oligosaccharides. *J. Am. Chem. Soc.* **1988**, *110* (16), 5583-5584.
44. Glaudemans, C. P. J.; Fletcher, H. G. J., Long-range effects of acyl groups in solvolysis of glycofuranosyl halides . synthesis of 2,3-di-O-benzyl-5-O-P-nitrobenzoyl-alpha-D-arabinofuranosyl chloride and of 2-O-benzyl-3,5-di-O-P-nitrobenzoyl-alpha-D-arabinofuranosyl chloride. *Journal of the American Chemical Society* **1965**, *87*, 4636-4641.
45. (a) Sanchez, S.; Bamhaoud, T.; Prandi, J., A comprehensive glycosylation system for the elaboration of oligoarabinofuranosides. *Tetrahedron Lett* **2000**, *41*, 7447-7452; (b) Bamhaoud, T.; Sanchez, S.; Prandi, J., 1,2,5-ortho esters of D-arabinose as versatile arabinofuranosidic building blocks. Concise synthesis of the tetrasaccharidic cap of the lipoarabinomannan of Mycobacterium tuberculosis. *Chemical Communications (Cambridge, United Kingdom)* **2000**, 659-660.
46. (a) Gadikota, R. R.; Callam, C. S.; Lowary, T. L., Stereocontrolled synthesis of 2,3-anhydro-beta-D-lyxofuranosyl glycosides. *Org. Lett.* **2001**, *3*, 607-610; (b) Gadikota, R. R.; Callam, C. S.; Wagner, T.; Del Fraino, B.; Lowary, T. L., 2,3-anhydro sugars in glycoside bond synthesis. Highly stereoselective syntheses of oligosaccharides containing alpha- and beta-arabinofuranosyl linkages. *J. Am. Chem. Soc.* **2003**, *125*, 4155-4165; (c) Callam, C. S.; Gadikota, R. R.; Krein, D. M.; Lowary, T. L., 2,3-anhydrosugars in glycoside bond synthesis. NMR and computational investigations into the mechanism of glycosylations with 2,3-anhydrofuranosyl glycosyl sulfoxides. *Journal of the American Chemical Society* **2003**, *125*, 13112-13119.
47. Zhu, X.; Kawatkar, S.; Rao, Y.; Boons, G. J., Practical approach for the stereoselective introduction of beta-arabinofuranosides. *Journal of the American Chemical Society* **2006**, *128*, 11948-11957.
48. (a) Crich, D.; Sun, S. X., Formation of beta-mannopyranosides of primary alcohols using the sulfoxide method. *J. Org. chem.* **1996**, *61*, 4506-4507; (b) Crich, D.; Sun, S. X., Direct chemical synthesis of beta-mannopyranosides and other glycosides via glycosyl triflates. *Tetrahedron* **1998**, *54*, 8321-8348.

49. Crich, D.; Pedersen, C. M.; Bowers, A. A.; Wink, D. J., On the use of 3,5-O-benzylidene and 3,5-O-(di-*tert*-butylsilylene)-2-O-benzylarabinothiofuranosides and their sulfoxides as glycosyl donors for the synthesis of beta-arabinofuranosides: Importance of the activation method. *J. Org. Chem.* **2007**, 72, 1553-1565.
50. Crich, D.; Li, H., Direct stereoselective synthesis of beta-thiomannoside. *J. Org. Chem.* **2000**, 65, 801-805.
51. Crich, D.; Lim, L. B. L., Glycosylation with sulfoxides and sulfinates as donors or promoters. *Org. React.* **2004**, (64).
52. Nacario, R. C.; Lowary, T. L.; McDonald, R., p-Tolyl 2-O-benzyl-3,5-O-(di-*tert*-butylsilanediyl)-1-thio-alpha-D-arabinofuranoside. *Acta Crystallographica Section E-Structure Reports Online* **2007**, 63, O498-O500.
53. Wang, Y. X.; Maguire-Boyle, S.; Dere, R. T.; Zhu, X., Synthesis of beta-D-arabinofuranosides: stereochemical differentiation between D- and L-enantiomers. *Carbohydr Res* **2008**, 343, 3100-3106.
54. Guthrie, R. D.; Smith, S. C., An Improved Preparation of 1,2,3,5-Tetra-O-Acetyl-Beta-D-Ribofuranose. *Chemistry & Industry* **1968**, 547-548.
55. Kam, B. L.; Barascut, J. L.; Imbach, J. L., General Method of Synthesis and Isolation, and an Nmr-Spectroscopic Study, of "Tetra-O-Acetyl-D-Aldopentofuranoses. *Carbohydr Res* **1979**, 69, 135-142.
56. Friedrich-Bochnitschek, S.; Waldmann, H.; Kunz, H., Allyl esters as carboxy protecting groups in the synthesis of O-glycopeptides. *J. Org. Chem.* **1989**, 54, 751-756.
57. Taylor, C. M.; Hardre, R.; Edwards, P. J. B., The impact of pyrrolidine hydroxylation on the conformation of proline-containing peptides. *J. Org. Chem.* **2005**, 70, 1306-1315.
58. Alabugin, I. V.; Zeidan, T. A., Stereoelectronic Effects and General Trends in Hyperconjugative Acceptor Ability of σ Bonds. *J. Am. Chem. Soc.* **2002**, 124, 3175-3185.
59. Kahne, D.; Walker, S.; Cheng, Y.; Vanengen, D., Glycosylation of Unreactive Substrates. *J. Am. Chem. Soc.* **1989**, 111, 6881-6882.
60. Ishiwata, A.; Munemura, Y.; Ito, Y., NAP ether mediated intramolecular aglycon delivery: A unified strategy for 1,2-cis-glycosylation. *Eur J Org Chem* **2008**, 4250-4263.
61. Ishiwata, A.; Akao, H.; Ito, Y., Stereoselective synthesis of a fragment of mycobacterial arabinan. *Org. Lett.* **2006**, 8, 5525-5528.
62. (a) D'Souza, F. W.; Lowary, T. L., The first total synthesis of a highly branched arabinofuranosyl hexasaccharide found at the nonreducing termini of mycobacterial arabinogalactan and lipoarabinomannan. *Org. Lett.* **2000**, 2, 1493-1495; (b) Yin, H. F.; D'Souza, F. W.; Lowary, T. L., Arabinofuranosides from mycobacteria: Synthesis of a highly branched hexasaccharide and related fragments containing beta-axabinofuranosyl residues. *J. Org. Chem.* **2002**, 67, 892-903.

63. (a) Sato, K.; Hada, N.; Takeda, T., Syntheses of new peptidic glycoclusters derived from beta-alanine: di- and trimerized glycoclusters and glycocluster-clusters. *Carbohydr Res* **2006**, *341*, 836-845; (b) Shaikh, H. A.; Sonnichsen, F. D.; Lindhorst, T. K., Synthesis of glycocluster peptides. *Carbohydr Res* **2008**, *343*, 1665-1674; (c) Bossu, I.; Sulc, M.; Krennek, K.; Dufour, E.; Garcia, J.; Berthet, N.; Dumy, P.; Kren, V.; Renaudet, O., Dendri-RAFTs: a second generation of cyclopeptide-based glycoclusters. *Org Biomol Chem* **2011**, *9*, 1948-1959.
64. (a) Lee, R. T.; Lee, Y. C., Affinity enhancement by multivalent lectin-carbohydrate interaction. *Glycoconjugate Journal* **2000**, *17*, 543-551; (b) Vargas-Berenguel, A.; Ortega-Caballero, F.; Casas-Solvas, J. M., Supramolecular chemistry of carbohydrate clusters with cores having guest binding abilities. *Mini-Reviews in Organic Chemistry* **2007**, *4*, 1-14.
65. Hollingsworth, M. A.; Swanson, B. J., Mucins in cancer: protection and control of the cell surface. *Nat Rev Cancer* **2004**, *4*, 45-60.
66. Braun, P.; Davies, G. M.; Price, M. R.; Williams, P. M.; Tendler, S. J. B.; Kunz, H., Effects of glycosylation on fragments of tumour associated human epithelial mucin MUC1. *Bioorgan Med Chem* **1998**, *6*, 1531-1545.
67. Braum, G.; Braun, P.; Kowalczyk, D.; Kunz, H., Enzymatic-hydrolysis of hydrophilic esters by lipases - carboxy deblocking of peptides and glycopeptides. *Tet Lett* **1993**, *34*, 3111-3114.
68. Kuduk, S. D.; Schwarz, J. B.; Chen, X. T.; Glunz, P. W.; Sames, D.; Ragupathi, G.; Livingston, P. O.; Danishefsky, S. J., Synthetic and immunological studies on clustered modes of mucin-related Tn and TF O-linked antigens: the preparation of a glycopeptide-based vaccine for clinical trials against prostate cancer. *Journal of the American Chemical Society* **1998**, *120*, 12474-12485.
69. Liu, M.; Barany, G.; Live, D., Parallel solid-phase synthesis of mucin-like glycopeptides. *Carbohydr Res* **2005**, *340*, 2111-2122.
70. Liu, M. A.; Borgert, A.; Barany, G.; Live, D., Conformational consequences of protein glycosylation: preparation of O-mannosyl serine and threonine building blocks, and their incorporation into glycopeptide sequences derived from alpha-dystroglycan. *Biopolymers* **2008**, *90*, 358-368.
71. Owens, N. W.; Stetefeld, J.; Lattova, E.; Schweizer, F., Contiguous O-galactosylation of 4(R)-hydroxy-L-proline residues forms very stable polyproline II helices. *Journal of the American Chemical Society* **2010**, *132*, 5036-5042.
72. (a) Friedrichbochnitschek, S.; Waldmann, H.; Kunz, H., Allyl esters as carboxy protecting groups in the synthesis of O-glycopeptides. *Journal of Organic Chemistry* **1989**, *54*, 751-756; (b) Zhang, H. X.; Guibe, F.; Balavoine, G., Selective palladium-catalyzed deprotection of the allyl and allyloxycarbonyl groups in phosphate chemistry and in the presence of propargyl and propargyloxycarbonyl groups. *Tet Lett* **1988**, *29*, 623-626.
73. Abdel-Magid, A. F.; Cohen, J. H.; Maryanoff, C. A.; Shah, R. D.; Villani, F. J.; Zhang, F., Hydrolysis of polypeptide esters with tetrabutylammonium hydroxide. *Tetrahedron Lett* **1998**, *39*, 3391-3394.

74. Frerot, E.; Coste, J.; Pantaloni, A.; Dufour, M. N.; Jouin, P., Pybop and Pybrop - 2 reagents for the difficult coupling of the alpha,alpha-dialkyl amino-acid, Aib. *Tetrahedron* **1991**, *47*, 259-270.
75. Valle, G.; Crisma, M.; Toniolo, C.; Beisswenger, R.; Rieker, A.; Jung, G., 1st observation of a helical peptide containing a chiral residue without a preferred screw sense. *Journal of the American Chemical Society* **1989**, *111*, 6828-6833.
76. Schmitt, H.; Jung, G., Total synthesis of the alpha-helical eicosapeptide antibiotic alamethicin. *Liebigs Ann Chem* **1985**, 321-344.
77. Castro, B.; Dormoy, J. R., Reaction of trisdimethylamino(pseudo)halophosphonium salts with carboxylic-acids. *Tetrahedron Lett* **1973**, 3243-3246.
78. Carpino, L. A.; Cohen, B. J.; Stephens, K. E.; Sadataalae, S. Y.; Tien, J. H.; Langridge, D. C., ((9-Fluorenylmethyl)oxy)carbonyl (Fmoc) amino-acid chlorides - synthesis, characterization, and application to the rapid synthesis of short peptide segments. *Journal of Organic Chemistry* **1986**, *51*, 3732-3734.
79. Carpino, L. A.; Sadataalae, D.; Chao, H. G.; Deselms, R. H., ((9-Fluorenylmethyl)oxy)carbonyl (Fmoc) amino-acid fluorides - convenient new peptide coupling reagents applicable to the Fmoc/*tert*-butyl strategy for solution and solid-phase syntheses. *Journal of the American Chemical Society* **1990**, *112*, 9651-9652.
80. Swain, C. G.; Scott, C. B., Rates of solvolysis of some alkyl fluorides and chlorides. *Journal of the American Chemical Society* **1953**, *75*, 246-248.
81. Bender, M. L.; Jones, J. M., Nucleophilic reactions of morpholine with benzoyl halides. The presence of an element effect. *Journal of Organic Chemistry* **1962**, *27*, 3771-3774.
82. Olah, G. A.; Nojima, M.; Kerekes, I., Synthetic methods and reactions. 4. Fluorination of carboxylic-acids with cyanuric fluoride. *Synthesis-Stuttgart* **1973**, 487-488.
83. Carpino, L. A.; Elfaham, A., Tetramethylfluoroformamidinium hexafluorophosphate - a rapid-acting peptide coupling reagent for solution and solid-phase peptide-synthesis. *Journal of the American Chemical Society* **1995**, *117*, 5401-5402.
84. (a) Jou, G.; Gonzalez, I.; Albericio, F.; LloydWilliams, P.; Giralt, E., Total synthesis of dehydroadipin B. Use of uronium and phosphonium salt coupling reagents in peptide synthesis in solution. *Journal of Organic Chemistry* **1997**, *62*, 354-366; (b) Ehrlich, A.; Heyne, H. U.; Winter, R.; Beyermann, M.; Haber, H.; Carpino, L. A.; Bienert, M., Cyclization of all-L-pentapeptides by means of 1-hydroxy-7-azabenzotriazole-derived uronium and phosphonium reagents. *Journal of Organic Chemistry* **1996**, *61*, 8831-8838; (c) El Haddadi, M.; Cavelier, F.; Vives, E.; Azmani, A.; Verducci, J.; Martinez, J., All-L-Leu-Pro-Leu-Pro: A challenging cyclization. *J Pept Sci* **2000**, *6*, 560-570; (d) Kamenecka, T. M.; Danishefsky, S. J., Discovery through total synthesis: A retrospective on the himastatin problem. *Chem-Eur J* **2001**, *7*, 41-63.
85. Carpino, L. A.; Elfaham, A.; Minor, C. A.; Albericio, F., Advantageous applications of azabenzotriazole (triazolopyridine)-based coupling reagents to solid-phase peptide-synthesis. *J Chem Soc Chem Comm* **1994**, 201-203.

86. Carpino, L. A., 1-Hydroxy-7-azabenzotriazole - an efficient peptide coupling additive. *Journal of the American Chemical Society* **1993**, 115, 4397-4398.
87. Carpino, L. A.; Imazumi, H.; El-Faham, A.; Ferrer, F. J.; Zhang, C. W.; Lee, Y. S.; Foxman, B. M.; Henklein, P.; Hanay, C.; Mugge, C.; Wenschuh, H.; Klose, K.; Beyermann, M.; Bienert, M., The uronium/guanidinium peptide coupling reagents: finally the true uronium salts. *Angewandte Chemie-International Edition* **2002**, 41, 442-445.
88. (a) Woody, R. W.; Sreerama, N., Circular Dichroism **2000**, Wiley-VCH, New York, N.Y., 601-620; (b) Kelly, S. M.; Jess, T. J.; Price, N. C., How to study proteins by circular dichroism. *BBA-Proteins Proteomics* **2005**, 1751, 119-139; (c) Johnson, W. C., Analyzing protein circular dichroism spectra for accurate secondary structures. *Proteins: Structure, Function, and Bioinformatics* **1999**, 35, 307-312.
89. Cowan, P. M.; McGavin, S., Structure of Poly-L-Proline. *Nature* **1955**, 176, 501-503.
90. Adzhubei, A. A.; Sternberg, M. J. E., Left-handed Polyproline II Helices Commonly Occur in Globular Proteins. *Journal of Molecular Biology* **1993**, 229, 472-493.
91. Bartlett, G. J.; Choudhary, A.; Raines, R. T.; Woolfson, D. N., $n \rightarrow \pi^*$ Interactions in proteins. *Nature Chemical Biology* **2010**, 6, 615-620.
92. Hinderaker, M. P.; Raines, R. T., An electronic effect on protein structure. *Protein Sci* **2003**, 12, 1188-1194.
93. Sreerama, N.; Woody, R. W., Poly(Pro)II Helices in Globular-Proteins - Identification and Circular Dichroic Analysis. *Biochemistry-Us* **1994**, 33, 10022-10025.
94. Ronish, E. W.; Krimm, S., The calculated circular dichroism of polyproline II in the polarizability approximation. *Biopolymers* **1974**, 13, 1635-1651.
95. Kelly, M. A.; Chellgren, B. W.; Rucker, A. L.; Troutman, J. M.; Fried, M. G.; Miller, A.-F.; Creamer, T. P., Host-Guest Study of Left-Handed Polyproline II Helix Formation. *Biochemistry-Us* **2001**, 40, 14376-14383.
96. Taylor, C. M.; Karunaratne, C. V.; Xie, N., Glycosides of hydroxyproline: Some recent, unusual discoveries. *Glycobiology* **2012**, 22, 757-767.
97. Ferris, P. J.; Woessner, J. P.; Waffenschmidt, S.; Kilz, S.; Drees, J.; Goodenough, U. W., Glycosylated Polyproline II Rods with Kinks as a Structural Motif in Plant Hydroxyproline-Rich Glycoproteins. *Biochemistry-Us* **2001**, 40, 2978-2987.
98. Pauling, L.; Corey, R. B., Structure of fibrous proteins of the collagen-gelatin group. *Proc Nat Acad Sci USA* **1951**, 37, 272-281.
99. Dedic, A.; Gadermaier, G.; Vogel, L.; Ebner, C.; Vieths, S.; Ferreira, F.; Egger, M., Immune recognition of novel isoforms and domains of the mugwort pollen major allergen Art v 1. *Molecular Immunology* **2009**, 46, 416-421.
100. Williamson, M. P., The structure and function of proline-rich regions in protein. *Biochemical Journal* **1994**, 297, 249-260.

101. Rothe, M.; Rott, M.; Mazanek, J., *Solid phase synthesis and conformation of monodisperse high molecular weight oligo-L-prolines*. Editions de l'Universite de Bruxelles: Brussels, 1976.
102. (a) Thomas, W. A.; Williams, M. K., C-13 NUCLEAR MAGNETIC-RESONANCE SPECTROSCOPY AND CIS-TRANS ISOMERISM IN DIPEPTIDES CONTAINING PROLINE. *J Chem Soc Chem Comm* **1972**, (17), 994; (b) Evans, C. A.; Rabenstein, D., NUCLEAR MAGNETIC-RESONANCE STUDIES OF ACID-BASE CHEMISTRY OF AMINO-ACIDS AND PEPTIDES .2. DEPENDENCE OF ACIDITY OF C-TERMINAL CARBOXYL GROUP ON CONFORMATION OF C-TERMINAL PEPTIDE-BOND. *Journal of the American Chemical Society* **1974**, 96 (23), 7312-7317; (c) Grathwohl, C.; Wüthrich, K., The X-Pro peptide bond as an nmr probe for conformational studies of flexible linear peptides. *Biopolymers* **1976**, 15 (10), 2025-2041; (d) Bedford, G. R.; Sadler, P. J., ¹³C magnetic resonance study of the ionization of N-acetyl-dl-proline in aqueous solution. *Biochimica et Biophysica Acta (BBA) - General Subjects* **1974**, 343, 656-662.
103. Helbecque, N.; Loucheux-Lefebvre, M. H., Critical chain length for polyproline-II structure formation in H-Gly-(Pro)_n-OH. *International Journal of Peptide and Protein Research* **1982**, 19, 94-101.
104. Creamer, T. P., Left-handed polyproline II helix formation is (very) locally driven. *Proteins-Structure Function and Genetics* **1998**, 33, 218-226.
105. MacArthur, M. W.; Thornton, J. M., Influence of proline residues on protein conformation. *Journal of Molecular Biology* **1991**, 218, 397-412.
106. Pysh, E. S., Random phase calculation of poly-L-proline II circular dichroism. *Biopolymers* **1974**, 13, 1563-1571.
107. Brahmachari, S. K.; Bansal, M.; Ananthanarayanan, V. S.; Sasisekharan, V., Structural investigations on poly(4-hydroxy-L-proline) 2. Physicochemical studies. *Macromolecules* **1979**, 12, 23-28.
108. Naziga, E. B.; Schweizer, F.; Wetmore, S. D., Solvent Interactions Stabilize the Polyproline II Conformation of Glycosylated Oligoproline. *Journal of Physical Chemistry B* **2013**, 117, 2671-2681.
109. Owens, N. W.; Lee, A.; Marat, K.; Schweizer, F., The Implications of (2S,4S)-Hydroxyproline 4-O-Glycosylation for Prolyl Amide Isomerization. *Chem-Eur J* **2009**, 15, 10649-10657.
110. Imamura, A.; Lowary, T., Chemical Synthesis of Furanose Glycosides. *Trends in Glycoscience and Glycotechnology* **2011**, 23, 134-152.
111. Cardoso, S. M.; Silva, A. M. S.; Coimbra, M. A., Structural characterisation of the olive pomace pectic polysaccharide arabinan side chains. *Carbohydr Res* **2002**, 337, 917-924.
112. Deber, C. M.; Bovey, F. A.; Carver, J. P.; Blout, E. R., Nuclear magnetic resonance evidence for cis-peptide bonds in proline oligomers. *Journal of the American Chemical Society* **1970**, 92, 6191-6198.

113. Svehla, E., The influence of weed pollen glycosylation on IgG-binding. *Master thesis at the University of Natural Resources and Life Sciences Vienna, Austria* **2013**.
114. Lisowska, E., The role of glycosylation in protein antigenic properties. *Cellular and Molecular Life Sciences* **2002**, *59*, 445-455.
115. Jones, C., Vaccines based on the cell surface carbohydrates of pathogenic bacteria. *Anais Da Academia Brasileira De Ciencias* **2005**, *77*, 293-324.
116. Wilson, I. B. H.; Harthill, J. E.; Mullin, N. P.; Ashford, D. A.; Altmann, F., Core alpha 1,3-fucose is a key part of the epitope recognized by antibodies reacting against plant N-linked oligosaccharides and is present in a wide variety of plant extracts. *Glycobiology* **1998**, *8*, 651-661.
117. Avery, O. T.; Goebel, W. F., Chemo-immunological studies on conjugated carbohydrate proteins. V. Immunological specificity of an antigen prepared by combining the capsular polysaccharide of type III pneumococcus with foreign protein. *J Exp Med* **1931**, *54*, 437-447.
118. (a) Schneerson, R.; Barrera, O.; Sutton, A.; Robbins, J. B., Preparation, characterization, and immunogenicity of Hemophilus-Influenzae type-B polysaccharide-protein conjugates. *J Exp Med* **1980**, *152*, 361-376; (b) Beuvery, E. C.; Leussink, A. B.; Vandelft, R. W.; Tiesjema, R. H.; Nagel, J., Immunoglobulin M and G antibody responses and persistence of these antibodies in adults after vaccination with a combined meningococcal group A and group C polysaccharide vaccine. *Infection and Immunity* **1982**, *37*, 579-585; (c) Beuvery, E. C.; Vanrossum, F.; Nagel, J., Comparison of the induction of immunoglobulin M and G antibodies in mice with purified pneumococcal type 3 and meningococcal group C polysaccharides and their protein conjugates. *Infection and Immunity* **1982**, *37*, 15-22.
119. (a) Gray, G. R., DIRECT COUPLING OF OLIGOSACCHARIDES TO PROTEINS AND DERIVATIZED GELS. *Archives of Biochemistry and Biophysics* **1974**, *163* (1), 426-428; (b) Roy, R.; Laferriere, C. A., Michael addition as the key step in the syntheses of sialyloligosaccharide-protein conjugates from N-acryloylated glycopyranosylamines. *J Chem Soc Chem Comm* **1990**, 1709-1711.
120. Taylor, C. M.; Hardré, R.; Edwards, P. J. B.; Park, J. H., Factors Affecting Conformation in Proline-Containing Peptides. *Organic Letters* **2003**, *5*, 4413-4416.
121. (a) Kang, Y. K.; Jhon, J. S.; Park, H. S., Conformational Preferences of Proline Oligopeptides. *The Journal of Physical Chemistry B* **2006**, *110*, 17645-17655; (b) Moradi, M.; Babin, V.; Roland, C.; Sagui, C., A classical molecular dynamics investigation of the free energy and structure of short polyproline conformers. *Journal of Chemical Physics* **2010**, *133*, 125104.
122. Weber, R. W., Cross-reactivity of pollen allergens: impact on allergen immunotherapy. *Annals of Allergy, Asthma & Immunology* **2007**, *99*, 203-212.
123. Lee, Y. W.; Choi, S. Y.; Lee, E. K.; Sohn, J. H.; Park, J.-W.; Hong, C.-S., Cross-allergenicity of pollens from the Compositae family: *Artemisia vulgaris*, *Dendranthema grandiflorum*, and *Taraxacum officinale*. *Annals of Allergy, Asthma & Immunology* **2007**, *99*, 526-533.

APPENDIX: LETTERS OF PERMISSION

Figure 1.6 – Page 17

To whom it may concern,

It is the policy of the American Society for Biochemistry and Molecular Biology to allow reuse of any material published in its journals (the Journal of Biological Chemistry, Molecular & Cellular Proteomics and the Journal of Lipid Research) in a thesis or dissertation at no cost and with no explicit permission needed. Please see our copyright permissions page on the journal site for more information.

Best wishes,

Sarah Crespi

American Society for Biochemistry and Molecular Biology

11200 Rockville Pike, Rockville, MD

Suite 302

240-283-6616

JBC | MCP | JLR

Tel:

ELSEVIER LICENSE

TERMS AND CONDITIONS

Jun 12, 2013

This is a License Agreement between Ning Xie ("You") and Elsevier ("Elsevier") provided by Copyright Clearance Center ("CCC"). The license consists of your order details, the terms and conditions provided by Elsevier, and the payment terms and conditions.

All payments must be made in full to CCC. For payment instructions, please see information listed at the bottom of this form.

Supplier	Elsevier Limited The Boulevard, Langford Lane Kidlington, Oxford, OX5 1GB, UK
Registered Company Number	1982084
Customer name	Ning Xie
Customer address	9430 Langham Dr Baton Rouge, LA 70810
License number	3130920906580
License date	Apr 16, 2013
Licensed content publisher	Elsevier
Licensed content publication	Structure
Licensed content title	Mapping the Interactions between a Major Pollen Allergen and Human IgE Antibodies
Licensed content author	Guilherme Razzera, Gabriele Gadermaier, Viviane de Paula, Marcius S. Almeida, Matthias Egger, Beatrice Jahn- Schmid, Fabio C.L. Almeida, Fatima Ferreira, Ana Paula Valente
Licensed content date	11 August 2010
Licensed content volume number	18
Licensed content issue number	8
Number of pages	11
Start Page	1011
End Page	1021
Type of Use	reuse in a thesis/dissertation
Portion	figures/tables/illustrations
Number of figures/tables/illustrations	1
Format	both print and electronic
Are you the author of this Elsevier article?	No
Will you be translating?	No
Order reference number	

Title of your thesis/dissertation	Oligomers of Beta-L-Arabinosides of Hydroxyproline: Synthesis of the Carbohydrate Epitope of the Art v 1 Allergen
Expected completion date	Aug 2013
Estimated size (number of pages)	150
Elsevier VAT number	GB 494 6272 12
Permissions price	0.00 USD
VAT/Local Sales Tax	0.0 USD / 0.0 GBP
Total	0.00 USD
Terms and Conditions	

Figure 2.5 – Page 26

Permission is hereby granted, on behalf of the IUCr, for you to reproduce the material specified below, subject to the following conditions:

1. Reproduction is intended in a primary journal, secondary journal, CD-ROM, book or thesis.
2. The original article in which the material appeared is cited.
3. IUCr's copyright permission is indicated next to the Figure in print. In electronic form, this acknowledgement must be visible at the same time as the Figure, and must be hyperlinked to the article (<http://dx.doi.org/10.1107/S1600536806054729>).

With best wishes,

Gillian

Dr Gillian Holmes (Managing Editor, Acta Crystallographica Section E)

International Union of Crystallography
5 Abbey Square, Chester, CH1 2HU, England

Figure 4.4 – Page 131; Figure 4.5 – Page 132

Title: Host–Guest Study of Left-
Handed Polyproline II Helix
Formation†
Author: Melissa A. Kelly et al.
Publication: Biochemistry
Publisher: American Chemical Society
Date: Dec 1, 2001
Copyright © 2001, American Chemical
Society

Logged in as:

Ning Xie

Account #:

3000646924

LOGOUT

PERMISSION/LICENSE IS GRANTED FOR YOUR ORDER AT NO CHARGE

This type of permission/license, instead of the standard Terms & Conditions, is sent to you because no fee is being charged for your order. Please note the following:

- Permission is granted for your request in both print and electronic formats, and translations.
- If figures and/or tables were requested, they may be adapted or used in part.
- Please print this page for your records and send a copy of it to your publisher/graduate school.
- Appropriate credit for the requested material should be given as follows: "Reprinted (adapted) with permission from (COMPLETE REFERENCE CITATION). Copyright (YEAR) American Chemical Society." Insert appropriate information in place of the capitalized words.
- One-time permission is granted only for the use specified in your request. No additional uses are granted (such as derivative works or other editions). For any other uses, please submit a new request.

If credit is given to another source for the material you requested, permission must be obtained from that source.

Figure 4.8 - Page 134

Title: Critical chain length for
polyproline-II structure
formation in H-Gly-(Pro)n-OH
Author: N. HELBECQUE,M.H.
LOUCHEUX-LEFEBVRE
Publication: Chemical Biology & Drug
Design
Publisher: John Wiley and Sons
Date: Jan 12, 2009
© 1982 Munksgaard International
Publishers Ltd.

Logged in as:

Ning Xie

Account #:

3000646924

LOGOUT

Order Completed

Thank you very much for your order.

This is a License Agreement between Ning Xie ("You") and John Wiley and Sons ("John Wiley and Sons"). The license consists of your order details, the terms and conditions provided by John Wiley and Sons, and the [payment terms and conditions](#).

[Get the printable license](#).

License Number	3166670470667
License date	Jun 12, 2013
Licensed content publisher	John Wiley and Sons
Licensed content publication	Chemical Biology & Drug Design
Licensed content title	Critical chain length for polyproline-II structure formation in H-Gly-(Pro)n-OH
Licensed copyright line	© 1982 Munksgaard International Publishers Ltd.
Licensed content author	N. HELBECQUE,M.H. LOUCHEUX-LEFEBVRE
Licensed content date	Jan 12, 2009
Start page	94
End page	101
Type of use	Dissertation/Thesis
Requestor type	University/Academic
Format	Print and electronic
Portion	Figure/table
Number of figures/tables	1
Original Wiley figure/table number(s)	Figure 2
Will you be translating?	No
Total	0.00 USD

Title: Contiguous O-Galactosylation
of 4(R)-Hydroxy-L-proline
Residues Forms Very Stable
Polyproline II Helices

Author: Neil W. Owens, Jörg Stetefeld,
Erika Lattová, and Frank
Schweizer

Publication: Journal of the American
Chemical Society

Publisher: American Chemical Society

Date: Apr 1, 2010

Copyright © 2010, American Chemical
Society

Logged in as:

Ning Xie

Account #:

3000646924

LOGOUT

PERMISSION/LICENSE IS GRANTED FOR YOUR ORDER AT NO CHARGE

This type of permission/license, instead of the standard Terms & Conditions, is sent to you because no fee is being charged for your order. Please note the following:

- Permission is granted for your request in both print and electronic formats, and translations.
- If figures and/or tables were requested, they may be adapted or used in part.
- Please print this page for your records and send a copy of it to your publisher/graduate school.
- Appropriate credit for the requested material should be given as follows: "Reprinted (adapted) with permission from (COMPLETE REFERENCE CITATION). Copyright (YEAR) American Chemical Society." Insert appropriate information in place of the capitalized words.
- One-time permission is granted only for the use specified in your request. No additional uses are granted (such as derivative works or other editions). For any other uses, please submit a new request.

If credit is given to another source for the material you requested, permission must be obtained from that source.

VITA

Ning Xie was born in Yangzhou, China, where he lived and attended school up until the 3rd grade. Two months before his 8th birthday, Ning came to Baton Rouge, Louisiana, to join his father, who was currently a doctoral candidate at Louisiana State University under Professor Milton C. Rush, and mother. He would live in Baton Rouge for the better part of his life, along with a short stint in Crowley, Louisiana.

Ning Xie received his Bachelor of Science degree in Chemistry in 2007 from LSU. He performed organic chemistry experiments as an undergraduate in the laboratory of Professor Robert Hammer where he first conducted peptide chemistry. In the fall of 2007, Ning was accepted into the doctoral program in the chemistry department at LSU where he is currently a doctoral candidate in organic chemistry working under the tutelage of Professor Carol M. Taylor. His graduate dissertation work involved the synthesis of oligomers of arabinosylated hydroxyproline and the investigation of their allergenic potential. Ning is a member of the American Chemical Society.